

**EPIGENETIC CHANGES INDUCED BY ADENOSINE AUGMENTATION
THERAPY PREVENT EPILEPTOGENESIS**

by

Rebecca Lynn Williams-Karnesky

A DISSERTATION

Presented to the Neuroscience Graduate Program

and the Oregon Health & Science University

in partial fulfillment of

the degree requirements for the degree of

Doctor of Philosophy

August 2012

School of Medicine
Oregon Health & Science University

CERTIFICATE OF APPROVAL

This is to certify that the Ph.D. dissertation of
REBECCA WILLIAMS-KARNESKY
has been approved on August 16, 2012

Advisor, Detlev Boison, PhD

Member and Chair, Steven Kohama, PhD

Member, Larry Sherman, PhD

Member, Buddy Ullman, PhD

Member, Julie Saugstad, PhD

TABLE OF CONTENTS

	Page
CERTIFICATE OF APPROVAL	
TABLE OF CONTENTS	i
LIST OF FIGURES	viii
LIST OF TABLES	xxi
LIST OF ABBREVIATIONS	xxiv
ACKNOWLEDGEMENTS	xxxiv
ABSTRACT	xxxvi
Chapter 1. Introduction	1
1. Neurological injury	2
1.1. Mechanism of ischemia-induced cell death	5
1.2. A brief history of therapeutic neuroprotection	8
1.3. Hibernation as an endogenous neuroprotective phenomenon	9
1.4. Early attempts at neuroprotection in clinical medicine	11
1.5. Beyond hypothermia – the evolution of neuroprotection	17
1.6. Neuroprotection via ischemic preconditioning	18
1.7. Cross tolerance – towards a unifying theory of preconditioning	21

2. The role of Toll-like receptors in neuroprotection	26
2.1. An Introduction to Toll-like Receptors	26
2.2. Toll-like receptor signaling pathways	28
2.3. Toll-like receptor expression	31
2.4. Toll-like receptor signaling in health and disease	33
2.5. Toll-like receptors and ischemic damage	34
2.6. Toll-like receptors and neuroprotection	38
2.7. TLR-mediated neuroprotection—reprogramming TLR signaling	43
3. The role of adenosine in neuroprotection	49
3.1. A brief history of adenosine-based therapies in neuroprotection	49
3.2. The basic physiology of adenosine and its receptors	50
3.3. The effects of adenosine release on the CNS during cerebral ischemia	51
3.4. A ₁ R effects in the CNS	54
3.5. A _{2A} R effects in the CNS	56
3.6. A _{2B} receptor effects in the CNS	58
3.7. A ₃ receptor effects in the CNS	60
3.8. Past complications in developing adenosine-based therapies for cerebral ischemia	61
3.9. Peripheral immune involvement and inflammatory cytokines in cerebral ischemia	62
3.10. The effects of adenosine on the peripheral immune system	65
3.11. Effects of adenosine on monocytes and macrophages	67
3.12. Effects of adenosine on T and B lymphocytes	68
3.13. Effects of adenosine on neutrophils and other granulocytes	69
3.14. A putative role for adenosine in preconditioning	71

Hypothesis and Specific Aims	75
Chapter 2. Manuscript #1: Proof of Concept: Pharmacological preconditioning with a Toll-like receptor agonist protects against cerebrovascular injury in a primate model of stroke	76
1. ABSTRACT	77
2. INTRODUCTION	78
3. MATERIALS AND METHODS	81
4. RESULTS	89
4.1. <i>Prophylactic administration of Kmix CpG ODNs significantly reduces infarct damage in mice</i>	89
4.2. <i>Prophylactic administration of Kmix CpG ODNs significantly reduces cortical damage in NHPs</i>	90
4.3. <i>Prophylactic administration of Kmix CpG ODNs improves neurological function in NHPs</i>	91
4.4. <i>Kmix CpG ODNs have no effect on blood cell composition following stroke</i>	92
4.5. <i>Plasma IL-6 and CRP are elevated following stroke in NHPs</i>	93
5. DISCUSSION	94

Chapter 3. Manuscript #2. Adenosine kinase determines the degree of brain injury after ischemic stroke in mice	112
1. ABSTRACT	113
2. INTRODUCTION	114
3. MATERIALS AND METHODS	116
4. RESULTS	124
4.1. <i>ADK expression levels in fb-Adk-def mice determine the tone of ambient adenosine</i>	124
4.2. <i>Cortical reduction of ADK provides regional protection from stroke</i>	126
4.3. <i>ADK activity negatively regulates LPS-induced stroke tolerance</i>	127
4.4. <i>Modulation of stroke susceptibility by regional overexpression or knockdown of ADK with an AAV-based vector system</i>	128
4.5. <i>AAV8-based knockdown of ADK reduces ischemic brain injury</i>	129
5. DISCUSSION	130
5.1. <i>Homeostatic bioenergetic network regulation through ADK</i>	131
5.2. <i>Adenosine and ADK in acute neuroprotection</i>	132
5.3. <i>Adenosine and ADK in ischemic tolerance</i>	133
5.4. <i>Therapeutic adenosine augmentation</i>	135

Chapter 4. Manuscript #3. Epigenetic changes induced by adenosine augmentation therapy prevent epileptogenesis	144
1. ABSTRACT	145
2. INTRODUCTION	146
3. MATERIALS AND METHODS	149
4. RESULTS	154
4.1. <i>Increased adenosine and reduced ADK expression induce DNA hypomethylation in the brain</i>	154
4.2. <i>The nuclear isoform of ADK plays a key role in the induction of DNA hypermethylation</i>	156
4.3. <i>Therapeutic delivery of adenosine modulates DNA methylation</i>	156
4.4. <i>Inhibition of DNA methylation attenuates seizures and kindling induced epileptogenesis</i>	157
4.5. <i>Intraventricular implants of adenosine-releasing silk reverse DNA hypermethylation in the epileptic brain</i>	158
4.6. <i>Adenosine-releasing silk prevents progression of epilepsy development</i>	160
4.7. <i>Adenosine-releasing silk implants prevent mossy fiber sprouting</i>	162
5. DISCUSSION	162

Chapter 5. Conclusions and Summary	177
1. Endogenous mechanisms can be harnessed for neuroprotection	178
2. CpG preconditioning relies on the peripheral immune response	181
3. Epigenetics: A universal mechanism of neuroprotection	184
3.1. Epigenetic changes in peripheral immune cells	185
3.2. Epigenetic changes in the CNS: Roles in disease and neuroprotection	189
3.3. Role of adenosine as an epigenetic modifier	193
3.4. Long-lasting potential of epigenetic therapies	197
4. Summary	197
References	200
Appendix	264
1. Appendix A: Studies exploring the role of the non-canonical NF κ B1 (p105/p50) signaling pathway in lipopolysaccharide-mediated ischemic tolerance in the brain.	265
2. Appendix B: Studies on the effectiveness of CpG ODNs via multiple routes of administration	279
3. Appendix C: Studies of the effectiveness of CpG preconditioning in epilepsy and permanent MCAO	284

4. Appendix D: Studies on the effectiveness of CpG preconditioning in ADK transgenic animals	293
5. Appendix E Studies on the role of adenosine A ₁ receptors on CpG mediated-preconditioning and infarct volume	301
6. Appendix F: Development an <i>in vitro</i> prescreening assay for assessing CpG response in non-human primates using peripheral mononuclear blood cells	308
7. Appendix G: Comparative assessment of three neurological scales for predicting function recovery between days 2 and 7 post-stroke in a non-human primate model	316
8. Appendix H: Manuscript #4: Changes in spontaneous activity assessed by accelerometry correlate with extent of cerebral ischemia-reperfusion injury in the nonhuman primate.	337
9. Appendix I: Characterization of the peripheral immune response following stroke in a non-human primate model	370
10. Appendix J: Characterization of the response to the two vessel occlusion model of cerebral ischemia in Chinese origin rhesus macaques	406
11. Appendix K: Supplemental figures referred to in the main text	418

LIST OF FIGURES

Chapter 1	Introduction	
Figure 1	<i>Representative dose-response curves for brain injury</i>	4
Figure 2	<i>Image of a page from the Edwin Smith papyrus dated 1500 BCE</i>	13
Figure 3	<i>Early application of systemic hypothermia to treat cerebral injury</i>	15
Figure 4	<i>Early approach to local hypothermia in the brain</i>	16
Figure 5	<i>Decreased myocardial infarct following preconditioning ischemia</i>	19
Figure 6	<i>Schematic overview of rapid and delayed ischemic preconditioning</i>	22
Figure 7	<i>Time course of delayed preconditioning</i>	23
Figure 8	<i>Representative heat map generated from microarray data following stroke in CpG-preconditioned and saline-treated animals</i>	24
Figure 9	<i>Genomic alterations in the blood following CpG preconditioning</i>	25
Figure 10	<i>Toll-like receptor signaling pathways</i>	29
Figure 11	<i>Toll-like receptor signaling in response to cerebral ischemia</i>	36
Figure 12	<i>Dose response of CpG preconditioning</i>	42
Figure 13	<i>Reprogramming the Toll-like receptor response to cerebral ischemia</i>	45
Figure 14	<i>Peripheral immune involvement following ischemic brain injury</i>	64
Figure 15	<i>Adenosine modulates peripheral immune cell function</i>	66

Chapter 2	Proof of Concept: Pharmacological preconditioning with a Toll-like receptor agonist protects against cerebrovascular injury in a primate model of stroke	
Figure 16	<i>Reduction in infarct volume following MCAO in mice preconditioned with CpG 1826 or Kmix CpG ODNs</i>	105
Figure 17	<i>Experimental timeline and surgical occlusion</i>	106
Figure 18	<i>Reduction in infarct volume following MCA and ACA occlusion in NHPs preconditioned with Kmix CpG ODNs</i>	107
Figure 19	<i>Cortical infarct is reduced following pretreatment with CpG ODNs as seen by T2 MRI</i>	108
Figure 20	<i>Neurological improvement following preconditioning with Kmix CpG ODNs</i>	109
Figure 21	<i>Plasma IL-6 and CRP are elevated following stroke in NHPs</i>	111

Chapter 3	Adenosine kinase determines the degree of brain injury after ischemic stroke in mice	
Figure 22	<i>Differential expression pattern of striatal and cortical ADK in fb-Adk-def mice</i>	137
Figure 23	<i>Regional ADK manipulation causes focal changes in adenosine levels</i>	138
Figure 24	<i>Local downregulation of ADK attenuates ischemic neuronal injury in the cortex</i>	139
Figure 25	<i>Increased ADK prevents LPS-induced ischemic tolerance in Adk-tg mutants</i>	140
Figure 26	<i>Modulation of ADK expression with an adeno associated virus (AAV) – based vector system</i>	141
Figure 27	<i>Modification of infarct volume by viral over- or under-expression of ADK</i>	143

Chapter 4	Epigenetic modifications induced by adenosine augmentation therapy prevent epileptogenesis	
Figure 28	<i>Increased adenosine and reduced ADK expression induces DNA hypomethylation in the brain; increased ADK expression induces DNA hypermethylation</i>	169
Figure 29	<i>The DNA methyltransferase inhibitor, 5-Aza-2dC attenuates ictogenesis and epileptogenesis</i>	171
Figure 30	<i>Intraventricular implants of adenosine-releasing silk polymer reverse DNA hypermethylation in the epileptic brain</i>	172
Figure 31	<i>Adenosine-releasing silk polymers prevent progression of epilepsy development</i>	173
Figure 32	<i>Adenosine-releasing silk polymer implants prevent mossy fiber sprouting</i>	175
Figure 33	<i>Model for the role of adenosine and associated DNA methylation changes in epileptogenesis</i>	176

Chapter 5	Conclusions and Summary	
Figure 34.	<i>Epigenetic reprogramming of immune cells following sepsis</i>	188
Figure 35	<i>Epigenetic mechanisms that underlie neural stem cell maintenance and maturation</i>	192
Figure 36	<i>Endogenous neural stem cell activation for the treatment of neurological disease</i>	196
Appendix A	Studies exploring the role of the non-canonical NFκB1 (p105/p50) signaling pathway in lipopolysaccharide-mediated ischemic tolerance in the brain.	
Figure 37	<i>Blood cytokine/chemokine profile following ip LPS administration.</i>	275
Figure 38	<i>NFκB Suppression following MCAO in LPS preconditioned animals</i>	276
Figure 39	<i>Reprogramming of TLR4 signaling and gene expression following stroke in LPS preconditioned animals</i>	277

**Appendix B Studies on effectiveness of CpG ODNs via multiple routes
of administration**

Figure 40	<i>Prophylactic CpG ODNs can induce neuroprotection via multiple routes of administration</i>	282
------------------	---	-----

**Appendix C Studies of the effectiveness of CpG preconditioning
in epilepsy and permanent MCAO**

Figure 41	<i>CpG preconditioning does not protect in a KA-induced model of excitotoxic cell death</i>	289
Figure 42	<i>CpG preconditioning does not reduce infarct volume in a model of permanent MCAO</i>	290
Figure 43	<i>Levels of serum TNF-α increase acutely following administration of CpG ODNs or LPS</i>	291

**Appendix D Studies of the effectiveness of CpG preconditioning
in ADK transgenic animals**

Figure 44	<i>Mice with increased adenosine tone in the brain can be preconditioned with CpG ODNs</i>	298
Figure 45	<i>Mice with increased adenosine tone in the forebrain can be preconditioned with CpG ODNs</i>	299
Figure 46	<i>Differential genomic response in blood and brain following preconditioning with ischemic, CpG or LPS</i>	300

**Appendix E Studies on the role of adenosine A₁ receptors on
CpG-mediated preconditioning and infarct volume
following MCAO**

Figure 47	<i>A₁R knockout mice have reduced infarct volume following transient MCAO</i>	306
Figure 48	<i>A₁R mice cannot be preconditioned with CpG ODNs</i>	307

Appendix H Manuscript #4: Changes in spontaneous activity assessed by accelerometry correlate with extent of cerebral ischemia-reperfusion injury in the nonhuman primate

Figure 57	<i>Daily schedule</i>	361
Figure 58	<i>Study timeline</i>	362
Figure 59	<i>Actogram representing a subset of continuous recordings made prior to and following stroke in a representative animal with a measured infarct volume of 26% by MRI method</i>	364
Figure 60	<i>Representative brain images showing infarct regions determined by T2-weighted MRI</i>	365
Figure 61	<i>Correlation between mean activity values versus infarct volume</i>	366
Figure 62	<i>Changes in total daily activity were related to the experimental procedure and infarct volume</i>	367
Figure 63	<i>Correlation between total cumulative neurological score and infarct volume</i>	368
Figure 64	<i>Correlation between percent change in mean activity counts and cumulative neurological scores</i>	369

Appendix I	Characterization of the peripheral immune response following stroke in a non-human primate model	
Figure 65	<i>Blood draw timeline</i>	381
Figure 66	<i>Gating strategy used to identifying PBMC subpopulations</i>	382
Figure 67	<i>Increase in white blood cells 48h post-stroke in NHPs is largely due to an increase in neutrophils</i>	384
Figure 68	<i>Red blood cell count, hematocrit and hemoglobin do not change following stroke in NHPs</i>	385
Figure 69	<i>Plasma C-reactive protein is elevated 48 hours after stroke in NHPs</i>	386
Figure 70	<i>Granulocytes are increased following stroke in NHPs</i>	387
Figure 71	<i>Monocytes are increased at 48 hours post-stroke, and remain elevated at 7 days post-infarct</i>	388
Figure 72	<i>Number of CD56+ but not CD16+ natural killer cells increase at 48 hours post stroke in NHPs</i>	389
Figure 73	<i>Natural killer cells become activated following stroke in NHPs</i>	390
Figure 74	<i>Lymphocytes decrease following stroke in NHPs</i>	391
Figure 75	<i>Slight decrease in number, but increase in activation status of CD4+ T cells following stroke in NHPs</i>	392
Figure 76	<i>Slight decrease in number, but increase in activation markers on CD8+ T cells following stroke in NHPs</i>	393

Figure 77	<i>CD25-CD3+CD8+ cells increase following stroke in NHPs</i>	394
Figure 78	<i>CD20+ B cells decrease acutely and become less activated following stroke in NHPs</i>	395
Figure 79	<i>CD4+ and CD8+ T regulatory cells increase following stroke in NHPs</i>	396
Figure 80	<i>CD3- CD20+ B cells have increases responsiveness to Toll-like receptor ligands following stroke in NHPs</i>	397
Figure 81	<i>CD3+CD4+ T cells and CD3+CD8+ T cells have decreased responsiveness to Toll-like receptor ligands following stroke in NHPs</i>	398
Figure 82	<i>Schematic representation of connections form the central nervous system and the peripheral immune system</i>	399
Figure 83	<i>Day 2 white blood cell count decreases as infarct volume increases</i>	400
Figure 84	<i>Day 7 white blood cell count increases with increasing infarct volume</i>	401
Figure 85	<i>CD4+ and CD8+ T cell, B cell, and NK cell counts increase with increasing with infarct volume</i>	402
Figure 86	<i>Ratio of CD4+ to CD8+ cells decreases with increasing infarct volume</i>	403
Figure 87	<i>High T to B cell ratio at time of stroke, but not after stroke, correlates with increased infarct volume</i>	404

**Appendix J Characterization of the response to the two vessel
occlusion model of cerebral ischemia in Chinese origin
rhesus macaques**

Figure 88	<i>Comparison of stroke volume with T2-weighted MRI across various durations of reversible, two-vessel occlusion in Indian origin animals</i>	410
Figure 89	<i>View of middle cerebral and anterior cerebral arteries from cranial window</i>	412
Figure 90	<i>Serial MRI section from Chinese or hybrid origin animals 2 days post occlusion</i>	413
Figure 91	<i>Vascular architecture of Indian origin rhesus compared to Chinese or hybrid origin</i>	414
Figure 92	<i>Representative MRIs from 8 Indian origin rhesus macaques 2 days post occlusion</i>	415
Figure 93	<i>Variable intensity but similar infarct volume in two separate T2 MRIs</i>	416

Appendix K Supplemental figures referred to in main text

Figure 94	<i>Reduction of MCAO-associated neurological deficit in mice following preconditioning with CpG ODNs</i>	418
Figure 95	<i>Boison Lab</i>	419

LIST OF TABLES

Chapter 1	Introduction	
Table 1	<i>Estimated pace of neural circuitry loss in typical large vessel, supratentorial acute ischemic stroke</i>	8
Table 2	<i>Endogenous Toll-like receptor ligands</i>	27
Table 3	<i>The endogenous roles of Toll-like receptors in cerebral ischemia</i>	37
Table 4	<i>Toll-like receptor ligands precondition against cerebral ischemia</i>	39
Chapter 2	Proof of Concept: Pharmacological preconditioning with a Toll-like receptor agonist protects against cerebrovascular injury in a primate model of stroke	
Table 5	<i>Complete Blood Count Summary</i>	110

Appendix F **Development an *in vitro* prescreening assay for assessing CpG response in non-human primates using peripheral mononuclear blood cells**

Table 6	<i>Response of peripheral blood mononuclear cells from individual non-human primates to CpG ODNs or LPS</i>	315
----------------	---	-----

Appendix G **Comparative assessment of three neurological scales for predicting function recovery between days 2 and 7 post-stroke in a non-human primate model**

Table 7	<i>Elaborated Spetzler neurological scale</i>	322
Table 8	<i>Elaborated Simon neurological scale</i>	324
Table 9	<i>Elaborated Lessov neurological scale</i>	326

Appendix H **Manuscript #4: Changes in spontaneous activity assessed by accelerometry correlate with extent of cerebral ischemia-reperfusion injury in the nonhuman primate**

Table 10 *Activity parameters* 363

Appendix I **Characterization of the peripheral immune response following stroke in a non-human primate model**

Table 11 *Cell surface activation markers used for PBMC population identification* 383

Appendix J **Characterization of the response to cerebral ischemia in Chinese origin rhesus macaques**

Table 12 *Summary of infarct volumes following 2 vessel occlusion in Indian origin animals* 411

LIST OF ABBREVIATIONS

5-Aza-2dC	5-Aza-2' deoxycytidine
5-ITU	5'-Iodotubercidin
8-CPT	8-Cyclo-pentyl theophylline
A ₁ R	Adenosine receptor 1
A _{2A} R	Adenosine receptor 2A
A _{2B} R	Adenosine receptor 2B
A ₃ R	Adenosine receptor 3
AAALAC	Association for the Assessment and Accreditation of Laboratory Animal Care
AAT	Adenosine augmentation therapy
AAV	Adeno-associated virus
ACA	Anterior cerebral artery
ADAC	Adenosine amine congener
<i>Adk</i>	Adenosine kinase gene
Adk-tg	Transgenic mice overexpressing <i>Adk</i> in the brain
ADK	Adenosine kinase

ADK-AS	Antisense orientation of <i>Adk</i>
ADK-L	Long isoform of <i>Adk</i>
ADK-S	Short isoform of <i>Adk</i>
ADK-SS	Sense orientation of <i>Adk</i>
ADO	Adenosine
AMP	5'-adenosine monophosphate
AMPA	2-amino-3-(5-methyl-3-oxo-1,2-oxazol-4-yl)propanoic acid
ANOVA	Analysis of variance
AP	Anterior-posterior
AP-1	Activator protein 1
ATL-146e	4-(3-[6-Amino-9-(5-ethylcarbamoyl-3,4-dihydroxy-tetrahydro-furan-2-yl)-9H-purin-2-yl]-prop-2-ynyl)-cyclohexanecarboxylic acid methyl ester
ATP	Adenosine triphosphate
BBB	Blood brain barrier
<i>Bdnf</i>	Brain derived neurotrophic factor gene
BDNF	Brain derived neurotrophic factor
BHK-AK2	Baby hamster kidney cells lacking <i>Adk</i>

BHK-WT	Wild-type baby hamster kidney cells
BMDC	Bone marrow derived cells
CA1	Cornu ammonis area 1 of the hippocampus
CA3	Cornu ammonis area 3 of the hippocampus
CBF	Cerebral blood flow
CCL5	Chemokine (C-C motif) ligand 5
CHA	N ⁶ -cyclohexyladenosine
CI-IB-MECA	2-chloro-N6-(3-iodobenzyl)adenosine-5'-N-methylcarboxamide
CMV	Cytomegalovirus
CNS	Central nervous system
CPA	N ⁶ -cyclopentyladenosine
CpG	Cytosine-guanine rich deoxyoligonucleotides
CpG ODNs	Unmethylated cytosine-guanine rich DNA Oligonucleotides
CRP	C-reactive protein
CXCL-10	C-X-C motif chemokine 10
DAB	3,3'-diaminobenzidine
DCs	Dendritic cells

DNMT	DNA methyltransferase
DPCPX	1,3-dipropyl-8-cyclopentylxanthine
dsRNA	Double stranded RNA
DV	Dorsal-ventral
EEG	Electroencephalogram
ELISA	Enzyme-linked immunosorbent assay
EMSA	Electrophoretic shift assay
EPSP	Excitatory postsynaptic potential
fb-Adk-def	Transgenic mouse lacking <i>Adk</i> in the forebrain
FDA	Food and Drug Administration
fEPSP	Field excitatory postsynaptic potential
GDNF	Glial-cell line derived neurotrophic factor
GDQ	Gardiquimod
GFP	Green fluorescent protein
GMC-SF	Granulocyte macrophage colony- stimulating factor
HBSS	HEPES-buffered saline solution
HCT	Hematocrit
HCY	Homocysteine

HDAC	Histone deacetylase
HMGB1	High-mobility group protein B1
HSP	Heat shock protein
HSP60	Heat shock protein 60
I κ B	Nuclear factor of κ light polypeptide gene enhancer in B-cells inhibitor
IACUC	Institutional Animal Care and Use Committee
ICAM	Intracellular adhesion molecule
i.c.v.	Intracerebroventricular
IFN	Type-1 interferon
IFN- β	Interferon- β
IFN- γ	Interferon- γ
IHC	Immunohistochemistry
IKK	I κ B kinase
IL-1 α	Interleukin-1 α
IL-1 β	Interleukin-1 β
IL-2	Interleukin-2
IL-6	Interleukin-6
IL-8	Interleukin-8

IL-10	Interleukin-10
IL-12	Interleukin-12
i.p.	Intraperitoneal
IRAK	Interleukin-1 receptor associated kinase
IRF3	Interferon regulatory factor 3
IRF5	Interferon regulatory factor 5
IRF7	Interferon regulatory factor 7
i.v.	Intravenous
JNK	c-Jun N terminal kinase
KA	Kainic acid
LOCF	Last measure observed carried forward
LPS	Lipopolysaccharide
MAPKK	Mitogen-activated protein kinase kinase
MCA	Middle cerebral artery
MCA/ACAO	Middle cerebral and anterior cerebral artery occlusion
MCAO	Middle cerebral artery occlusion
MCP-1	Monocyte chemoattractant protein-1
MeCP2	Methyl CpG binding protein 2
MFI	Mean fluorescence intensity

MIP-1 α	Macrophage inflammatory protein-1 α
ML	Medial-lateral
MR	Magnetic resonance
MRI	Magnetic resonance imaging
mTLE	Mesio-temporal lobe epilepsy
MyD88	Myeloid differentiation primary response gene 88
NECA	Adenosine-5'-N-ethylcarboxamide
NF κ B	Nuclear factor-kappa B
NHP	Non-human primate
NIH	National Institute of Health
NMDA	<i>N</i> -methyl-D-aspartate
ONPRC	Oregon National Primate Research Center
OTS-1	Oligonucleotide transport system-1
PBMC	Peripheral blood mononuclear cell
pDC	Plasmacytoid dendritic cell
PET	Positron emission tomography
pMCAO	Permanent middle cerebral artery occlusion
PTZ	Pentylenetetrazol

RANTES	Chemokine (C-C motif) ligand 5 (CCL5), also known as regulated upon activation, normal T-cell expressed, and secreted
RBC	Red blood cell
RMR	Resting metabolic rate
ROS	Reactive oxygen species
SAH	S-adenosylmethionine hydrolase
SAL	Saline
SAM	S-adenosylmethionine
SD	Standard deviation
SE	Status epilepticus
SEM	Standard error of the mean
SRS	Spontaneous recurrent seizures
ssRNA	Single stranded RNA
STAIR	Stroke Therapeutic Academic Industry Roundtable
T _{reg}	T regulatory cell
TAK1	TGF- β activated kinase 1
TBI	Traumatic brain injury
TIA	Transient ischemic attack

TIR	Toll-interleukin 1 receptor
TIRAP	TIR domain containing adaptor protein
TLE	Temporal lobe epilepsy
TLR	Toll-like receptor
TLR2	Toll-like receptor 2
TLR3	Toll-like receptor 3
TLR4	Toll-like receptor 4
TLR7	Toll-like receptor 7
TLR9	Toll-like receptor 9
tMCAO	Transient middle cerebral artery occlusion
TNF- α	Tumor necrosis factor- α
TNFR	TNF- α receptor
TRAF	TNF receptor associated factor 6
TRAP	Transiently reduced availability of peripheral-blood leukocytes
TRIF	TIR domain containing adaptor inducible IFN- β
TSA	Triclostatin A
TTC	2,3,5-triphenyltetrazolium hydrochloride
VCAM	Vascular cell adhesion molecule

VEGF

Vascular endothelial growth factor

WBC

White blood cell

WT

Wild-type

ACKNOWLEDGEMENTS

First and foremost, I would like to acknowledge my funding sources without whom the work in this thesis would not have been possible, including grants from the NIH (F30 NS070359-01), and OHSU (MMI Departmental T32 training award, UPTEC scholarship).

Next, I would like to thank my mentor, Dr. Detlev Boison, for his willingness to invite me into his laboratory. Detlev has been a fabulous mentor, allowing me to pursue independent work, while always being available to offer guidance and steer me in the right direction. I have so enjoyed working under your tutelage; you have created an amazing lab environment of collaboration where it feels safe to take unique, creative approaches to science. I would also like to thank all of the wonderful members of the Boison lab (**Figure 95**), who make coming to work every day a joyous experience. I am so lucky to be able to consider you all not only colleagues, but friends, and I will miss interacting with you all on a daily basis.

The work in this thesis is not merely the product of my time in the Boison lab, but also a result of the exceptional mentoring I have received throughout my graduate education. Thus, I would like to extend my sincere thanks to Dr. Mary Stenzel-Poore and the members of the Stenzel-Poore lab for their contributions to my scientific development. Many thanks also go to my thesis advisory committee, Dr. Steven Kohama, Dr. Lawrence Sherman, Dr. Buddy Ullman and Dr. Julie Saugstad, who have challenged and supported me throughout this process.

Completing my graduate work would not have been possible without the support of many individuals not involved with my work in the lab. Many deep bows are due to the entire Dharma Rain Zen Center sangha for their continuous support and loving kindness throughout this process. I am so grateful to be part of such an amazing community. Special thanks to my teacher, Gyokuko Carlson, for her patience, guidance and wisdom.

Thank you to my family, for loving and supporting me unconditionally through this often challenging time. Perhaps the hardest part of completing my thesis was not being able to spend more time with all of you. Your love means the world to me.

Finally, I would like to thank my darling Benjamin. You have been so patient, supportive, loving, funny and understanding, throughout this process. It is hard to express just how much you have helped me during graduate school, but I know I would not be in such a wonderful place today if it were not for you. I feel truly blessed to have you as a partner.

ABSTRACT

The brain is exquisitely sensitive to changes in nutrient availability, thus it is selectively vulnerable to the changes in homeostasis which occur in hypoxic, ischemic, or excitotoxic conditions. However, the brain has the ability to make use of several endogenous neuroprotective responses to such conditions. By understanding these innate mechanisms, it is possible to harness the protection conferred by these processes and to elicit them pharmacologically. Stimulating of Toll-like receptors is one means of conferring prophylactic neuroprotection to the brain in anticipation of an ischemic injury, and adenosine augmentation therapy represents an additional means by which endogenous neuroprotective responses can be elicited to reinstate equilibrium following disruption of homeostasis.

The underlying mechanisms governing the induction of neuroprotection are becoming increasingly linked to complex genomic reprogramming. This reprogramming is likely occurring via modification of the epigenetic landscape in the central nervous system (CNS) as well as in the periphery. Exquisitely sensitive and responsive to changes in equilibrium, release of the endogenous molecule adenosine is likely a key player in these epigenetic changes, though other factors are likely at work as well. The studies herein show that surges of adenosine can modify methylation status of DNA in the brain. This action likely extends to histones and other proteins as well. Release of adenosine is a characteristic component of most, if not all, preconditioning paradigms,

and may be crucial for the induction of ischemic or excitotoxic tolerance via epigenetic reprogramming both in the periphery and in the CNS.

Future therapeutics aimed at inducing prophylactic neuroprotection or repair damage following neurological injuries that utilize epigenetic changes will likely revolutionize the field of neuroprotection. Focal adenosine augmentation delivery from biodegradable polymer is an example of one epigenetic neuroprotective therapy that could progress quickly to the clinical setting. Other common pharmacological compound and endogenous molecules are likely to be found to have epigenome-modifying effects, opening the way for their use in numerous neurological disease states.

CHAPTER 1

INTRODUCTION

“Great minds can sometimes guess the truth before they have either the evidence or arguments for it.” –Nicholas Humphrey, theoretical psychologist [1]

1. Neurological injury

In humans, the brain is the largest single consumer of glucose and oxygen of all the organs in the body, accounting for approximately 25% of the resting metabolic rate (RMR) [2]. This is over twice the proportion of energy expenditure of other (non-human) primates, which allocate 8-10% of their RMR to their brains [2], and over five times that of other (non-primate) mammals, which only allocate 3-5% of RMR to their brains [3]. This means the human brain alone utilizes nearly 450 kcal/day or 400 kcal/day for adult males and females, respectively [2]. The protein pumps that maintain the ion gradients in neurons to allow for electrical signaling account for over half of the energy consumption of the brain [4]. The metabolic demands of the human brain arise largely from cost of processing neural information [4], the price of increasing complexity and information processing ability. This increase in brain power has been compensated for by an increase in dietary quality, and a decrease in other tissue types with high metabolic demand, such as intestines and skeletal muscle [2, 5].

Due to its high metabolic demands, and the fact that it does not store glycogen but instead relies exclusively on glucose from the blood, the brain is exquisitely sensitive

to fluctuations in availability of essential nutrients, such as oxygen and glucose (**Figure 1**). Cessation of blood flow to the brain, or cerebral ischemia, can occur due to blockage of an artery or cessation of cardiac function and rapidly leads to irreversible cellular damage of neural tissues [6].

Neurological diseases are highly prevalent and represent a significant proportion of health care cost in the US. The most recent survey by the Center for Disease Control and Prevention ranks cardiovascular disease as the leading cause of death in 2010 in the United States, and cerebrovascular accidents (including stroke) as the fourth leading cause of death in the United States, and a leading cause of life-long disability [7]. Together, these two diseases account for over one third of all US deaths, with the economic burden of treating individuals with these disorders totaling over \$444 billion dollars annually [8]. Epilepsy, another of the US's most common chronic neurological disorders, affects over 2 million people nationwide and represents a health care burden of over \$15.5 billion dollars annually [8]. The brain pathophysiologies of these diseases share some common mechanisms, including hypoxia, ischemia, and excitotoxic cell death. Indeed, cerebral ischemia is a leading cause of acquired epilepsy [9], illustrating the interrelatedness of these diseases. For practical purposes, this introduction will focus primarily on transient cerebral ischemia and reperfusion injury – with mention of other neurological disorders when appropriate. The term “stroke” may be used interchangeably when referring to cerebral ischemia, particularly in a clinical context.

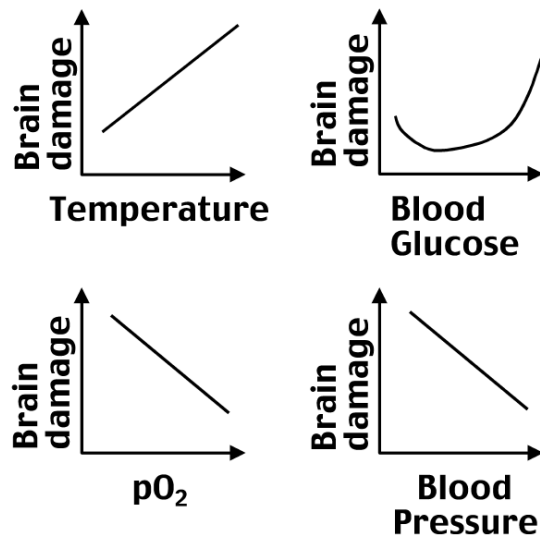


Figure 1. Representative dose-response curves for brain injury

Brain damage decreases with decreasing body temperature (hypothermia). Conversely, brain damage increases with decreasing oxygen and blood pressure. Brain damage increases with very low or very high levels of blood glucose. Adapted from *Annals NY Academy of Science* 939, 2001 [10]. Roland N. Auer, "Non-pharmacologic (physiologic) neuroprotection in the treatment of brain ischemia" pp. 272-282.

1.1. Mechanism of ischemia-induced cell death

To understand how the brain protects itself from ischemic injury, it is pertinent to review how ischemia leads to cell death. Pathophysiological events such as thrombosis, embolism or systemic hypo-perfusion restrict blood flow to the brain. Cellular homeostasis cannot be supported by insufficient oxygen and glucose levels, and multiple cellular processes are thus initiated which lead to cell death, including ion imbalance and excitotoxicity, oxidative stress, inflammation, and apoptosis [11, 12].

During prolonged ischemia, cellular energy, in the form of ATP, is depleted due to lack of substrate. Without adequate ATP to maintain them, neuronal ion channels such as Na^+/K^+ ATPase and Ca^{2+} ATPase are unable to function, leading to ionic imbalance across cellular membranes and increases in cytoplasmic Ca^{2+} concentration. Plasma membrane depolarization results in presynaptic release of the excitatory neurotransmitter glutamate which, when bound to post-synaptic NMDA and AMPA receptors, opens these Ca^{2+} permeable channels [13]. Lack of ATP also reduces synaptic glutamate retrieval by neurons and astrocytes, resulting in sustained stimulation of post-synaptic neurons, causing a cascade of excitotoxic stimulation through adjacent brain regions. Increase in cytoplasmic Ca^{2+} results in Ca^{2+} flow into mitochondria through the Na-Ca uniporter [14]. As the mitochondrial matrix is depolarized, oxidative phosphorylation is impaired, leading to further ATP depletion [15]. The ionic imbalance

leads to swelling of the mitochondria, membrane rupture, and release of pro-apoptotic proteins and mitochondrial Ca^{2+} stores [16-18]. Calcium overload, activating many if not all calcium dependent proteases, lipases and DNAses [19], causes cells in the ischemic core to die from simple catabolism.

High levels of intracellular Ca^{2+} , Na^{2+} and ADP cause mitochondria to produce harmful levels of reactive oxygen species (ROS). The brain is especially vulnerable to ROS as neurons have relatively low levels of endogenous antioxidants [20] and are thus highly susceptible to the destruction of cellular macromolecules by oxidative damage [21, 22]. Further, reperfusion brings reoxygenation, and with it an excessive amount of substrate for oxidation reactions, causing a surge in the production of reactive molecules such as superoxide, NO and peroxynitrate. In addition to their destructive effects on cellular mitochondria, DNA, proteins and lipids, these radicals activate matrix metalloproteases, which degrade collagen and laminins in the basal lamina, disrupting vascular wall integrity and increasing blood-brain barrier permeability. Together this can lead to parenchymal hemorrhage and vasogenic brain edema.

Oxidative stress also triggers the activation of resident inflammatory cells in the brain, namely microglia and astrocytes. Once activated, these cells release cytokines and chemokines, which aid in leukocyte migration and accumulation into ischemic brain tissue. Production of IL-1 is increased after permanent or transient cerebral ischemia in microglia, astrocytes, and neurons. IL-1 causes up-regulation of the adhesion molecules E-selectin, ICAM-1, ICAM-2, and VCAM-1 on cerebral endothelial cells thereby aiding neutrophil infiltration [23, 24]. Production of $\text{TNF-}\alpha$ is also

increased after ischemia, and has been observed in the same cell types as IL-1. Like IL-1, TNF- α induces adhesion molecule expression in cerebral endothelial cells and promotes neutrophil accumulation and transmigration. TNF- α can also lead directly to apoptotic cell death by activation of the death domain in its receptors (TNFR-1 and TNFR-2), which leads to caspase activation. Importantly, inhibition of either IL-1 β or TNF- α protects the brain from injury [24].

Stroke-induced cytokine activation of the cerebral endothelium is accompanied by chemokine recruitment of inflammatory cells to the brain. Monocyte chemoattractant protein-1 (MCP-1 α) and macrophage inflammatory protein-1 (MIP-1 α) are both increased after focal ischemia. Consistent with a deleterious role for these chemokines, inhibition of either reduces cerebral ischemic injury [25]. Neutrophils are generally the first leukocyte subtype to penetrate into the ischemic brain, followed by macrophage and lymphocytes [26, 27]. Neutrophils potentiate tissue damage and cell death by releasing oxygen free radicals and proteolytic enzymes. Lymphocytes, too, have strong proinflammatory and tissue-damaging properties. Together, infiltrating inflammatory cells cause secondary damage to potentially salvageable tissue surrounding the ischemic core.

As mentioned previously, when the brain is deprived of nutrients, cell death occurs rapidly. Rough calculations done to quantify the rate of cell death in large vessel supratentorial stroke, the most common ischemic stroke subtype estimate a loss of 1.9 million neurons per minute (**Table 1**) [6]. Thus, therapies that can halt neurological damage as soon as it occurs, or ideally, to prevent damage before it occurs, are a major

focus of current therapeutic neuroscience research. Not surprisingly, humans have long been interested in finding ways to protect the brain from injury; this interest in self preservation has given rise to the field of neuroprotection.

Table 1. *Estimated pace of neural circuitry loss in typical large vessel, supratentorial acute ischemic stroke*

	Neurons Lost	Synapses Lost	Myelinated Fibers Lost
Per Stroke	1.2 billion	8.3 trillion	7140 km / 4470 miles
Per Hour	120 million	830 billion	714 km / 447 miles
Per Minute	1.9 million	14 billion	12 km / 7.5 miles
Per Second	32,000	230 million	200 meters / 218 yards

Modified from *Stroke* (37), 2005 [6]. Jeffery L. Saver, “Time is brain – quantified” pp. 263-266.

1.2. A brief history of therapeutic neuroprotection

Neuroprotection is defined as any therapeutic modality that prevents, retards or reverses neuronal death from primary neuronal lesions [28]. This definition can be expanded to include preservation of other essential brain components, such as astrocytes, microglia and oligodendrocytes, and can be applied to the central as well as peripheral nervous system. When designing a neuroprotective strategy for ameliorating damage due to a lack of delivery of blood and/or oxygen, as is the case in cerebral ischemia, two simplified general approaches immediately come to mind: augmenting

nutrient delivery to starving tissue, or decreasing nutrient demand in the tissue. The first approach, augmenting blood flow and/or oxygen and glucose delivery to the starving brain, occurs rapidly via endogenous mechanisms originating in the autonomic nervous system [29]. This autonomic neuroprotective mechanism involving differential excitation of sympathetic neurons throughout the body is exemplified by the 'diving' or 'oxygen conserving' reflex initiated when a vertebrate bird or mammal is submerged in water [30, 31]. Mediated by excitation of oxygen-sensitive neurons in the rostral ventrolateral medulla oblongata (RVLM), this reflex decreases in blood flow to the muscles, gut and kidney via sympathetic afferents, and increases blood flow to the heart and cerebral circulation via vasodilation and bradycardia [32]. The second approach, to decrease the metabolic demands of the brain, can also be found to occur endogenously in certain mammals, in the form of hibernation.

1.3. Hibernation as an endogenous neuroprotective phenomenon

The idea that the brain has developed endogenous mechanisms to protect itself from injury during periods of low blood flow may appear novel at the outset, but is not surprising when considering that the mammalian brain has successfully adapted to this condition as part of a natural behavior: hibernation. During hibernation, animals enter a unique physiological state of reduced energy consumption, thought to be beneficial for survival during periods of food shortage combined with periods of extremely low

ambient temperature which would normally have a high associated energy cost [33, 34]. Hibernation is characterized by extended bouts of torpor that can last for days to weeks, interrupted periodically by arousal last from 12-24 hours [35, 36]. During hibernation, animals undergo dramatic drops in body temperature, oxygen consumption and heart rate, but suffer no damage due to cerebral hypoxia/ischemia [33, 37-40]. Further, heterothermic animals have been found to be more resistant to ischemic injury even out of hibernation than euthermic animals [41].

Studies using arctic ground squirrels show that these animals undergo a dramatic drop in cerebral blood flow (CBF) during hibernation [37]. This drop in blood flow is associated with decreased respiratory rate as well as decreased electrographic activity in the brain, but is not associated with hypoxic damage even in neuronal population that are normally highly sensitive to hypoxic/ischemic damage, such as those in the hippocampal CA1 region [37]. Similarly, acute hippocampal slices taken from hibernating squirrels are tolerant to hypoxic and aglycemic conditions *in vitro* [42]. Elucidation of the endogenous mechanisms used by the hibernating brain has consequently become an area of focus in neuroprotection.

The hibernating brain is metabolically depressed, significantly decreasing nutrient demand on the tissue and cellular levels. Some of the ways the brain appears to suppress metabolism during hibernation include decreased activity of ion channels [43-45], arrest of protein synthesis [42], and dendritic remodeling [46]. There is an accompanying increase in resistance to antioxidant stress: levels of ascorbate (Vitamin

C) are increased in the serum and cerebrospinal fluid (CSF) [40, 47, 48], and there is increased superoxide dismutase (SOD), particularly in brown fat where mitochondrial transport chain is uncoupled for thermogenesis [49-51]. During hibernation the brain is also protected by systemic changes including hypocoagulation [52-54] and immune suppression [55-57]. Perhaps the most observable trait of hibernating animals is their profoundly reduced body temperature [35, 36]. Hypothermia alone confers some level of neuroprotection via metabolic suppression [58-62] among other mechanisms and was one of the first neuroprotective therapies to be actively research for clinical use.

1.4. Early attempts at neuroprotection in clinical medicine

Some of the earliest investigations into neuroprotection were carried out by ancient Egyptian, Greek and Roman physicians, who used various forms of hypothermia to treat head injury [63-65]. The Edwin Smith papyrus, a fragment of a larger treatise on the surgical treatment of injuries beginning with the head, is the first text to describe the cranial architecture, the meninges, cerebral spinal fluid, pulsation of the brain and paralysis (**Figure 2**) [66-68]. Dated 1500 BCE, the Edwin Smith papyrus is thought by some to have been originally authored by Imhotep in 3000-2500 BCE [66, 67]. The text offers a number of case studies of head injuries, including diagnosis and treatment, which often included application of cold, heat, fresh meat or honey and grease [66, 67]. The ancient Greeks also studied head injuries, and Hippocrates authored many treatises

focused on treating such wounds [69]. In addition to advocating trepanation in the treatment of head injuries to relieve intracranial pressure, Hippocrates also recommended the use of ice to slow blood loss [69-71].

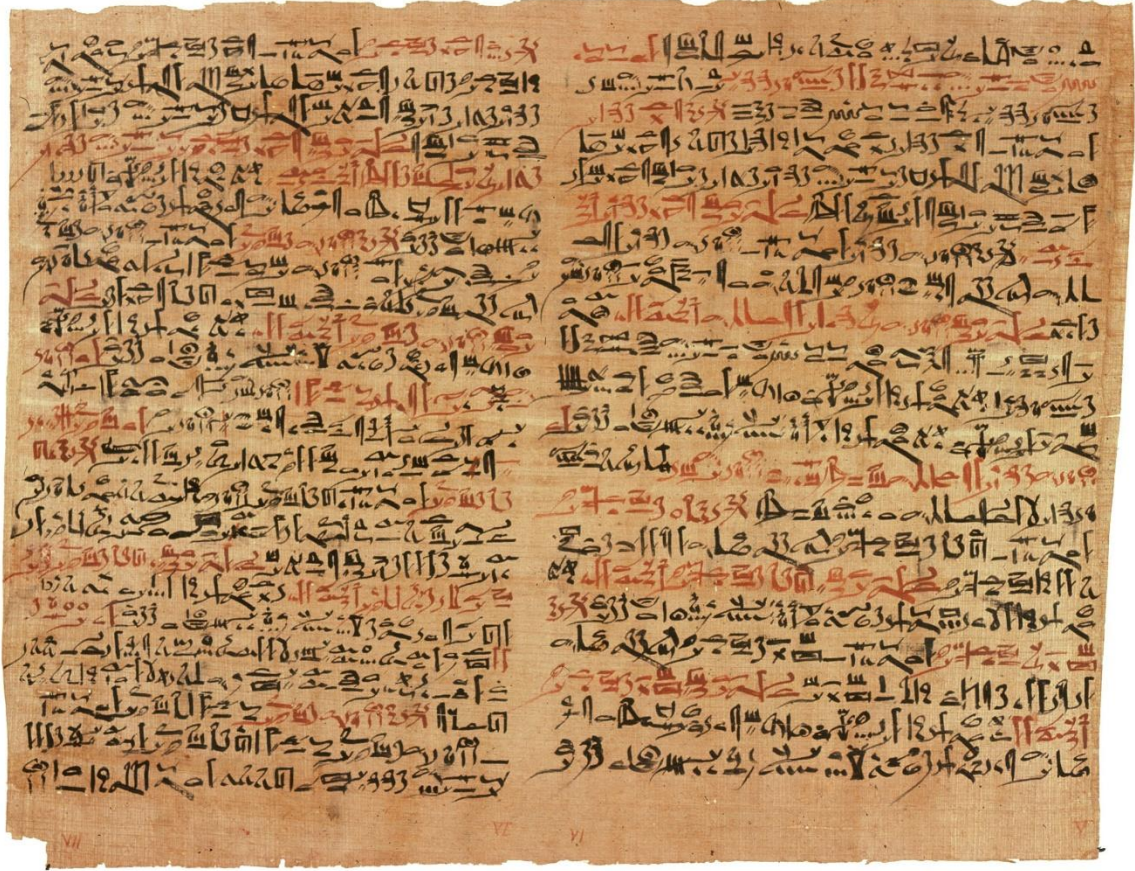


Figure 2. Image of a page from the Edwin Smith papyrus dated 1500 BCE

The Edwin Smith papyrus from ancient Egypt is the earliest written medical text documenting the diagnosis and treatment of head injuries. Though the papyrus itself is dated to 1500 BCE, it is believed to have been originally authored by Imhotep in 3000-2500 BCE. Edwin Smith Papyrus Plate V and VI, Photograph © 2004 The Metropolitan Museum of Art.

The first modern attempts at neuroprotection also utilized hypothermia [72, 73], spurred largely in the 1930's and 40's by reports documenting successful resuscitation of drowning victims who were hypothermic, even after prolonged asphyxia [74]. In 1943 Dr. Temple Fay published his positive findings on the use of full body hypothermia to treat traumatic brain injury (**Figure 3**) [73]. Dr. Fay went on to further refine the hypothermic technique for local application (**Figure 4**) [72], a technique that continues to be utilized to a limited degree in a refined form in some neurological intensive care units. Indeed, for every 10°C decrease in temperature, cerebral oxygen uptake decreases by 50% [75-77]. Induction of hypothermia for neuroprotective purposes continued to be actively researched and used in the context of neurological and open heart surgery [78-80]. Studies in the late 1950's and early 60's shows benefit from moderate hypothermia during and after brain ischemia and traumatic brain injury (TBI) in dogs [81, 82]. These promising results were followed up with humans studies [83, 84], but these early attempts at hypothermia were abandoned due to difficulties in clinical management and side effects [83, 85].

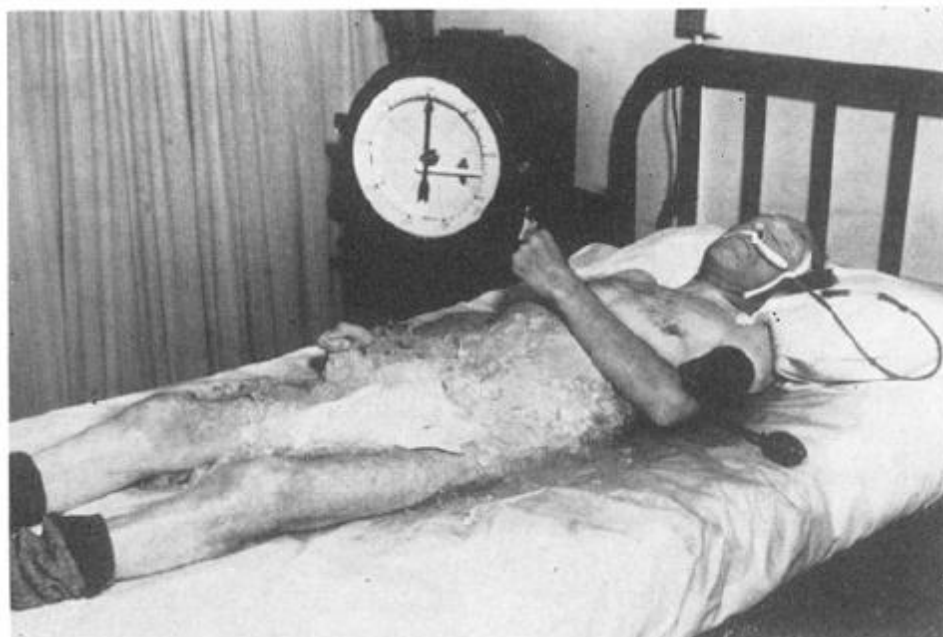


Figure 3. *Early application of systemic hypothermia to treat cerebral injury*

Example of an early clinical application of hypothermia to treat neurological injury. Patient's body temperature was continuously measured with a rectal thermocouple (89.5°F). Patient was anesthetized with Sodium Amytal, choral hydrate and paraldehyde. Patient was cooled with ice on a mattress due to objections from the nurses to total submersion in an ice bath. It is noted in the original paper that "this patient (a physician) insisted upon keeping socks on". Later attempts at fully body cooling were facilitated by the development of blankets that circulated chilled solutions and could cover the entire patient, including the head. Reprinted with modifications from the *Journal of Neurosurgery* (16), 1959 [72]. Temple Fay "Early experiences with local and general refrigeration of the human brain" pp. 239-260.



Figure 4. *Early approach to local hypothermia in the brain*

Intracranial refrigeration applied in a patient with a brain abscess and diffuse cerebritis. Sterile refrigerated boric acid and Dakin's solution were used alternately to irrigate the intracranial area using gravity to maintain flow. The technique was reportedly "extremely well tolerated and [the] clinical results were very satisfactory". Reprinted with modifications from the *Journal of Neurosurgery* (16), 1959 [72]. Temple Fay "Early experiences with local and general refrigeration of the human brain" pp. 239-260.

1.5. Beyond hypothermia – the evolution of neuroprotection

Other early published attempts at neuroprotection included the use of barbiturates and anesthetics to mimic the decreased metabolic effects seen in hypothermia [58-62], which were thought to be the cause of neuroprotection. As the field of neuroprotection began to grow, research was undertaken to understand the mechanisms underlying the neuroprotective phenomenon. In 1954, Hegnaeur and D'Arnato showed that hypothermia decreased oxygen demand in dogs [86], linking decreased metabolic demand to neuroprotection. Further work in the 60's applied the concept of perfusion disturbance to neuronal injury in ischemia [87], an idea adopted from myocardial research. The idea of the penumbra, ischemic but still viable tissue lying outside the core of an infarcted area, was proposed in 1976, along with the concept of differential susceptibility to ischemia by brain region [88].

In the late 1970's, Steen and Michenfelder suggested that the protective effects of barbiturates and anesthetics were occurring through additional mechanisms besides their metabolic depressive effects [89, 90]. Interest in identifying additional pharmacological agents that could induce neuroprotection intensified during the early 1980's. The role of excitatory neurotransmitters such as glutamate and aspartate in ischemic cell death also became an area of focus in the field of neuroprotection [91-93]. Selective excitatory amino acid receptor antagonists, particularly those for the NMDA

receptor subtypes, were one novel class of drugs shown to be protective in the context of ischemia and anoxia *in vivo* [94-96].

1.6. Neuroprotection via ischemic preconditioning

Coinciding with work on hypothermia, in the 1960's researchers in the field of neuroprotection discovered, but did not capitalize on, the phenomenon of cerebral ischemic tolerance [97]. Ischemic tolerance is a phenomenon whereby the brain can be preconditioned to be resistant to an otherwise damaging event (e.g. a prolonged period of ischemia) by a prior exposure to a non-damaging stimulus (e.g. a brief period of ischemia). The first experiment published on this phenomenon demonstrated the increased glycolytic capacity of the rat brain following exposure of brief anoxia, and the increased the survival time of these pre-exposed animals to subsequent prolonged anoxia [97]. Unfortunately, the field of ischemic preconditioning was largely silent until the publication of a seminal paper in 1986, when Murry and colleagues showed that following exposure to four 5 minute periods of coronary occlusion, the myocardium in dogs had significantly reduced damage when exposed to a 40 minute coronary occlusion **(Figure 5)** [98].

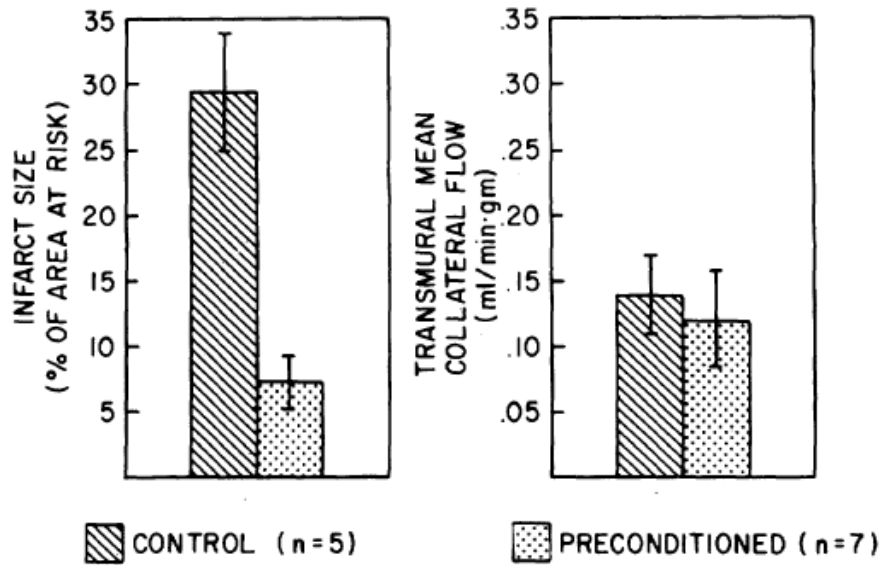


Figure 5. *Decreased myocardial infarct following preconditioning ischemia*

Dogs exposed to four 5 minute periods of preconditioning ischemia have significantly smaller infarct volumes following a subsequent 40 minutes of cerebral ischemia than dogs not exposed to preconditioning ischemia. Collateral blood flow to the ischemic tissue was not significantly different between the two groups, indicating that increased blood flow to the area was not the mechanism of protection. Adapted from *Circulation* (74) 1986 [98]. Charles E. Murry, Robert B. Jennings and Keith A. Reimer, "Preconditioning with ischemia: a delay of lethal cell injury in ischemic myocardium," pp. 1124-1136.

The pace of ischemic preconditioning research continued to accelerate in cardiology [99, 100], but it wasn't until 1990 that ischemic preconditioning was reported in cerebral tissue [101]. In their landmark paper Kitagawa *et al* [101] documented protection of normally vulnerable neurons in the hippocampal CA1 region following bilateral carotid artery occlusion when preceded by one or two minutes of transient carotid artery occlusion. Kitagawa *et al* went on to document this phenomenon in various regions of the brain, and coined the term 'ischemic tolerance' [101, 102]. Interestingly, this same group recognized the significance of an earlier discovery reported by another lab [103]: that hyperthermia could precondition against ischemic injury. Kitagawa *et al* went on to reproduce this result [104], pioneering research in cross-tolerance – tolerance to a noxious insult that can be elicited by a non-identical preconditioning stimulus. In a separate paper from the following year it was observed that “cells exposed to various types of stress acquire resistance or tolerance to subsequent lethal insults” [105]. Indeed, preconditioning appears to be a universal phenomenon, occurring across species, organ systems and tissue types.

Research into the mechanism behind preconditioning began expanding from simply looking at reduction in metabolic demand to encompass the molecular signaling pathways that were elicited following preconditioning stimuli. Discovery of the production of heat shock proteins (HSPs) as an endogenous response to various forms of stress [106-110] made them early candidates for mediating ischemic tolerance [105, 106, 111]. Prior to their discovery in ischemic tolerance, HSPs were being investigated for their role in mediating thermal tolerance, or the ability of cells to withstand an

otherwise lethal heat exposure following brief exposure to a non-lethal heat treatment [112, 113]. However, other mediators of damage in cerebral ischemia had been identified and were viewed as potential targets for neuroprotection, including excitotoxins [114], calcium [115], free radicals [116], leukocytes [117], and eicosanoids [118, 119].

1.7. Cross tolerance – towards a unifying theory of preconditioning

As research into cross-tolerance progressed, multiple stimuli were shown to confer tolerance to cerebral ischemia: global cerebral ischemia [101], focal cerebral ischemia [120], hyperbaric oxygen [121], cortical spreading depression [122], hyperthermia [103], hypothermia [123], cerebellar stimulation [124], metabolic inhibition [125], and inflammation [126, 127]. Preconditioning was also recognized to occur with two distinct temporal profiles (**Figure 6**): rapid preconditioning, which occurred within a matter of minutes [128, 129], and delayed preconditioning, which took hours or days to develop and generally involved *de novo* protein synthesis [130]. Interestingly, most stimuli can elicit both types of preconditioning. However, the window of effectiveness differs greatly between the two paradigms. Just as it is quickly initiated, protection from rapid preconditioning only lasts on the order of hours, while delayed preconditioning can last for several days [131]. Generally, delayed preconditioning requires 24 to 48 hours to establish the tolerant phenotype, tolerance is

at its maximum at 72 hours after the preconditioning stimulus, and tolerance decreases over the course of one week (**Figure 7**).

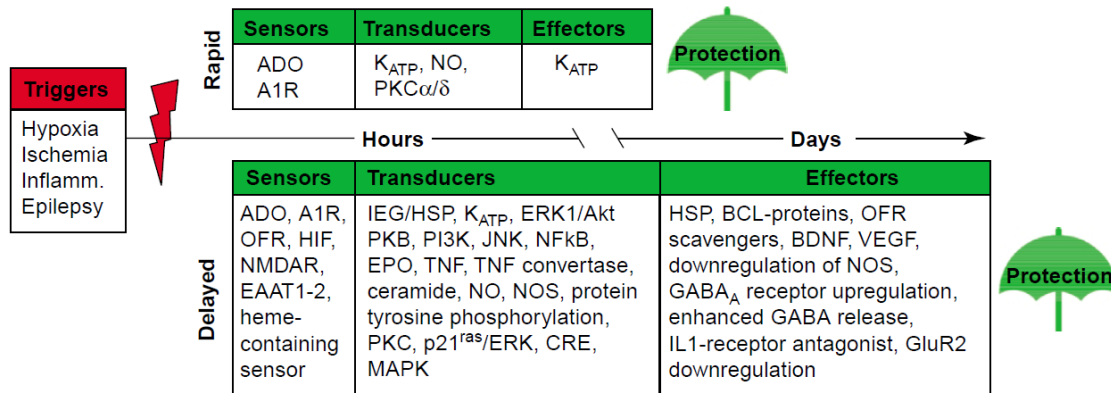


Figure 6. Schematic overview of rapid and delayed ischemic preconditioning

Abbreviations: A1R, adenosine receptor type 1; ADO, adenosine; Akt, a serine/threonine kinase family; BDNF, brain derived neurotrophic factor; CRE, cAMP-response element; EAAT, excitatory amino acid transporter; EPO, erythropoietin; ERK, extracellular signal-regulated kinase, GluR2, glutamate-receptor subunit 2; HIF, hypoxia inducible factor; HSP, heat shock protein; IEG, immediate early gene; IL-1, interleukin-1; Inflamm, inflammation; JNK, c-Jun N terminal kinase, K_{ATP}, ATP sensitive K⁺ channel; MAPK, mitogen-activated protein kinase; NF κ B, nuclear factor κ B; NGF, nerve growth factor; NMDAR, NMDA receptor; NO, nitric oxide; NOS, nitric oxide synthase; ORF, oxygen free radical; PI3K, phosphoinositide-3 kinase, PKB, protein kinase B, PKC, protein kinase C; TNF, tumor necrosis factor; VEGF, vascular-endothelial growth factor. Adapted from *TRENDS in Neurosciences* (26)5, 2003 [131]. Ulrich Dirnagl, Roger P. Simon and John M. Hallenbeck, "Ischemic tolerance and endogenous neuroprotection," pp. 248-254.

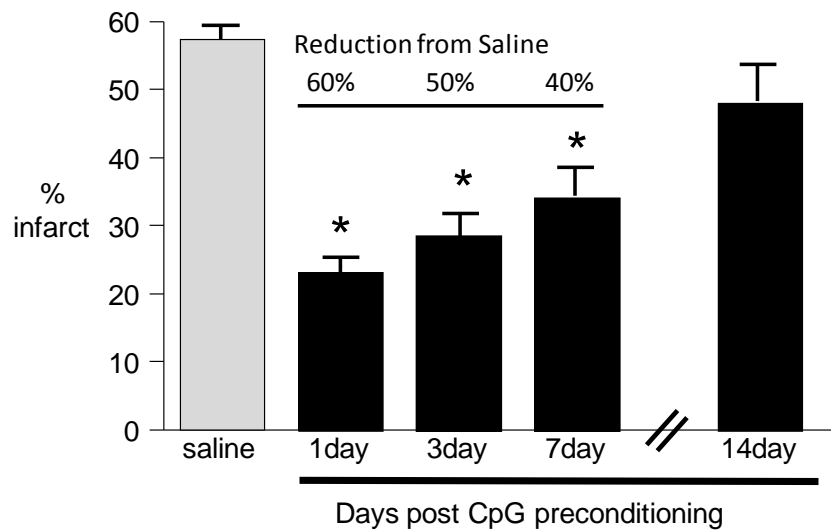


Figure 7. Time course of delayed preconditioning

Delayed preconditioning induced with the Toll-like receptor 9 agonist CpG. A single intraperitoneal injection of 20µg CpG ODN 1826 was given to adult male C57Bl/6 mice prior to 60 minute transient middle cerebral artery occlusion. Indirect infarct volume was assessed after 24 hours of reperfusion via TTC staining. Value are group means ± SEM. * indicates p < 0.05 comparison to saline controls.

Recent work has shown that to induce a state of delayed tolerance, a reprogramming of the genomic response to injury is required (**Figures 8 and 9**) [130, 132]. This finding was made, in part, by directly comparing the genomic response following ischemic preconditioning to the genomic response to preconditioning via an inflammatory stimulus, specifically Lipopolysaccharide (LPS, also referred to as bacterial endotoxin) [132]. LPS was first used as the prototypic stimulus for eliciting a robust inflammatory response. LPS is sensed by the innate immune system, resulting in the release of a cascade of inflammatory cytokines. Systemic application of LPS confers protection to ischemia in kidney [133] and heart [134] as well as brain. Interestingly, advances in the understanding of innate immunology, specifically the discovery of mammalian analogues of the Toll-like receptor family of proteins [135], coincided with the growth of the field of preconditioning, offering a unique insight into a potential unifying mechanism of preconditioning.

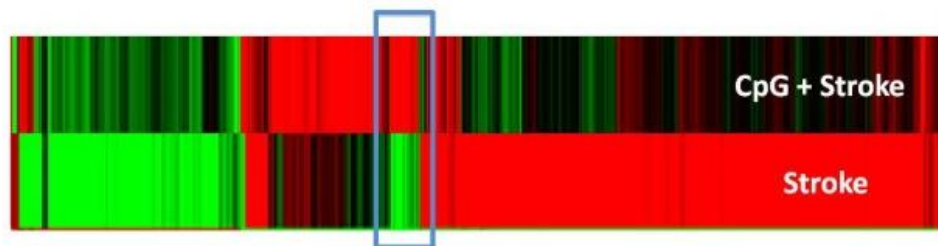


Figure 8. *Representative heat map generated from microarray data following stroke in CpG-preconditioned and saline-treated animals*

Upregulated genes compared to non-stroked controls are red, while down regulated genes are green. Non-regulated genes are black. The boxed region encompasses erythropoiesis-related transcripts that are upregulated following stroke only in CpG-preconditioned animals, not in vehicle-treated controls.

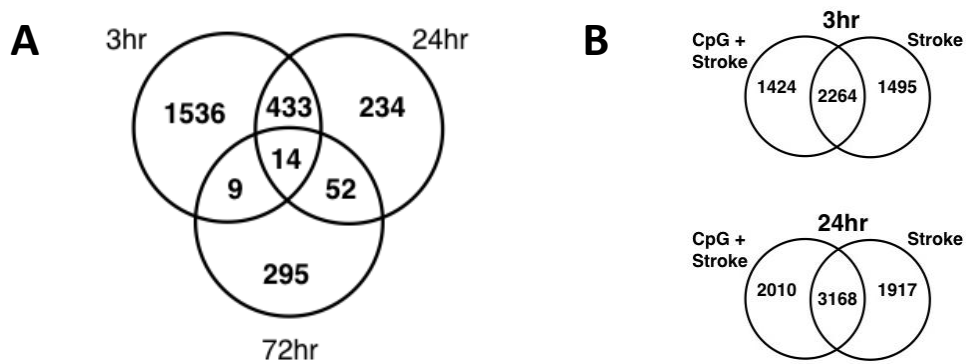


Figure 9. *Genomic alterations in the blood following CpG preconditioning*

(A) Venn diagrams showing the number of transcripts regulated at 3, 24 and 72hr post systemic CpG administration (i.p. 0.8mg/kg). Criteria for regulation: fdr adjusted $p < 0.05$ and ≥ 2 fold regulation compared to non-treated mice. **(B)** Venn diagrams showing the number of transcripts regulated at 3 and 24 hr post MCAO in mice preconditioned with CpG compared to stroke alone. Criteria for regulation: fdr adjusted $p < 0.05$ and ≥ 2 fold regulation compared to non-stroked mice.

2. The role of Toll-like receptors in neuroprotection

2.1. An Introduction to Toll-like Receptors

The Toll-like receptors (TLRs), so-called because of their homology to the *Drosophila* Toll receptor, were first characterized in mammals by their ability to recognize pathogen-associated molecular patterns such as those found in the bacterial cell wall components peptidoglycan (TLR2) and lipopolysaccharide (LPS) (TLR4), as well as viral dsRNA (TLR3), ssRNA (TLR7), and nonmethylated cytosine-guanine (CpG) DNA (TLR9). Recently it has been found that in addition to their role in pathogen detection and defense, TLRs act as sentinels of tissue damage and mediate inflammatory responses to aseptic tissue injury. Host-endogenous molecules associated with damaged cells and tissues have also been shown to activate TLRs (**Table 2**). Surfactant, HSP60, components of the extracellular matrix, and fibrinogen have all been shown to activate TLR4, while host HMGB1, as well as host mRNA and DNA are endogenous ligands of TLR2 (and TLR4), TLR3 and TLR9, respectively.

TLRs, upon activation by either pathogen- or host-derived ligands, induce downstream signals that lead to cytokine and chemokine production and thereby initiate inflammatory responses. TLRs are located on antigen presenting cells such as B cells, dendritic cells, monocytes/ macrophages and microglia. In addition, these

Table 2. Endogenous Toll-like receptor ligands

TLRs	Endogenous Ligand	Ligand Source	Response	Reference
TLR 2 and 4	Hsp60	Necrotic cells	TNF- α and NO in macrophages	Ohashi K, et al. J Immunol. 2000; 164(2): 558-61. Vabulas RM, et al. J Biol Chem. 2001; 276(33): 31332-9.
	Hsp70	Necrotic cells	IL-12 and ELAM-1 (endothelial cell-leukocyte adhesion molecule-1) in macrophages	Asea A, et al. J Biol Chem. 2002; 277(17): 15028-34. Vabulas RM, et al. J Biol Chem. 2002; 277(17): 15107-12.
	gp96	Necrotic cells	IL-12 in DCs	Vabulas RM, et al. J Biol Chem. 2002; 277(23): 2084-53.
	High mobility group box 1 (HMGB1)	Released from nucleus in inflammation	Lethality in sepsis reperfusion injury	Parks JS, et al. J Biol Chem. 2004; 279(9): 7370-7.
	Urate crystal	Deposition in joints and bursal tissues in gout	TNF- α , IL-1 β , TGF- β 1 in macrophages	Liu-Bryan R, et al. Arthritis Rheum. 2005; 52(9): 2934-46.
	Biglycan	Released from ECM	TNF- α , MIP in macrophages/DCs	Schaefer L, et al. J Clin Invest. 2005; 115(8): 2223-33.
	Hyaluronan	Degraded from larger species in ECM	Chemokine production in macrophages, activation of DCs via TLR4	Jiang D, et al. Nat Med. 2005; 11(11): 1173-9. Termeer C, et al. J Exp Med. 2002; 195(1): 99-111.
TLR 4	Hsp22 (HspB8)	Synovial fluid in rheumatoid arthritis	IL-6, TNF- α , upregulation of co-stimulatory molecules in DCs	Roelofs MF, et al. J Immunol. 2006; 176(11): 7021-7.
	Fibronectin extradomain A	Tissue damage	MMP-9 in human macrophages	Okamura Y, et al. J Biol Chem. 2001; 276(13): 10229-33.
	Surfactant protein-A	Lung surfactant	TNF- α and IL-10 in macrophages	Guillot L, et al. J Immunol. 2002; 168(12): 5989-92.
	Fibrinogen	Extravated from vasculature in response to endothelial cell retraction	Chemokine production in macrophages	Smiley ST, et al. J Immunol. 2001; 167(5): 2887-94.
	Heparin sulfate	Released from ECM, cell membranes	Maturation and up-regulation of co-stimulator molecules in DCs	Johnson GB, et al. J Immunol. 2002; 168(10): 5233-9.
	Beta-defensin 2-fusion protein (rmDF-2/rfv)	Epithelial antibacterial peptides	Maturation and up-regulation of co-stimulator molecules in DCs	Birgyn A, et al. Science. 2002; 298(5595): 1025-9.
	Mimimally modified (oxidized) low density lipoprotein	Pro-inflammatory and pro-atherogenic protein	Actin polymerization and spreading of macrophages	Miller Y1, et al. J Biol Chem. 2003; 278(3): 1561-8.
	Pancreatic elastase	Pancreatic elastase	TNF- α secretion in THP-1 cells	Hietaranta A, et al. Biochem Biophys Res Commun. 2004; 323(1): 192-6.
	Alpha-A crystallin	<i>Necrotic cells</i>	Activation of DCs	Roelofs MF, et al. J Immunol. 2006; 176(11): 7021-7.
TLR 7	RNA immune complex	<i>Necrotic cells</i>	IFN- α production by PDCs	Barrat FJ, et al. J Exp Med. 2005; 202(8): 1131-9.
TLR 7 and 8	siRNAs* when encapsulated into liposomes	<i>Necrotic cells</i>	Induction of TNF- α and IL-6 in PBMCs	Sioud M. J Mol Biol. 2005; 348(5): 1079-90.
TLR 9	Chromatin immune complex	<i>Necrotic cells</i>	DC activation	Boule MW, et al. J Exp Med. 2004; 199(12): 1631-40.
	DNA immune complex	<i>Necrotic cells</i>	IFN- α production by PDCs	Barrat FJ, et al. J Exp Med. 2005; 202(8): 1131-9.
TLR 3	mRNA* when complexed with lipofectin	<i>Necrotic cells</i>	Activation and TNF- α production by human DCs	Kariko K, et al. J Biol Chem. 2004; 279(13): 12542-50.

Adapted from *Neuroscience* 158(3) 2009 [136]. Brenda J. Marsh, Rebecca L. Williams-Karnesky and Mary P. Stenzel-Poore, "Toll-like receptor signaling in endogenous neuroprotection and stroke," pp. 1007-20.

receptors can be expressed by the cerebral endothelium and by cells within the brain parenchyma such as astrocytes, oligodendrocytes, and neurons [137-140].

2.2. Toll-like receptors signaling pathways

The TLRs signal through common intracellular pathways, which ultimately lead to transcription factor activation, and the subsequent generation of cytokines and chemokines (**Figure 10**) [141, 142]. Each TLR family member, with the exception of TLR3, initiates intracellular signaling via recruitment of the intracellular Toll-interleukin 1 receptor (TIR)-domain-containing adaptor myeloid differentiation primary response gene 88 (MyD88). When recruited to plasma membrane-associated TLRs, either directly (TLRs 5 and 11) or via the TIR domain containing adaptor protein (TIRAP) adaptor (TLRs 1, 2, 4, 6), MyD88 enlists members of the interleukin-1 receptor associated kinase (IRAK) family, including IRAK1, IRAK2, and IRAK4, to begin a process of auto- and cross-phosphorylation among the IRAK molecules. Once phosphorylated, IRAKs dissociate from MyD88 and bind TNF receptor associated factor 6 (TRAF6), an E3 ligase. TRAF6 in turn activates TGF- β activated kinase 1 (TAK1) which itself activates the I κ B kinase (IKK) complex and mitogen-activated protein kinase kinases (MAPKKs). The IKK complex, composed of IKK α , IKK β and the regulatory subunit IKK γ /NEMO, phosphorylates I κ B proteins. This phosphorylation is necessary for the ubiquitination and proteosomal degradation of I κ Bs and the subsequent nuclear translocation of the transcription factor

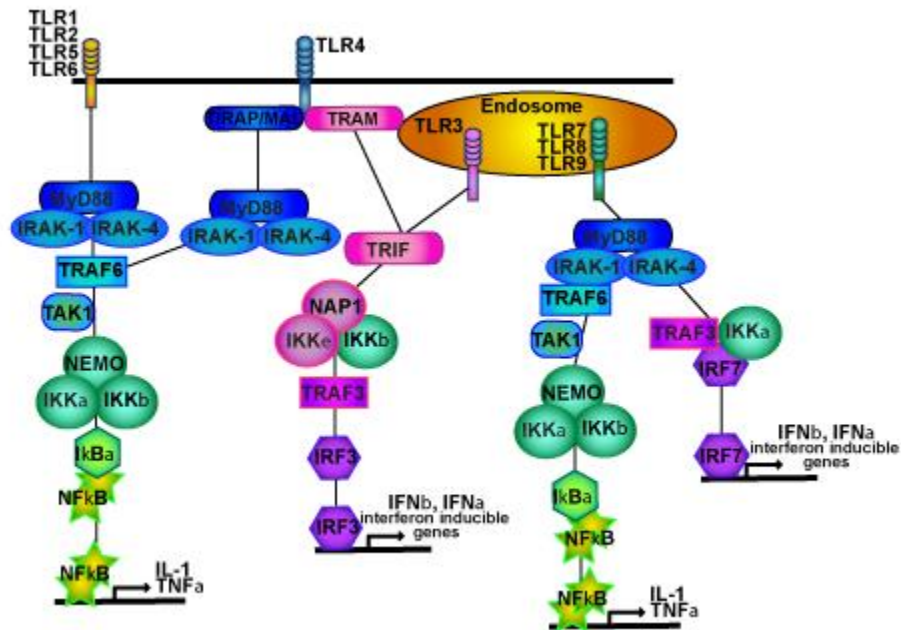


Figure 10. Toll-like receptor signaling pathways

TLRs signal through three primary pathways: an NFκB-inducing pathway, an AP-1-inducing pathway, and an IRF-inducing pathway. Cross-talk between these pathways allows for specific responses to a diverse array of pathogen- and host-associated molecules. Adapted from *Neuroscience* (158) 2009 [136]. Brenda J. Marsh, Rebecca L. Williams-Karnesky and Mary P. Stenzel-Poore, "Toll-like receptor signaling in endogenous neuroprotection and stroke," pp. 1007-1020.

NFκB. Members of the MAPK family phosphorylate and activate components of the transcription factor activator protein 1 (AP-1). Together, these transcription factors induce inflammatory cytokine production (e.g. TNF-α, IL-1).

MyD88 is also recruited to the endosomal receptors TLR7 and TLR9 again enlisting members of the IRAK family. Due to the endosomal location of the complex, the phosphorylated IRAKs are able to bind TRAF3 in addition to TRAF6. Activation of TRAF3 leads to phosphorylation, dimerization, and nuclear localization of the transcription factors IRF3, IRF5, and IRF7 with resultant Type I interferon (IFN) production. Hence these endosomal TLRs are capable of signaling to NFκB, AP-1 and IRFs, resulting in a diverse genomic response.

Endosomal TLR3 is unique among the TLRs because it does not signal through MyD88 but signals instead via recruitment of the TIR domain-containing adaptor inducing IFNβ (TRIF). TRIF enlists the noncanonical IKKs, TBK1 and IKKε, which activate IRF3. Further, TRIF recruits TRAF6 and RIP-1, which results in activation of MAPK and IKKα/β. Hence TLR3, like the other endosomal receptors, is capable of activating NFκB, AP-1 and IRFs. Of all the TLRs, only TLR4 can recruit either MyD88 (via TIRAP) or TRIF (via TRAM) and can thus induce either the pro-inflammatory cytokines TNF-α and IL1 via NFκB or the anti-viral IFNβ via IRF3.

2.3. Toll-like receptor expression

The complement of TLR family members expressed by a cell depends on its identity and its activation status. Constitutive expression of TLRs within the brain occurs in microglia and astrocytes and is largely restricted to the circumventricular organs and meninges—areas with direct access to the circulation [143-145]. Human and murine microglia express TLRs 1-9 and generate cytokine profiles specifically tailored by the TLR stimulated [137, 139, 146]. Similarly, human and murine astrocytes express multiple TLRs, with particularly prominent TLR3 expression [137, 139, 140, 147, 148]. Microglia and astrocytes respond differently to specific TLR engagement reflective of their distinct roles in the brain. Microglia initiate robust cytokine and chemokine responses to stimulation of TLR2 (TNF- α , IL-6, IL-10), TLR3 (TNF- α , IL-6, IL-10, IL-12, CXCL-10, IFN- γ), and TLR4 (TNF- α , IL-6, IL-10, CXCL-10, IFN- γ), yet astrocytes initiate only minor IL-6 responses to all but TLR3 stimulation [139].

Microglia express TLR3 and TLR4 at the cell surface while astrocytes express these receptors intracellularly [137]. The cellular location of TLRs affects their downstream signaling cascades [149], which may explain the different responses of these cells to TLR stimulation. The inflammatory milieu also plays a critical role in regulating TLR expression. Microglia stimulated with CpG specifically up-regulate TLR9, whereas those stimulated with a synthetic TLR3 ligand suppress all TLRs except TLR3 [146]. Similarly, astrocytes stimulated with LPS up-regulate TLRs 2 and 3 but suppress

TLR4, while astrocytes exposed to RNA viruses up-regulate TLR3 and TLR9 [148]. Thus microglia and astrocytes initiate a layered and multifaceted response to TLR engagement.

Oligodendrocytes and endothelial cells express a relatively limited repertoire of TLRs. Oligodendrocytes express TLRs 2 and 3 [137], while cerebral endothelial cells constitutively express TLRs 2, 4, and 9 [150] and increase their expression of these TLRs in response to stressful stimuli, including systemic LPS and cerebral ischemia [138, 151, 152]. In response to LPS, endothelial cells up-regulate E-selectin, an NF κ B-dependent molecule, and IFN γ , an IRF3-dependent molecule, indicating that these cells utilize the TLR-NF κ B and the TLR-IRF3 signaling pathways [153].

Neurons express TLR3 and generate inflammatory cytokines (TNF- α , IL-6), chemokines (CCL5, CXCL10) and antiviral molecules (IFN γ) in response to dsRNA [154]. Neurons also employ TLRs in their development and differentiation. TLRs 3 and 8 are expressed on murine neurons early in development and inhibit neurite outgrowth in a MyD88- and NF κ B-independent manner [155]. TLR2 and TLR4 have been found on adult neural progenitor cells where they appear to elicit opposing effects. While TLR2 activation stimulates neuronal differentiation of these cells, TLR4 activation decreases proliferation and neuronal differentiation, driving these cells toward an astrocytic fate [156]. Curiously, both TLRs exert these endogenous effects in a MyD88-dependent manner, suggesting that these molecules utilize MyD88 in distinct ways. Hence even

minor alterations of these fine-tuned endogenous pathways can have profound effects on cellular responses to TLR engagement.

2.4. Toll-like receptor signaling in health and disease

Studies with TLR knockout mice illustrate the endogenous function of TLRs in health and disease. TLR2 and TLR4 have been shown to play detrimental roles in the development of congestive heart failure and cardiac hypertrophy, respectively, by signaling through MyD88 and NF κ B [157, 158]. TLR2 has additionally been found to be proatherogenic in hyperlipidaemic mice [159], and TLR4 has been shown to produce inflammatory reactions in adipose tissue and thereby mediates obesity and insulin resistance [160, 161]. Conversely, TLR2 and TLR4 activation by hyaluronic acid protect lung tissue from non-infectious injury [162], and TLR4 has been shown to help maintain lung integrity, and prevent the development of emphysema, by modulating oxidant generation [163].

The effects of endogenous TLR stimulation are clearly varied, depending on the cell and tissue type in which the receptors are found and on the disease process in which they are involved. The overwhelming and generally damaging inflammatory response of TLRs to aseptic tissue injury may be a consequence of TLR evolution in response to pathogens. In the setting of pathogen invasion, an inflammatory deluge

may be the most effective means to clear microorganisms. The activation and influx of leukocytes, with the concomitant release of free radicals and tissue-destroying enzymes, assails not only the invading pathogen but any host cells that harbor the pathogen. However, when this same powerful response is co-opted by the host to clear and resolve tissue damage, it can destroy the very cells it is meant to save. This damage promoting characteristic is prominently observed following brain ischemia, where inflammation plays a critical role in both injury progression and resolution.

2.5. Toll-like receptors and ischemic damage

A significant portion of the damage associated with stroke injury is due to the resultant inflammatory response. This aspect of the innate immune response is exemplified by the fact that some anti-inflammatory strategies have been shown to ameliorate ischemic damage [164-166]. The inflammatory response to stroke is initiated by the detection of injury-associated molecules by local cells such as microglia and astrocytes. The response is further promoted by infiltrating neutrophils and macrophages, resulting in the production of inflammatory cytokines, proteolytic enzymes, and other cytotoxic mediators. In the mouse, leukocytes and brain cells (microglia, astrocytes and neurons) express TLRs [146, 167]. Hence, injury-associated molecules such as HSP60 and HMGB1 may act as endogenous ligands for TLRs, thereby initiating the damaging inflammatory response to stroke.

It is increasingly clear that TLRs do in fact play a role in ischemic damage (**Figure 11**). The pathogenic role of TLRs in ischemic processes was first demonstrated in a mouse model of myocardial ischemia/reperfusion injury, because mice lacking functional TLR4 incur less damage than wild type mice [168]. Since then, TLR2 has also been shown to cause dysfunction following cardiac ischemia and both have been shown to exacerbate renal ischemic damage, in a MyD88-dependent and a MyD88-independent manner [169, 170]. However, the particular pathway responsible for the damaging effects of TLR activation may differ depending on the cell type or organ affected as TLR4 worsens ischemic damage following liver transplant in a MyD88-independent, IRF3 dependent fashion [171, 172].

Importantly, TLR2 and TLR4 have been shown to play a role in cerebral ischemic damage (**Table 3**). Mice lacking either functional TLR2 or TLR4 are less susceptible to transient focal cerebral ischemia/reperfusion damage, demonstrating smaller infarcts than wild type controls [152, 173, 174]. Further, mice lacking TLR4 incur less damage following global cerebral ischemia and permanent focal ischemia [175, 176]. The TLR endogenous ligands HSP 60, HSP70 and HMGB1 are found in the brain following injury [177-179]. Hence these molecules may activate TLR2 and TLR4 within the brain itself, leading to the generation of inflammatory mediators such as TNF- α , IL-1, IL-6, and iNOS, all known to be associated with stroke damage.

Cerebral Ischemia

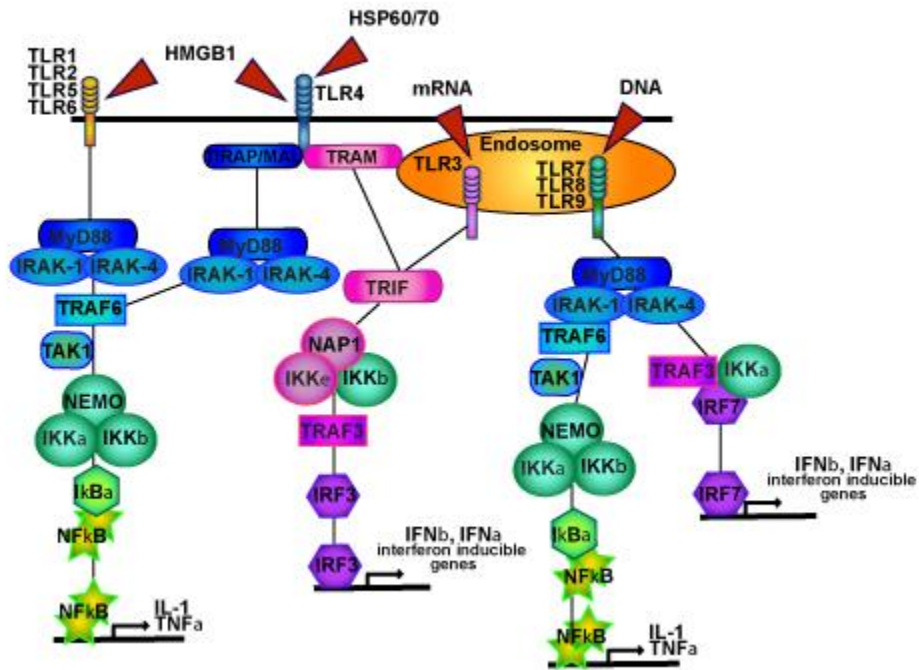


Figure 11. Toll-like receptor signaling in response to cerebral ischemia

TLR signaling following cerebral ischemia is likely initiated by endogenous molecules released from stressed cells and tissues (red arrowheads). In the case of TLR2 and TLR4, ischemia-induced signaling contributes to tissue damage. Other TLRs may also respond to ischemic injury. Differences in TLR signaling pathways suggest that these responses may differ in both magnitude and quality from those of TLR2 and TLR4. Adapted from *Neuroscience* (158) 2009 [136]. Brenda J. Marsh, Rebecca L. Williams-Karnesky and Mary P. Stenzel-Poore, "Toll-like receptor signaling in endogenous neuroprotection and stroke," pp. 1007-1020.

Table 3. *The endogenous roles of Toll-like receptors in cerebral ischemia*

TLR knock-out	Stroke model	Animal model	Outcome	Proposed mechanism	Citation
TLR 2	MCAO via filament, 60 min, 48h reperfusion	Mouse, C57BL/6J, male, 10-12 week, tlr 2 -/-	Decreased infarct in TLR2 -/-	TLR2 signaling	Ziegler G, et al. <i>Biochem biophys Res Commun.</i> 2007; 359(3): 574-9.
	MCAO via filament, 60min, 24 and 72h reperfusion	Mouse, C57BL/6J, male, 13-15 week, tlr 2 -/-	Decreased infarct in TLR2 -/-	TLR2 in microglia	Lehnardt S, et al. <i>J Neuroimmunol.</i> 2007; 190(1-2): 28-33.
	MCAO via filament, 60 min, 72h reperfusion	Mouse, tlr 2 -/-	Decreased infarct in TLR2 -/-		Tang SC, et al. <i>Proc Nat Acad Sci USA.</i> 2007; 104(34):13798-803.
TLR 4	Permanent MCAO via electrocoagulation, 24h and 7d preperfusion	Mouse, male, adult, tlr 4 -/- (C3H/HeJ and C57BL/10ScCr)	Decreased infarct in TLR4 -/-	Decreased inflammatory response, i.e. MMP9	Caso JR, et al. <i>Circulation.</i> 2007; 115(12): 1599-608.
	MCAO, 6h, embolism, 24h reperfusion	Mouse, C3H/HeJ, female, 8 week, tlr 4 -/-	Decreased infarct in TLR4 -/-	Decreased inflammatory cytokines i.e. TNF-alpha, IL-6	Cao CX, et al. <i>Biochem Biophys Res Commun.</i> 2007; 353(2):509-14.
	MCAO via filament, 60 min, 72h reperfusion	Mouse, tlr 4 -/-	Decreased infarct in TLR4 -/-		Tang SC, et al. <i>Proc Nat Acad Sci USA.</i> 2007; 104(34):13798-803.
	Global cerebral ischemia/reperfusion via occlusion of CCA, LSA and RSA, 12 min, 6h reperfusion	Mouse, C57BL/10ScCr, male, 8-12 week, tlr 4 -/-	Decreased infarct in TLR4 -/-	Decrease pIkkappa-B and NFkB	Hua F, et al. <i>J Neuroimmunol.</i> 2007; 190(1-2): 101-11.

Adapted from *Neuroscience* 158(3) 2009 [136]. Brenda J. Marsh, Rebecca L. Williams-Karnesky and Mary P. Stenzel-Poore, "Toll-like receptor signaling in endogenous neuroprotection and stroke," pp. 1007-20.

2.6. Toll-like receptors and neuroprotection

In contrast to the detrimental role of TLRs in response to ischemia, stimulation of these receptors prior to ischemia provides robust neuroprotection (**Table 4**). TLR4-induced tolerance to cerebral ischemia was first demonstrated with low dose systemic administration of LPS, which caused spontaneously hypertensive rats to become tolerant to subsequent ischemic brain damage induced by middle cerebral artery occlusion (MCAO) [126]. Since then, LPS induced tolerance to brain ischemia has been demonstrated in a mouse model of stroke and in a porcine model of deep hypothermic circulatory arrest [180, 181].

As with other stimuli that induce delayed preconditioning, neuroprotection conferred by LPS is time and dose-dependent. Tolerance appears by 24 hours after LPS administration and extends out to 7 days, but is gone by 14 days [182]. Protective doses of LPS appear to depend on the animal model of stroke and the route of systemic administration, ranging from 0.02 to 1mg/kg [126, 181-186]. Tolerance induction has been shown to require new protein synthesis and a modest inflammatory response, as it can be blocked by prior administration of cyclohexamide or dexamethasone [184]. Specifically, TNF- α has been implicated as a mediator of LPS-induced ischemic tolerance because inhibition of TNF- α systemically [126] or within the brain [182] blocks neuroprotection, and mice lacking TNF- α fail to be protected by LPS preconditioning [182].

Table 4. Toll-like receptor ligands precondition against cerebral ischemia

TLR	Treatment	Stroke model	Animal model	Outcome	Proposed mechanism	Citation
LPS (TLR 4)	LPS, 0.2 mg/kg, IP, 72h prior	MCAO via filament, 60 min, 24h reperfusion	C57BL/6 mice, 8-10 weeks, male	Reduced infarct in LPS preconditioned	TNF-alpha	Rozenweig HL, et al. J Cereb Blood Flow Metab. 2007; 27(10): 1663-74.
	LPS, 0.2 mg/kg, IP, 48h prior	MCAO via filament, 60 min, 48h reperfusion	C57BL/6 mice, 8-10 weeks, male	Reduced infarct in LPS preconditioned	Suppression of cellular inflammation	Rozenweig HL, et al. Stroke. 2004; 35(11): 2576-81.
	LPS, 0.5 mg/kg, IP, 24h prior	MCAO via filament, 25min, 72h reperfusion	C57BL/6 mice, 2-3 months, male	Reduced infarct in LPS preconditioned	iNOS, preservation of neurovascular function and CBF	Kunz A, et al. J Neurosci. 2007; 27(27): 7083-93.
	LPS 0.9mg/kg, IV, 72h prior	focal cerebral ischemia, 6h, 24h, 7d and 14d reperfusion	Rat, spontaneously hypertensive	Reduced infarct in LPS preconditioned	Preservation of local cerebral blood flow, upregulation of eNOS	Furuya K, et al. J Neurosurg. 2005; 103(4): 715-23.
	LPS 0.9mg/kg, IV, 1-7d prior	permanent MCAO via electrocoagulation, 24h reperfusion	Rat, adult, male, spontaneously hypertensive	Reduced infarct in LPS preconditioned	IL-1, TNF-alpha	Tasaki K, et al. Brain Res. 1997; 748(1-2): 267-70.
	LPS, 0.9mg/kg, IV, 72h prior	permanent MCAO via electrocoagulation, 24h reperfusion	Rat, adult, male, spontaneously hypertensive	Reduced infarct in LPS preconditioned	Maintainance of microvascular patency	Dawson DA, et al. J Cereb Blood Flow Metab. 1999; 19(6): 616-23.
CpG ODN (TLR 9)	CpG ODN 1826, 20 ug, IP, 72h prior	MCAO via filament, 60 min, 24h reperfusion	C57BL/6 mice, 8-10 weeks, male	Reduced infarct in CpG preconditioned	Reprogramming of TLR9 signalling pathway	Stevens SL, et al. J Cereb Blood Flow Metab. 2008; 28(5): 1040-7.
	CpG ODN, 0.3mg/kg, IM, 72h prior	MCA/ACAO via aneurism clip, 60 min, 48h reperfusion	Rhesus macaque, adult, male	Reduced infarct, increased motor function in CpG preconditioned	Reprogramming of TLR9 signalling pathway	Bahjat and Williams-Karnesky et al. J Cereb Blood Flow Metab. 2011; 31(5):1229-42.
Poly-ICLC (TLR 3)	Poly-ICLC, 1.6mg/kg, subcutaneous, 72h prior	MCAO via filament, 45 min, 24h reperfusion	C57BL/6 mice, 8-10 weeks, male	Reduced infarct in polyIC preconditioned, improved motor function	TNF-alpha independent, Type 1 interferon	Packard et al. J Cereb Blood Flow Metab. 2012; 32: 242-7.
GDO (TLR 7)	GDO, 10, 20 or 40ug, subcutaneous, 72h prior	MCAO via filament, 45 min, 24h reperfusion	C57BL/6 mice, 8-10 weeks, male	Reduced infarct in GDO preconditioned improved motor function	TNF-alpha independent, Type 1 interferon	Leung et al, Stroke. 2012; 43: 1383-9

Adapted from *Neuroscience* 158(3) 2009 [136]. Brenda J. Marsh, Rebecca L. Williams-Karnesky and Mary P. Stenzel-Poore, "Toll-like receptor signaling in endogenous neuroprotection and stroke," pp. 1007-20.

In addition to its neuroprotective effects, LPS preconditioning has vasculoprotective efficacy. Nitric oxide appears to play a critical role in the protective effects of LPS. Mice lacking iNOS expression fail to be protected by LPS pretreatment [186], and eNOS expression within the brain is directly correlated to the time window of LPS-induced neuroprotection [185]. LPS pretreatment has further been shown to prevent the impairment of endothelial and smooth muscle relaxation normally induced by ischemia/reperfusion injury [187], resulting in normalization of cerebral blood flow in peri-infarct regions lasting out to 24 hours after MCAO [185, 188].

LPS-induced ischemic protection requires an inflammatory response *prior* to the ischemic event, yet protection occurs through modulation of the inflammatory response *following* ischemia. Rosenzweig and colleagues have shown that LPS preconditioning changes the response of circulating leukocytes to stroke, attenuating stroke-induced neutrophilia, lymphopenia, and monocyte activation [180]. This altered inflammatory response extends into the brain itself. LPS preconditioning attenuates activation of microglia after stroke and reduces neutrophil infiltration into the ischemic hemisphere [180]. Hence, LPS induced preservation of microvascular function following MCAO may be due to suppressed lymphocyte adhesion to activated endothelium, either by TNF- α -induced suppression of endothelial activation and adhesion molecules [183, 189] or by prevention of cellular inflammatory responses to ischemia [180].

One hallmark of LPS preconditioning is suppression of cytotoxic TNF- α signaling following stroke. Mice that have been preconditioned with LPS prior to ischemia display

a pronounced suppression of the TNF- α pathway following stroke, as evinced by reduced TNF- α in the serum, decreased levels of cellular TNFR1, and enhanced levels of neutralizing soluble-TNFR1. These mice are thus protected from the cytotoxic effects of TNF- α after cerebral ischemia [182]. Collectively, these mechanisms lead to a muted TNF- α response to ischemic injury and increased cell survival.

As with TLR4 and LPS, stimulation of TLR9 by systemically administered CpG oligodeoxynucleotides induces robust protection against brain ischemia in a time (**Figure 7**) and dose-dependent manner (**Figure 12**). CpG pretreatment protects neurons in both *in vivo* and *in vitro* models of stroke, including in non-human primates [190, 191]. As with LPS preconditioning, the protection afforded by CpG depends on TNF- α in mice, as systemic CpG administration acutely and significantly increases serum TNF- α , and TNF- α knock-out mice fail to be protected by CpG preconditioning. Similarities among the known TLR signaling pathways and their shared ability to induce TNF- α , itself a potent preconditioning stimulus, suggests that stimulation of TLR4 and TLR9 may induce ischemic tolerance by similar means.

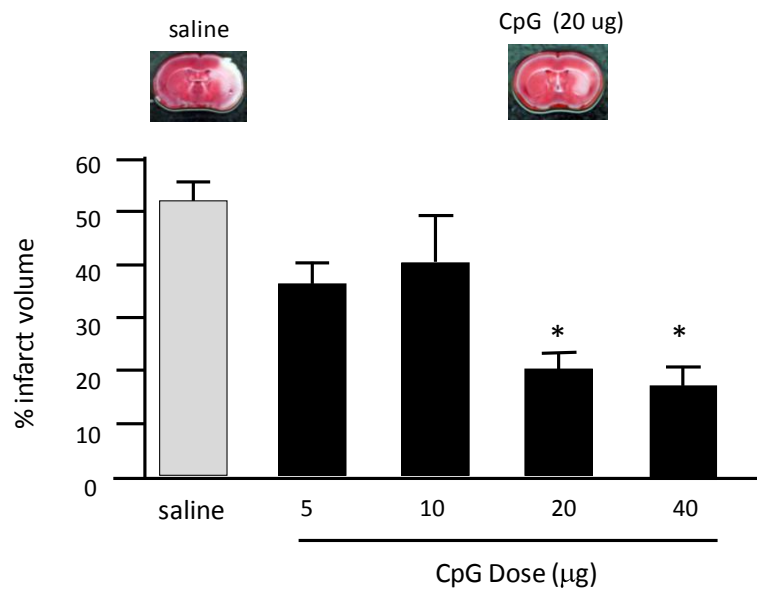


Figure 12. Dose response of CpG preconditioning

Preconditioning induced with the Toll-like receptor 9 agonist CpG. A single intraperitoneal injection of 5-40µg CpG ODN 1826 was given to adult male C57Bl/6 mice prior to 60 minute transient middle cerebral artery occlusion. Indirect infarct volume was assessed after 24 hours of reperfusion via TTC staining (representative images above graph). Value are group means ± SEM. * indicates $p < 0.05$ comparison to saline controls.

2.7. TLR-mediated neuroprotection—reprogramming TLR signaling

The finding that TLRs are mediators of ischemic injury provides insight into the potential mechanisms of LPS- and CpG-induced neuroprotection. In fact, TLR-induced tolerance to subsequent ischemia may occur by the same mechanisms that govern a very similar phenomenon—that of LPS-induced tolerance to subsequent LPS exposure. The latter phenomenon is known as “endotoxin tolerance” and occurs when pretreatment with a low dose of LPS renders cells or whole animals tolerant to the normally detrimental effects of a second, higher dose of LPS.

Cells that are tolerant to LPS are defined by their inability to generate TNF- α in response to TLR4 activation. Upon TLR4 ligation, LPS tolerant cells, unlike naive cells, do not recruit MyD88 to TLR4, and fail to activate IRAK-1 and NF κ B [192]. The TLR4- NF κ B signaling axis becomes decommissioned following a primary exposure to LPS via an elaborate negative feedback loop that involves known inhibitors of TLR signaling. Among those inhibitors are: Ship-1, which prevents TLR4-MyD88 interaction, IRAK-M, a non-functional IRAK decoy, and TRIM30 α , which destabilized the TAK1 complex [193-195]. Thus, subsequent signaling of TLR4 to NF κ B is blocked and inflammatory cytokine production is suppressed. Conversely, secondary exposure causes *enhanced* IFN β release, suggesting increased signaling via the TLR4-IRF3 axis [196]. Thus, pretreatment with LPS causes cells to switch their transcriptional response to TLR4 stimulation by

enhancing the IRF3- induced cytokine IFN β and suppressing the NF κ B-induced cytokine TNF- α .

Similar to endotoxin tolerance, priming TLR9 with its ligand, CpG, induces a state of hypo-responsiveness to subsequent challenge with CpGs [197]. Interestingly, cross-tolerance between the two receptors has also been reported, as ligands for TLR9 induce tolerance against a subsequent challenge with a TLR4 ligand [196, 198]. CpG-pretreated cells not only produce less TNF- α when secondarily challenged with LPS, they also produce significantly higher levels of IFN β [196]. Together, the aforementioned studies suggest the intriguing possibility that TLR stimulation prior to stroke may reprogram ischemia-induced TLR activation (**Figure 13 A and B**).

Specifically, administration of LPS or CpG may activate TLR4 and TLR9, respectively, causing a small inflammatory response, with an initial rise in TNF- α . Cells would then regulate their inflammatory response through expression of negative feedback inhibitors of the TLR4-NF κ B signaling axis that remain present when cells are subsequently exposed to endogenous TLR ligands generated from ischemia-injured tissue. Within this new cellular environment, stimulated TLRs such as TLR2 and TLR4 would be unable to activate NF κ B-inducing pathways. Because of this, stroke-induced TLR2 signaling may be blocked completely leading to reduced injury, and stroke induced TLR4 signaling would shift from NF κ B induction to IRF3 induction. Suppression of NF κ B induction would be expected to protect the brain, as mice lacking the p50 subunit of NF κ B suffer less cerebral ischemic damage than wild type mice [199]. Enhancement of

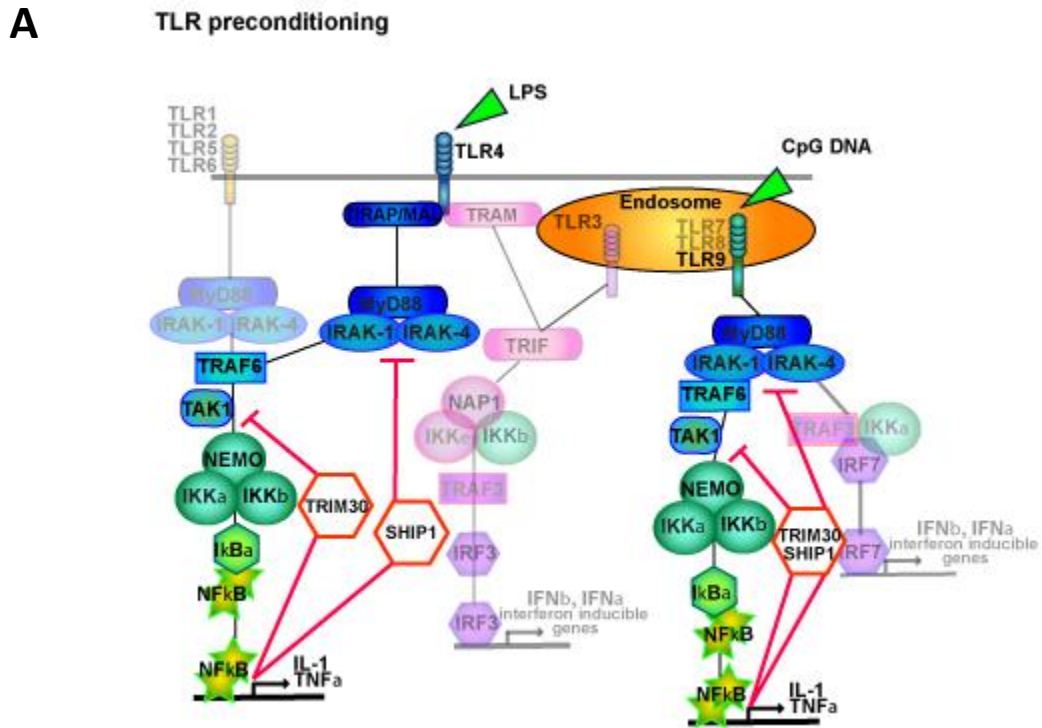


Figure 13. Reprogramming the Toll-like receptor response to cerebral ischemia

(A) Toll-like receptor signaling in response to preconditioning stimuli. Stimulation of TLR4 with LPS causes a primary inflammatory response, via release of pro-inflammatory cytokines, and a secondary inhibition of inflammation, via upregulation of pathway inhibitors, Trim30 and Ship-1. Stimulation of TLR9 with CpG may cause a similar response. Adapted from *Neuroscience* 158(3) 2009 [136]. Brenda J. Marsh, Rebecca L. Williams-Karnesky and Mary P. Stenzel-Poore, "Toll-like receptor signaling in endogenous neuroprotection and stroke," pp. 1007-20.

B Cerebral Ischemia Following TLR preconditioning

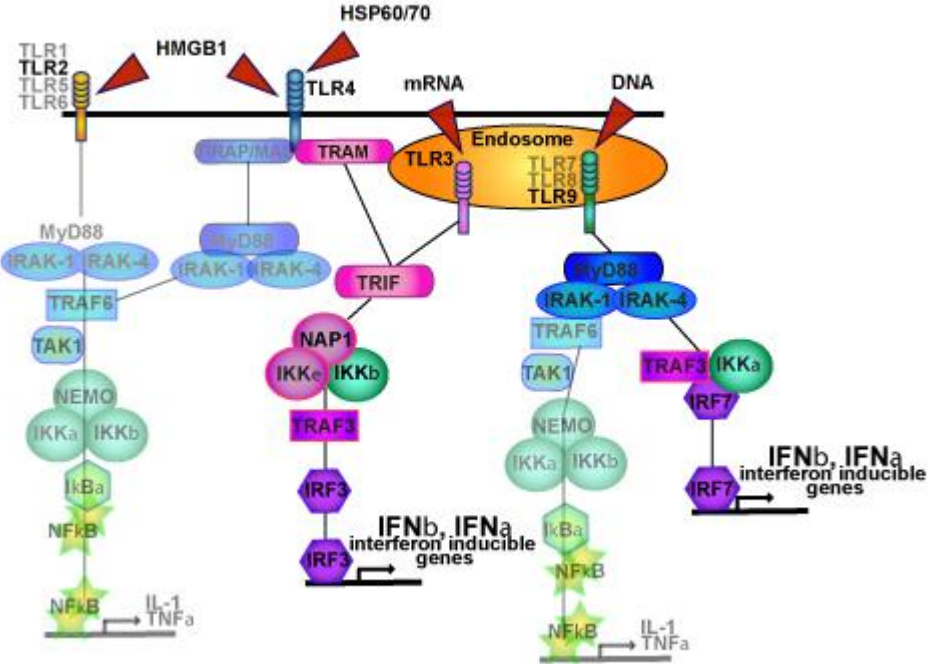


Figure 13. Reprogramming the Toll-like receptor response to cerebral ischemia.

(B) Reprogrammed Toll-like receptor signaling following cerebral ischemia in the context of preconditioning. The presence of pathway inhibitors may block ischemia-induced TLR signaling to NFκB and thereby shunt signaling towards IRFs. Adapted from *Neuroscience* 158(3) 2009 [136]. Brenda J. Marsh, Rebecca L. Williams-Karnesky and Mary P. Stenzel-Poore, “Toll-like receptor signaling in endogenous neuroprotection and stroke,” pp. 1007-20.

IRF signaling would also be expected to protect the brain, as IFN β , a downstream product of IRF3 induction, has been shown to act as an acute neuroprotectant [200, 201].

IFN β , best known for its anti-viral effects, has potent anti-inflammatory activities as well. Several studies have shown that IFN β can stabilize the blood-brain barrier, potentially by reducing matrix metalloprotease production by activated glia [202-204]. Similarly, it has been shown to inhibit monocyte migration across human brain-derived endothelial cells [205] and reduce cellular infiltration into damaged brain regions [202].

On a cellular level, IFN β has been shown to reduce reactive oxygen species [206-208], suppress inflammatory cytokine production and induce IL-1Ra [209, 210], promote nerve growth factor production by astrocytes [211] and protect neurons from toxicity induced by activated microglia [212]. In addition, systemic administration of IFN β has been shown to reduce infarct damage in rat and rabbit models of ischemic stroke [200, 201]. Therefore, in the setting of LPS preconditioning, upregulation of this cytokine following stroke would be expected to contribute to neuroprotection.

IFN β may not be the only neuroprotective molecule downstream of IRF signaling. TLR3 signals exclusively through the TRIF-dependent pathway and stimulation of TLR3 in human astrocyte cultures induces the expression of several neuroprotective molecules such as brain derived neurotrophic factor, neurotrophin 4, pleiotrophin, and TGF β 2 [140], all of which have been implicated in endogenous neuroprotection [213-215].

Astrocytic TLR3 stimulation also results in production of the anti-inflammatory cytokine IL-10 [140]. Conditioned media from these cultures enhances neuronal survival and suppresses astrocyte growth in slice cultures. Interestingly, LPS stimulation of macrophages has been shown to upregulate TLR3 expression [216], inviting the possibility that LPS preconditioning may upregulate TLR3 in the brain, further enhancing stroke induced IRF signaling.

Pretreatment with TLR ligands appears to reprogram the brain's response to ischemia and alters endogenous stroke-induced TLR signaling by suppression of the NF κ B-inducing pathway and upregulation of the IRF-inducing pathway. Reprogramming causes a finely controlled shift in the balance of proinflammatory and anti-inflammatory cytokines, and represents an endogenously orchestrated mechanism that protects the organism from additional damage. Reprogramming of endogenous TLR signaling, with the subsequent generation of neuroprotective Type I IFNs, may be a unifying property of the neuroprotected phenotype. Interestingly, the story becomes more complex: recent evidence suggests that the purine nucleoside adenosine may also play a role in the genomic reprogramming required for ischemic and TLR-mediated preconditioning.

3. The role of adenosine in neuroprotection

Adenosine, an endogenous purine nucleoside that modulates many physiological processes, and its receptors have shown great promise as therapeutic targets to reduce of damage following experimental stroke. In addition to their value as post-stroke treatments that reduce the extent of ischemic damage, these compounds have been prime candidates for prophylactic neuroprotection.

3.1. A brief history of adenosine-based therapies in neuroprotection

For some time adenosine and its receptors have been viewed as potential therapeutic targets for the treatment of neurological injury. In practice, however, adenosine-based therapies for the treatment of cerebral ischemia have proven complex in their implementation [217]. Difficulties stem from the widespread distribution of adenosine receptors within the central nervous system (CNS) and throughout the body. For this reason, even direct targeting of specific adenosine receptors leads to widespread off-target effects. Further complications in developing robust adenosine-based therapeutics include imperfect targeting of specific receptor subtypes by agonists and antagonists. Finally, as mentioned previously, cerebral ischemia is comprised of a

complex set of pathophysiological processes that are influenced differentially by adenosine spatially and temporally.

3.2. The basic physiology of adenosine and its receptors

The adenosine receptor family consists of four members: A_1 , A_{2A} , A_{2B} and A_3 receptors. Adenosine receptors consist of seven transmembrane spanning regions, and are coupled to G proteins, which activate a number of intracellular signaling pathways [218]. Adenosine receptors are broadly grouped into two categories: A_1 and A_3 receptors, which couple to inhibitory G proteins, and A_{2A} and A_{2B} receptors, which couple to stimulatory G proteins. However, adenosine receptors are pleiotropic; they can couple with various G proteins and transduction systems according to their degree of activation and their particular cellular or subcellular location [219].

Extracellular adenosine levels are low under normal conditions, but increase substantially in response to metabolic stress [218, 220, 221]. Extracellular adenosine levels are increased under stress via several mechanisms: 1) inhibition of equilibrative nucleoside transporters, 2) increased release of ATP from cells and stimulation of extracellular breakdown of ATP by ectonucleotidases, and 3) inhibition of intracellular adenosine removal [220, 221]. Rapid elevations in adenosine occur following ischemia *in vitro* such that within 10 minutes of ischemia adenosine levels in hippocampal slices are

increased by more than 20 μ M [222]. *In vivo* studies also show increases in adenosine in the CNS with cerebral ischemia [223]. Interestingly, increased levels of adenosine during stroke are not limited to the CNS, as adenosine levels in serum have also been shown to increase following transient ischemic attack (TIA) and stroke in humans [224].

3.3. The effects of adenosine release on the CNS during cerebral ischemia

Adenosine is a potent endogenous neuromodulator with known neuroprotective properties [225-227]. Administration of adenosine to the brain at the time of stroke ameliorates damage [228]. Further, transgenic overexpression of adenosine kinase, the primary negative enzymatic regulator of adenosine, leads to increased vulnerability to ischemic cell death, presumably due to decreased levels of adenosine in the CNS [229]. In practice, however, the clinical use of adenosine as a neuroprotectant during stroke has been unsuccessful. Adenosine is an imperfect neuroprotectant, as it can provide benefit in some cases and exacerbate tissue damage in other conditions [225, 230].

Adenosine receptors are distributed throughout the body, and play a prominent role in cardiac and renal system function. When administered intravenously, adenosine at bolus doses of 6-12mg is used to treat patients with paroxysmal supraventricular tachycardia to restore normal sinus rhythm by slowing conduction through the A-V node in the heart [231]. At higher doses, adenosine causes decreased blood pressure by

decreasing vascular resistance. Adenosine is also a respiratory stimulant, and intravenous administration has been shown to increase ventilation and reduce arterial PCO₂ causing respiratory alkalosis. Decreased blood flow and respiration compound cerebral ischemic injury, superseding the potential neuroprotective properties of systemically administered adenosine.

Targeted delivery of adenosine to the CNS in a controlled manner has also proven problematic. Adenosine has a very short half-life in human plasma (<5 seconds), and low blood brain barrier permeability [232]. Molecules with greater plasma stability have been tested such as adenosine analogs, receptor-specific agonists and antagonists, and enzymatic regulators of adenosine. For example, pretreatment with the unspecified adenosine agonist NECA (adenosine-5'-N-ethylcarboxamide) protects human astrocytoma cells from apoptosis under hypoxic conditions *in vitro* [233]. Success has also been reported with adenosine agonists in rodent models of cerebral ischemia. Systemic administration of the adenosine kinase inhibitor GP683 at a moderate, but not high or low dose, to rats within 270 minutes of onset of surgical ischemia reduced cerebral damage significantly [234].

Unfortunately, the optimal window of administration for adenosine-modulating drugs has been difficult to determine. This is a common problem encountered by many potential stroke therapeutics that show promise in animal models, as accurate determination of the time of onset of cerebral ischemia is difficult in human patients. Patients suffering from cerebral ischemia routinely face delays in access to clinical care,

often due to a failure to recognize symptoms of neurological damage. The mean hospital arrival time for patients suffering from cerebral ischemia is approximately 11 hours after the onset of vessel obstruction [235]. Once patients have been admitted to the hospital, more time may elapse before accurate diagnosis and treatment begins. Thus, therapies for cerebral ischemia with long time windows of efficacy are most desirable. In the case of adenosine, there is the added complication of a diverse distribution of adenosine receptors in the brain, whose actions can be opposing either spatial or temporally. While administration of a specific adenosine receptor agonist early on may be protective, administration of the same drug late in the course of stroke may exacerbate ischemic damage.

Direct administration of adenosine-modulating drugs to the CNS is used in animal models to dissect the systemic and CNS effects of adenosine in stroke. These targeted experimental therapies have shown efficacy in reducing ischemic damage in small animal models of stroke. For example, intracerebral ventricular (i.c.v.) administration of the selective A₃R agonist Cl-IB-MECA (2-chloro-N⁶-(3-iodobenzyl)adenosine-5'-N-methylcarboxamide) decreased infarct volume in a mouse model of transient ischemia [236]. Clinically, i.c.v. administration of drugs is impractical and the uncertainty about the diverse temporal effects of adenosine receptor activation and blockade remains problematic. While animal experiments using i.c.v. administration might not translate directly into clinical therapies, they provide insight into the local temporal effects of adenosine on the CNS.

3.4. A₁R effects in the CNS

In the brain, the A₁ subgroup is the most abundant and widespread of the adenosine receptors [219]. A₁ receptors have the highest affinity for adenosine of all the subtypes [221]. Under basal conditions, adenosine likely acts via this receptor subtype. Based on immunohistochemical studies, A₁ receptor expression has been shown to be high in the hippocampus, cerebral cortex, basal ganglia, and some thalamic nuclei in humans and a variety of animals [219]. A₁ receptor expression is highest in neurons, but the receptor is also present on astrocytes, microglia, and oligodendrocytes [219]. A₁ receptors are a central focus in the study of the neuroprotective role of adenosine in stroke due to their high concentration and affinity for adenosine, known coupling to inhibitory G proteins and the large number of selective agonists and antagonists available for use.

Activation of A₁ receptors is generally considered protective in the context of noxious stimuli. The brain uses vast amounts of ATP generated by oxidative phosphorylation to maintain control of K⁺ and Na⁺ gradients in neurons. Function of the Na⁺/K⁺ ATPase is disrupted during ischemia because mitochondria are unable to make ATP when glucose and oxygen levels are low. Altered Na⁺/K⁺ ATPase activity leads to depolarization of the neuronal plasma membrane and subsequent release of excitatory neurotransmitters. As a result, calcium-permeable NMDA channels open causing calcium-mediated cell death. A₁ receptors are linked to inhibitory G proteins, which

inhibit adenylyl cyclase, activate inward rectifying K⁺ channels, inhibit Ca²⁺ channels, and activate phospholipase C [220]. This has the cumulative effect of decreasing neuronal excitability. Activation of A₁ receptors also leads to feedback inhibition of the release of presynaptic excitatory neurotransmitters, such as glutamate. Stimulation of A₁ receptors can therefore lead to prevention of excitotoxic cell death under ischemic conditions.

In practice, A₁ receptor activation has been shown to produce conflicting effects in both *in vivo* and *in vitro* models of cerebral ischemia. As neurons in the CA1 region of the hippocampus are particularly susceptible to hypoxic cell death, this region is often the selected indicator of tissue damage in both *in vitro* and *in vivo* models of ischemia. In hippocampal slice preparations recovery following hypoxia, as measured by restoration of the CA1 field EPSP (fEPSP), was attenuated by the application of the A₁R antagonist DPCPX (1,3-dipropyl-8-cyclopentylxanthine) [237]. This result would suggest that antagonists of A₁R have a detrimental effect in hypoxia, at least at the neuronal level. However, application of the A₁R antagonist 8-CPT (8-cyclo-pentyl theophylline) to hippocampal slices at the time of insult did not exacerbate hypoxia induced cell death in the CA1 [238]. Hippocampal slices from A₁R knockout mice subjected to hypoxia showed a small, though not statistically significant decrease in damage to neurons in the CA1 region [238]. A₁R knockout mice, when exposed to global ischemia, showed no increased neuronal damage in the CA1 region of the hippocampus, the cortex, or the striatum as compared to wildtype controls [238]. In the same study, mice treated with 8-CPT at the time of global ischemia has a significant increase in cell death in the CA1 region, the cortex and the striatum when compared to control-treated animals. Taken

together, these results suggest that the protective effects of A₁R activation may be temporally regulated. Perhaps acute stimulation via A₁ receptors provides protection by decreasing synaptic transmission, but during recovery from ischemia-induced down-regulation of A₁ receptors may be beneficial.

3.5. A_{2A}R effects in the CNS

A_{2A} receptors are also distributed widely throughout the brain. However, they are expressed at lower density in most regions than A₁ receptors [219]. The highest density of A_{2A} receptors can be found in the striatum [221]. The affinity of A_{2A} receptors for adenosine is also relatively high. The advent of more selective A_{2A} receptor agonists and antagonists, and the generation of A_{2A} knockout mice, has revealed an important role of A_{2A} receptors as mediators of neuroprotection in stroke. Because they are coupled to excitatory G proteins, it would seem that stimulation of A_{2A} receptors would exacerbate ischemic damage. Indeed, when applied centrally, A_{2A} receptor antagonists afford protection in several *in vivo* models of ischemic injury [239-243]. Further, A_{2A} receptor knockout animals show a significant decrease in damage following focal cerebral ischemia [244]. The location of A_{2A} receptors in the brain may also influence ischemic injury. In a model of permanent focal ischemia, a decrease in A_{2A} receptor ligand affinity and an increase in receptor expression were seen in the striatum, but not the cortex [245]. Stroke can occur in diverse regions of the brain depending on the

specific vessels involved. It may be possible to tailor adenosine receptor modulating drugs to patients based on the area of ischemia as more is learned of the location specific properties of adenosine receptors. Perhaps for patients with strokes in the striatum, A_{2A} receptor antagonism would be a more potent therapy than for patients with primarily cortical injury.

Surprisingly, peripheral stimulation of A_{2A} receptors has also been shown to provide protection to cerebral ischemia *in vivo* [243]. Systemic administration of A_{2A} receptor agonists also protects against spinal cord ischemia-reperfusion and traumatic spinal cord injury *in vivo* [246, 247]. Further, direct administration of A_{2A} receptor agonists to the brain immediately preceding intracerebral hemorrhage reduces cell death [248]. In these cases, protection afforded by A_{2A} receptor agonists is attributed to a reduction of neutrophil infiltration into the affected tissue. Stimulation of A_{2A} receptors has been shown to decrease production of proinflammatory cytokines by peripheral immune cells [249, 250]. Inflammatory cytokines may play a role in exacerbating injury in the CNS. However, elucidation of the distinct contributions of A_{2A} receptors in the CNS and in the periphery to ischemic damage has proven difficult.

A_{2A}R knockout bone marrow chimera mice have been created to separately address the peripheral and CNS effects of A_{2A} receptors. As stated previously, A_{2A}R knockout mice are protected from cerebral ischemic damage [244]. Similarly, A_{2A}R knockout mice are protected from compression injury of the spinal cord when compared to wild-type controls [251]. Chimeric mice lacking A_{2A} receptors in non-bone

marrow derived cells (BMDCs) also show protection from compression, but only a small reduction in infarct is seen these mice. Notably, protection in spinal compression injury is abolished in wild-type/knockout bone marrow chimera mice that lack the A_{2A} receptor in BMDCs but is retained in cerebral ischemia [244, 251]. Interestingly, the amelioration of damage in chimeric mice lacking A_{2A} receptors on BMDCs is not as robust as in A_{2A} knockout animals. These results suggest that neuroprotection in these two models of injury may be mediated differentially. In the case of ischemic injury, over 90% of the microglia in the damaged area of chimeric mice were found to be brain derived, indicating that suppression of inflammation in peripheral BMDCs may not have been significant in this circumstance [244]. A_{2A} receptor activation may be beneficial acutely in the periphery by acting on brain endothelium to increase cerebral blood flow and by reducing inflammatory cytokine production by immune cells, while A_{2A} receptor antagonism may be beneficial in the CNS during later stages of ischemia, when prolonged activation of neurons could be detrimental.

3.6. A_{2B} receptor effects in the CNS

The effects of adenosine A_{2B} receptors during ischemia are not as well characterized as those of A_{2A} receptors. A_{2B} receptors are perhaps the least studied member of the adenosine receptor family. A_{2B} receptors are present on vascular smooth muscle and endothelial cells, as well as on astrocytes [252, 253]. Due to their low affinity

for adenosine, and their relative paucity in the brain, A_{2B} receptors seem to be activated only under hypoxic or ischemic conditions, when levels of adenosine surge [254, 255]. Recent *in vitro* studies have suggested a role for A_{2B} receptors in production of glial cell line-derived neurotrophic factor (GDNF) by astrocytes [256]. Adenovirus-mediated GDNF pretreatment has been shown to reduce cell death following MCAO by both intracerebral and systemic administration [257, 258]. Intracerebral infusion of GDNF post-MCAO increases striatal neurogenesis in rat, indicating a possible role in regeneration as well as protection [259].

A_{2B} receptors may also regulate vascular leak during hypoxia [260], potentially contributing to increased blood flow to affect tissues. Studies of si-RNA mediated A_{2B} receptor suppression *in vitro* have shown increased endothelial leak in response to hypoxia, and A_{2B} receptor knockout animals show increased vascular permeability as compared to wildtype or other adenosine receptor knockout animals [260]. The ablation of the A_{2B} receptor in mice leads to a basal level of low-grade inflammation and increased leukocyte adhesion to the vasculature [261]. A_{2B} receptor mice also display an enhance expression of pro-inflammatory cytokines as compared to control mice. Bone marrow transplantation studies indicate that these processes are regulated primarily by bone marrow and, to lesser extent, vascular, A_{2B} receptors [261]. Taken together, these results indicated that A_{2B} receptors might afford protection to the CNS when activated under ischemic conditions, either directly or by decreasing inflammation and reducing immune cell adhesion to vascular endothelium.

3.7. A₃ receptor effects in the CNS

A₃ receptors stimulate inhibitory G proteins; like A₁ receptors, A₃ receptor activation inhibits adenylyl cyclase and leads to the activation of phospholipase C. However, the affinity of A₃ receptors for adenosine is the lowest of all subgroups, on the order of 6500 nM, which is roughly 100 times lower than the affinity of A₁ receptors [221]. A₃ receptors are found throughout the brain, though they are present at levels 10-30 fold lower than A₁ or A₂ receptors [262]. Interestingly, A₃ receptors on CNS cells have been shown to be involved in both cell survival and death, depending on the degree of receptor activation and the specific pathophysiological conditions [263].

More specifically, long duration activation of A₃ receptors leads to cell death via necrosis or apoptosis, while short-term stimulation of central A₃ receptors prior to injury may reduce spontaneous apoptosis [264]. Application of A₃ receptor antagonists to hippocampal slices during prolonged oxygen-glucose deprivation (OGD) prevented neuronal loss in the CA1 region [265]. Interesting, during brief periods of OGD, A₃ receptors antagonism resulted in faster recovery of fEPSP, indicating an inhibitory role of these receptors during initial hypoxia [265]. Chronic pre-exposure to A₃ agonist is protective *in vivo*; this may be due to rapid desensitization of A₃ receptors [266, 267]. Intravenous or i.c.v. administration of the selective A₃ receptor agonist CI-IB-MECA 165 minutes and 15 minutes prior to the onset of transient ischemia was protective in rats [236]. Consistent with these results, A₃ knockout animals have increased susceptibility

to transient cerebral ischemic injury [236]. Post ischemic administration of CI-IB-MECA is also protective *in vivo* [217]. Interestingly, in contrast to *in vitro* results, an acute, single dose of CI-IB-MECA given acutely during focal ischemia increased infarct volume [264]. These results suggest that the effects of A₃ receptor signaling during ischemic injury may be beneficial or detrimental depending on the specific circumstances in which the stimulus occurs. Correctly timed, A₃ receptor modulation may be a potential target for therapeutic intervention. Early chronic stimulation of A₃ receptors leading to their down regulation, or acute A₃ receptor blockade, may be one strategy for inducing prophylactic neuroprotection in advance of predicted ischemic injury.

3.8. Past complications in developing adenosine-based therapies for cerebral ischemia

A major stumbling block in the development of adenosine-based neuroprotective strategies has been the dramatic systemic effects of adenosine which include decreased heart rate, blood pressure and body temperature, and sedation [268]. As more specific adenosine receptor agonists and antagonists are developed, drugs with fewer off-target effects may emerge. Novel therapeutic methods, such as biodegradable brain implants [269] may also allow for easier local delivery of adenosine, or modulators of specific adenosine receptors, to the central nervous system. Additionally, the systemic effects of adenosine may yet be harnessed to ameliorate damage caused by ischemic stroke.

3.9. Peripheral immune involvement and inflammatory cytokines in cerebral ischemia

In the context of a pathogen invasion, a vigorous inflammatory response is an effective means to clear an invasive microorganism. Responding immune cells kill not only pathogens, but also the cells harboring them. However, when this same response is co-opted by the host to clear infarcted tissue, it can damage the very cells it is intending to save. Much of the damage associated with brain ischemia is due to the resultant inflammatory response. This has been demonstrated by the amelioration of ischemic damage through the use of anti-inflammatory strategies [164-166]. Inflammation following stroke originates with microglia and astrocytes, which detect injury-associated molecules and produce pro-inflammatory cytokines [270, 271]. Vascular endothelium becomes activated, signaling to the periphery and increasing blood brain barrier permeability [272, 273]. The inflammatory response is further promoted by the infiltration of macrophages and neutrophils. These cells produce proteolytic enzymes, inflammatory cytokines and other cytotoxic molecules.

Proinflammatory cytokine have been implicated in exacerbating the damage in stroke by increasing neuroinflammation, with particular attention paid to TNF- α [274]. TNF- α is pleiotropic inflammatory cytokine that is produced by a variety of cell types, including peripheral immune cells and cells that are resident in the CNS (**Figure 14**). Intravenous administration of anti-TNF- α antibody to mice following transient cerebral ischemia has been shown to ameliorate damage and reduce edema [275]. Adenosine

receptor agonists and antagonists are both effective suppressors of TNF- α through their actions on various cell types. In rabbits undergoing transient spinal cord ischemia, lower levels of plasma TNF- α and decreased damage were seen following intravenous administration of ATL-146e (4-(3-[6-amino-9-(5-ethylcarbamoyl-3,4-dihydroxy-tetrahydro-furan-2-yl)-9H-purin-2-yl]-prop-2-ynyl)-cyclohexanecarboxylic acid methyl ester) [276]. Understanding how adenosine modulates the release of TNF- α by both peripheral immune cells and by cells in the CNS may be particularly beneficial when developing adenosine based therapies for the treatment of stroke. The effects of TNF- α on adenosine receptor expression may also provide insight into the phenomenon of ischemic preconditioning, a phenomenon in which a brief noxious stimuli induce changes in the CNS and in the periphery that result in endogenous neuroprotection from stroke.

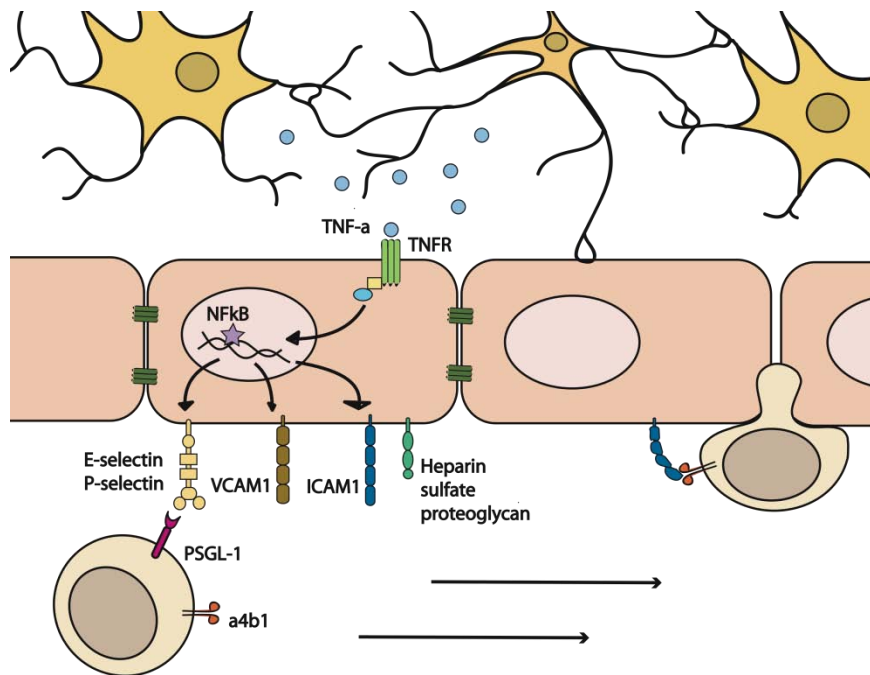


Figure 14. *Peripheral immune involvement following ischemic brain injury*

Neurons and astrocytes damaged by ischemia release pro-inflammatory factors such as TNF- α into the brain parenchyma. These pro-inflammatory molecules in turn diffuse and bind receptors on vascular endothelial cells. Activation of endothelial cells via TNF- α and related receptors leads to nuclear factor kappa B (NF κ B) activation and nuclear translocation. In the nucleus, NF κ B activity induces transcription of adhesion molecules and chemokines, including E-selectin, P-selectin, vascular cell adhesion molecule (VCAM1), intercellular adhesion molecule (ICAM1) and heparin sulfate proteoglycan. Peripheral immune cells traveling through the vasculature express receptors to adhesion molecules (i.e. PSGL-1 for selectins, α 4- β integrin for VCAM1). As they survey the body, leukocytes roll along the activated endothelium, adhere via adhesion molecules and become activated themselves, then extravasate into the brain parenchyma. Adapted from *Current Pharmacology* 7(3) 2009 [277]. Rebecca L. Williams-Karnesky and Mary P. Stenzel-Poore, "Adenosine and stroke: Maximizing the therapeutic potential of adenosine as a prophylactic and acute neuroprotectant," pp. 217-27.

3.10. The effects of adenosine on the peripheral immune system

Adenosine may play a role in modulating systemic immune involvement in stroke that is in addition to its role in the CNS. Adenosine levels in serum increase following stroke [224]. This finding may be particularly significant, as peripheral immune cells express functional adenosine receptors, and respond to changes in extracellular adenosine (**Figure 15**). It is also important to consider the peripheral effects of adenosine-based therapeutics, as systemic administration of adenosine-modulating drugs affect immune cells as well its direct effects on the CNS.

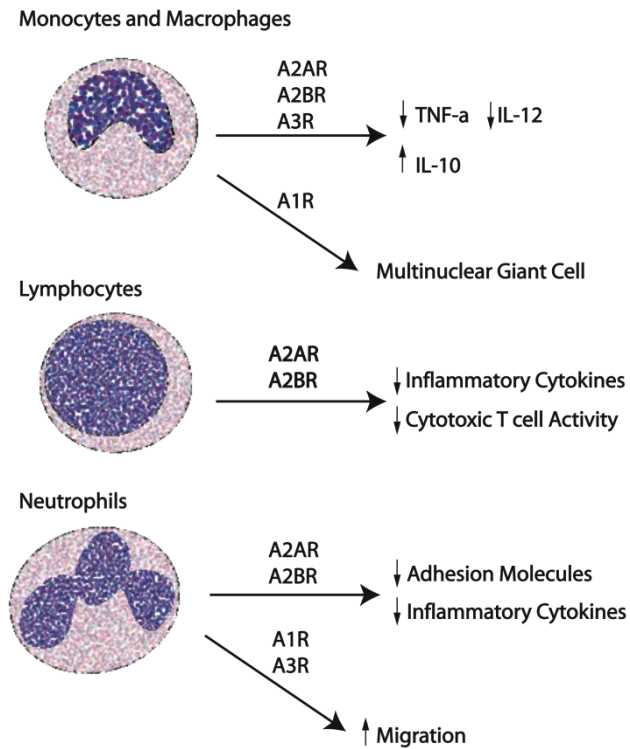


Figure 15. Adenosine modulates peripheral immune cell function

Adenosine modulates the activity of peripheral immune cells differentially depending on the receptors that are activated. Overall, activation of A_{2A} and A_{2B} receptors directs immune cells to an anti-inflammatory response. This property could be harnessed in stroke to reduce inflammatory damage in the CNS caused by infiltrating activated immune cells. Stimulation via A₁ receptors on immune cells tends to increase migration and activity, but also leads to angiogenesis through their interaction with cerebral vascular endothelial cells. Adapted from *Current Pharmacology* 7(3) 2009 [277]. Rebecca L Williams-Karnesky and Mary P. Stenzel-Poore, "Adenosine and stroke: Maximizing the therapeutic potential of adenosine as a prophylactic and acute neuroprotectant," pp. 217-27.

3.11. Effects of adenosine on monocytes and macrophages

Monocytes and macrophages express the full complement of A_1 , A_{2A} , A_{2B} , and A_3 receptors. Stimulation via adenosine receptors not only shapes macrophage function, but can also influence differentiation. High levels of extracellular adenosine can delay monocyte maturation [278]. Broadly, extracellular adenosine has the effect of changing the response of macrophages from proinflammatory to anti-inflammatory. Adenosine inhibits TNF- α and IL-12 production, while increasing IL-10 production by macrophages [279]. These effects appear to be primarily mediated via A_{2A} , A_{2B} and A_3 receptors [280]. Studies have shown that A_{2B} receptor activation with the selective agonist BAY 60-6583 on macrophages *in vitro* and *in vivo* leads to decreased production of TNF- α following injurious stimuli [281]. However, it should be noted that adenosine has differential effects on macrophage development depending on the receptor it stimulates. For instance, stimulation via A_1 receptors has been found to influence monocytes to become phagocytic multinuclear giant cells, while stimulation via A_{2A} and A_{2B} receptors has been shown to inhibit this process [282].

Monocytes also affect resolution of ischemic damage by influencing vascular endothelial cells. Application of the selective A_1 receptor agonist CPA (N^6 -cyclopentyladenosine) to macrophages results in increased production of vascular endothelial growth factor (VEGF), leading to an increase in capillary formation *in vitro* [283]. When activated, macrophages can themselves be a source of extracellular

adenosine, via ATP production [279]. Through this local extracellular production of adenosine, macrophages may also suppress the inflammatory response of other immune cells. Monocytes and macrophages exert broad influence on damage and healing following stroke. Stimulation of the A_{2A} receptor mediates inhibits production of $TNF-\alpha$, decreasing inflammation at the time of ischemia. Therapies that increase the expression of A_{2A} receptors for adenosine, such as the Toll-like receptor 4 (TLR4) agonist lipopolysaccharide (LPS) [284], may be useful as a prophylactic to modulate the response of macrophages to endogenous adenosine release during ischemic injury.

3.12. Effects of adenosine on T and B lymphocytes

Recruitment of activated lymphocytes to the brain parenchyma following stroke leads to increased tissue damage [26]. Adenosine may serve as a negative regulator of lymphocyte activation, and thereby reduce damage caused by an excessive inflammatory response. Lymphocytes express A_{2A} , A_{2B} and A_3 adenosine receptor subtypes [285]. Similar to that seen in macrophages, stimulation of adenosine receptors on lymphocytes has the net effect of suppressing activation. The adenosine A_{2A} receptor has been directly implicated in adenosine-mediated suppression of cytokine production and cytotoxic activity in natural killer T cells, a highly specialized group of T lymphocytes [286].

Additionally, evidence is mounting to support the hypothesis that adenosine mediates the formation of T regulatory cells [280, 287]. Unlike cytotoxic T lymphocytes, regulatory T cells serve as suppressors of inflammation, which can limit damage to healthy tissues caused by overactivated immune cells. Surprisingly, the regulatory function of T regulatory cells has been linked to their ability to produce adenosine [288]. A_{2A} receptors appear to be the dominant receptor subtype mediating the immunosuppressive effects of adenosine on lymphocytes. Stimulation of the A_{2A} receptor in mixed lymphocyte populations leads to a decrease in expression of the intercellular adhesion molecule ICAM, decreased production of several proinflammatory cytokines, and decreased proliferation [289]. However, it should be remembered that the actions of A_{2A} receptor stimulation could be blocked via A_1 or A_3 receptor activation [289]. While this may be relevant with acute systemic administration of adenosine-based therapeutics selective for A_1 and A_3 agonists, the negative consequences could potentially be overcome by using short-acting, CNS-targeted drugs.

3.13. Effects of adenosine on neutrophils and other granulocytes

Neutrophils are granulocytes, members of the polymorphonuclear family of cells, which also includes eosinophils and basophils. Following activation by cytokines and chemokines, neutrophils upregulate intracellular adhesion molecules, adhere to vascular endothelium and migrate into damaged tissue. Migration of neutrophils occurs

well before migration of monocytes or lymphocytes [290]. Once at the site of inflammation, neutrophils release preformed granule constituents, lytic enzymes, reactive oxygen species and inflammatory cytokines, such as TNF- α .

While helpful in the context of response to infection with a pathogen, as with other immune cells, overactivation of neutrophils at sites of injury can exacerbate damage of healthy tissue. Neutrophils in particular are strongly recruited following ischemic-reperfusion injury, and have been shown to contribute significantly to subsequent neuroinflammatory damage [291]. Adenosine promotes migration of neutrophils, a process which appears to occur via stimulation of A₁ and A₃ receptors [292, 293].

Conversely, by acting via A_{2A} receptors, adenosine downregulates surface expression of adhesion molecules, and decreases the production of pro-inflammatory cytokines [280]. Application of the adenosine kinase inhibitor GP515 attenuates neutrophil degranulation via an adenosine-mediated action [294]. This action appears to be mediated strongly by A₃ receptors, as well as by A_{2A} receptors, but not by A₁ receptors [294]. In mast cells, A_{2A} receptor stimulation also blocks degranulation, while A_{2B} receptor activation causes release of VEGF [283]. Taken together, these results indicate that A_{2A} receptors serve as a negative regulator of granulocyte-induced inflammation, while A₁ receptors may promote the inflammatory properties of these cells. A₃ receptors appear to have mixed effects on neutrophils, depending on the context in which the stimulation occurs.

Neutrophils infiltrate into the brain parenchyma following ischemic injury, contributing to immune mediated inflammatory damage following stroke; adenosine receptors provide an accessible, potential target for modulation of the proinflammatory properties of these cells. Overall, A_{2A} receptor stimulation on neutrophils acutely and immediately following stroke likely decreases inflammatory damage. Compounds that directly induce expression of A_{2A} receptors on neutrophils such as LPS, or those that elicit the release of cytokines like TNF- α , Interleukin 1 β (IL-1 β) [295], may be useful as prophylactic neuroprotectants by reprogramming the response of neutrophils to stroke.

3.14. A putative role for adenosine in preconditioning

Ischemic preconditioning can be induced by a variety of noxious stimuli, including short periods of hypoxia or ischemia, cortical spreading depression, brief seizure, exposure to inhaled anesthetic or a low dose of bacterial endotoxin [131]. Preconditioning that occurs rapidly, immediately following stimulation, is termed acute preconditioning. Local increase of adenosine in the brain is likely one of the mechanisms by which acute preconditioning occurs [219]. Rapid upregulation of neuroprotective A₁ receptors in the brain have been shown to be one mechanism of adenosine-mediated acute preconditioning. When given during a brief conditioning period of ischemia, the selective A₁ receptor agonist DPCPX attenuates the protective effects of preconditioning [296, 297]. Rapid tolerance against focal ischemia by isoflurane is also attenuated by

DPCPX administration [298]. As an additional mechanism, rapid adenosine receptor desensitization may contribute to acute neuroprotective as is seen following chronic A₃ receptor agonism [266].

Neuroprotection that develops over a period of several hours or days and requires new protein synthesis is termed delayed preconditioning. As in acute preconditioning, adenosine may play a role in delayed preconditioning. ATP diphosphohydrolase and 5'-nucleotidase, two enzymes involved in the local production of adenosine from ATP via hydrolysis, showed enhanced activity in the CA1 region of the hippocampus following brief ischemia. This increase in enzymatic activity correlated with protection in the CA1 region from subsequent ischemic injury, given 48 hours later. Adenosine receptor antagonists block tolerance to ischemia induced by preconditioning. As with acute preconditioning, the neuroprotective effects of ischemic preconditioning are attenuated with the administration of the selective A₁ agonist DPCPX at the time of conditioning ischemia [299, 300]. Interestingly, DPCPX administered at the time of ischemia, 72 hours after preconditioning, does not reverse protection, implying a role for A₁ receptors during conditioning ischemia [300].

Unmethylated cytosine-guanine rich oligodinucleotides (CpG ODNs), which act on Toll-like receptor 9 (TLR9), have been shown to be a highly effective means of prophylactic neuroprotection in a mouse model of cerebral ischemia [190]. The delayed neuroprotection afforded by CpG ODNs occurs following the systemic injection. CpG ODNs also confer protection from oxygen-glucose deprivation in mixed cortical cultures

in vitro. Similar findings have been previously reported for the TLR4 agonist LPS [180]. An increase in systemic levels of TNF- α is required for neuroprotection in both LPS- and CpG-mediated preconditioning [180, 190]. Interestingly, proinflammatory cytokines such as TNF- α increase the expression and signaling of A₁ receptors in the brain [301]. Upregulation of A₁ receptors in the CNS, effectively preparing the brain for ischemic insult, may be one mechanism by which TLR agonists elicit endogenous neuroprotection. TNF- α upregulates A_{2A} and A_{2B} receptor expression on endothelial cells, which may contribute to suppression of inflammation following ischemic injury [302, 303]. This contribution may be highly relevant, as stimulation of these receptors on vascular endothelial cells suppresses expression of adhesion molecules such as E-selectin and vascular cell adhesion molecule (VCAM-1) [304]. Stimulation of excitatory A_{2A} receptors enhances nitric oxide release and vasodilation [305], and stimulation of A_{2B} receptors leads to expression of angiogenic factors [306]. TNF- α also leads to the upregulation of A_{2A} receptors on peripheral immune cells [307]. Similarly, upregulation of A_{2A} receptors on neutrophils is seen following stimulation with TNF- α , which may reduce the damage caused by inflammatory immune infiltrate into the brain following stroke [295].

Following exposure to TNF- α , as in the context of preconditioning, expression of A_{2A} and A_{2B} receptors are increased. When combined with the surge of adenosine that accompanies neurological injury this likely causes immune cells to produce an anti-inflammatory response. In support of this idea, A_{2A} receptors have been shown to decrease TNF- α production and adhesion molecule expression following stimulation

with TLR4 agonists [308], which are also released endogenously following stroke [309]. Indeed, synergism between adenosine and TLRs are well documented, especially in peripheral immune cells [310-312]. While the involvement of adenosine receptors in TLR-mediated preconditioning has not been confirmed, direct regulation of adenosine-related gene products is also seen via microarray analysis in both brain and blood following TLR-mediated preconditioning (Stenzel-Poore lab, unpublished observation.) Further, systemic administration of LPS has been shown to lead to elevated adenosine levels in the brain [313]. Thus, endogenous release of adenosine following preconditioning ischemia may be a mediator of the tolerance phenotype. A greater understanding of the role of adenosine in endogenous neuroprotection may lead to interventions and therapeutic strategies useful in ischemia. A focus on the interaction between TLRs and adenosine receptors may be appropriate because systemic TNF- α levels remain lower—a feature that is preferable in the treatment of patients.

Hypothesis and Specific Aims of this Thesis

The long-term goal of this research was to better illuminate the mechanisms underlying the induction of neuroprotective phenotypes for the ultimate development of clinical therapeutic neuroprotectants. It is highly likely that the genomic reprogramming required in diverse forms of preconditioning may have overlapping mechanisms of induction. Toll-like receptors, with their ability to sense both endogenous and foreign danger signals, and adenosine, with its rapid release kinetics in response to damage signals, its wide receptor distribution, and potential role as an epigenetic modulator, may be key players in the induction of neuroprotection. The elucidation of a unifying theory of preconditioning could generate development of better neuroprotective therapies, lead to synergistic use of existing compounds, and enable of exploitation of existing, but heretofore undiscovered, endogenous protective mechanisms.

Specific Aims:

- 1. Test the efficacy of the preconditioning using the TLR9 agonist CpG in a non-human primate model of stroke to assess the potential translational potential of this therapy.**
- 2. Determine if adenosine is required for TLR-mediated preconditioning.**
- 3. Investigate the potential of adenosine to induce neuroprotection via epigenetic reprogramming.**

CHAPTER 2

Manuscript #1

Proof of Concept: Pharmacological preconditioning protects against cerebrovascular injury in a primate model of stroke

Frances Rena Bahjat^{1,*}, **Rebecca L. Williams-Karnesky^{1,*}**, Steven G. Kohama²,
G. Alexander West³, Kristian P. Doyle⁴, Nikola S. Lessov¹, Maxwell D. Spector¹,
Theodore R. Hobbs⁵, Mary Stenzel-Poore¹

***These authors contributed equally to this work.**

¹Department of Molecular Microbiology and Immunology, Oregon Health & Science University, Portland, Oregon, USA; ²Division of Neuroscience, Oregon National Primate Research Center, Beaverton, Oregon, USA; ³Colorado Brain & Spine Institute, Neurotrauma Research Laboratory, Swedish Medical Center, Englewood, Colorado, USA; ⁴ Department of Neurology and Neurological Sciences, Stanford University School of Medicine, Stanford, CA; ⁵Division of Animal Resources, Oregon National Primate Research Center, Beaverton, Oregon, USA

Chapter 2 is modified from the original paper published in the *Journal of Cerebral Blood Flow and Metabolism* on February 2nd, 2011 [191].

ABSTRACT

Cerebral ischemic injury represents a significant portion of the burden of disease in developed countries; rates of mortality are high and the costs associated with morbidity are enormous. Recent therapeutic approaches have aimed at mitigating the extent of damage and/or promoting repair once injury has occurred. Many patients at high risk of ischemic injury are easily identifiable, thus neuroprotective agents that can prevent brain injury before an insult occurs represent the holy grail in stroke therapeutics. Agents that stimulate the innate pattern recognition receptor, Toll-like receptor 9, have been shown to precondition the brain to ischemic injury in a mouse model of stroke. Here, we demonstrate for the first time that pharmacological preconditioning against cerebrovascular ischemic injury is also possible in a non-human primate model of stroke in the rhesus macaque. The model of stroke used for this study is a minimally invasive transient vascular occlusion resulting in primarily cortical damage; a model with clinical relevance. Finally, K-type (a.k.a. B-type) CpG oligonucleotides, the class of agents employed in this study, are currently in use in human clinical trials, underscoring the feasibility of this treatment in patients at risk of cerebral ischemia.

INTRODUCTION

Cerebral ischemic injury is the third leading cause of death and the leading cause of serious, long-term disability in the United States. Therapies for the treatment of stroke are often targeted toward the acute event, but neuroprotective strategies designed to reduce the damage caused by ischemic injury are highly feasible. Despite demonstrated efficacy in preclinical studies, a huge number of putative neuroprotective compounds have failed in clinical trials [314]. The discussion over reasons for failure has highlighted the need to vet potential neuroprotective compounds in nonhuman primate (NHP) models of stroke [315]. Unlike rodents, NHP have similar neuroanatomy and vasculature as compared to humans; rodents have lissencephalic brains, while humans and NHPs have gyrencephalic brains [316]. Moreover, NHP models of stroke offer the potential for more advanced neurological assessment compared to rodents, possibly providing a second outcome measure in addition to infarct volume [316-319]. Other similarities between human and NHPs include the ratio of gray to white matter and the threshold of these tissues to injury, which is important since these different tissues respond differently to therapeutic interventions and have different responses to brain ischemic injury [320-322]. For example, it has been shown that patients who survived a brief period of cardiac arrest had only minor changes in white matter, despite laminar necrosis in the cerebral cortex and severe ischemic changes in the basal ganglia [323]. Because they do differ in their neurochemical response to ischemia, amelioration of damage in gray and white matter will likely require different therapeutic approaches

and different models to test candidate therapeutics. Finally, studies performed in NHPs better extrapolate efficacious and toxic dose ranges for human subjects.

In response to the paucity of adequate NHP models of stroke, our laboratory recently developed a novel model of stroke in the rhesus macaque (*Macaca mulatta*) [324], an Old World monkey. In this model, the middle cerebral and anterior cerebral arteries are transiently occluded using a minimally-invasive transorbital approach, resulting in a highly reproducible stroke with good survivability. This remains the only NHP model of stroke that results in an infarct primarily involving cortical gray matter, allowing for targeted study of therapies designed to prevent cortical gray matter injury. Additionally, by producing a reliable pattern of damage centered on the primary motor cortex, the resulting neurological deficit in this model is plegia of the upper and lower extremities. This type of motor deficit is quantifiable in the NHP, whereas changes in alertness or cognition are not as readily ascertainable.

In many instances, patients can be identified as being at high risk for an ischemic event. For example, approximately half of patients undergoing coronary artery bypass surgery suffer long-term cognitive decline from intra-operative focal or global ischemia [325]. For these patients, prophylactic neuroprotection would be extremely beneficial and, as the results from this study show, this may soon become a viable clinical option. Specifically, Toll-like receptor (TLR) activation has shown great potential in prophylactic neuroprotection [326, 327]. TLRs sense pathogen-associated molecular patterns, both natural (i.e. bacterial lipopolysaccharide (LPS), bacterial DNA, and single-stranded RNA)

and synthetic (i.e. unmethylated cytosine-guanine rich DNA oligonucleotides (CpG ODNs), imidazoquinolines and polyinosinic:polycytidylic acid (poly I:C)). In addition to acting as sensors of invading pathogens, TLRs also act as sentinels of tissue damage and mediate inflammatory responses to aseptic tissue injury. When given in advance of ischemic injury in rodent models of cerebral ischemia, TLR ligands have demonstrated robust neuroprotective potential, likely through the reprogramming of the innate immune response to injury [126, 180, 183, 190, 328]. Prophylactic LPS has also been shown to salvage hippocampal neurons from ischemic death in a pig model of cardiopulmonary bypass [181], indicating the potential for broad utility of TLR ligands as neuroprotectants in a diverse range of conditions that result in cerebral ischemic injury. Importantly, TLR ligands are being developed for use in humans for a variety of clinical indications, both as monotherapies and as components of various FDA-approved and novel vaccine technologies [329]. Several CpG ODNs have shown reasonable safety profiles in humans and have been explored in numerous human clinical trials [329].

The goal of the present work was to evaluate the efficacy of a mixture of K-type CpG ODNs optimized for human immunostimulatory activity as a prophylactic neuroprotectant using this clinically-relevant NHP stroke model. These data satisfy the Stroke Therapeutics Academic Industry Roundtable recommendations [315] and are deemed a necessary precursor to advancement of these compounds to human clinical trials. To our knowledge, this is the first demonstration that a pharmacological preconditioning agent can protect the central nervous system from ischemic damage in the non-human primate.

MATERIALS AND METHODS

Animals

Nonhuman primates

Thirty adult, male rhesus macaques (*Macaca mulatta*; Oregon National Primate Research Center (ONPRC), Beaverton, OR) with an average age of 8.8 ± 2.3 years and an average body weight of 8.4 ± 1.7 kg, were selected for this study. Animals were single-housed indoors in double cages on a 12h:12h light/dark cycle, with lights-on from 0700 to 1900h, and at a constant temperature of $24 \pm 2^\circ\text{C}$. Laboratory diet was provided bi-daily (Lab Diet 5047, PMI Nutrition International, Richmond, IN) supplemented with fresh fruits and vegetables, and drinking water was provided *ad libitum*. The animal care program is compliant with federal and local regulations regarding the care and use of research animals and is Association for Assessment and Accreditation of Laboratory Animal Care (AAALAC)-accredited. All animal experiments were subject to approval by the Institutional Animal Care and Use Committee (IACUC) at the Oregon National Primate Research Center.

Mice

C57BL/6J mice (male, 8 to 10 weeks of age) were obtained from Jackson Laboratories (West Sacramento, CA, USA). All mice were housed in a facility approved by the AAALAC, met National Institute of Health guidelines, and were approved by the Oregon Health and Science University IACUC.

Reagents

ODN 1826 (tccatgacgttcctgacgtt), a mouse specific phosphorothioate CpG ODN was obtained from Invivogen (San Diego, CA, USA). Endotoxin levels were determined to be negligible (<0.125 EU/mg). Kmix CpG ODN, a 1:1:1 mixture of 3 human specific phosphorothioate K type ODNs (K3: ATC GAC TCT CGA GCG TTC TC; K23: TCG AGC GTT CTC; K123: TCG TTC GTT CTC), [330] was kindly provided by Dr. Dennis Klinman for mouse studies or obtained from Oligos Etc. (Wilsonville, OR, USA) for NHP studies.

Drug Treatments

For mice, a volume of 200 μ L of CpG ODN 1826, Kmix CpG ODNs, or saline vehicle was administered by intraperitoneal injection at indicated doses 72 hours before middle cerebral artery occlusion (MCAO). For NHP, a fixed dose volume of 1 mL of Kmix CpG ODN solution or saline vehicle was administered by intramuscular injection 72 hours before middle cerebral artery and anterior cerebral artery occlusion (MCA/ACAO). Animals were randomized to receive 0.06 mg/kg Kmix CpG (low dose), 0.3 mg/kg Kmix CpG (high dose) or saline. Investigators were blinded to treatments. The experimental timeline is depicted in **Figure 16A**.

Surgery

Mouse MCAO model

Cerebral focal ischemia was induced by MCAO as published previously [331]. Mice were anesthetized with 3% isoflurane and maintained with 1.5% to 2% isoflurane throughout the surgery. All surgical procedures were performed under an operating stereomicroscope. The middle cerebral artery was blocked by threading a silicone-coated 8-0 monofilament nylon surgical suture through the external carotid artery to the internal carotid artery, and blocking its bifurcation into the middle cerebral artery. The filament was maintained in place for 35 minutes while the mice were maintained under anesthesia; then the filament was removed and blood flow restored. Cerebral blood flow was monitored with laser Doppler flowmetry (Transonic System Inc., Ithaca, NY, USA). Temperature was monitored with a rectal thermometer and maintained at $37^{\circ}\text{C}\pm 0.5^{\circ}\text{C}$ with a controlled heating pad and lamp (Harvard Apparatus, Holliston, MA, USA). Mice were survived for 24 hours with access to soft food and water until euthanasia.

Two-vessel Occlusion Protocol in NHP

Two weeks before surgery, animals were screened for general health, endemic disease, and neurological disorders. The right middle cerebral artery (distal to the orbitofrontal branch) and both anterior cerebral arteries were exposed and occluded with vascular clips, as previously described [324]. Surgical procedures were conducted

by a single surgeon. Briefly, anesthesia was induced with ketamine (~10 mg/kg, intramuscular injection) and animals were then intubated and maintained under general anesthesia using 0.8% to 1.3% isoflurane vaporized in 100% oxygen. A blood sample was taken and a venous line was placed for fluid replacement. An arterial line was established for blood pressure monitoring throughout surgery to maintain a mean arterial blood pressure of 60 to 80mmHg. End-tidal CO₂ and arterial blood gases were continuously monitored to titrate ventilation to achieve a goal PaCO₂ of 35 to 40 mm Hg. The surgery was performed as described previously [324]. Post-operative analgesia consisted of intramuscular hydromorphone HCl and buprenorphine.

Infarct Measurements

Mouse

Mice were deeply anesthetized with isoflurane, and then perfused with ice-cold saline containing 2U/mL heparin. Brains were removed rapidly, placed on a tissue slicer, and covered with agarose (1.5%). The olfactory bulbs were removed and the remainder of the brain was sectioned into 1mm slices beginning from the rostral end into a total of seven slices. The area of infarction was visualized by incubating the sections in 1.5% TTC (2,3,5-triphenyltetrazolium chloride; Sigma Aldrich) in PBS for 15 mins at 37°C. The sections were then transferred to 10% formalin (Sigma Aldrich). Images of the sections were scanned, and the hemispheres and areas of infarct were measured using NIH ImageJ v1.38 software (Bethesda, MD, USA). The measurements were multiplied by the

section thickness and summed over the entire brain to yield volume measurements. Data of ischemic damage were calculated using the indirect method to minimize error introduced from edema. Percent infarct = (contralateral hemisphere volume – volume of noninfarcted tissue of the ipsilateral hemisphere)/(contralateral hemisphere volume) x100 [332].

Nonhuman primate

Measurement of infarct volume was performed using T₂-weighted magnetic resonance images taken after 48 hours of reperfusion [324]. All scans were performed on a Siemen's 3T Trio system, housed near the surgical suite at ONPRC. Because of the small filling capacity of the rhesus macaque head, an extremity coil was used to achieve better image quality of the brain. Anesthesia was induced initially with ketamine (10mg/kg intramuscular injection) and a blood sample was obtained. The animals were then intubated and administered 1% isoflurane vaporized in 100% oxygen for anesthesia maintenance. Animals were scanned in the supine position 2 days after surgery, and most animals also received baseline scans before surgery. Animals were monitored for physiologic signs, including pulse-oximetry, end-tidal CO₂, and respiration rate. All animals received anatomical MRI scans, which included T₁- and T₂-weighted, high-resolution time of flight scans, and a diffusion-weighted scan. The T₁ scan was an MPRAGE protocol, with TR=2500ms, TE=4.38ms, number of averages=1 and the flip angle=12°. Full brain coverage was attained at a resolution of 0.5mm isovoxel. The T₂ scan was a turbo spin-echo experiment, with TR=5280ms, TE=57ms, number of

averages=4, an echo train length of 5, and a refocusing pulse flip angle of 120°. The entire brain was imaged with a 0.5x0.5 mm in-plane resolution and a slice thickness of 1mm. For visualization of the region of infarction, sections were immediately placed in 1.5% 2,3,5-triphenyl tetrazolium chloride (TTC, Sigma) in 0.9% phosphate-buffered saline and stained for 15-45 mins at 37°C, as appropriate. Images from T2-weighted MRIs and TTC stained sections were examined for the location of infarction, and the total affected area measured using ImageJ, as previously described [324]. Each of the techniques (MRI, TTC) analyzed comparable anatomical regions and sampled approximately 15 slices (4mm each). Measurements of infarct volume as a percentage of the ipsilateral hemisphere or cortex were made using the following formula: (area damaged/total area)x100%.

Neurologic Assessment in NHP

Neurologic assessments were performed by a single observer, as previously described [333]. The scale evaluates motor function, behavior (mental status), and cranial nerve deficit and higher scores represent better functional outcomes. Motor function scores from 1 to 70, according to severity of hemiparesis in the left extremities, are presented. A score of 10=severe hemiparesis, 25=mild hemiparesis, 55=favors normal side, or 70=normal ability. Behavior and alertness scores are presented, ranging from 0 to 20, with 0=dead, 1=comatose, 5=aware but inactive, 15=aware but less active, and 20=normal.

Tissue Collection in NHP

Animals were euthanized 2 days after stroke; animals were taken directly from MRI to necropsy under sedation followed by deep anesthesia with 25mg/kg pentobarbital. Blood samples were drawn before exsanguination and perfusion with cold heparinized saline (2U/ml) through the ascending aorta. Brains were rapidly removed, placed in a rhesus brain matrix (ASI, Warren, MI, USA) and cut into 15 consecutive, 4-mm thick coronal slabs per brain.

Adverse Events in NHP Study

Two NHPs died during the surgical procedure. One animal from the 0.3 mg/kg Kmix CpG group died when the dura mater was ruptured prior to occlusion. One animal in the saline control group died 24 hours following surgery, and was found upon necropsy to have an abnormally enlarged heart, deemed the likely cause of death. Two primates in the saline control group were excluded from the study following surgery. One animal was excluded due to an intracranial bleed that continued post-surgically; the other was excluded due to a clotting problem that resulted in an extreme hemorrhagic transformation at the site of occlusion in addition to other subcutaneous hemorrhage events found at necropsy. Injections for two animals in the 0.3mg/kg Kmix CpG group were actually 0.24 and 0.37 mg/kg. No drug related adverse events were apparent. A third saline-treated animal was excluded from the dataset due to early termination at 24 hours post-occlusion. Exclusion of data for this animal did not alter the significance of the findings.

Inclusion of non-saline treatment controls in NHP Study

In order to account for excluded saline-treated control animals and increase the power of the study, five untreated animals were included in the control group for data analysis purposes. Untreated controls differed only in that they did not receive an intramuscular-injection of saline 72 hours prior to onset of surgical occlusion. There was no statistically significant difference in infarct volume between saline-treated ($41.6 \pm 2.0\%$) and untreated ($33.3 \pm 4.1\%$) animals ($p=0.12$ with Student's T test).

Plasma and Blood Analyses in NHP

Levels of GMC-SF, IFN- γ , IL-1 β , IL-2, IL-6, IL-8, IL-10, IL-12p70, and TNF- α were assayed using a 9-plex Proinflammatory Multiplex Human Cytokine ELISA Array (Meso Scale Design, Gaithersburg, MD). The limits of detection of plasma levels of all cytokines were 0.6 pg/ml; average levels of GMC-SF, IFN- γ , IL-1 β , IL-2, IL-8, IL-10, IL-12p70, and TNF- α were below detectable limit for most samples and group means were <5pg/mL. C-reactive protein was measured by human-specific Active[®] ELISA (Beckman Diagnostics, Brea, CA). Hematology parameters were determined using an ABX Pentra 60 analyzer (Horiba Medical, Irvine, CA).

Statistical Analyses

All statistical analyses were performed using Prism (Graphpad Software, La Jolla, CA). Group means were compared using a one-way ANOVA with Bonferroni's multiple

comparison *post-hoc* test. For data with repeated measurements, data were compared using a two-way ANOVA with Bonferroni's *post hoc* test. Data represent mean \pm standard error of the mean (SEM), unless otherwise noted. Differences were considered statistically significant when $p < 0.05$.

RESULTS

Prophylactic administration of Kmix CpG ODNs significantly reduces infarct damage in mice

Prior to testing in NHPs, the neuroprotective potential of prophylactic treatment with Kmix CpG ODNs was evaluated using a mouse MCAO model (**Figure 16**). Kmix CpG ODNs represent a mixture of three CpG DNA sequences, shown by Klinman and colleagues to optimally stimulate peripheral blood mononuclear cells (PBMC) from a heterogeneous human population [330]. This mixture of K-type ODNs was shown to have similar broad stimulatory activity in PBMC from rhesus macaques [334] and showed sufficient activity to be tested in mice, according to our studies. Results were compared to preconditioning with CpG ODN-1826, which has been previously shown to be neuroprotective in mice [190]. Three days prior to stroke, C57BL/6J mice ($n=4-8$) were treated with a single dose of increasing concentrations of Kmix CpG ODN or a single dose of ODN-1826 and infarct volumes were quantified at 24 hours following

reperfusion. Preconditioning with 0.8 mg/kg Kmix CpG ODNs resulted in a significant reduction in mean infarct volume in mice (**Figure 1**), demonstrating a $16.5 \pm 4.4\%$ infarct compared to $36.7 \pm 3.7\%$ for controls ($p < 0.05$). An equivalent dose of 0.8 mg/kg CpG ODN-1826 resulted in a similar decrease in mean infarct volume, from $36.7 \pm 3.7\%$ in control group to $17.8 \pm 4.6\%$ ($p < 0.05$).

Prophylactic administration of Kmix CpG ODNs significantly reduces cortical damage in NHPs

Using the optimal time window determined from mouse studies [190], Kmix CpG ODNs were administered 72 hours prior to surgical occlusion (**Figure 17A**). All doses of CpG were well tolerated by the rhesus macaque with no apparent toxicities. Prophylactic systemic administration of Kmix CpG ODNs significantly reduced cortical damage resulting from surgical occlusion (depicted in **Figure 17B and C**) in a dose-related manner, as assessed by T_2 MR imaging 48 hours after reperfusion (**Figure 18A and 19**). As compared to the control group ($37.0 \pm 2.64\%$ infarct volume), doses of 0.06 mg/kg and 0.3 mg/kg Kmix CpG ODNs reduced cortical damage to $27.3 \pm 4.8\%$ ($p > 0.05$) and $21.3 \pm 5.0\%$ ($p < 0.05$), respectively (**Figure 18A**). In addition to cortical stroke volume measurements using T_2 MR imaging, TTC staining of coronal sections was also performed and the area of infarct as a percent of ipsilateral hemisphere was determined (**Figure 18B**), rather than percent of cortex. Since the colorless TTC is enzymatically reduced to a red formazan product by dehydrogenases abundant in mitochondria, the

red intensity roughly correlates with the number and functional activity of mitochondria representing undamaged tissue [335]. Quantitation of infarct as a percent of cortex using TTC staining was not performed due to the unreliable nature of macroscopic identification of cortical regions in coronal tissue sections of the rhesus macaque. Importantly though, nearly identical magnitudes of neuroprotection were observed using both measurement approaches, despite the different nature of each measurement (**Figure 18B**). Specifically, a 42% reduction in mean infarct volume was observed between saline and 0.3mg/kg treated groups, when determined as a percent of ipsilateral hemisphere using TTC staining (**Figure 18B**); the magnitude of neuroprotection was identical to that obtained for percent of cortex using serial MR imaging approach (**Figure 18A**). Our previous studies show a significant correlation between percent of hemisphere infarct volumes measured using TTC staining and T₂ MR imaging methods [324]. Similarly, the current study showed a significant correlation between percent of hemisphere measurements derived using TTC and MRI approaches ($r=0.86$ by Spearman r correlation analysis, $p<0.0001$; data not shown).

Prophylactic administration of Kmix CpG ODNs improves neurological function in NHPs

In addition to assessment of infarct volume via T₂ MRI, animals were also examined for improvement in neurological function resulting from preconditioning using the modified Spetzler neurological scale adapted for evaluation of NHPs [333]. Groups receiving either 0.06mg/kg or 0.3mg/kg Kmix CpG ODNs prior to surgical

occlusion demonstrated an approximately 40% increase in motor function (27 ± 7 and 27 ± 8 , respectively) above that observed for the control group (19 ± 3) (**Figure 20A**). Though functionally relevant, this level of improvement was not dose-dependent or statistically significant in this study ($p>0.05$). As might be expected from a primarily cortical model of stroke, no significant difference in behavior and alertness was observed between control and CpG ODN-treated animals (**Figure 20B**).

Kmix CpG ODNs have no effect on blood cell composition following stroke

To monitor for potential effects of prophylactic CpG ODN administration on blood composition, basic hematological parameters at baseline (two weeks before surgery), at 72 hours post-drug administration just prior to surgery, and at the time of necropsy (48 hours after surgery) were assessed. No significant changes were observed between prescreen and surgery values for any of the treatment groups, suggesting that CpG treatment had no effect on the measured parameters at the time of stroke induction (**Table 5**). At 48 hours following surgery, there were no significant differences in mean WBC counts among groups, including animals receiving CpG treatment. In contrast, a statistically significant reduction in mean lymphocyte count was observed 48 hours after stroke in all groups compared to their respective prescreen values (**Table 5**). These results are consistent with findings in humans [336]. When compared to blood taken just prior to surgical occlusion, mean neutrophil count showed a trend for elevation in samples taken at the time of necropsy in all groups (**Table 5**), which also

correlates well with findings in humans after stroke [337]. These results also confirm our previous findings in stroked rhesus macaque [324].

Plasma IL-6 and CRP are elevated following stroke in NHPs

To investigate the effects of stroke and/or potential mechanisms of action of CpG ODNs in neuroprotection, plasma levels of key proinflammatory cytokines were measured. GM-CSF, IFN- γ , IL-1 β , IL-2, IL-6, IL-8, IL-10, IL-12p70, and TNF- α were measured. In our rodent model of stroke, we have found that elevation of systemic TNF- α is required for preconditioning with CpG ODNs [190]. Following administration of Kmix CpG ODNs in the non-human primates, very little detectable systemic TNF- α was observed at the time point measured, with the exception of a single animal (data not shown). This is not surprising given that the systemic increase seen in mice following CpG administration occurs one hour post drug administration, with a return to undetectable levels by three hours post-administration. Blood collection at earlier time points was not viable for the current study due to the necessity of anesthesia and/or the potential for introduction of stress, both of which have been shown to be neuroprotective. Following stroke, systemic levels of IL-6 were detectable at 48 hours post-stroke in all animals (**Figure 21A**), which correlates well with data from human stroke patients [338]. Mean levels of plasma C-reactive protein (CRP) (**Figure 21B**) were also significantly increased following stroke in all groups. While elevated plasma CRP levels are not disease specific, it can be a sensitive marker for tissue injury and

inflammation. Interestingly, there was no significant difference in mean systemic levels of CRP between treatment groups, despite an observed reduction in mean infarct volume following Kmix preconditioning. The animal with high TNF- α and IL-6 levels had unusually low WBC counts at all time points with no differences observed prior to or following treatment or stroke; however, no elevations in CRP were seen at prescreen or surgery time points (data not shown). All other cytokines were either below the detectable limit or present at very low levels with no differences observed between the time points examined.

DISCUSSION

Prophylactic CpG ODNs are a promising candidate therapy for individuals at high risk of cerebral ischemic injury. The therapeutic potential of CpG ODNs and other TLR ligands has been well documented in rodent studies [126, 180, 183, 190]; however, this is the first study to evaluate CpG ODNs as a prophylactic neuroprotective therapy in an NHP model of stroke. To our knowledge, this is the first proof of concept study to demonstrate pharmacological preconditioning protects the brain from ischemic injury in a clinically-relevant non-human primate model. In our study, two doses of Kmix CpG ODNs were given systemically 72 hours prior to occlusion. Our results demonstrate a significant, dose-related reduction in tissue damage and a trend towards improved neurological outcome at 48 hours post-reperfusion in animals receiving prophylactic

treatment with CpG ODNs. Importantly, no adverse drug-related events were apparent during the course of the study. Moreover, we show that inflammatory sequelae and hematological changes fitting with the human condition are present in this NHP model of stroke. These data further strengthen the value of this model for use as a preclinical testing ground for potential therapeutics and provides additional endpoints that might be useful biomarkers for later clinical efficacy assessment. Congruent with our previous findings, we also demonstrate that infarct volume determined using a functional measure of dehydrogenase activity (TTC method) correlates well with infarct volume determined using serial MR images. T₂ MR imaging is highly sensitive to water content producing a strong signal in areas of damage following cerebral ischemia [319]. In contrast, TTC staining is largely reflective of metabolic processes carried out by mitochondria in living tissue. Studies have shown that TTC-stained infarct regions correspond to the location and area of hyperintensity on MR images of the same brain [319]. Despite the differences in these independent parameters measured by two different techniques, similar magnitudes of neuroprotection were derived, further validating our results.

The three different CpG ODNs used in this study (referred to as K mix) were selected based on their potential to broadly stimulate an immune response in peripheral blood cells from a majority of the human population. Previous work by Klinman and others has shown that there is variation in the individual response of human immune cells based on differences in CpG ODN sequence and length [330]. While individual CpG ODN sequences are capable of eliciting robust responses in a given

inbred rodent strain, outbred populations, such as non-human primates and humans, show more highly variable and even absent immune responses with a given CpG ODN. Further, structural differences between various classes of CpG ODNs have been shown to selectively stimulate distinct cell populations, allowing these compounds to be used selectively to achieve specific therapeutic goals. K-type (also called B-type) ODNs predominantly stimulate B cells to proliferate and produce IgM and IL-6, while D-type (also called A-type) CpG ODNs predominantly elicit plasmacytoid dendritic cell production of type I IFNs and NK cell production of IFN- γ [334].

Prior to use in our non-human primate model of stroke, we tested Kmix CpG ODNs in our mouse MCAO model. Mouse models of stroke allow for easier manipulation and afford more flexibility when dissecting the mechanisms involved in drug efficacy. While rodent models are essential for the selection and validation of potential therapeutic targets, additional validation in primates is often warranted to enhance the chances of success in human clinical trials. To bridge this translational gap, models of stroke in animals genetically closer to humans have been called for by numerous groups [339]. By first testing our selected compound in rodents prior to testing in non-human primates, we sought to validate the use of both models for preclinical testing of TLR activators as neuroprotective agents. Understanding the limitations of both model systems for modeling human stroke with particular therapeutic targets may allow for more rapid validation or exclusion of development candidates. By showing that Kmix CpG ODNs are efficacious in both our mouse and NHP models of stroke, we confirm that

both systems can be used synergistically to investigate the mechanisms involved in TLR-induced preconditioning.

Though much work is needed to elucidate the precise mechanism of neuroprotection induced by CpG ODNs, we can begin to speculate based on data gathered from investigations in the rodent. It has come to be appreciated that reprogramming of the innate immune response appears to be a crucial part of the phenomenon of TLR-induced neuroprotection. Aside from functioning merely as sensors of invading pathogens, innate immune receptors are being increasingly recognized for their ability to also sense and alert the host immune system to endogenous damage as well. Though recruitment of immune cells to a site of injury can lead to removal of debris and dying cells and stimulation of repair processes, when inappropriately activated, this response can paradoxically lead to an exacerbation of damage, as demonstrated in sepsis. Through complex feedback mechanisms, signaling in the immune system is regulated to allow the appropriate response to various stimuli. In the case of TLRs, stimulation leads to the activation of two distinct signaling pathways, culminating in the activation of either NF κ B or IRF3 and IRF7 pathways and resultant production of TNF- α or type 1 interferons, respectively [340]. During a stroke, damaged and dying cells lead to a local release of endogenous molecules that stimulate TLRs [341]. These endogenous ligands promote the activation of NF κ B and downstream production of proinflammatory cytokines such as TNF- α , which can exacerbate injury. In mice lacking TLR4, which initially signals predominantly through the canonical NF κ B

pathway, damage due to ischemia is reduced [173, 342]. Also, intracerebroventricular (i.c.v.) injection of TNF- α at the time of stroke exacerbates ischemic damage [182].

In TLR preconditioning, much like in endotoxin tolerance, a small amount of stimulation leads to NF κ B activation and production of TNF- α , followed by the transcription of inhibitory molecules for the NF κ B signaling arm of the pathway. Thus, when a subsequent stimulatory event occurs (i.e., the release of endogenous TLR ligands in the case of stroke), TLR signaling is redirected to the IRF3 arm, resulting in increased production of type 1 interferons [196]. In addition to reducing the amount of inflammatory cytokines produced following signaling, the increased production of type 1 interferons may be directly beneficial. Data show that i.c.v. injection of IFN- β is protective at the time of stroke [201, 309]. The exact location of the TLR reprogramming event, either in the central nervous system or periphery, is still a matter of investigation. The fact that prophylactic TLR ligands are administered systemically at very low levels and these antigens have not been readily shown to cross the blood brain barrier, argues for some involvement of the periphery. However, direct changes in gene transcription and protein levels in the brain following drug treatment suggest a strong central nervous system component as well [309]. Repeated administration of CpG ODN in mice results in increased TNF mRNA in the brain, which is sustained following cessation of treatment [343]. These data suggest there may be a potential link between the peripheral and central compartments following systemic CpG ODN treatment.

Several studies have evaluated the ability of anti-sense ODNs to cross the blood brain barrier [344-346], which could result in direct stimulation of brain TLR9-expressing cells. One such study in mice showed that peripheral administration of a 42-mer phosphorothioate ODN (P-ODN) directed against the amyloid β protein resulted in brain distribution of this molecule [345]. P-ODNs were shown to cross the BBB via a saturable transporter termed oligonucleotide transport system-1 (OTS-1) and similar concentrations of P-ODN were observed between the cerebral spinal fluid and brain compartments. While it is conceivable that our phosphorothioate CpG ODNs may also cross the BBB, peripheral responses could also play a role. For instance, cerebrovascular endothelial cells may be critical mediators of the neuroprotection following systemic administration of CpG ODNs, as they may convey activating or inhibitory signals from the periphery to the CNS either directly via modulation of BBB permeability or indirectly.

The area of the brain that is protected by preconditioning may give further clues about possible mechanisms of action. Prophylactic administration of Kmix CpG ODNs resulted in a reduction in tissue damage primarily in the cortex of NHPs, similar to data in the mouse MCAO model [190]. Interestingly, previous studies in NHPs using PET to compare histology and oxygen metabolism between transient and permanent MCA occlusion show significantly greater damage to the cortex in transient ischemia [347]. This effect has been attributed to post-ischemic hyperperfusion observed in the cortex, but not the striatum; therefore, it would be reasonable to speculate that mechanisms of CpG-induced protection may include an attenuation of reperfusion injury.

In addition to collecting infarct volume data, we sought to enhance the current study by gathering functional neurological data from the animals post-ischemia. A trend for improvement in motor function was seen in CpG ODN treated animals, though differences were not statistically significant. Additionally, no differences in behavioral outcome were seen between control and CpG ODN-treated animals. There are several factors that may have contributed to the limited improvement of neurological parameters. All animals were maintained on post-operative analgesia for 48 hours following stroke, limiting our ability to accurately assess behavior and alertness of animals. Longer-term survival of animals and eventual discontinuation of analgesics would allow for a more accurate behavioral and motor deficit assessment. Additionally, the scale used to assess motor deficit does not clearly differentiate proximal versus distal functional deficits in the upper and lower extremities. Based on location of the infarct induced in this model, animals showing less severe deficits are characterized primarily by distal weakness, while dysfunction in more severely affected animals extends more proximally. Finally, assessing behavioral changes in rhesus macaques is challenging compared to humans, given their tendencies to mask physical deficits as a survival mechanism. A more extensive neurological scale designed to assess the specific deficits seen in this model is under development by our laboratory, which may provide greater insight into functional outcomes in future studies. Despite these complexities, cortical infarct volume was directly related to motor function outcome when considering data from all animals together, as statistical analysis revealed a significant correlation between these values ($p=0.04$ using Spearman's correlation and r value = -

0.42; data not shown). Specifically, as the infarct volume increased the extent of motor deficit observed increased, as indicated by a decrease in the motor score.

Utilizing a therapy that likely modulates the innate immune response may require fine-tuning of dose and regimen to elicit the desired response; too little preconditioning agent may not provide a strong enough signal for upregulation of neuroprotective molecules, too high of a dose may cause an adverse reaction. Based on data from the mouse, it appears that Kmix CpG ODNs afford protection over a specific concentration range, as efficacy is lost when the concentration of drug is too low or too high. In our study, no adverse events related to administration of drug were observed, and no increases in serum proinflammatory cytokine levels were observed at the time points measured. Further testing of additional doses and dose regimens in NHPs, as part of pharmacokinetic and pharmacodynamic studies, will help further define the optimal conditions for use of Kmix CpG ODNs.

Though Kmix CpG ODNs were administered systemically, no significant changes were seen in hematological parameters 72 hours after treatment, just prior to stroke induction. This result was not entirely surprising, as TLR preconditioning in mice appears to induce only a transient change in gene expression [136]. Also, a TLR7 ligand given systemically in mice has been shown to induce transient reversible leukocyte depletion from the blood [348]. These studies showed that peripheral blood leukocyte levels were reduced as early as one hour following TLR7 ligand treatment and were returned to normal by 24 to 48 hours. The resulting “transiently reduced availability of

peripheral-blood leukocytes” is referred to as “TRAP” and occurs due to increased endothelial adhesiveness contributing to increased leukocyte tissue residence time [348]. Overall, the lack of modulation of absolute numbers of peripheral lymphocytes and neutrophils observed between drug-treated (protected) and control (non-protected) animals could indicate that cells in the peripheral circulation are not responsible for the protective phenotype. An alternate hypothesis is that the peripheral blood cells have been reprogrammed to a less damaging or more protective phenotype, rather than being expanded or eliminated from the blood. A third possibility is that the effect of drug treatment on peripheral cells occurs transiently at a very early stage and the resultant signals responsible for later neuroprotection are conveyed at that time. Changes in circulating cells prior to day 3 following administration of CpG ODNs were not evaluated due to the potential negative effects on our stroke model, therefore, further study will be necessary to examine potential protective mechanisms.

Pretreatment with Kmix CpG ODNs also did not significantly alter the post-stroke distribution of peripheral blood cells in stroked NHPs. The magnitude of post-stroke lymphopenia was comparable in all groups, mirroring the results seen in humans with stroke. In humans, stroke typically induces a transient immediate loss of T-lymphocytes peaking at 12 hours after onset of stroke, which is recovered between day 7 and 14 post-stroke [336]. In our study, NHPs demonstrated neutrophilia following stroke, which has also been noted in humans. In one study conducted using stroke patients, a greater than 50 percent increase in neutrophil count was observed following stroke and changes were maintained for over 14 days post-stroke [336]. Another study in human stroke

patients showed that the magnitude of early neutrophilia correlated well with cerebral infarct size, as determined by MR imaging [337], although a direct cause-effect relationship could not be determined. The role of neutrophils in damage following ischemic injury has long been debated. Neutrophils are proposed to be important mediators of post-ischemic cerebral damage [349, 350], although more recent findings suggest that the presence of neutrophils may only be correlative with extent of pathology [351]. Interestingly, increases in blood neutrophil counts were observed in the most neuroprotected animals receiving 0.3 mg/kg Kmix CpG ODNs. This result agrees with studies by Ahmed and colleagues [183], whereby LPS preconditioned rats showed increased neutrophil infiltration with concomitant reduction in damage to the brain following MCAO. Due to the lack of modulation of absolute number of neutrophils, despite an observed reduction of infarct volume, it is plausible to speculate that these cells are either 1) not contributing to damage, or 2) are reprogrammed and thus less destructive following preconditioning.

Despite a decrease in tissue damage in our preconditioned animals, levels of CRP and IL-6 were similarly elevated at 48 hours following stroke in all treatment groups. Increases in CRP and IL-6 are seen acutely following stroke in humans, and these markers are considered potential biomarkers for infarct severity [338] [352, 353]. The increase seen despite reduction in infarct volume may be due to the non-specific association of these proteins with cerebral injury. Specifically, the surgical model itself or stress involved in animal manipulations may induce changes in levels of these acute phase reactants or their inducers, as our model involves manipulation of the dura mater

and cerebral vessels and post-surgical recovery. Of note, this study did not examine specific lymphocyte subpopulations, such as T regulatory cells, which may be altered by TLR preconditioning and may contribute to the protection conferred by these agents.

Based on data from our laboratory and others, prophylactic administration of TLR ligands has been shown to result in robust neuroprotection in rodents. Importantly, this work is the first demonstration that these neuroprotective agents are also efficacious in a nonhuman primate stroke model. These data provide important insights for the process of stroke drug development. The demonstrated congruence between data from mouse and NHP models is an important step in the preclinical development of TLR ligands as neuroprotectants. These data intimate that the mouse stroke model could serve to be a valuable tool for the development of this class of agents for stroke. Thus, CpG ODNs are highly promising therapeutics for clinical stroke prevention due to their favorable safety profile in humans. Determining how CpG ODNs precondition the brain to subsequent injury continues to be a subject of intense study. Of additional importance, this NHP stroke model demonstrates key clinical phenotypes observed in human stroke patients. In conclusion, our data support the idea that this model has good predictive value, serves as a valuable preclinical tool to validate potential therapeutic targets, and will allow for more adequate establishment of efficacious dose ranges and regimens for clinical studies in humans.

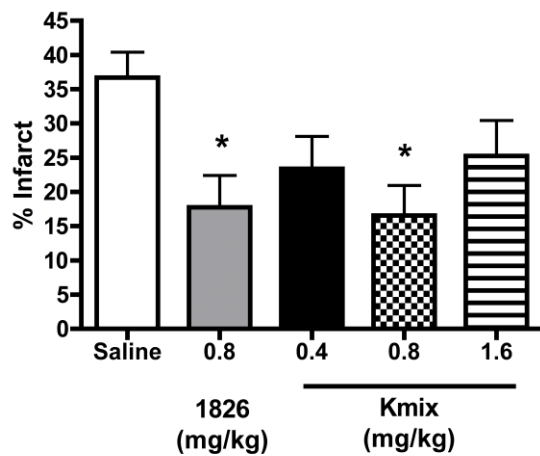


Figure 16. Reduction in infarct volume following MCAO in mice preconditioned with CpG 1826 or *Kmix* CpG ODNs

CpG ODNs or saline control was administered in a final volume of 200µl via intraperitoneal injection 72 hours prior to the onset of surgical occlusion. All animals were subjected to 35 minutes of MCA occlusion and infarct volumes were measured 24 hours following reperfusion. Data are displayed as mean ± SEM of n=4-7 per group and * denotes p<0.05 by one-way ANOVA and Bonferroni *post-hoc* test.

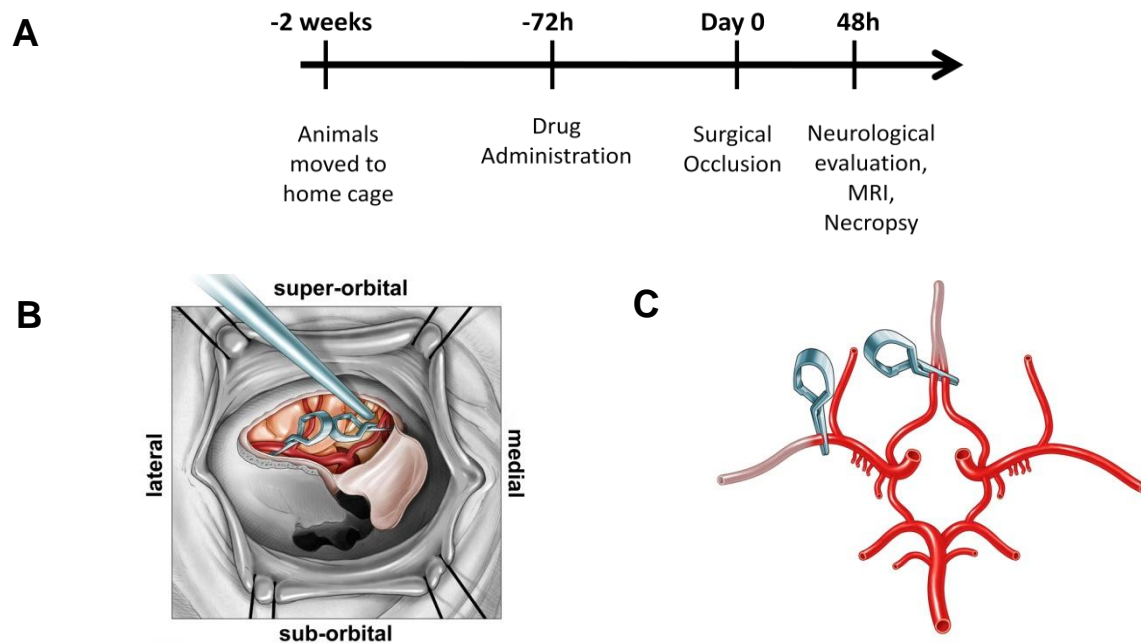


Figure 17. *Experimental timeline and surgical occlusion*

(A) Animals were assessed for physical health, blood was drawn for baseline prescreening and they were transferred to their home cages two weeks prior to surgery for acclimation. Kmix CpG ODNs or saline control was given 72 hours prior to surgery. Just prior to surgery, blood was drawn to assess drug-induced changes to peripheral cell populations and plasma cytokines. After 48 hours of reperfusion, animals were taken to MRI for imaging of final infarct volume. Following MRI, animals were taken directly to necropsy and tissues were collected. **(B,C)** Reproduction of schematic of the surgical site and vasculature of the rhesus two-vessel occlusion model from West *et al*, *Journal of Cerebral Blood Flow & Metabolism* (2009) 29, 1175–1186. **(B)** *In situ* surgical view of the right orbit of the rhesus macaque illustrating the exposure of major cerebral arteries and positioning of aneurysm clips for occlusion of the right middle cerebral artery and bilateral anterior cerebral arteries. **(C)** *Ex vivo* illustration of the Circle of Willis with one clip on the middle cerebral artery distal to the orbitofrontal artery (lateral clip) and a second clip on both anterior cerebral arteries (medial clip) just before the vessels join to form a single pericallosal artery.

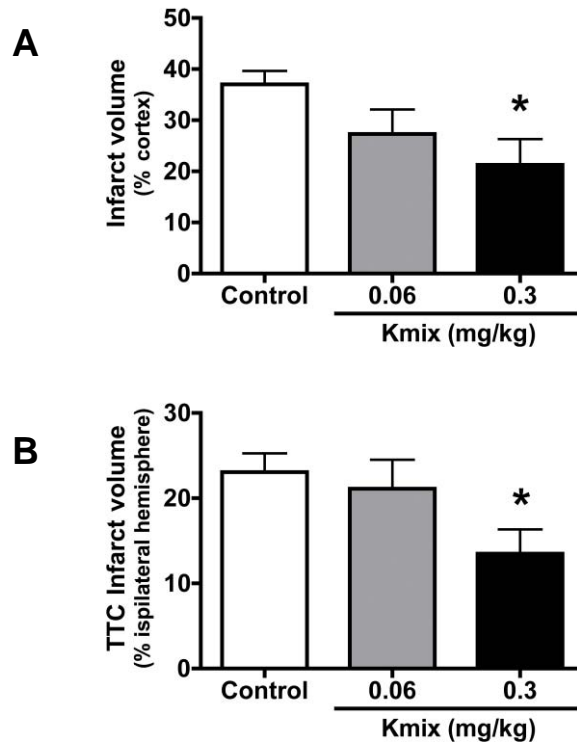


Figure 18. Reduction in infarct volume following MCA and ACA occlusion in NHPs preconditioned with Kmix CpG ODNs

Kmix ODNs or saline control was administered 72 hours prior to the onset of surgical occlusion via intra-muscular injection in a final volume of 1 ml. Infarct volume was measured 48 hours after reperfusion using **(A)** T₂ MRI scans to determine percent infarct of ipsilateral cortex and **(B)** TTC staining to determine infarct as a percent of ipsilateral hemisphere. Data are expressed as mean ± SEM and * denotes p<0.05 using one-way ANOVA with Bonferroni *post-hoc* test.

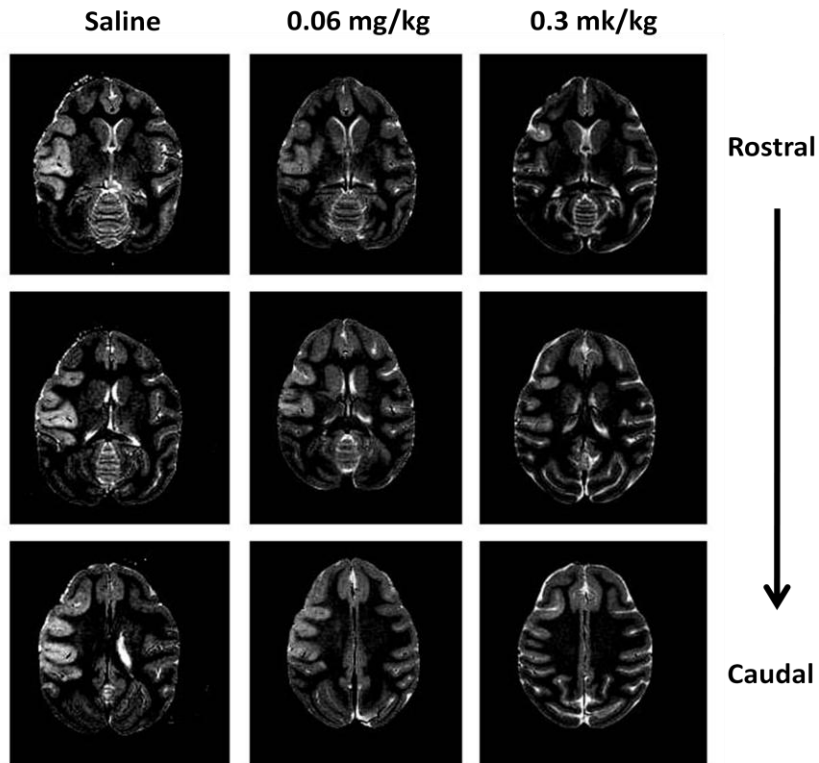


Figure19. Cortical infarct is reduced following pretreatment with CpG ODNs as seen by T2 MRI

Imaging was performed 48 hours following 60 minutes of surgical occlusion of the right MCA and both ACAs. Images shown depict infarct progression at various levels of the brain from rostral to caudal with left of image reflecting the right hemisphere; each column displays one representative animal from each treatment group. Infarct appears light on image, while non-infarcted tissue appears dark.

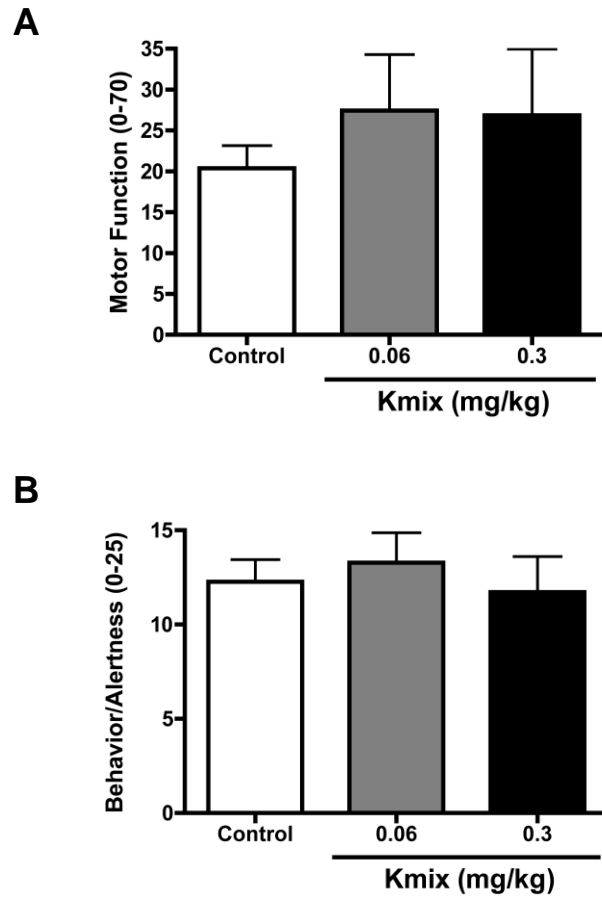


Figure 20. Neurological improvement following preconditioning with Kmix CpG ODNs

(A) Motor function and **(B)** behavior and alertness were assessed using the modified Spetzler neurological scale at 48 hours following surgical occlusion, prior to sedation for MRI. To minimize the sedative effects of post-operative analgesics animals were assessed in the morning, at least 6 hours after their last dose of pain medications. Data displayed are mean \pm SEM.

Table 5. Complete Blood Count Summary

Prescreen	WBC (10 ³ /mm ³)	Neutrophils (10 ³ /mm ³)	Lymphocytes (10 ³ /mm ³)	Monocytes (10 ³ /mm ³)	Eosinophils (10 ³ /mm ³)	Basophils (10 ³ /mm ³)	RBC (10 ⁶ /mm ³)	Platelets (10 ³ /mm ³)	HCT (%)
Control	8.63±2.12 ^A	4.16±2.21	3.94±1.09	0.33±0.14	0.10±0.05	0.08±0.02	5.61±0.42	255.2±81.1	40.5±2.5
0.06 mg/kg Kmix CpG	7.61±2.21	4.24±1.71	2.68±0.73	0.31±0.13	0.16±0.11	0.08±0.05	5.61±0.42	322.4±61.3	40.0±2.3
0.3 mg/kg Kmix CpG	9.63±5.05	4.37±3.39	4.87±2.40 ^C	0.38±0.22	0.30±0.29	0.011±0.08	5.64±0.42	317.3±96.9	41.1±2.2
Surgery									
Control	6.35±3.04	2.82±1.81	3.12±1.18	0.24±0.21	0.10±0.09	0.05±0.06	5.35±0.42	300.5±72.9	38.6±2.6
0.06 mg/kg Kmix CpG	6.79±2.95	3.54±2.43	2.30±0.68	0.28±0.10	0.09±0.04	0.03±0.02	5.23±0.25	295.3±83.4	38.1±2.3
0.3 mg/kg Kmix CpG	7.04±2.37	3.07±1.44	3.45±1.22	0.31±0.09	0.14±0.09	0.09±0.09	5.53±0.29	284.0±48.5	39.9±1.6
Necropsy									
Control	6.91±3.41	4.27±1.97	1.79±0.94 ^{A,B}	0.52±0.38 ^A	0.09±0.07	0.06±0.07	4.77±0.48	280.2±70.9	34.9±1.0
0.06 mg/kg Kmix CpG	6.44±2.40	4.72±2.17	1.67±0.81 ^E	0.47±0.19	0.09±0.08	0.05±0.03	4.98±0.57	301.1±45.6	36.4±4.3
0.3 mg/kg Kmix CpG	7.60±2.32	4.55±1.72	2.34±1.11 ^D	0.62±0.26 ^C	0.10±0.07	0.07±0.04	5.00±0.90	267.6±68.3	36.2±2.6

Data represent mean ± SD of n=7 for Kmix groups and n= 11 for control group. Prescreen denotes analysis of blood drawn two weeks prior to occlusion, surgery denotes blood draw at the time of surgery (72 hours post-treatment and prior to occlusion), and necropsy denotes 48 hours after reperfusion. WBC denotes white blood cells, RBC denotes red blood cells, HCT denotes hematocrit. Two-way ANOVA comparisons of timepoints with Bonferroni post-hoc test indicated significance of ^Ap<0.05 versus control surgery value, ^Bp<0.001 versus control prescreen, ^Cp<0.05 versus 0.3mg/kg surgery value and ^Dp<0.001 versus 0.3 mg/kg prescreen value; and comparisons of group means indicated ^Ep<0.01 versus 0.3 mg/kg prescreen value.

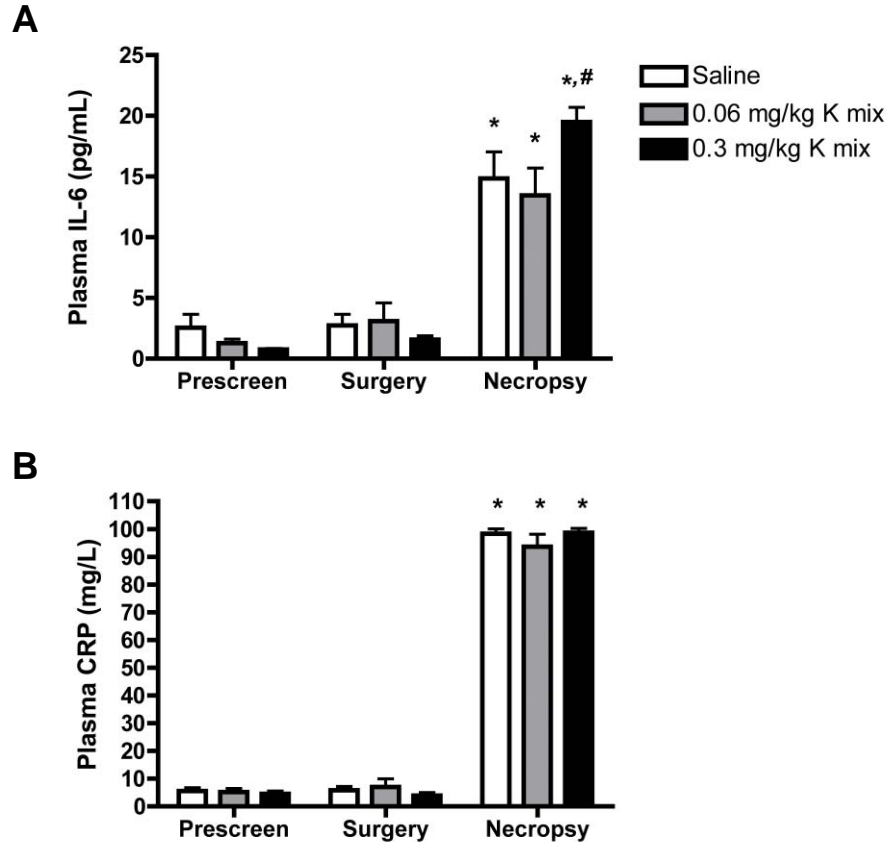


Figure 21. Plasma IL-6 and CRP are elevated following stroke in NHPs

Blood samples for plasma cytokine analysis were taken at 48 hours following vessel reperfusion. (A) Plasma IL-6 and (B) CRP levels were measured and * denotes $p < 0.05$ for all groups at time of necropsy versus all other timepoints. One outlier was excluded for IL-6 values from 0.06mg/kg group, as animal demonstrated 1 log higher values for IL-6 (range 166-170pg/mL) and TNF- α (range 650-857pg/mL) at all time points with no deviation post-ischemia. Data are displayed as mean \pm SEM of $n=6-7$ /group. Using Two-way ANOVA with Bonferroni *post-hoc* test, * denotes $p < 0.05$ versus prescreen and surgery timepoints and # denotes significance versus saline ($p < 0.05$) and 0.06 mg/kg ($p < 0.01$) groups at necropsy.

CHAPTER 3

Manuscript #2

Adenosine kinase determines the degree of brain injury after ischemic stroke in mice

Hai-Ying Shen¹, Theresa A Lusardi¹, **Rebecca L Williams-Karnesky^{1,2}**, Jing-Quan Lan¹,

David J Poulsen³, and Detlev Boison^{1,2}

¹ Robert Stone Dow Neurobiology Laboratories, Legacy Research Institute, Portland, OR 97232, USA. ² Dept of Neurology, Oregon Health and Science University, Portland, OR 97239, USA. ³ Dept of Biomedical and Pharmaceutical Sciences, University of Montana, Missoula, MT 59812, USA.

Chapter 3 is modified from the original paper published in the *Journal of Cerebral Blood Flow and Metabolism* on March 23, 2011 [354].

ABSTRACT

Adenosine kinase (ADK) is the major negative metabolic regulator of the endogenous neuroprotectant and homeostatic bioenergetic network regulator adenosine. We used three independent experimental approaches to determine the role of ADK as a molecular target for predicting the brain's susceptibility to ischemic stroke. First, when subjected to a middle cerebral artery occlusion (MCAO) model of focal cerebral ischemia, transgenic fb-Adk-def mice, which have increased ADK expression in striatum (164%) and reduced ADK expression in cortical forebrain (65%), demonstrate increased striatal infarct volume (126%) but almost complete protection of cortex (27%) compared to wild-type controls, indicating that cerebral injury levels directly correlate to levels of ADK in the CNS. Second, we demonstrate abrogation of lipopolysaccharide (LPS)-induced ischemic preconditioning in transgenic mice with brain-wide ADK overexpression (Adk-tg), indicating that ADK-activity negatively regulates LPS-induced tolerance to stroke. Third, using adeno associated virus (AAV)-based vectors that carry *Adk*-sense or -antisense constructs to overexpress or knockdown ADK *in vivo*, we demonstrate increased (126%) or decreased (51%) infarct volume, respectively, four weeks after injection into the striatum of wild-type mice. Together, our data define ADK as a possible therapeutic target for modulating the degree of stroke-induced brain injury.

INTRODUCTION

Despite intensive research into the development of neuroprotective drugs, to date no clinically viable pharmacological therapy exists to prevent neuronal injury after stroke [355]. Therefore, endogenous neuroprotective mechanisms are of critical importance [356] and might be exploited as alternative therapeutic approaches. Several endogenous neuroprotectant mechanisms are known, including the phenomenon of ischemic tolerance, in which a “preconditioning” event (e.g. a mild stroke, or a challenge with an endotoxin, such as lipopolysaccharide, LPS) protects the brain against a subsequent stroke [356]. Although effective in blunting the deleterious effects of a stroke, the underlying mechanisms of ischemic preconditioning are only partly understood. Epigenetic mechanisms might be involved in this phenomenon [130], as direct neuroprotective mediators have been identified by genomic and proteomic analyses [357].

The purine ribonucleoside adenosine is an endogenous neuroprotectant of the brain, which is uniquely poised to provide homeostatic bioenergetic network regulation due to its direct biochemical and pharmacological interactions with energy homeostasis, nucleic acid metabolism, methylation status, and adenosine receptor dependent signaling pathways [219, 255, 358-361]. In brain, synaptic levels of adenosine are largely regulated by an astrocyte-based adenosine cycle [362]. Astrocytes express two types of equilibrative nucleoside transporters and reuptake of adenosine is driven by intracellular phosphorylation of adenosine into 5'-adenosine monophosphate (AMP) via adenosine kinase (ADK) [362].

Brain injury is characterized by a global acute surge of adenosine, which likely constitutes an endogenous protective response of the brain [363]. Specifically, adenosine levels have been shown to increase rapidly in both the infarct and non-infarcted hemispheres following the induction of MCAO [364]. This increase in adenosine may act as an acute neuroprotectant, as well as an inducer of delayed neuroprotection. Strikingly, the key regulatory enzyme of adenosine, ADK, is also endogenously regulated following stroke, and its expression is decreased following onset of injury thus potentiating the adenosine surge [365]. Thus, expression levels of ADK might play a crucial role in determining the brain's susceptibility to stroke-induced injury. Indeed, transgenic mice overexpressing ADK are highly susceptible to stroke-induced brain injury [229]. We therefore hypothesized that experimental or therapeutic manipulations that reduce ADK expression would confer a neuroprotective phenotype to the brain similar to ischemic preconditioning. This finding would be highly meaningful, as modulation of brain ADK levels may be a viable target for therapeutic manipulation in clinical stroke. We further hypothesized that ischemic preconditioning would be abrogated under conditions of increased adenosine clearance, such as ADK overexpression, as an acute surge of adenosine may serve as a key initiator of delayed ischemic tolerance.

To address our research hypotheses we pursued three independent experimental approaches:

(i) Using a transgenic mouse model with reduced ADK in forebrain (fb-Adk-def), we demonstrate almost complete protection of cortical structures from the deleterious

effects of 60 minutes of middle cerebral artery occlusion (MCAO). (ii) Using a transgenic mice with brain-wide overexpression of ADK (Adk-tg) we demonstrate abrogation of ischemic preconditioning. (iii) Using an AAV-based gene therapy approach, we demonstrate that knockdown of ADK can protect the brain from the effects of a stroke. Together, our data define a novel role for ADK as a critical molecular determinant of injury severity following stroke; in addition, our data imply that a knockdown of ADK in the brain may lead to a state of permanent ischemic tolerance.

MATERIALS AND METHODS

Animals

All animal procedures were conducted in a facility accredited by the Association for Assessment and Accreditation of Laboratory Animal Care (AAALAC) in accordance with protocols approved by the Legacy Institutional Animal Care and Use Committee (IACUC) and the principles outlined by the National Institute of Health (NIH). Male C57BL/6 wild-type (WT) mice (Charles River, Wilmington, MA, USA) and fb-Adk-def and Adk-tg mutants of the same genetic background weighing 25 to 30 g were housed under diurnal lighting conditions (12 h/12 h cycle). The fb-Adk-def mutant line was recently created by cross-breeding *Emx1-Cre-Tg3* mice expressing Cre-recombinase in neurons and astrocytes of the telencephalon with ADK transgenic mice (“Adk-tg mice”) carrying a *loxP*-flanked ADK transgene (*Adktm1^{-/-}:TgUbiAdk*) in an otherwise lethal ADK knockout (*Adktm1^{-/-}*) background [366]. The resulting *Adktm1^{-/-}:Tg(UbiAdk):Emx1-Cre-Tg3* mice

(referred to as “fb-Adk-def mice”) are triple mutants homozygous for the deletion of the endogenous *Adk* gene, homozygous for the *Adk*-transgene, and heterozygous for Cre. These animals have a forebrain-selective reduction of ADK in cortical and hippocampal regions, while ADK continues to be overexpressed in striatum in analogy with the *Adk*-tg mice. Mutant animals for this study were generated by breeding *Adk*-tg mice with fb-*Adk*-def mice, resulting in both genotypes as littermates in a 1:1 ratio.

Focal Ischemia reperfusion model

Transient focal ischemia (30 or 60 min) was induced by occlusion of the middle cerebral artery in mice anesthetized using 1.5% isoflurane, 70% N₂O and 28.5% O₂. Ischemia was induced by introducing a coated filament (6.0; Doccol, Redlands, CA, USA) from the external carotid artery into the internal carotid and advancing it into the arterial Circle of Willis, thereby occluding the middle cerebral artery. The suture was maintained intraluminally for 30 or 60 minutes, and was then removed to restore blood flow. Regional cerebral blood flow was monitored by transcranial laser Doppler flowmetry (Transonic System Inc., Ithaca, NY, USA) throughout surgery to confirm occlusion of the MCA. Mouse body temperature was maintained at 36 °C ± 0.5°C with a thermostat-controlled heating pad (Harvard Apparatus, MA, USA). All surgical procedures were performed under an operating stereomicroscope.

Lipopolysaccharide (LPS) preconditioning

LPS preconditioning was conducted as previously described [180] with minor modifications. Briefly, adult male wild-type C57BL/6 mice and Adk-tg mutants received an intraperitoneal injection of phenol-extracted LPS (0.2mg/kg, in a volume of 0.1ml/10g bodyweight) from *Escherichia coli* 055:B5 (L-2880; Sigma, St Louis, MO, USA). Control mice received an intraperitoneal injection of sterile saline of the same volume. Three days after injection all mice were challenged with either 30 min or 60 min of MCAO. After 23 h of reperfusion mice were sacrificed for histological evaluation of infarct volume.

Determination of the infarct volume

To quantify infarct volume, two methods were used: 2,3,5-triphenyltetrazolium hydrochloride (TTC) staining and Nissl staining. Mice subjected to MCAO were sacrificed 23 h after ischemia. For TTC staining, perfused mouse brains were removed and placed into a mouse brain mold calibrated for dissection of 1 mm slices at regular intervals. Six adjacent 1 mm thick coronal sections were stained by immersion in 2% (w/v) TTC. For Nissl staining, mouse brains were first processed as described in the Immunohistochemistry section below and then subjected to a standard Nissl staining procedure [367]. Infarct-volume was calculated according to published procedures [180]. Cortical and striatal infarct volumes were calculated separately by subtracting undamaged areas of the ipsilateral hemisphere from the contralateral non-ischemic

hemisphere. Total infarct volume was calculated by summing area of infarct from 6 sections and multiplying by slice thickness. Percent infarct was calculated as described previously; results are reported as indirect infarct volume [229].

Intrastriatal delivery of AAV8

Generation of adeno associated virus (AAV)-based vectors targeting adenosine kinase was performed as described [368]. Briefly, constructs expressing the cytoplasmic isoform of ADK in either sense, to overexpress ADK (“ADK-SS”), or antisense orientation, to knockdown ADK (“ADK-AS”), under the control of the *gfaABC1D* promoter [369], to express the constructs selectively in astrocytes, were packaged into AAV serotype 8 – based vectors. Control vectors contained either an empty vector backbone (“AAV-null”) or expressed a green fluorescent protein under the control of the same promoter (“AAV-GFP”). To manipulate local ADK expression, intrastriatal injections of ADK-SS, ADK-AS, AAV-Null, and AAV-GFP were performed in adult male wild-type C57BL/6 mice under general anesthesia (1.5% isoflurane, 30% O₂, and 68.5% N₂O) using stereotactic procedures (AP = 1.0 mm; ML = -1.6 mm; DV = -3.4 mm). Viral particles were unilaterally injected using a 5- μ l Hamilton syringe with a 34-gauge stainless steel injector (Plastics One, Roanoke, VA) in 2 μ l of concentrated viral solutions (10¹² genomic particles/ml) at a rate of 0.5 μ l/min. The needle was left in place for an additional 3 minutes after injection to minimize reflux. Four weeks after virus injection, animals were subjected to MCAO followed by histological analysis. To evaluate efficiency of

virus delivery, AAV-GFP was co-injected with ADK-SS or ADK-AS at a 1:1 (v/v) ratio in another set of animals, which were also sacrificed at four weeks for histological evaluation.

Immunohistochemistry

To determine changes in the pattern of ADK expression, naïve fb-Adk-def and WT mice as well as virus-injected WT mice that were not subjected to MCAO were sacrificed for immunohistochemical analysis as previously described [370] with slight modification. Mice were transcardially perfused with saline followed by 4% paraformaldehyde. Brains were removed and post-fixed in 4% paraformaldehyde, cryoprotected in 10% dimethylsulfoxide in phosphate-buffered saline (v/v, PBS) overnight, and then sectioned into 40- μ m coronal sections using a vibratome (Leica, VT 1000s). For the detection of ADK, brain slices were incubated overnight at 4°C with primary anti-ADK diluted 1:5000 in Tris-Triton, pH 7.4 with 2% normal serum and 0.2% Triton X-100. Sections were then washed in TBS plus 0.05% Triton X-100, pH 7.4. For Immunofluorescence staining, this was followed by a 30 min incubation at room temperature in donkey anti-mouse secondary antibody, conjugated to Cy3 (1:300) (Jackson Immuno Research, West Grove, PA, USA). The sections were then washed and mounted on gelatin-coated slides and coverslipped with Dako fluorescent mounting medium (Carpentaria, CA, USA). For Immunoperoxidase-staining, after incubation with primary anti-ADK antiserum, slices were incubated for 30 min in a biotinylated goat anti-

rabbit secondary antibody (1:300). After washing, brain slices were incubated with avidin-biotin enzyme complex (Vectastain Elite Kit; Vector Labs, Burlingame, CA) for 20-30 min, followed by incubation in hydrogen peroxide and 3,3'-diaminobenzidine (DAB) hydrochloride (Sigma, St Louis, MO). The sections were mounted on gelatin-coated slides, air-dried, dehydrated, and cover slipped [370]. Digital images of ADK immunohistochemistry were acquired using a Zeiss AxioPlan inverted microscope equipped with an AxioCam 1Cc1 camera (Carl Zeiss MicroImaging, Inc., Thornwood, NY); all images were acquired under identical conditions and all image processing was applied identically across different experimental groups.

Western blot analysis

To quantify ADK expression, the striatum or cortex of naïve adult fb-Adk-def mutants and WT mice (n=5 per genotype), or AAV8-virus injected WT mice (n = 4 per AAV8-virus subtype) were processed for aqueous protein extraction as described [371]. Cell extracts were standardized to 40 µg proteins per lane, and electrophoresed in a 10% Tris-glycine gel. After transfer, membranes were incubated in polyclonal rabbit antiserum against ADK (1:5000), followed by incubation with peroxidase-conjugated anti-rabbit antibody (#7074, 1:8000, Cell Signaling, MA). Immunoblots were quantified using a Kodak Scientific Imaging System (v3.6.5.k2, Kodak). To normalize ADK immunoreactivity to protein loading, a mouse monoclonal anti- α -tubulin antibody (# sc-

8035, 1:5000; Santa Cruz, CA) was used to reprobe the same blot and the OD ratio of ADK to α -tubulin was calculated.

In vivo biosensor measurements

The adenosine biosensors used in this study were microelectrodes covered with an enzyme matrix containing adenosine deaminase and xanthine oxidase. Enzymatic degradation of adenosine creates an electrochemical gradient that can be quantified using a potentiostat. Selectivity for adenosine is controlled for by including inosine sensors that do not contain adenosine deaminase. Subtraction of the “inosine” signal (background) from the “adenosine” signal is used to calculate the tone of adenosine. This method has been described in detail elsewhere [372]. Adenosine (ADO, #SA-1003-05) and inosine (INO, #SA-1004-05) microelectrode biosensors were purchased from Sarissa Biomedical (Coventry, UK). Prior to use the sensors were rehydrated in buffer A (2 mM NaH_2PO_4 buffer, pH 7.4, 100 mM NaCl, 1 mM MgCl_2 , 2 mM glycerol) overnight and pre-calibrated with 40 μM adenosine or inosine in Buffer A, according to the manufacturer’s protocol. To measure *in vivo* adenosine levels, mice were affixed in a stereotactic frame under anesthesia (1.5% isoflurane, 70% N_2O and 28.5% O_2). A 15 mm skin incision was made along the sagittal suture to expose the skull of the animals, and a hole was drilled through the skull with the center corresponding to the following coordinates: AP -1.00 mm, ML +1.60 mm. After breaching the dura a mini-reservoir was created around the hole using a silicon gasket (diameter of 8 mm) affixed to the skull

using Loctite glue (#01-06966, Henkel Co.) (**Figure 23B**). The mini-reservoir was continuously perfused with HEPES-buffered saline (HBSS, containing 140 mM NaCl, 2 mM CaCl₂, 1 mM MgCl₂, 3 mM KCl, 10mM HEPES, and 10 mM glucose, 7.4 pH, sterile filtered) throughout the experiment. Pre-calibration to determine sensor response was performed by adding solutions of adenosine, inosine and serotonin to the mini-reservoir (**Figure 23B**). The biosensor was mounted on a stereotaxic manipulator and inserted into the brain at the following coordinates: AP -1.00 mm, ML +1.60 mm and DV -1.50 mm, and AP -1.00 mm, ML +1.60 mm and DV -3.40 mm, for cortical and striatal adenosine quantifications, respectively. Sensor signals were amplified using a Duostat ME 200+ Amplifier (Sarissa, UK), digitized (PowerLab, AD Instruments, Colorado Springs, CO), and recorded using LabChart Pro (AD Instruments). Adenosine tone was calculated using averages after currents had stabilized (typically 35 minutes after probe insertion into brain). Following removal from the brain sensors were allowed to equilibrate in HBSS (**Figure 23A**). The difference between the in-brain and in-HBSS measurements corresponds to local adenosine [or inosine] tone. INO sensors were used to normalize adenosine levels following the same procedure. After each measurement, the sensor was re-calibrated using 10 μM adenosine or 10 μM inosine, as appropriate, in HBSS with 1 μM NaH₂PO₄, and the inosine signal was subtracted from the adenosine signal to calculate the adenosine tone. Data from fb-Adk-def mice (n = 3) were normalized against data derived from WT mice (n = 3) using the same approach.

Statistical analysis

Values are expressed as means \pm SEM. Statistical analysis was performed with one way ANOVA followed by post-hoc analysis or student t-test. $P < 0.05$ and $P < 0.01$ were accepted as statistical significance.

RESULTS

ADK expression levels in fb-Adk-def mice determine the tone of ambient adenosine

To determine whether experimental manipulation of ADK expression affects the tone of ambient adenosine, we made use of transgenic mice with a dichotomous expression pattern of ADK in brain: fb-Adk-def mice are triple mutants based on (i) systemic deletion of the endogenous (subject to endogenous regulation) *Adk*-gene, (ii) expression of a ubiquitously (not subject to endogenous regulation) expressed loxP-flanked *Adk*-transgene leading to brain-wide overexpression of ADK, and (iii) expression of Cre-recombinase under the control of an *Emx1*-promoter leading to forebrain-selective reduction of ADK [367]. To assess the consequences of this genetic manipulation on ADK expression levels within the striatum and cerebral cortex, we first performed ADK immunohistochemistry on brains from naïve adult male fb-Adk-def or wild-type (WT) mice. As expected, fb-Adk-def mice had significantly reduced cortical ADK expression compared to WT mice, whereas expression levels of striatal ADK remained high as seen in *Adk*-tg mice (**Figure 22A**). The regional changes in ADK

expression were further characterized by Western blot analysis performed using micro-dissected brain regions, i.e. cortex and striatum, derived from fb-Adk-def and WT mice (**Figure 22B, upper panel**). Quantification of the Western blot by densitometry confirmed the immunohistochemical findings of reduced ADK levels in the cortex of fb-Adk-def mice ($64.6 \pm 4.6\%$, $n=10$, $p<0.01$) and increased ADK levels in the striatum ($163.6 \pm 6.4\%$, $n=10$, $p<0.01$, **Figure 22B, lower panel**), compared to WT controls.

Since ADK is the key adenosine metabolizing enzyme in the adult mouse brain, any change in ADK expression is expected to result in changes in ambient adenosine. To quantify changes in ambient adenosine (adenosine tone) as a result of the genetic manipulation in fb-Adk-def mutants, we used adenosine (ADO) microelectrode biosensors [373] to measure regional adenosine levels in real-time *in vivo* (**Figure 23A and 23B**) thereby minimizing potential artifacts that are frequently associated with postmortem quantifications of adenosine [374]. Corresponding to the regional overexpression of ADK, striatal adenosine levels in fb-Adk-def mice were significantly lower ($50.4 \pm 3.9\%$) than in the striatum of WT mice ($n=3$, $p<0.01$). Conversely, cortical adenosine levels in fb-Adk-def mice were significantly higher ($163.3 \pm 17\%$) than in WT mice ($n=3$, $p<0.05$, **Figure 23C**), in line with reduced ADK expression in cerebral cortex. To control for the specificity of the ADO-biosensor measurements to adenosine we performed analogous inosine-biosensor recordings and found no differences between cortical and striatal inosine levels in the fb-Adk-def mutants (data not shown). Our data demonstrate that regionally restricted changes in ADK expression translate into significant changes in ambient adenosine levels.

Cortical reduction of ADK provides regional protection from stroke

To test whether the genetic reduction of ADK in the cortex of fb-Adk-def mice could confer resistance to stroke-induced brain injury, we subjected fb-Adk-def mice to a paradigm of middle cerebral artery occlusion (MCAO) that modeled transient focal ischemia. Adult male WT (n=10) and fb-Adk-def mice (overexpression of ADK in striatum, but reduced expression of ADK in cortex, **Figure 22**) (n=11) were subjected to 60 minutes of MCAO followed by 23 h of reperfusion. In contrast to the lethal outcome of 60 minutes of MCAO in Adk-tg mice (which globally overexpress ADK in the brain) [229], all WT and fb-Adk-def mice survived until sacrifice 23 hours after injury (data not shown). Thus, the regional reduction of ADK in the cortex of an ADK-overexpressing brain is sufficient to prevent a lethal outcome after focal ischemia.

To investigate whether the local reduction of ADK in the cortex of fb-Adk-def mice provides regional or global protection against ischemic neuronal cell death, we evaluated the infarct volume of the cortex and striatum separately by 2,3,5-triphenyltetrazolium chloride (TTC) staining of brain sections after 23 hours of reperfusion. In WT mice the indirect striatal and cortical infarct volumes were $56.1 \pm 4.7\%$ and $68.3 \pm 4.4\%$, respectively, as compared to the volume of the contralateral hemisphere (n=10, WT mice, **Figure 24**). In contrast fb-Adk-def mice had significant increase in ($69.3 \pm 4.5\%$) indirect infarct volume in striatum (n=11, $P < 0.05$ versus WT, **Figure 24**), which equated to a 126% increase in infarct size relative to the WT controls. Most strikingly, in the cortex the indirect infarct volume in fb-Adk-def mice was reduced to $18.5 \pm 2.5\%$ (n=11, $P < 0.01$, versus WT, **Figure 24**), a 73% reduction in cortical infarct

volume relative to WT controls. These data indicate that a regional downregulation of ADK in the cortex provides localized protection against ischemic injury, even when in direct proximity to an area (striatum) with increased ADK and increased injury. Additionally, protection of the cortex in fb-Adk-def mice was found to be sufficient to prevent the lethal outcome seen after ischemia associated with global ADK overexpression in Adk-tg mice.

ADK activity negatively regulates LPS-induced stroke tolerance

To assess whether ADK activity modulates ischemic tolerance, Adk-tg mutants, which have brain-wide overexpression of ADK, and WT mice were subjected to a single systemic injection of LPS, a known preconditioning agent, 3 days prior to MCAO (**Figure 25A**). In the absence of LPS-preconditioning, saline injected Adk-tg mice demonstrated significantly enlarged ($59.8 \pm 4.9\%$) infarct volume following 30 min of MCAO, compared with WT controls ($40.2 \pm 3.5\%$, $P < 0.05$, $n = 8/\text{group}$, **Figure 25B**). In WT mice, LPS preconditioning provided protection against stroke following either 30 min or 60 min of MCAO by significantly reducing infarct volume (30 min of MCAO: $21.2 \pm 3.2\%$ versus $40.2 \pm 3.5\%$ of control; and 60 min of MCAO: $28.9 \pm 3.4\%$ versus $52.8 \pm 4.2\%$ of control, $P < 0.01$, $n = 8/\text{group}$, **Figure 25B,C**). The level of protection afforded by LPS-preconditioning in WT mice in this study is consistent with previous studies [180]. Interestingly, LPS-mediated ischemic tolerance was blunted by ADK overexpression in Adk-tg mice. This falls in line with our hypothesis that an acute surge of adenosine is

required to initiate preconditioning as previous work using real-time biosensor measurements in vivo have shown levels of adenosine increase significantly following systemic administration of LPS [313]. In addition, we have demonstrated previously that adenosine levels in brain rise as a consequence of ischemic preconditioning [365]. LPS-preconditioned Adk-tg mice subjected to 30 min of MCAO had only a moderate decrease in infarct volume ($43.6 \pm 6.7\%$, $P=0.04$, versus $59.8 \pm 4.9\%$ of control, $P<0.05$, $n=7-8/\text{group}$, **Figure 25B**); and 60 min of MCAO was found to be lethal in Adk-tg mice with or without LPS preconditioning (**Figure 25C**). Together, these data demonstrate that increased ADK activity exacerbates stroke-related injury and attenuates the endogenous neuroprotective mechanism of LPS- induced ischemic preconditioning.

Modulation of stroke susceptibility by regional overexpression or knockdown of ADK with an AAV-based vector system

To determine if selective targeting of ADK expression has therapeutic potential in reducing stroke-induced brain injury we constructed two novel AAV8-based vectors expressing ADK in either a sense (AAV8-pGfa-Adk-SS, "ADK-SS") or antisense (AAV8-pGfa-Adk-AS, "ADK-AS") orientation under the control of an astrocyte-specific gfaABC1D promoter [369]. First, to evaluate the regional pattern of ADK expression following viral manipulation, ADK-SS or ADK-AS was unilaterally co-injected with an AAV8-GFP reporter virus (1:1 of volume) into the striatum of naïve C57BL/6 mice. Four weeks after intrastriatal injection, the ADK-SS/AAV-GFP-injected mice were characterized by a

robust increase in ADK expression (**Figure 26A, d-f**), compared to basal ADK levels observed in mice that received only AAV-GFP injection (**Figure 5A, a-c**). At higher magnification the ADK-SS/AAV-GFP-injected striatum showed cellular features indicative of ADK overexpression that colocalized with, and was confined to AAV-GFP infected cells (**Figure 5A, g-i; arrows**). Conversely, the ADK-AS/AAV-GFP -injected mice demonstrated a moderate decrease in ADK expression (**Figure 26A, j-l**), as compared to endogenous ADK levels in the AAV-GFP injected striatum (**Figure 26A, a**). Abrogation of ADK expression was most prominent in GFP-expressing cells (**Figure 26A, m-o; arrows**).

Regional changes in ADK expression were quantified by Western blot analysis using the entire striatum from WT mice injected with ADK-AS, ADK-SS, or AAV-Null viruses (n=4, each group). Four weeks after intrastriatal injection of virus we observed a 17% decrease and 18% increase in striatal ADK expression levels in mice receiving ADK-AS or ADK-SS, respectively (p<0.05 versus the AAV-Null control, **Figure 26B**). Together, these data demonstrate that our novel AAV8-gfap-Adk-SS and AAV8-gfap-Adk-AS viral vectors are effective in modulating ADK expression levels *in vivo*.

AAV8-based knockdown of ADK reduces ischemic brain injury

To assess whether AAV8-based overexpression of ADK renders the brain more vulnerable to cerebral ischemic injury and to evaluate whether viral downregulation of ADK is effective in protecting the brain against injury induced by stroke, we subjected ADK-SS and ADK-AS injected mice (n=7-8 per group) to 60 min of MCAO. Brain infarct

volumes were evaluated after 23 hours of ischemia-reperfusion (**Figure 27A**). As expected, the ADK-AS and ADK-SS viruses had opposing effects on the degree of cerebral ischemic injury. Compared to the AAV-Null virus injected mice, which had an infarct volume of $48.6 \pm 2 \%$ ($n = 8$), the ADK-SS virus-injected mice displayed a significantly enlarged infarct volume of $61.8 \pm 4.4 \%$ ($n=7$, $P<0.05$, **Figure 27B**). This is equivalent to a 25.9% increase relative to the AAV-Null controls. More importantly, brain injury in ADK-AS virus injected mice was significantly attenuated, resulting in a final infarct volume of $24.8 \pm 2.9\%$ ($n=7$, $P<0.05$), a 48.8% reduction compared with the Null-virus injected mice (**Figure 27B**). These data indicate that viral-mediated downregulation of ADK protects the brain against ischemic injury whereas upregulation of ADK exacerbates stroke-induced neuronal cell death. Taken together, these results provide proof of the concept that therapeutic manipulations that decrease levels of ADK in the brain can protect the brain from ischemic injury.

DISCUSSION

Acute brain injury can result in neuroprotection and tolerance to subsequent injury [356]. However, the molecular effectors of this endogenous neuroprotection are incompletely known. Acute brain injury, in particular after trauma, stroke, or seizures, is associated with a surge of the brain's endogenous neuroprotectant adenosine [363, 365], which can (i) increase the acute neuroprotective capacity of the brain, and (ii)

trigger downstream events that create a state of delayed protection that can protect the brain from subsequent injury. As increases in brain adenosine, in response to changes in ADK expression, have been shown to be both neuroprotective and antiepileptic in acute seizure models [367], ADK expression levels may also determine the degree of neuroprotection and tolerance in ischemia. Thus, the adenosine-ADK system may be a candidate as an endogenous effector of acute and delayed neuroprotection (tolerance).

Homeostatic bioenergetic network regulation through ADK

In contrast to conventional pharmacotherapeutic approaches that aim to achieve specificity by selective targeting of specific molecular pathways, our goal here was to broadly affect homeostatic bioenergetic network regulation by modulating the availability of adenosine through ADK manipulation. Biochemically, adenosine links energy homeostasis with nucleic acid metabolism [360] and is an important feedback regulator of transmethylation reactions [358, 370], including DNA methylation, and thus ideally posed to regulate homeostatic networks through bioenergetic and epigenetic mechanisms. Those adenosine receptor independent activities of adenosine need to be distinguished from signaling pathways that depend on stimulation of four types of G-protein coupled adenosine receptors (A_1 , A_{2A} , A_{2B} , A_3). Adenosine receptor dependent pathways are known to contribute to the protective role of adenosine in the delayed response to ischemic injury through its anti-inflammatory actions [375], modulation of

the neuro-immune response and role in promoting angiogenesis and tissue remodeling [218]. The role of specific adenosine receptors in the context of stroke however varies with level and duration of stimulation, and is highly affected by temporal and spatial relationships. As such, the precise timing, duration and level of stimulation needed at the receptor level to provide neuroprotection is likely to be impossible to mimic pharmacologically. For this reason, we have focused on using homeostatic bioenergetic network regulation as a novel strategy to manipulate global adenosine expression through its key regulatory enzyme, ADK. In this manner, we can optimally take advantage of synergistic homeostatic bioenergetic network effects of adenosine, mediated through the sum of all adenosine receptor dependent and independent effector systems. Using transgenic as well as gene therapy-based manipulations of ADK in mice we were uniquely poised to study the net-effects of adenosine modulation on acute and delayed neuroprotection.

Adenosine and ADK in acute neuroprotection

Adenosine has long been recognized for its potential as an acute neuroprotectant in the context of cerebral ischemic injury [219, 376, 377]. Levels of adenosine are tightly regulated by physiological and pathophysiological changes that occur during the acute phase of ischemic injury, such as metabolic stress, vasodilation or vasoconstriction, platelet aggregation [242] and the release of excitatory neurotransmitters [377]. Despite promise in rodent models of stroke [228], the direct

administration of adenosine has not been translated to clinical therapy as it has a short physiological half-life and causes many unwanted central and peripheral side effects, including suppression of cardiac function, sedation and renal impairment. For these reasons we focused on the key adenosine removing enzyme in brain, ADK, as a novel therapeutic target to reduce ischemic neuronal cell death [362]. Recent work in our laboratory has shown that acute downregulation of endogenous ADK in response to stroke might be an innate neuroprotective mechanism aimed at potentiating ambient levels of adenosine [365].

Using complementary transgene and gene therapy-based approaches we demonstrate here that the degree of acute brain injury directly depends on expression levels of ADK and the resulting tone in ambient adenosine. Most importantly, in fb-Adk-def mice that have increased ADK in forebrain and decreased ADK in striatum ambient levels of adenosine directly correspond to ADK expression levels (**Figure 2**), and the regional susceptibility to stroke-induced brain injury is governed by the regional expression profile of ADK (**Figures 1A and 3A**). These findings indicate that adenosine-dependent acute neuroprotection depends on local rather than systemic responses.

Adenosine and ADK in ischemic tolerance

The brain has evolved endogenous mechanisms to regulate, limit and repair damage in response to injury. The phenomenon of ischemic tolerance takes advantage of these feedback mechanisms to confer a state of decreased susceptibility to ischemic

injury. By applying a noxious stimulus at just below the level of inducing damage, natural protective responses can be elicited prior to a larger subsequent, otherwise injurious, stimulus. Ischemic tolerance can be divided into two broad categories: acute preconditioning, which develops over minutes or hours, and delayed preconditioning, which takes 24-72 hours to develop and involves gene regulation and protein synthesis [130]. The role of adenosine in ischemic preconditioning has been studied extensively in the heart [378], however less is known about its role in cerebral ischemia. In acute cerebral preconditioning the adenosine system is a well-accepted candidate to the development of ischemic tolerance [297, 379].

Data from the current study show that adenosine plays a novel role in promoting delayed ischemic tolerance. If adenosine is a required component of biochemical and physiological pathways leading to tolerance, then abrogation of the adenosine response by increasing the metabolic clearance of adenosine should abrogate the phenomenon of ischemic tolerance elicited by delayed preconditioning. Here, we clearly demonstrate that transgenic animals with increased metabolic adenosine clearance due to overexpression of ADK throughout the brain (Adk-tg mice), remain susceptible to ischemic injury despite a standard preconditioning treatment with LPS. Our current results, using transgenic animals with increased adenosine clearance due to overexpression of ADK in brain (Adk-tg) illustrate the essential role of adenosine in the CNS in LPS-induced delayed-type preconditioning. Further, it is tempting to deduce, particularly in light of our current data showing that animals with increased adenosine

clearance cannot be preconditioned, that an adenosine signal – triggered by a preconditioning stimulus – is needed for the development of ischemic tolerance.

Therapeutic adenosine augmentation

The question remains as to whether the acute or long-term effects of adenosine dominate in the phenomenon of ischemic tolerance. Acutely, adenosine has been shown to exert neuroprotective effects via signaling through inhibitory A₁ receptors; however mice lacking A₁ receptors do not show increased susceptibility to ischemic damage [238]. In line with this, mice globally lacking excitatory A_{2A} receptor have reduced susceptibility to stroke [244]. Further, systemic, but not central, administration of A_{2A} receptor antagonists have been shown to reduce infarct volume in several *in vivo* models of ischemic injury [243]. This protection was shown to be largely dependent on A_{2A} receptors present on bone marrow-derived cells [375]. Paradoxically, systemic activation of A_{2A} receptors also led to protection against cerebral ischemic damage [380]. These partly contradictory findings suggest that adenosine receptor independent mechanisms might also contribute to neuroprotection. Thus, the global net effect of homeostatic network regulation determines the susceptibility to neuronal cell death in stroke. Therefore, we did not aim to investigate specific pathways or molecular components of downstream effector systems, but elected to augment the natural production of adenosine in response to injury by decreasing the abundance of its key regulatory enzyme ADK. The novel therapeutic concept of decreasing ADK without

drastically affecting its temporal regulation may be the most practical immediate therapeutic approach to harnessing the adenosine system for ischemic neuroprotection. We have previously suggested that polymer-based, stem cell-based, and gene therapy-based adenosine augmentation therapies might uniquely be suited to suppress seizures in epilepsy [381].

Though we have shown viral knock down of ADK *in vivo* to be a successful neuroprotective strategy that induces a state of permanent tolerance to ischemia, at this time we do not propose the use gene therapy as prophylactic to treat patients at risk of cerebral ischemia. Rather, in lieu of the development of more targeted pharmacological approaches, it may be possible to pursue other, less invasive, methods to raise basal levels of adenosine in the brain of patients and thereby mimic the features of ADK downregulation. One such possibility might be the ketogenic diet, which is currently used to treat intractable epilepsy and other neurological disorders [382], and has recently been shown to increase A₁R activation in the brain [383]. In summary, modulation of adenosine levels via its key regulatory enzyme ADK may be used therapeutically to mimic essential features of preconditioning resulting in a phenotype of ischemic tolerance in patients at risk of cerebral ischemic injury.

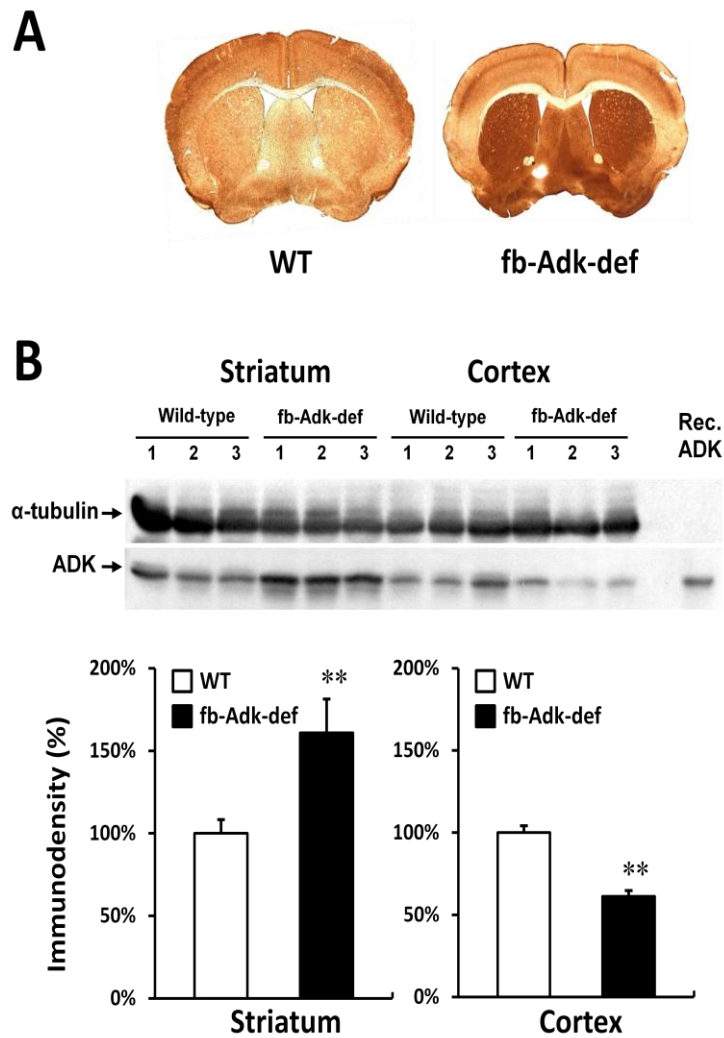


Figure 22. *Differential expression pattern of striatal and cortical ADK in fb-Adk-def mice*

Regional expression of ADK was evaluated in the brain of naïve wild-type (WT) and fb-Adk-def mice. **(A)** Representative immunohistochemical staining with ADK primary antibody in WT (left) and fb-Adk-def (right) mice. **(B)** Top: Representative Western blot of ADK from the striatum or cortex of adult WT and fb-Adk-def mutant mice. Bottom: Quantitative analysis of striatal (left panel) and cortical (right panel) ADK levels based on two replicates of western blots performed with samples from $n = 5$ animals from each genotype. ADK levels were first normalized for loading using a α -tubulin standard. ADK levels are shown as relative to striatal or cortical ADK levels in WT mice (set as 100%). Data are displayed as mean \pm SEM of 10 measurements. * $P < 0.05$; ** $P < 0.01$ paired comparisons t -test.

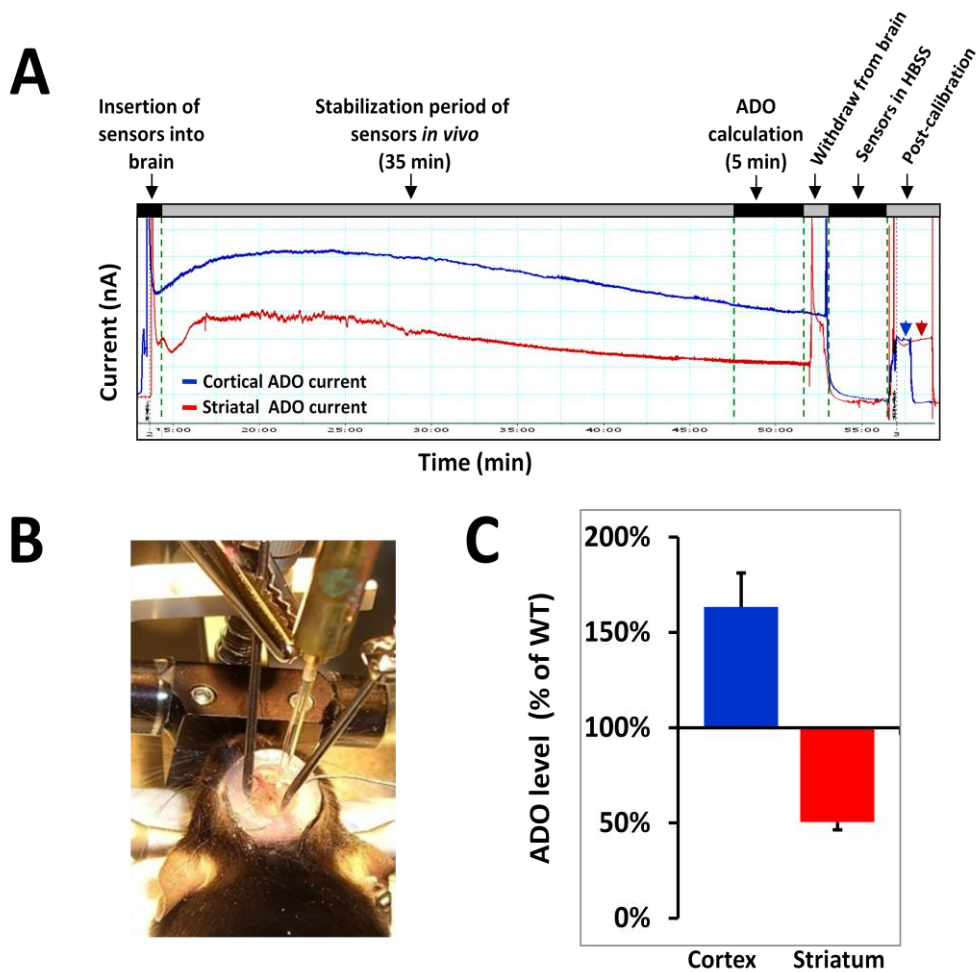


Figure 23. Regional ADK manipulation causes focal changes in adenosine levels

The adenosine and inosine biosensors were used for *in vivo* real-time determination of adenosine levels in the striatum of fb-Adk-def mutants. Fb-Adk-def mutant mice have increased adenosine in the cortex, and reduced adenosine in the striatum when compared to wild-type mice. **(A)** Representative traces of the real-time adenosine measurements and post-calibration. Biosensors were precalibrated with adenosine, inosine and serotonin then inserted into the cortex or striatum for real-time measurement. After removal, biosensors were post-calibrated with adenosine. **(B)** Biosensors were mounted on a stereotaxic manipulator and *in vivo* measurements were performed in a mini-reservoir that was continuously perfused with HEPES-buffered saline. **(C)** Statistic analysis of cortical and striatal adenosine (ADO) levels in fb-Adk-def mutants versus WT mice (n=3, per genotype). * P<0.05 and ** P<0.01 versus cortex or striatum in WT mice, respectively.

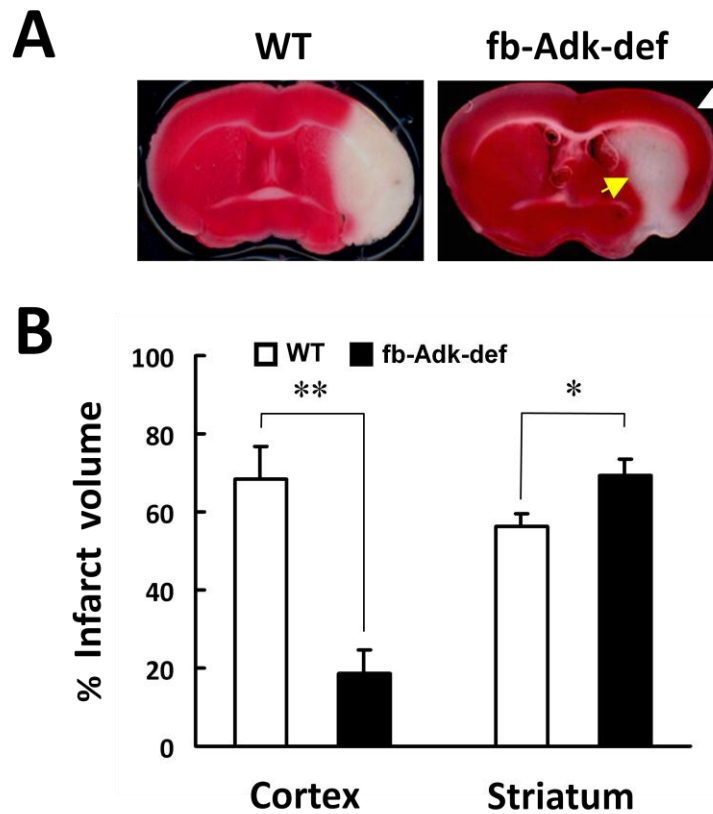


Figure 24. *Local downregulation of ADK attenuates ischemic neuronal injury in the cortex*

After 60 min of MCAO and 23 h of reperfusion, mice were sacrificed and the brains were TTC stained to evaluate ischemic damage. Healthy tissue stains pink, while damaged tissue remains white. **(A)** Representative TTC staining of wild-type (WT, left) and fb-Adk-def (right) mice. The white arrow indicates the cortical region protected against MCAO, while the yellow arrow indicates the region of exacerbated damage in the striatum of fb-Adk-def mice. **(B)** Quantification of indirect infarct volume in the cortex (left panel) and striatum (right panel) of WT (white bars, n=10) and fb-Adk-def mutant (black bars, n=11) mice. Data are displayed as mean \pm SEM. * $P < 0.05$ and ** $P < 0.01$, versus WT mice.

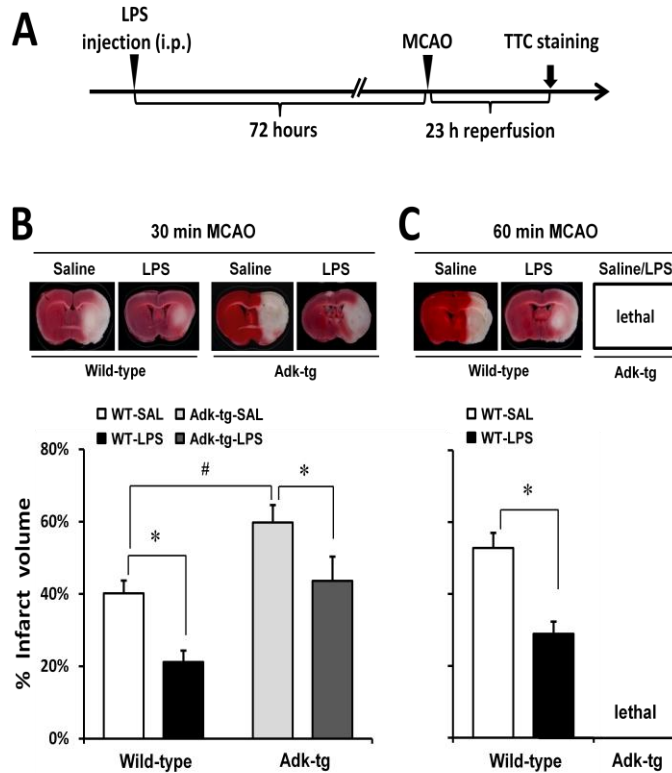


Figure 25. Increased ADK prevents LPS-induced ischemic tolerance in Adk-tg mutants

(A) Schematic illustration of the treatment paradigm for LPS-preconditioning. 3 days post LPS (0.2mg/kg, i.p.) mice received either 30 or 60 min of MCAO. Animals were sacrificed after 23 hours of reperfusion and the brains were collected for TTC staining. **(B)** Top: Representative TTC staining from wild type (WT) and Adk-tg mice injected with LPS (0.2mg/kg, i.p.). Mice were given 30 min MCAO followed by 23 h of reperfusion. Bottom: Quantification of indirect infarct volume in WT and Adk-tg mice injected with either LPS (0.2mg/kg, i.p.) or saline (SAL) 72 hours prior to 30 min MCAO and 23 h reperfusion (n = 7-8/per group). **(C)** Top: Representative TTC staining from WT mice injected with LPS (0.2mg/kg, i.p.) 72 hours prior to 60 min MCAO and 23 h reperfusion. Bottom: Quantification of indirect infarct volume (n = 7-8/per group). Data are shown as mean ± SEM. * P<0.05 versus saline-injected mice with MCAO within corresponding genotype. # P< 0.01 versus saline-injected WT controls.

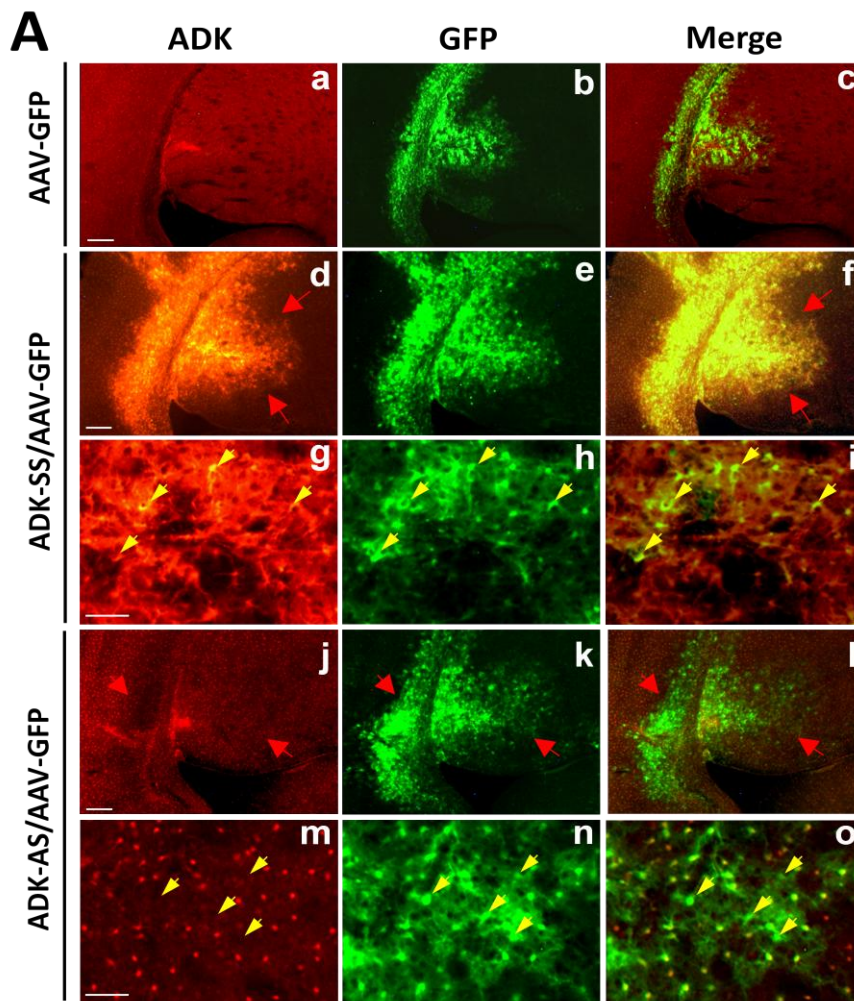


Figure 26. Modulation of ADK expression with an adeno associated virus (AAV) – based vector system

(A) Immunohistofluorescence of ADK (red) and GFP (green) in WT mice injected with AAV-GFP (**a-c**), or co-injection of AAV-GFP with either ADK-SS (**d-i**), or ADK-AS (**j-o**). **(a-c)** Representative immunohistofluorescence showing basal ADK levels and AAV-virus expression pattern in AAV-GFP injected WT mice. **(d-f)** ADK-SS / AAV-GFP co-injection causes a robust increase in ADK immunoreactivity (red arrows). **(g-i)** Higher magnification images of the ADK-SS / AAV-GFP co-injection site shows that ADK colocalizes with AAV-GFP infected cells (yellow arrows). **(j-l)** ADK-AS / AAV-GFP co-injection in WT mice causes a decrease in ADK immunoreactivity (red arrows). **(m-o)** Higher magnification images of the ADK-AS / AAV-GFP co-injection site show that cells lacking ADK colocalize with AAV-GFP infected cells (yellow arrows).

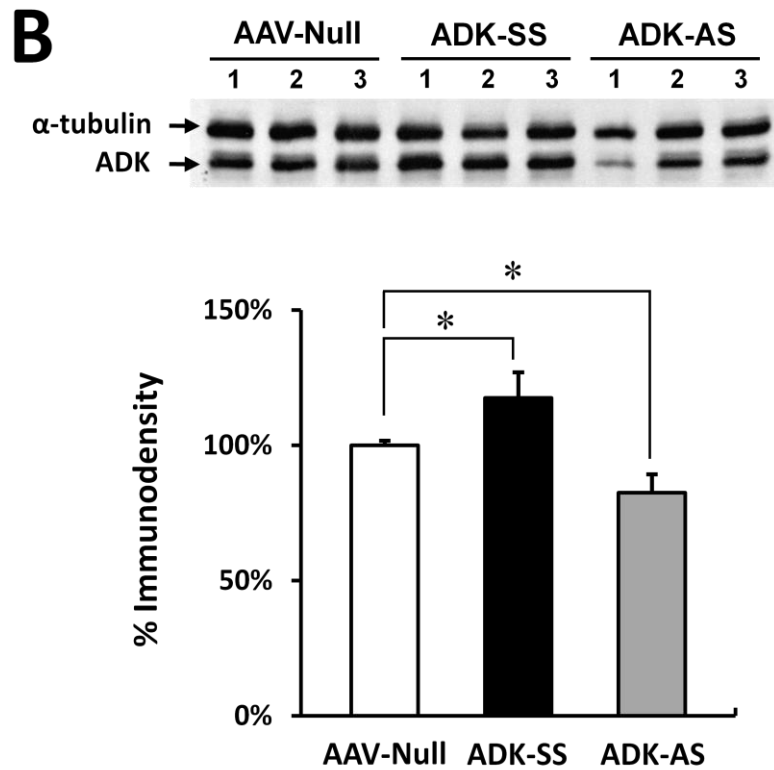


Figure 26, continued. *Modulation of ADK expression with an adeno associated virus (AAV) – based vector system*

(B) Top: Representative Western blot of ADK from adult WT mice injected with either AAV-Null, ADK-SS or ADK-AS virus. Bottom: Quantitative analysis of ADK levels based on two separate Western blots performed with samples from $n = 4$ animals for each injection type. Protein loading was normalized to the α -tubulin standard prior to inter-group comparison. Values are displayed as relative to ADK protein levels in AAV-Null (set as 100%) brain. Data represent the mean \pm SEM, $n=4$. * $P<0.05$ versus AAV-Null group.

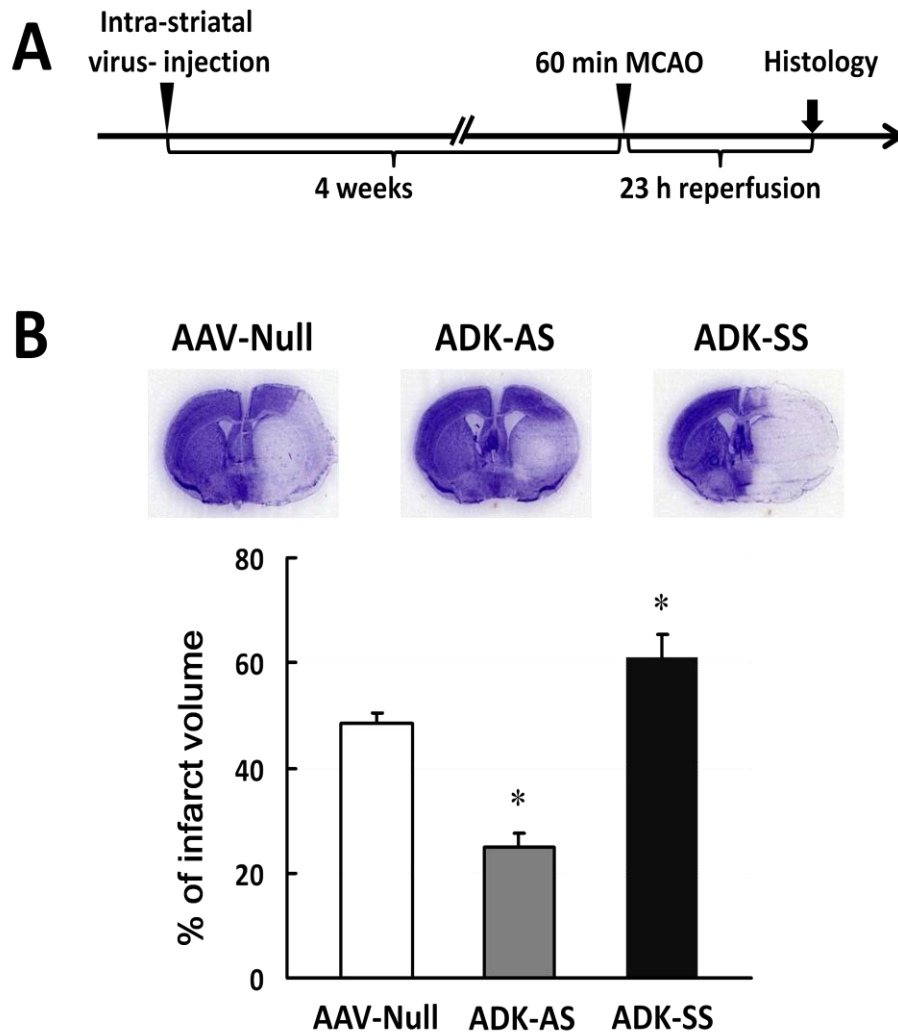


Figure 27. Modification of infarct volume by viral over- or under- expression of ADK

(A) Schematic illustration of the treatment paradigm for WT mice given intra-striatal virus injection (AAV-Null, ADK-AS or ADK-SS) followed by 60 min MCAO (4 weeks post virus injection) followed by 23 h of reperfusion. **(B)** Top: Representative Nissl staining of brain from WT mice injected with either AAV-Null, ADK-AS or ADK-SS, followed after 4 weeks with 60 min MCAO and 23 h of reperfusion. Mice that received ADK-AS virus injections had smaller infarcts and mice who received ADK-SS virus had larger infarct volumes when compared to mice that received an injection of AAV-Null virus. Bottom: Quantification of indirect infarct volume in WT mice injected with either AAV-Null, ADK-AS or ADK-SS virus ($n = 7-8$ per group) prior to 60 min MCAO followed by 23 h reperfusion. Data are shown as mean \pm SEM. * $P < 0.05$, versus AAV-Null virus injected controls.

CHAPTER 4

Manuscript #3

Epigenetic changes induced by adenosine augmentation therapy prevent epileptogenesis

Rebecca L. Williams-Karnesky^{a,b}, Nikki K. Lytle^a, Ursula S. Sandau^a, Joseph M. Farrell^a,
Eleanor M. Pritchard^c, David L. Kaplan^c and Detlev Boison^{a,b}

^aRobert Stone Dow Neurobiology Laboratories, Legacy Research Institute,
Portland, Oregon 97232, USA. ^bDepartment of Neurology, Oregon Health and Science
University, Portland, Oregon, 97233, USA. ^cDepartment for Biomedical Engineering,
Tufts University, Medford, MA 02155, USA

Chapter 4 is modified from the original paper submitted to *The Journal of Clinical Investigation* on July 3, 2012.

ABSTRACT

Epigenetic modifications, including changes in DNA methylation, lead to altered gene expression and thus may underlie epileptogenesis via induction of permanent changes in neuronal excitability. Therapies that could inhibit or reverse these changes may be highly effective in halting disease progression. Here we identify an epigenetic function of the brain's endogenous anticonvulsant adenosine, showing that this compound induces hypomethylation of DNA via biochemical interference with the transmethylation pathway. We show that inhibition of DNA methylation can inhibit epileptogenesis in multiple seizure models. Using a rat model of temporal lobe epilepsy we identify an increase in hippocampal DNA methylation, which correlates with increased DNA methyltransferase activity, disruption of adenosine homeostasis, and with spontaneous recurrent seizures. Finally, we use bioengineered silk implants to deliver a defined dose of adenosine over 10 days to the brains of epileptic rats. This transient therapeutic intervention reversed the DNA hypermethylation seen in the epileptic brain, inhibited sprouting of mossy fibers in the hippocampus, and prevented the progression of epilepsy for at least 3 months. Thus, pathological changes in DNA methylation status may underlie epileptogenesis, and reversal of these epigenetic changes via therapeutic adenosine augmentation to the brain after the onset of epilepsy may halt disease progression.

INTRODUCTION

Epilepsy is the third most common neurological disorder in the US after Alzheimer's disease and stroke, affecting nearly 3 million Americans and 50 million people worldwide. Despite decades of research, seizure suppression is still only achieved in just over half of affected individuals. Long term outcomes depend on patient compliance, an important consideration since many antiepileptic drugs have negative side effects. Current antiepileptic therapies fail to address the underlying causes of epilepsy, (i.e. changes in gene transcription), and do not halt epileptogenesis [384]. Epileptogenesis is characterized by a progressive increase in frequency and severity of spontaneous recurrent seizures (SRS). Several mechanisms are thought to be implicated in the epileptogenic cascade including neuro-inflammatory responses, selective neuronal cell loss, mossy fiber sprouting, aberrant connectivity, and gliosis coupled with adenosine dysfunction [385]. One potential unifying factor behind many of the pathological changes in epileptogenesis may be epigenetic modifications, which are likely further potentiated by epileptogenesis itself [386-388]. Epigenetic modifications, which alter gene transcription without modifying the underlying DNA sequence, are highly plastic and can respond rapidly in response to environmental cues, an important endogenous mechanism for temporally and spatially controlling gene expression. Changes in histone acetylation and methylation, as well as changes in DNA methylation, once thought to occur only in dividing cells, have been shown to occur in mature cells in the central nervous system (CNS) [389, 390]. Tellingly, these changes occur regularly and rapidly. Even a single initial episode of neural synchronization exceeding 30 seconds in

the hippocampus induces DNA methylation-dependent epigenetic alterations in transcription of immediate early genes and initiates a cascade of transcription factors contributing to long-term neuronal and circuit alterations [391].

Methylation of DNA in the CNS has attracted increasing attention recently, with new research showing activity-induced proliferation of neural precursors via active DNA demethylation [390]. Altered DNA methylation in the brain has also been implicated in psychiatric and neurological conditions, including epilepsy [390, 392, 393]. The methylation hypothesis of epileptogenesis suggests that seizures by themselves can induce epigenetic chromatin modifications and thereby aggravate the epileptogenic condition [387]. Interestingly, Valproic acid, used for decades as an antiepileptic drug, has since been shown to function as a histone deacetylase inhibitor [386, 394], and more recently as an inhibitor of DNA methylation [395]. Despite these new insights into the role of pathological DNA methylation changes in disease, and the fact that two DNA methyltransferase (DNMT) inhibitors are currently FDA approved (azacitidine and decitabine), direct manipulation of DNA methylation has not been tested in human epilepsy or in animals models of disease [396].

DNA methylation requires the donation of a methyl group from S-adenosylmethionine (SAM), a process that is facilitated by DNA methyltransferase enzymes (**Figure 28A**). The resulting product, S-adenosylhomocysteine (SAH) is then further converted into adenosine (ADO) and homocysteine (HCY) by SAH hydrolase. Critically, the equilibrium constant of the SAH hydrolase enzyme lies in the direction of SAH formation [397]; therefore, the reaction will only proceed when adenosine and

homocysteine are constantly removed [358, 397]. In the adult brain, removal of adenosine occurs largely via the astrocyte-based enzyme adenosine kinase (ADK) [220, 398]. Interestingly, concurrent with transcriptional changes seen in epilepsy there is a progressive increase in growth of astrocytic processes and an increase in expression in ADK expression, resulting in hippocampal adenosine deficiency [367, 399, 400].

Adenosine is an endogenous anticonvulsant in the brain [220, 401] as well as an obligatory end product of transmethylation reactions [358]. Previous work has focused on adenosine's anticonvulsant activity, which is largely mediated via activation of pre- and postsynaptic adenosine A₁ receptors to decrease neuronal excitability [402, 403]. The ambient tone of adenosine is determined by neuronal adenosine release [404] and ADK-driven reuptake through equilibrative nucleoside transporters in astrocytes, which form a 'sink' for adenosine [362]. Since disruption of adenosine homeostasis and adenosine deficiency has been implicated in epileptogenesis, local therapeutic adenosine augmentation has been shown to be an effective strategy to acutely suppress seizures in modeled epilepsy [362, 405]. However, the epigenetic effects of adenosine augmentation in the treatment of epilepsy, including the potential to modulate DNA methylation status, have not been well characterized. Based on adenosine's role as an obligatory end product of DNA methylation, we hypothesized that an increase in ADK and the resulting decrease in adenosine, as seen in chronic epilepsy [367, 383], would lead to an increase in global DNA methylation in the brain. Further, we hypothesized that therapeutic adenosine augmentation might be an effective strategy to reverse this pathological DNA hypermethylation and thereby prevent the progression of epilepsy.

MATERIALS AND METHODS

Animals, PTZ threshold, kindling model, mesial temporal lobe epilepsy model, and seizure monitoring.

All animal procedures were conducted in a facility accredited by the Association for Assessment and Accreditation of Laboratory Animal Care (AAALAC) in accordance with protocols approved by the Institutional Animal Care and Use Committee. For seizure threshold testing, male CD-1 mice (25-35g) were used. 0.75% (w/v) pentylenetetrazol (PTZ) was prepared in isotonic saline. 5-Aza-2'deoxyctidine (5-Aza-2dC) was prepared in isotonic saline and administered via tail vein 10 minutes prior to initiation of PTZ infusion. PTZ was infused via tail vein, at a rate of 0.2ml/min using a Hamilton microsyringe (Harvard Apparatus, USA), in freely moving animals. Time to first twitch, first clonus and final extensor phase was recorded. Infusion was stopped after a final extension or at a maximum volume of 0.9ml, whichever came first.

For the kindling model and associated 5-Aza-2dC drug testing male Sprague Dawley rats (300-350g) were implanted with bipolar, coated stainless steel electrodes (0.20 mm in diameter, Plastics One, Roanoke, VA) into the right hippocampus (stereotactic coordinates relative to Bregma: AP -4.2 mm; ML -4.6; DV -5.6). Experiment 1 (acute 5-Aza-2dC): The animals were kindled based on a rapid kindling protocol [406, 407]. Briefly, using a Grass S-88 stimulator rats received 12 stimulations per day (1-ms square wave pulses of 200 μ A, 50-Hz frequency, 10 s duration at an interval of 30 minutes between stimulations) every 2 – 3 days until a stable Racine stage 5 seizure was

generated. Following a 2 d stimulus free period the testing was initiated. Rats received two stimulations then a single i.p.bolus of either saline or 5-Aza-2dC (0.5 mg/kg) 15 min prior to a subsequent series of 9 stimulations. All stimulations were delivered at an interval of 30 minutes and rats were scored for mean Racine score and after discharge duration. There was a 5 day drug and stimulus free period between the saline and 5-Aza-2dC trials. Experiment 2 (chronic 5-Aza-2dC): Animals were kindled as described above while being chronically treated with either saline or 5-Aza-2dC (0.4 mg/kg, i.p.) administered 12 hours prior to the first kindling session and every successive 12 hours until the saline injected controls achieved a stable Racine stage 5 seizure score. Following an 11 day drug and stimulus free period animals received a stimulus and were scored for seizure stage and duration.

For the mesial temporal lobe epilepsy model young male Sprague Dawley rats (130 – 150g) received a single acute dose of KA (12 mg/kg i.p.) to trigger status epilepticus (SE). Only rats that exhibited at least 3 h of convulsive Racine stage 4 seizures were used. Starting 4 weeks post-KA animals were continuously video monitored to quantify the number of convulsive stage 4-5 seizures per week [408]. The number of stage 4-5 seizures typically increased to >3 seizures per week at 9 weeks post-KA, and animals experienced at least 10 spontaneous convulsive stage 4-5 seizures (inclusion criterion). All animals were further monitored during weeks 10-13 and 18-21 post-KA. Behavioral seizures were confirmed by EEG analysis in selected animals. Briefly, bipolar, coated, stainless steel recording electrodes (0.20 mm in diameter, Plastics One, Roanoke, VA) were implanted into the right hippocampus and fixed with a head-set of

dental acrylate. Coordinates for the hippocampal electrodes were 4.2 mm caudal to bregma, 3 mm lateral to midline, and 3.3 mm ventral to dura. Electrical brain activity was amplified (Grass Technologies, West Warwick, RI) and digitized (powerLab, AD Instruments, Colorado Springs, CO). EEG file was analyzed manually by an observer blinded to the animal's treatment. EEG seizure activity was defined as high-amplitude rhythmic discharges that clearly represented a new pattern of tracing (repetitive spikes, spike- and wave discharges, and slow waves) that lasted at least 5 s. Epileptic events occurring with an interval less than 5 s without the EEG returning to baseline were defined as belonging to the same seizure.

Immunohistochemistry.

Staining for ADK was performed as previously described [370]. Digital images were acquired under identical conditions and all image processing was applied identically across experimental groups. ADK expression was quantified by densitometry by analyzing fields of 500 μ m encompassing the entire CA1 region. Corresponding fields from 2 sections from each animal ($n = 3$ animals per group) were analyzed using ImageJ. Levels in each analysis field were measured as arbitrary density units and are represented as averages \pm SEM normalized to controls. Timm staining was performed [409] and quantified as described [410].

Cell culture.

BHK-WT and BHK-AK2 cells were cultured in Dulbecco's Modified Eagle Media (supplemented with 10% FBS). A pc-DNA3.1 vector with a human CMV promoter was used to drive expression of the ADK-long or ADK-short cDNA. Transfection was carried out in parallel experimental replicates using a standard calcium phosphate transfection protocol. Subsequently, cells were harvested for DNA from three separate experimental replicates or, to quantify ADK protein expression three transfection replicates were pooled and used for Western blotting.

Western blotting.

To quantify ADK expression, cells were harvested for aqueous protein extraction. 25 µg of protein were loaded into a 10% Bis-Tris gel, separated by standard gel electrophoresis, transferred, and incubated overnight using a primary ADK antibody (1:5000) [411]. To normalize ADK immunoreactivity with protein loading, a mouse monoclonal anti- α -tubulin antibody (sc-8035, 1:5000; Santa Cruz, CA) was used to reprobe the same blot and the optical density ratio of ADK to α -tubulin was calculated.

Polymer implant design and implantation, and i.c.v. drug injections.

Cylindrical silk-based polymer implants designed to deliver the target dose of 250 ng adenosine per day for a limited period of 10 days were designed and fabricated as described [269, 412]. Consistency of adenosine release and *in vivo* efficacy have

previously been validated [412]. Adenosine releasing polymers (250 ng adenosine/day) or control polymers (0 ng adenosine/day) were implanted bilaterally into both lateral brain ventricles using a stereotactic implantation device as described [413]. i.c.v. injections were performed using similar surgical techniques and identical stereotactic coordinates, but with drugs (adenosine, homocysteine, S-adenosylmethionine or diluent) injected using a transiently placed guide cannula and injection volumes of 5 μ l.

Global DNA Methylation Assay.

Total genomic DNA was isolated from fresh frozen tissues using a DNeasy Blood and Tissue Kit (Qiagen, Valencia, CA, USA). Global DNA methylation status was assessed using the MethylFlash Methylated DNA quantification kit from Epigentek (Farmingdale, NY, USA) as per manufacturer's instructions. Data are presented as average \pm SEM normalized to control values.

DNA Methyltransferase Activity Assay.

Nuclear proteins were isolated from fresh frozen tissue using an EpiQuik Nuclear Extraction Kit I per manufacturer's instruction (Epigentek, Farmingdale, NY, USA). DNMT activity was quantified from freshly isolated nuclear proteins using a fluorimetric EpiQuik DNMT Activity/Inhibition Assay Ultra kit per manufacturer's instruction (Epigentek, Farmingdale, NY, USA). Data are presented as average \pm SEM normalized to control values.

Statistics.

Quantitative data were analyzed using GraphPAD Prism software (GraphPAD Software, La Jolla, CA). *In vivo* seizure data are based on $N = 8$ for adenosine and $N = 5$ to 8 for controls depending on drop outs (weeks 18-21 post-KA) due to lethal seizures in the control groups. Stage 4 and 5 seizure counts were averaged by experimental group as seizures per week and analyzed in one-week bins. Seizure data are presented as \pm SEM and were analyzed using two-way ANOVA on ranks using an unweighted means analysis followed by a Bonferroni test. Global methylation and immunohistochemistry (IHC) data are presented as average \pm SEM, and were analyzed using a Student's *t*-test.

RESULTS

Increased adenosine and reduced ADK expression induce DNA hypomethylation in the brain.

To provide mechanistic evidence that adenosine contributes to the regulation of DNA methylation in the brain we used a variety of techniques to manipulate adenosine tone. First, we generated direct evidence that adenosine can regulate DNA methylation biochemically by using individual reaction precursor or products. Thus, we administered a bilateral i.c.v. bolus of adenosine (ADO, 5 μ g/ventricle), homocysteine (HCY, 250 μ g/ventricle) or S-adenosylhomocysteine (SAM, 8.14 μ g/ventricle) to definitively identify the role these biochemical agents play *in vivo* to regulate DNA transmethylation (**Figure**

28A). ADO and HCY, both end-products in the transmethylation pathway, significantly decreased global DNA methylation in the hippocampus within 24 h, an effect that was maintained for at least 5d post infusion (**Figure 28B**). Conversely, injection of SAM, the primary methyl donor for transmethylation reactions, transiently increased global methylation by 24% at 24 hours (**Figure 28B**).

Having shown that it was possible to manipulate DNA methylation status *in vivo* biochemically, we next sought to determine whether changes in ADK expression, as seen in epilepsy, might modulate DNA methylation in the brain. To begin with, we examined transgenic mice (fb-Adk-def mice) with a forebrain-selective reduction of ADK expression in the cortex [354, 367]. We predicted that the resulting 3.3-fold increase in hippocampal adenosine tone [354] would suppress transmethylation and result in decreased DNA methylation. Indeed, a significant 31% decrease in global DNA methylation was seen in hippocampal isolates from fb-Adk-def mice (**Figure 28C**). Likewise, chronic administration of the specific ADK-inhibitor 5-iodotubercidin (5-ITU, 3.1 mg/kg i.p. once every day, for 5 days) led to a significant 35% decrease in global DNA methylation in the hippocampus of wild-type mice (**Figure 28D**). These findings show that modulating adenosine tone directly, or via modulation of ADK expression, can affect DNA methylation status in the hippocampus.

The nuclear isoform of ADK plays a key role in the induction of DNA hypermethylation.

Mammalian ADK exists in two alternatively spliced isoforms, ADK long (ADK-L) and ADK short (ADK-S), which reside in the nucleus and cytoplasm, respectively [414]. Importantly, the nuclear isoform of ADK undergoes coordinated developmental expression changes during early postnatal brain development suggesting a potential link with gene regulation [370]. To investigate whether the nuclear isoform of ADK plays a unique role in the regulation of DNA methylation we transfected cultured ADK-deficient BHK-AK2 cells [405] separately with an expression plasmid for either ADK-L or ADK-S and quantified global DNA methylation. Compared to mock-transfected BHK-AK2 cells, 24 hours after transfection, recipients of ADK-L showed a robust 400% increase in global DNA methylation, whereas the recipients of ADK-S showed only a modest 50% increase in global DNA methylation (**Figure 28D**). These results demonstrate that an increase of the nuclear isoform of ADK causes increases in global DNA methylation. These results also suggest a link between ADK dysregulation, decreased ADO tone and DNA hypermethylation in the epileptic brain.

Therapeutic delivery of adenosine modulates DNA methylation.

To investigate the therapeutic potential of adenosine, we used adenosine-releasing silk-based polymer implants to alter DNA methylation. We previously generated and characterized silk-based biodegradable brain implants able to deliver local doses of 8 to 1000 ng adenosine per day [269, 412]. These implants were able to

successfully suppress seizures in kindled rats [412] with no adverse effects. Here we used implants designed to release a controlled dose of 250 ng adenosine per implant per day during a restricted time frame of 10 days [412]. Five days following bilateral intraventricular implantation of adenosine releasing polymers in naïve animals, global DNA methylation was significantly reduced by 51% in the hippocampus when compared to animals receiving control polymers (**Figure 28E**). These data suggest that adenosine releasing polymers could be used as therapeutic delivery device to modulate DNA methylation *in vivo*.

Inhibition of DNA methylation attenuates seizures and kindling induced epileptogenesis.

We have previously shown that independent of an acute injury a sufficient trigger for spontaneous focal seizures is increased ADK expression and the resulting decrease in adenosine tone within the cortex and hippocampus [367]. Here we establish that these conditions contribute to increased DNA methylation (**Figure 28**). Thus we sought to determine if changes in DNA methylation are integral to ictogenesis and epileptogenesis. To address this question we first performed a dose response of the DNA methyltransferase inhibitor 5-Aza-2'deoxyCytidine (5-Aza-2dC) in a timed pentylenetetrazol (PTZ) threshold test. Wild-type mice treated with the highest dose of 5-Aza-2dC (5.0 mg/kg,i.v.) 10 minutes prior to continuous PTZ infusion had a significant delay in latency to the extensor phase of seizures (**Figure 29A**). Similarly, in fully kindled rats that have reproducible Racine stage 5 seizures either prior to drug injection (**Figure**

29B, pre-5-Aza-2dC) or when treated with saline (volume matched control, i.v.) an acute bolus of 5-Aza-2dC (5 mg/kg, i.v.) significantly attenuates the average Racine score to 3.48 (**Figure 29B**); however, there was no difference in afterdischarge duration (data not shown). Next we assessed whether inhibiting DNA methyltransferase activity while rats are kindled would suppress epileptogenesis. Following an 11 day drug and stimulus free period, rats that were treated with 5-Aza-2dC (0.4 mg/kg,i.p.every 12 hours) throughout kindling paradigm had a significantly reduced average Racine score after receiving a single test stimulation compared to saline treated controls. Furthermore, the average afterdischarge duration was reduced by 51% in animals kindled under the presence of 5-Aza-2dC (**Figure 29C**).

Intraventricular implants of adenosine-releasing silk reverse DNA hypermethylation in the epileptic brain.

Astrogliosis-associated increases in ADK expression and resulting adenosine deficiency have been independently identified as pathological hallmarks of the epileptic brain [367, 383]. Based on our findings linking the adenosine tone to the global DNA methylation status, we predicted that increased ADK expression in epilepsy would lead to increased DNA methylation. To investigate this hypothesis we used a model of temporal lobe epilepsy (TLE) in rats characterized by the development of spontaneous recurrent seizures (SRS) triggered by systemic kainic acid (KA) induced SE [415] (**Figure 30A**). Nine weeks after SE all animals experienced >10 SRS (inclusion criterion) and

hypermethylation of DNA associated with a 37% increase of ADK in the epileptic hippocampus (**Figure 30B**). Global DNA methylation in whole hippocampal isolates was also increased at 9 weeks after KA-injection compared to naïve animals (166%, $P= 0.012$) (**Figure 30C**). To test whether transient adenosine delivery could reduce DNA methylation in the epileptic brain, the same adenosine releasing polymers that we found to reduce DNA methylation in naïve rats (**Figure 28E**) were implanted into the brain ventricles of epileptic animals at 9 weeks following systemic administration of KA (**Figure 30A**). Compared to rats 9 week post-KA global DNA methylation was decreased by 29% in the hippocampi of epileptic animals 5 days after receiving adenosine releasing polymer and reached levels of DNA methylation comparable to that of naïve rats ($P=0.60$) (**Figure 30C**). Importantly, this change persisted for at least 3 weeks after cessation of adenosine release from the polymers (4 weeks post implantation) (**Figure 30C**). These data suggest that a transient dose of adenosine delivered locally can have a long-lasting effect on the DNA methylation status. To understand the mechanism by which adenosine augmentation changes DNA methylation status, we quantified the enzymatic activity of DNA methyltransferases (DNMT) in epileptic rats. Nine weeks following the systemic injection of KA, DNMT activity in the epileptic animals was elevated almost two-fold (174%) compared to sham-injected non-epileptic control animals (**Figure 29D**) consistent with hypermethylation of hippocampal DNA in those animals (**Figure 30C**). 5 days following the intraventricular delivery of 250 ng adenosine per day by silk-based implants, DNMT activity was almost completely blocked (15%; $P<0.03$ 5d post ADO vs 9 weeks post KA) (**Figure 30D**) consistent with restoration of

normal DNA methylation status in the epileptic animals (**Figure 30C**), which our data suggests may be mediated in part by inhibition of DNMT activity.

Adenosine-releasing silk prevents progression of epilepsy development.

Considering that ictogenesis and epileptogenesis are partially dependent on changes in DNA methylation (**Figure 29**) we hypothesized that if in the epileptic brain the pathological increase in DNA methylation is blocked by augmenting adenosine tone we could halt long-term epilepsy progression. Epileptogenesis is a life-long process that continues after onset of the first SRS and leads to a progression in seizure frequency and severity [416]. As a result, previous studies aimed at the identification of antiepileptogenic drugs have been frequently confounded by early initiation of treatment [384]. Therefore, to rigorously test the antiepileptogenic potential of transient adenosine augmentation, we chose to initiate treatment in ‘early epilepsy’ after the onset of SRS using the systemic KA model of TLE (**Figure 31A**). Epilepsy progression was continuously monitored (24/7) by video from weeks 5-9 following systemic KA administration. Continuous epileptogenesis was reflected by a progressive increase in number of seizures after initial SE (control animals, **Figure 31B**) [415, 417]. Epileptic animals (9 weeks after SE; >10 SRS) subsequently received bilateral intraventricular polymer implants releasing 250 ng adenosine each for a limited duration of 10 days (**Figure 31A**) [412]. Following polymer implantation, epilepsy progression was monitored in two 4-week recording sessions from weeks 10-13 and weeks 18-21 (i.e. weeks 1-4 and

9-12 post polymer implantation) (**Figure 31A**). As expected, adenosine releasing polymers almost completely prevented any seizures during the first week following implantation (**Figure 31B**). Remarkably, significantly reduced seizure activity was maintained far beyond the time window of active adenosine release (first 10 days), up to at least 12 weeks after polymer implantation (75% reduction of SRS incidence, 250 ng vs. 0 ng adenosine/day, $P < 0.001$) (**Figure 31B**). Importantly, during weeks 18-21 following KA, animals that were transiently exposed to adenosine did not show a significant increase in seizure frequency, while control animals continued to worsen and 3 died due to excessive seizures. Together, these data demonstrate a potent antiepileptogenic role of transient focal adenosine delivery. EEG recordings were performed in a separate cohort of animals to avoid potential confounds on DNA methylation analysis and histopathology. Those animals received intrahippocampal and cortical EEG recording electrodes during the polymer implantation surgery. Electrographic seizures were monitored in these animals from weeks 10-13 post-KA (weeks 1-4 post polymer implantation). Whereas sham or control-polymer receiving animals displayed robust seizures in the EEG (**Figure 31C**), seizure activity was markedly attenuated in recipients of the adenosine-releasing silk polymers (**Figure 31D**).

Adenosine-releasing silk implants prevent mossy fiber sprouting.

The antiepileptogenic role of silk-based adenosine delivery was further validated by assessing the degree of granule cell axon (mossy fiber) sprouting as an independent histological outcome parameter of epileptogenesis (**Figure 32A**). Mossy fiber sprouting is thought to be a fundamental epileptogenic mechanism responsible for the formation of new recurrent excitatory circuits in the dentate gyrus [418]. Nine weeks after SE, epileptic rats showed a significant increase in mossy fiber sprouting when compared to naïve control animals, with visible axons beginning to spread from the hilar layer into the granular cell layer (**Figure 32A, bottom row – white arrow**). In sham animals mossy fiber sprouting was progressive; at 21 weeks post-KA, axon sprouting increased and Timm granules, which correspond to mossy fiber synaptic terminals, presented throughout the molecular layer of the dentate gyrus (**Figure 32B, middle row – black arrow**). In stark contrast, animals that had transiently been exposed to adenosine at 9 weeks after SE had no significant change in mossy fiber sprouting 12 weeks later (**Figure 32A, B**). Thus, transient exposure to adenosine prevented mossy fiber sprouting, a major contributor to disease progression in epilepsy.

DISCUSSION

The epigenetic landscape of the brain has come under increasing scrutiny in recent years, in part due to the increasing number of techniques available for surveying the epigenome, and in part due to several seminal discoveries and ‘re-discoveries’. DNA methylation in particular has garnered favor, thanks in part to the ‘re-discovery’ of the

sixth base of the genome, 5-hydroxymethylcytosine [419] an oxidative intermediate of DNA demethylation, and the characterization of the Tet family of proteins responsible for facilitating active DNA demethylation [420]. Shown to be integral to memory formation [421], active DNA methylation is maintained in nondividing, post-mitotic neurons via DNMTs 1 and 3a [389]. DNMT activity has also been shown to regulate synaptic plasticity in the hippocampus [422]. Subsequent work has shown that active DNA demethylation is induced by neuronal activity in mature neurons [423], leading in turn to adult neurogenesis [390].

Several lines of evidence now support the notion that epigenetic changes, including DNA methylation, histone modifications, chromatin remodeling, noncoding RNAs, and RNA editing, are pathological hallmarks of human epilepsy syndromes and intrinsically linked to the process of epileptogenesis [388]. DNA methyltransferases 1 and 3 have been found to be overexpressed in the brains of patients with temporal lobe epilepsy (TLE) [424]. Increased Reelin promoter methylation has been associated with granule cell dispersion in human TLE [392]. Genes associated with DNA methylation (e.g. MeCP2) have been shown to be elevated in human epilepsy and animal seizure models [425]. Further, it has recently been discovered that several commonly used antiepileptic drugs have epigenetic effects [394, 395] which may be responsible for their efficacy.

In the present study we demonstrate that there is an increase in DNA methylation in the hippocampi of epileptic animals, and show that epileptogenesis can be attenuated by systemic administration of the DNA methyltransferase inhibitor 5-Aza-2dC. This last finding directly supports the 'methylation hypothesis of epileptogenesis',

which suggests that seizures can induce epigenetic modifications and thereby aggravate the epileptogenic condition [387]. This finding also has direct translational potential, as two inhibitors of DNA methylation (azacytidine and decitabine) are FDA approved for use in treating myelodysplastic syndromes [426]. However, these drugs require complicated dosing regimens and have numerous side effects [426, 427] which may make them unsuitable for treating epilepsy. In order to circumvent the potential side effects caused by systemic administration of demethylating agents, we took advantage of the novel epigenetic properties of the abundant biological compound adenosine.

Adenosine is a well-recognized endogenous anticonvulsant and mediator of seizure cessation [428]. It has been shown previously that adenosine augmentation therapy effectively suppresses seizures via adenosine A₁ receptor activation [362]; however, these receptor-mediated effects are limited to the time of adenosine delivery [412]. Here, we show that adenosine tone can directly modulate DNA methylation *in vivo*. Adenosine may also exert additional epigenetic effects via biochemical interference with the transmethylation reaction (e.g. modulation of histone methylation) though we did not examine this possibility in the present study. Indeed, aberrant patterns of histone methylation have been implicated in epileptogenesis [387]. Further, it has been suggested that specific alterations in histone methylation drive changes in DNA methylation, and that DNA methylation, in turn, might exert positive feedback inducing lysine methylation on histones [429]. These possibilities pose tantalizing questions for future studies.

There is increasing evidence to support the idea that even a brief exposure to an epigenetic modulator may lead to long-standing changes in gene expression [430]. Recent work in cancer biology has shown that exposure to transient low doses of DNA demethylating agents can produce long-term anti-tumor effects, modulated by genome wide promoter methylation, which persist long after drug withdrawal [431]. By broadly targeting multiple intracellular pathways via genome-wide altered DNA methylation status, we hypothesized that adenosine-induced epigenetic reprogramming could be used to directly address a major weakness of current epilepsy treatments: inability to halt long-term disease progression [432]. We theorized that it might be possible to use a transient treatment to induce durable therapeutic changes via epigenetic reprogramming.

Using a biodegradable silk polymer to deliver defined amounts of adenosine locally over pre-defined periods of time, we determined we would have the unique ability to induce epigenetic changes locally with a transient treatment. Following surgical resection of an epileptogenic focus, seizures recur in about 50% of patients, and secondary epileptogenesis is a significant problem [433, 434]. Placement of adenosine-releasing silk into the resection cavity following epilepsy surgery might be used as preventative treatment. Similarly, transient adenosine delivery might be used as preventative treatment in patients at risk for developing epilepsy, e.g. following a severe traumatic brain injury. Finally, since epileptogenesis is a life-long ongoing process in patients with epilepsy, local treatment with adenosine-releasing silk might be envisioned

as a feasible therapeutic strategy to prevent disease progression with its sequelae of comorbidities and pharmacoresistance.

The studies presented here show that local augmentation of adenosine via implantable biodegradable polymers can inhibit DNA methylation in the CNS of both healthy and epileptic animals. This transient biochemical manipulation has long-lasting effects, preventing seizure progression and mossy fiber sprouting for at least 3 months in a model of mesial temporal lobe epilepsy. In order for a new antiepileptogenesis intervention to be clinically relevant, the window of effectiveness is particularly important. Previous reports on 'antiepileptogenesis' were based on early intervention within hours or a few days before or after an epileptogenesis-precipitating injury. Even though partial 'antiepileptogenic' effects were reported in some studies, it is not clear whether epileptogenesis was truly suppressed or whether the precipitating injury was modified [384]. Our present study differs because we delayed therapeutic intervention until all animals developed at least 10 SRS ('early epilepsy'); thus we were able to monitor long-term disease progression (i.e. epileptogenesis) without any confounds related to injury modification.

In future studies it will become necessary to identify those genes that are regulated in response to adenosine-dependent changes in DNA methylation. Conventionally, gene transcription has thought to be repressed by methylation of cytosine and guanosine residues in so-called 'CpG islands' that are located in promoter regions of genes. However, this view of the complex role of DNA methylation seems to be limited in scope, as DNA methylation occurring in non-CpG rich regions [435], as well

as an non-CpG sites [436], has been shown to occur. Interestingly, the promoter of the gene encoding brain derived neurotrophic factor (BDNF) is subject to regulation by promoter methylation [437]. BDNF in turn has been linked to the alteration of epileptogenesis genes [438] and localized overexpression of BDNF has been shown to suppress mossy fiber sprouting [439]. Thus, the adenosine-induced suppression of mossy fiber sprouting documented here (**Figure 31**) might be due to decreasing the methylation status of the *Bdnf* gene promoter and leading to increased expression of BDNF. This is an intriguing hypothesis warranting further investigation.

Previous work by our lab and others has shown that dysregulation of adenosine homeostasis due to overexpression of the key adenosine metabolizing enzyme ADK leads to exacerbation of epilepsy [367, 399]. In light of the recent epigenetic findings presented herein we propose a refined model of the adenosine kinase hypothesis of epileptogenesis [440] (**Figure 32**). Epileptogenesis is triggered by a surge in high levels of adenosine that can result from injuries such as SE, stroke, or brain trauma [363, 365, 411]. As our current findings suggest, high levels of acute adenosine induce DNA hypomethylation, which in turn could permit the expression of early epilepsy genes that contribute to initiating epileptogenesis. Epileptogenesis in turn is associated with astrogliosis, overexpression of ADK and resulting adenosine deficiency [367, 383, 399]. Once these changes in ADK expression are established, they result in pathological hypermethylation of DNA. This in turn could lead to suppression of neurogenesis genes, perpetuating and exacerbating epileptogenesis. Alternatively, this increase in DNA methylation might occur in gene bodies [441], leading to increased gene transcription of

inflammatory or excitatory pathway intermediates. Herein it is important to note that an intracellular change in ADK expression within astrocytes may have both cell autonomous and non-autonomous ramifications. Adenosine levels within astrocytes and neurons are regulated by equilibrative and concentrative nucleoside transporters [442-444]. Thus an increase in ADK in astrocytes, as observed in the epileptic hippocampus, may directly affect DNA methylation within the affected astrocyte. Additionally, increased ADK in astrocytes reduce the global adenosine tone through transport of extracellular adenosine and subsequent metabolism to AMP creating the potential for pathological levels of astocytic ADK to indirectly modulate the activity of neighboring cells (i.e. epigenetic changes in neurons). By the same principal we show that a transient therapeutic dose of adenosine can disrupt this vicious cycle, via epigenetic reprogramming, blocking further progression of epilepsy. Thus, adenosine-induced modulation of DNA methylation has the potential to be a clinically-relevant therapeutic strategy uniquely suited to prevent epileptogenesis.

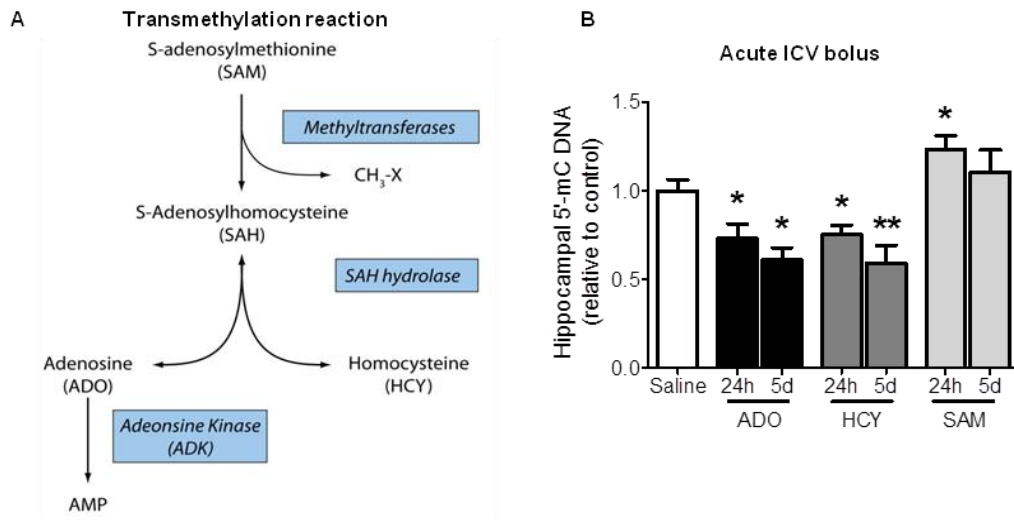


Figure 28. Increased adenosine and reduced ADK expression induce DNA hypomethylation in the brain; increased ADK expression induces DNA hypermethylation

(A) Biochemistry of the transmethylation reaction. **(B)** Adenosine (ADO) or homocysteine (HCY) significantly decreases global DNA methylation at 24 hours (h), a change that is maintained for 5 days (d) post injection; while S-adenosylmethionine (SAM) significantly increases levels at 24 h. Global DNA methylation was assessed 24 h and 5 d after bilateral i.c.v bolus of saline, ADO (5 mg/ventricle), HCY (250 mg/ventricle) or SAM (16.28 mg/ventricle).

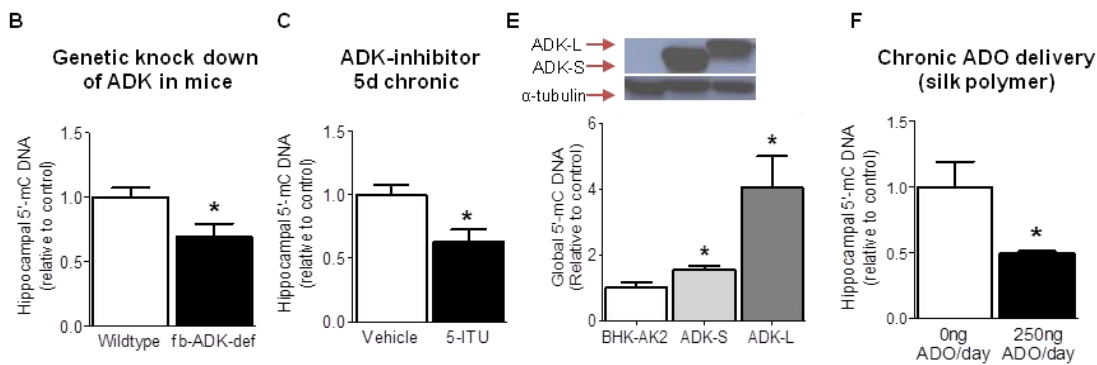


Figure 28, continued. *Increased adenosine and reduced ADK expression induce DNA hypomethylation in the brain; increased ADK expression induces DNA hypermethylation*

(C) Reduced ADK expression leads to a significant decrease in global DNA methylation *in vivo* as seen in hippocampus of transgenic fb-Adk-def mice with reduced ADK expression in forebrain. **(D)** 5'-iodotubercidin, an ADK-inhibitor (5-ITU, 3.1 mg/kg i.p., once daily for 5 d) reduces global DNA methylation in hippocampus of wild-type mice. **(E)** Transient overexpression of ADK leads to DNA hypermethylation in ADK-deficient BHK cells (BHK-AK2). Western blot shows protein expression from 3 pooled experimental replicates of BHK-AK2 cells transfected with the nuclear (ADK-L) or cytoplasmic (ADK-S) isoform of ADK and non-transfected control cells. Quantification of DNA methylation was assessed using three experimental replicates. ADK-L increases DNA methylation to a greater extent than ADK-S. **(F)** ADO releasing polymer decreases global DNA methylation in hippocampus of naïve rats. The level of global DNA methylation was assessed 5 d after implantation of silk-based polymer releasing either 0ng (control) of 250ng ADO/ventricle/d. Data are displayed as average \pm SEM; * < 0.05 and ** < 0.01; n=5 for panel B and n=3-4 for all other groups.

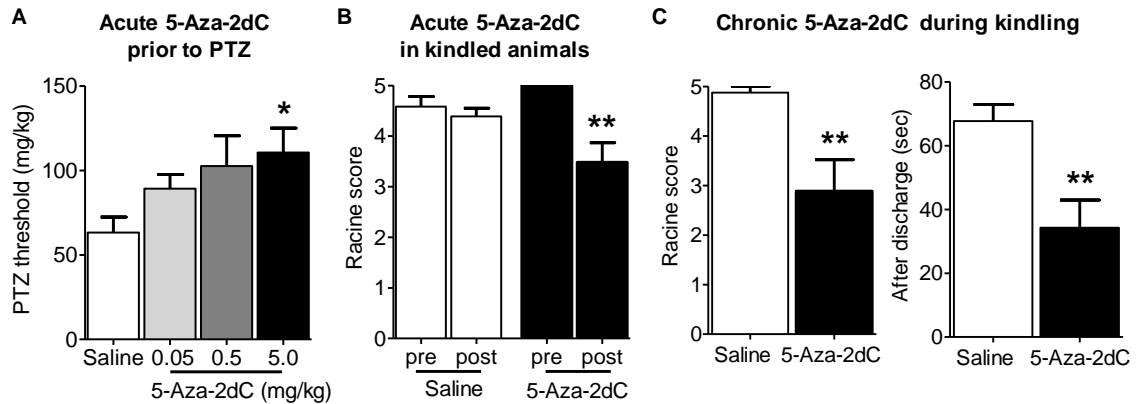


Figure 29. *The DNA methyltransferase inhibitor, 5-Aza-2dC attenuates ictogenesis and epileptogenesis.*

(A) Dose response of wild-type mice pretreated with 5-Aza-2dC (0.05, 0.5, 5.0 mg/kg) 10 minutes prior to continuous pentylenetetrazol (PTZ) infusion shows a significant increase in seizure threshold with the high dose 5-Aza-2dC (5.0 mg/kg) compared to saline treated controls. **(B)** A single injection of 5-Aza-2dC (0.5 mg/kg, ip) administered to fully kindled rats significantly reduces the average Racine score in subsequent stimulations (post-5-Aza-2dC) compared to the average Racine score prior to 5-Aza-2dC treatment (pre-5-Aza-2dC). There was no difference in the average Racine score in the rats prior to (pre-saline) or following (post-saline) vehicle injection. **(C)** Rats kindled while being chronically treated with 5-Aza-2dC (0.4 mg/kg, i.p. every 12 hours) have a significant decrease in the average Racine score and after discharge duration compared to control kindled rats in response to a test stimulation (ip saline, volume matched). The test stimulation was administered after an 11 day stimulus and drug free period. Data are displayed as the average \pm SEM; * < 0.05 and ** < 0.01; n = 6-8 PTZ threshold; n = 6 acute 5-Aza-2dC kindling, n = 8-9 chronic 5-Aza-2dC kindling.

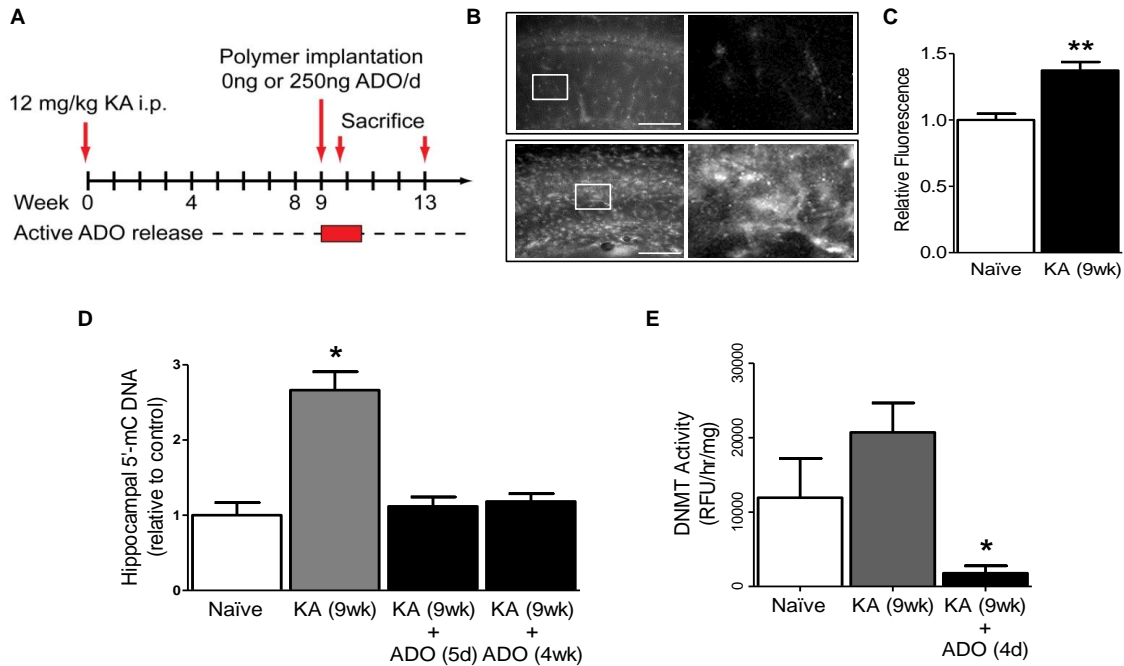


Figure 30. Intraventricular implants of adenosine-releasing silk polymer reverse DNA hypermethylation in the epileptic brain.

(A) Experimental timeline. **(B)** Coronal brain sections of the hippocampal CA1 subregion showing normal ADK expression in non-injured control rats (upper panels) and increased ADK expression in epileptic animals at 9 weeks (wk) after kainic acid (KA) injection (12 mg/kg ip; lower panels). Scale bar = 100 μ m. **(C)** Quantification of ADK immunoreactive material indicates a significant upregulation of ADK in the CA1 subregion of the hippocampus 9 wk after KA injection, compared to naïve controls. **(D)** Adenosine (ADO) releasing polymer attenuates the KA induced increase in global DNA methylation in the hippocampus of epileptic rats. Nine wk post KA (12 mg/kg, i.p.) there is a significant increase in global DNA methylation in the hippocampus of epileptic animals compared to the naïve controls. Bilateral implantation of ADO releasing polymer [250ng/ventricle/day (d) for 10 d] at 9 wk post KA significantly decreases DNA methylation compared to KA rats. Note that DNA methylation in ADO polymer treated KA rats was restored to naïve levels. This reversal in hypermethylation persisted for at least 4 wk following cessation of ADO release from the polymers. **(E)** DNA methyltransferase (DNMT) activity increases in epileptic animals 9 wk after systemic KA, an effect that was strongly and significantly suppressed by ADO released from the polymer. Data are displayed as average \pm SEM; * < 0.05 and ** 0.01; n=3 for all groups.

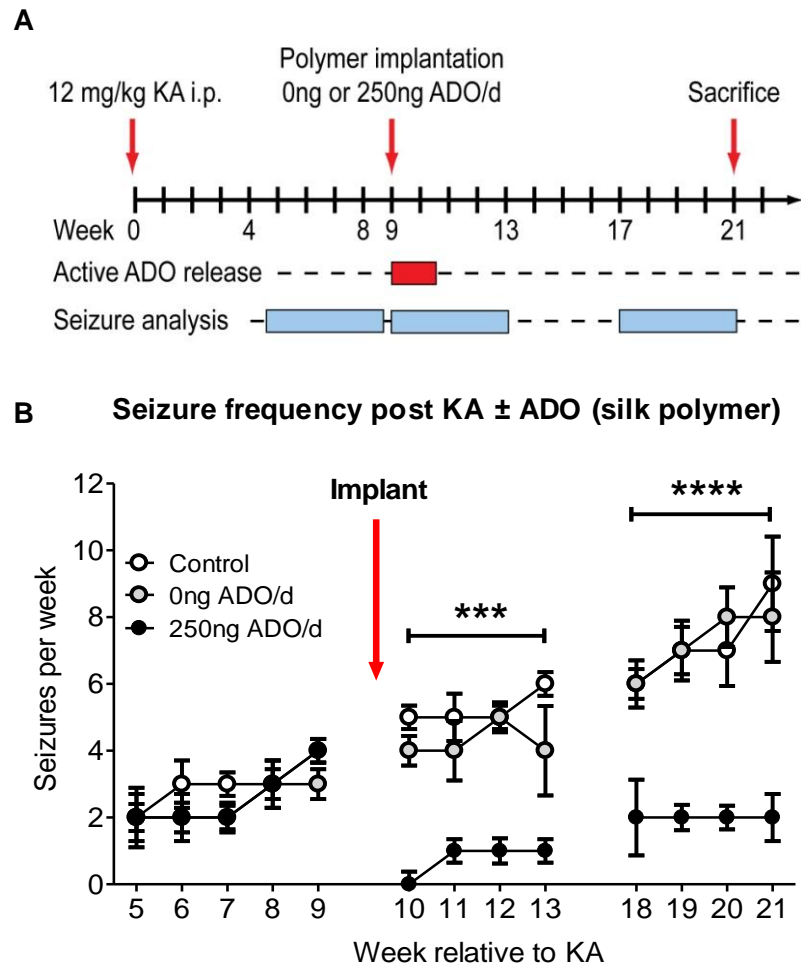


Figure 31. Adenosine-releasing silk polymers prevent progression of epilepsy development.

(A) Experimental design. **(B)** Prevention of epileptogenesis by adenosine (ADO)-releasing silk. 9 weeks (wk) after kainic acid (KA)-injection, epileptic rats received bilateral intraventricular implants of silk-based polymers releasing either 250ng (closed circles ●) or 0ng (gray circles ●) ADO/day (d), or underwent sham surgery (open circles ○). Polymers transiently released a therapeutic dose of ADO for 10 d. Seizures were monitored by video analysis and weekly seizure numbers are presented. Data are displayed as average ± SEM, n=8 for ADO-implant recipients and 5-8 for control groups. Significant differences represent between group comparisons (ADO vs. controls) as analyzed by a two-way ANOVA; *** < 0.001 and **** < 0.0001.

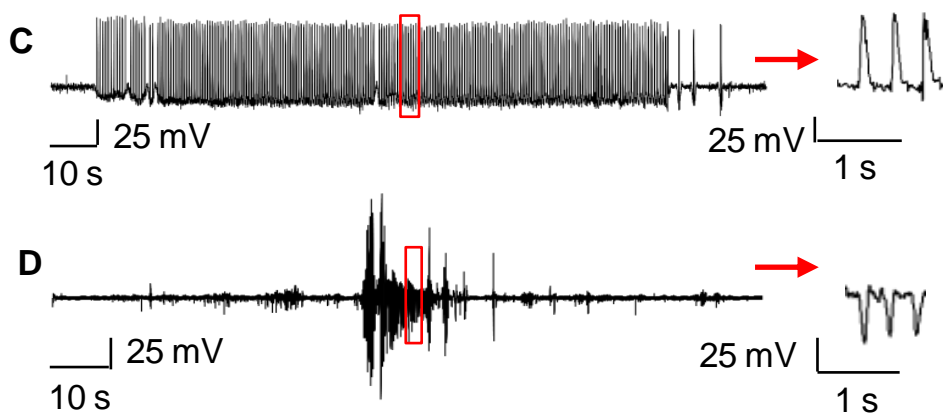


Figure 31, continued. *Adenosine-releasing silk polymers prevent progression of epilepsy development.*

(C) Representative hippocampal EEG trace showing a 2-minute seizure in an animal that received control polymer (0ng ADO/d) 9 wk after systemic administration of KA. **(D)** Example of an epileptiform burst in an animal that received ADO releasing polymer (250ng/d) 9 wk after KA. Note, these events were rare in ADO treated animals and lasted <15 seconds. Higher resolution traces (**regions demarcated by red boxes in panels C & D**) are depicted to the right of the red arrows.

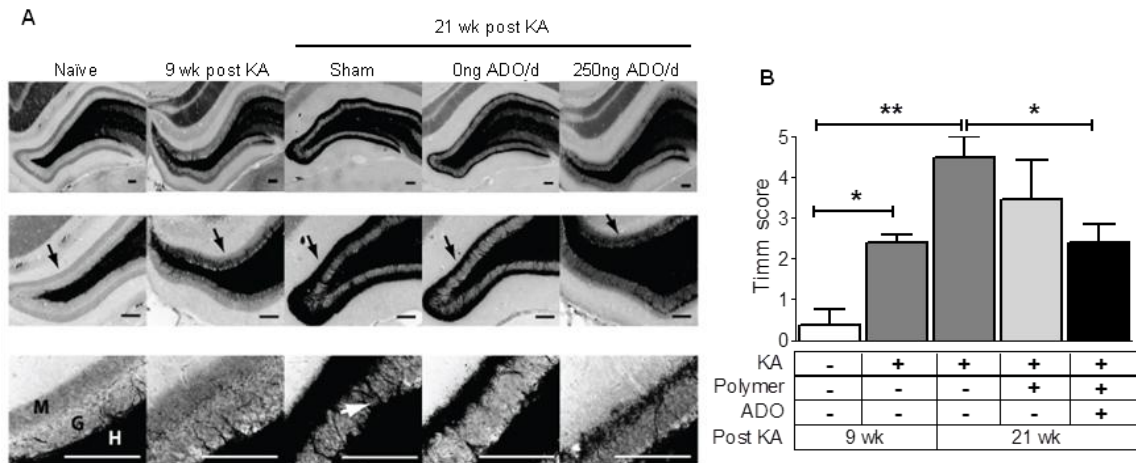


Figure 32. Adenosine-releasing silk polymer implants prevent mossy fiber sprouting.

(A) Transient adenosine (ADO) augmentation therapy in epileptic rats prevents mossy fiber sprouting in the dentate gyrus. Top row: Representative low magnification (5x) images of Timm staining of mossy fibers in hippocampus in naïve animals, animals 9 weeks (wk) post-KA, animals 21 wk post-KA (Sham), and animals 21 wk post-KA that received polymers releasing either 0ng (control) or 250ng ADO/day (d) for a duration of 10 d, (implanted 9 wk post-KA). Middle row: Higher magnification (10x) images that depict Timm granules (black arrows) that correspond to mossy fiber synaptic terminals present in 21 wk post-KA Sham and 0ng ADO/d animals, but not in the 250ng ADO/d animals. Bottom row: High magnification (40x) images that illustrate extensive sprouting of mossy fiber axons in 21 wk post-KA animals (white arrow). M=molecular layer, G= granular layer, H= hilus. Scale bars:500 μ m. **(B)** Quantitative analysis of Timm staining shows that transient ADO delivery significantly reduced mossy fiber sprouting compared to 21 wk post-KA (Sham) animals within the 3 month time span between week 9 and 21. Data represent group average Timm score in hippocampus and are displayed as mean \pm SEM; * < 0.05 and ** < 0.01; n=3 for all groups.

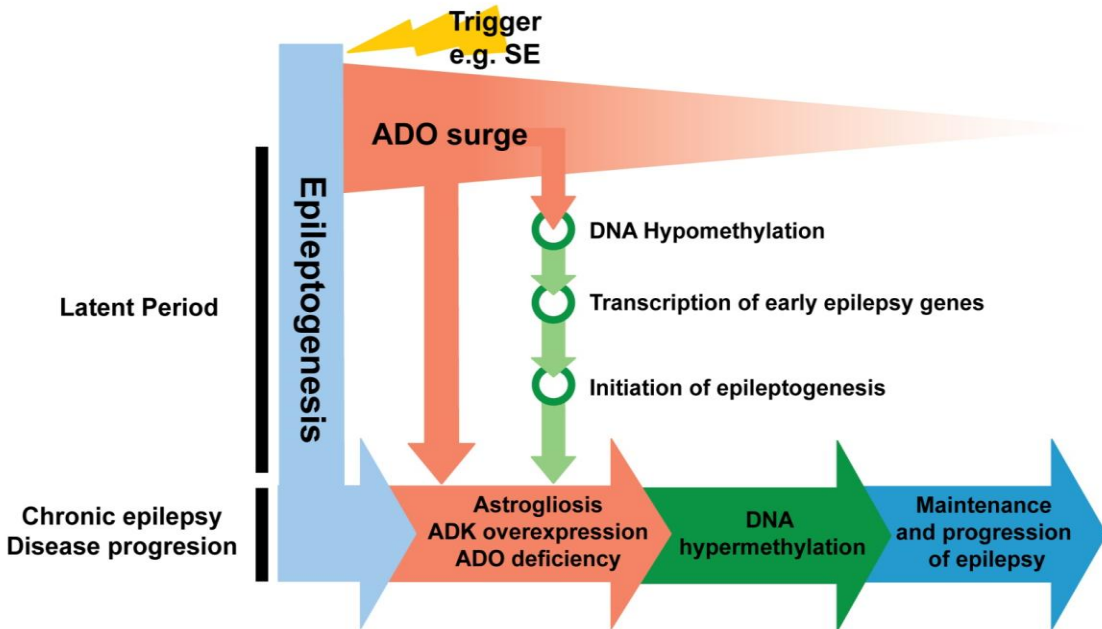


Figure 33. Model for the role of adenosine and associated DNA methylation changes in epileptogenesis.

Epileptogenesis is triggered by a surge of adenosine (ADO), which first induces DNA hypomethylation and the induction of epileptogenesis genes. As part of ongoing epileptogenesis astrogliosis with associated overexpression of ADK occurs, which results in subsequent ADO deficiency. These alterations lead to DNA hypermethylation and maintenance and progression of the epileptic phenotype.

CHAPTER 5

CONCLUSIONS AND SUMMARY

"Why then can one desire too much of a good thing?"

Rosalind to Orlando in *As You Like It*, (Act IV, Scene I), William Shakespeare [445]

1. Endogenous mechanisms can be harnessed for neuroprotection

Too much of a good thing can indeed be bad – consider the immune response: When activated appropriately, the immune system is able to sense and respond to invading pathogens and clear them from the infected host. However, this same response can become dysregulated, producing excessive inflammatory cytokines and other inflammatory mediators, which can also overwhelm and kill the very host it is trying to protect. This is the case in sepsis [446]; the host does not die from the invading pathogens in their system, but from the overwhelming production of inflammatory molecules by the immune system, which triggers widespread inflammation leading to blood clots, leaky blood vessels and potentially organ failure. Termed systemic inflammatory response syndrome (SIRS), death from septic shock following any infection encountered by a host is not a desirable or evolutionarily advantageous outcome. Thus, the immune system has evolved to strategies to regulate itself, tailoring the inflammatory response such that invading pathogens are cleared while doing minimal damage to the host. These self-regulatory mechanisms include upregulation of genes coding anti-inflammatory molecules, and downregulation of genes coding pro-inflammatory molecules.

Just as the body is able to regulate its response to an inflammatory stimulus, organisms are able to respond with adaptive mechanisms to possible recurring threats, whether those threats are external or internal. This is also found to be true at the organ and tissue level. Thus, though it may be highly vulnerable to injury on a cellular level, the brain has developed complex system of neuroprotective strategies to shield itself from injury during times of stress. Following brief non-damaging exposure to an otherwise harmful stimulus the brain induces endogenous mechanisms to prevent exacerbation of damage [131]. By understanding the ways in which the brain is able to alter its response to noxious stimuli, it is then possible to exploit these strategies therapeutically.

Induction of tolerance to cerebral ischemia via Toll-like receptor (TLR)-mediated preconditioning is one such example of the therapeutic application of knowledge about an endogenous protective mechanism to a clinical disease. Low-dose exposure to various TLR ligands including LPS (TLR-4), CpG ODNs (TLR-9), Poly I:C (TLR-3) and Gardiquimod (TLR-7) prior to ischemia have been shown to provide robust reduction in infarct volume in rodents [180, 181, 190, 447, 448]. As previously shown, this protection also extends to a non-human primate model of stroke [191]. The classical TLR ligand, and the first TLR ligand used to confer prophylactic neuroprotection was bacterial endotoxin, LPS.

Preconditioning with LPS has been shown to reduce cerebral damage by several labs in multiple models of transient ischemia [180, 182, 185, 186], as well as permanent

ischemia [126, 188]. This protection has been shown to occur in young healthy animals [180, 182, 186], as well as in animals with co-morbidities (e.g. spontaneously hypertensive rats) [126, 185, 188]. Prevention of ischemic tissue damage by LPS has been shown to extend to other organs, such as the heart [449-451], kidney [133], lung [452], and liver [453, 454]. Preconditioning with LPS has also been shown to reduce brain damage as well as neurological deficits in a rat model of traumatic brain injury [455], and appears to attenuate neuronal death and seizures in pilocarpine-induced epilepsy [456, 457]. However, LPS also triggers the complement, coagulation, fibrinolytic, and kinin pathways to release vasoactive peptides and also the release of an array of cytokine mediators from macrophages and monocytes [458]. The effects of even low dose endotoxin exposure include fever, platelet aggregation, thrombocytopenia, leukocytosis and coagulopathies. Thus, LPS-induced preconditioning is not a good candidate for advancement to clinical use, as endotoxin causes severe inflammatory reactions, including sepsis, in humans.

For these reasons, other TLR ligands are being investigated for clinical use. CpG ODNs are one such promising compound. Currently in use in Phase II and III human clinical trials as vaccine adjuvants, as well as cancer and asthma therapeutics [329], CpG ODNs are particularly well suited for therapeutic development. Preconditioning with CpG ODNs has been shown to confer protection in mixed cortical cultures from oxygen/glucose deprivation (OGD) *in vitro* and from transient MCAO in rodents and primates *in vivo* [190, 191]. The window of protection is similar to that induced by LPS [180, 190], and reduces ischemia-related neurological deficits in rodents (**Figure 83,**

Appendix J). Further, CpG ODNs provide protection from cerebral ischemia when administered by a variety of routes, including intramuscular [191], intraperitoneal, subcutaneous and intranasal (**Figure 40, Appendix B**).

2. CpG preconditioning relies on the peripheral immune response

However, the protection elicited by CpG ODNs is not perfect. In putting forth recommendations for the testing of potential stroke therapeutics, the Stroke Therapeutic Academic and Industry Roundtable (STAIR) recommended testing of compounds in multiple stroke models including transient and permanent occlusion models. To date, all published studies of CpG preconditioning have been completed in transient occlusion models [190, 191]. When tested in a model of permanent occlusion, CpG ODNs failed to reduce ischemic damage (**Figure 42, Appendix C**). Similarly, prophylactic CpG ODNs did not prevent excitotoxic cell death resulting from intrahippocampal administration of KA (**Figure 41, Appendix C**). The finding that CpG ODNs do not seem to protect in permanent occlusion may be explained by their mechanism of action being highly dependent on the peripheral immune response.

The route of administration of CpG ODNs has a large impact on their absorption, distribution, metabolism and elimination. When given subcutaneously, CpG ODNs are slowly absorbed, concentrating in the draining lymph node for several days following administration, and then entering the systemic circulation [329]. Once in the circulation, CpG ODNs bind to plasma proteins, particularly albumin and are rapidly cleared into tissues, favoring kidney, liver and spleen. Interestingly, CpG ODNs do not seem to cross

the blood-testes or blood brain barrier [329]. Further, because TLR9 is endosomal, CpG ODNs must be internalized prior to elicit a response [459]. Thus, CpG ODNs are predominantly sensed by phagocytic cells, such as plasmacytoid dendritic cells (pDCs) [460]. Interestingly, most immune cells do not express TLR9, and so do not respond directly to CpG ODNs, but rather become activated indirectly by contact with pDCs which excrete IFN- α and drive pDC accumulation in the marginal zone and outer T cell area of the lymph node [329, 461]. B cells can also sense CpG DNA, and actively engage in cross-talk with pDCs to modulate immune cell function [460-462].

Administration of subcutaneous CpG ODNs induces high levels of serum cytokines and chemokines, while intravenous administration of the same CpG ODNs fails to induce a measurable cytokine response in humans [463]. As might be predicted, subcutaneous administration of CpG ODNs confers the highest level of ischemic neuroprotection in rodents (**Figure 40, Appendix B**). Tellingly, brains from mice taken following exposure to preconditioning doses of CpG ODNs, show significant (>1.5 fold) regulation of only 2 unique transcripts, where as brains from mice exposed to LPS show regulation of over 140 unique transcripts (**Figure 46, Appendix D**). This change in LPS but not CpG preconditioned animals is on the same magnitude as the change seen in ischemic preconditioning.

In mice, the initiation of a neuroprotective state appears to be at least partially mediated via TNF- α in both LPS and CpG preconditioning. TNF- α levels increase acutely in the serum of mice following i.p. LPS or CpG administration, and TNF- α deficient mice

cannot be preconditioned with LPS or CpG ODNs [182, 190]. However, the blood levels of TNF- α seen after administration of CpG ODNs in mice are nearly 100 fold lower than those seen following LPS administration (**Figure 43, Appendix C**). Thus, CpG and LPS may induce protection via slightly different mechanisms; because it induces such a large release of TNF- α , LPS might induce protection via TNF- α -mediated reprogramming of resident cells in the CNS, while CpG might induce more potent changes to peripheral immune cells, and may have a smaller effect on resident CNS cells. Further, humans and non-human primates do not secrete high levels of TNF- α following administration [463], but NHPs can be robustly protected from transient cerebral ischemia by CpG ODNs [191]. This observation again argues for a predominantly peripheral mechanism of action for CpG ODNs, particularly in non-rodent models of injury.

Lending support to argument in favor of the role of CpG ODNs inducing preconditioning by modulation of the peripheral immune response, CpG ODNs have been shown to induce B, T and Natural Killer cells to secrete cytokines more readily than LPS [464]. Further, CpG ODNs have been shown to induce DCs to establish unidirectional intracellular cross-talk to induce T cell responses [465]. In DCs stimulated with K-type CpG ODNs, this process occurs via a MyD88-dependent, c-Jun N-terminal kinase (JNK)-amplified mechanism, resulting in MyD88-dependent cytokine production [465]. This MyD88-dependent cytokine amplification may then be self-controlled through production of regulatory cytokines such as IL-10. Hence, when injury occurs after preconditioning with CpG ODNs, lymphocytes may be reprogrammed to produce anti-inflammatory cytokines. Thus, CpG ODNs may fail to offer protection in models of

neurological injury where damage is less-dependent on extravasion of peripheral immune cells into the brain parenchyma, such as seizure or permanent occlusion [466].

In vitro experiments have shown that when applied directly to mixed cortical cultures, CpG ODNs preconditioning can protect from OGD [190]. This finding is not surprising as astrocytes, microglia and neurons express TLRs, including TLR9 [146, 467, 468]. TLR9 preconditioning in this system may modulate the cytokine response to injury via stimulation of microglial cells [469], thereby indirectly protecting neurons. As CpG ODNs do not readily cross the blood brain barrier, an interesting *in vivo* correlate to this experiment would be to apply CpG ODNs directly to the CNS (e.g. i.c.v.) and then see if neuroprotection could be elicited. By reprogramming CNS cells directly, it is likely that this route of administration would provide ischemic neuroprotection, both in transient and permanent occlusion. Similarly, i.c.v. administration would likely provide protection from excitotoxic cell death in seizure models.

3. Epigenetics: A universal mechanism of neuroprotection

Robust neuroprotection can be elicited by a wide variety preconditioning stimuli: brief seizure, global or focal cerebral ischemia, hyper- or hypothermia, metabolic inhibition, dietary restriction, sleep deprivation, and inflammation [101, 103, 120-127, 470-472]. Interestingly, the unifying mechanism behind these strategies appears to be reprogramming of the genomic response to injury [130-132, 473, 474]. This is true in ischemic tolerance induced by preconditioning exposure to ischemia [130, 357], hypoxia

[475, 476] or Toll-like receptor ligands [132], as well as in epileptic tolerance [477, 478]. Indeed, tolerance seems to require a broad modification of gene expression, altering expression of genes from throughout the genome. Thus, approaches that have targeted single gene targets to induce neuroprotection have largely failed. The question remains: what exactly is controlling these genomic changes?

The signature of ischemic tolerance appears to largely involve transcriptional suppression and proteomic enrichment of epigenetic gene silencers [132, 473, 479]. By having the ability to affect the entire genome, epigenetic modification at the histone or DNA level may provide the comprehensive remodeling of genomic architecture needed to induce robust neuroprotection. Thus, epigenetic modifications may represent a universal mechanism for the induction of neuroprotection.

3.1 Epigenetic changes in peripheral immune cells

Epigenetic modifications, which alter gene transcription without modifying the underlying DNA sequence, are highly plastic and can respond rapidly in response to environmental cues, an important endogenous mechanism for temporally and spatially controlling gene expression. Epigenetic modifications occur in cells throughout the body, and may play a critical role in mediating immune cell response to inflammatory signals. Patients who survive SIRS often go on to have long term immune deficiencies, termed compensatory anti-inflammatory response syndrome (CARS) [480]. Thought to be due to an attempt by the body to regulate the harmful systemic T_H1 immune

response driving systemic inflammation and organ failure [481], CARS is characterized by upregulation of anti-inflammatory cytokines such as IL-10 [482] and increase susceptibility to infection that can last for days, weeks or even years [483]. Both SIRS and CARS are caused by dysregulation of pro- or anti-inflammatory cytokines. In immune cells, expression of these proteins can be regulated by at the pre- and post-translation level. It is becoming increasingly clear that epigenetics play an important role in mediating these changes. CARS is hypothesized to be driven by production of anti-inflammatory molecules elicited to counteract the overwhelming inflammatory profile in SIRS, but may also be caused by suppression of these gene loci at the cellular level via epigenetic changes in mature immune cells [480].

Notably, tolerance to innate immune ligands such as LPS seems to be driven by cell-intrinsic mechanisms that have an epigenetic basis (**Figure 34**). Following LPS exposure, dimethylation at histone 3 lysine residue 9 (H₃K₉me₂) in the IL-1 β and TNF- α promoters specifically suppresses these gene loci, inhibiting transactivation of these genes by NF κ B [484]. LPS stimulation also leads to increases in the histone demethylase KDM6B (JMJD3) via NF κ B [485]. Further, binding of H3K9 histone methyltransferase G9a to the TNF- α promoter during LPS induced tolerance leads DNA methylation-induced suppression of gene expression via recruitment of DNA methyltransferase (DNMT) 3a/b [486]. Production of TNF- α by immune cells has been shown to also requires active epigenetic modifications, as application of the broad histone deacetylase (HDAC) inhibitor triclostatin A (TSA) inhibits this process [487]. Finally, recently it has been shown that microRNAs, small non-coding RNAs that inhibit translation by targeted

degradation of mRNA, serve as mediators of LPS-tolerance via transcriptional silencing [488].

The activity of adaptive immune cells is also shaped by epigenetic modifications. Perturbations in epigenetic activation or silencing of genes can have deleterious effects on the ability of naïve T cells to commit to a lineage [480]. Further, maturation of anti-inflammatory T_{regulatory} (T_{reg}) cells requires histone methylation and acetylation as well as DNA methylation at promoter and enhancer regions of the *Foxp3* locus [489, 490]. It is highly likely that similar epigenetic processes are essential to the implementation of the reprogramming of the inflammatory response seen in TLR-mediated preconditioning, as well as in preconditioning elicited by other methods.

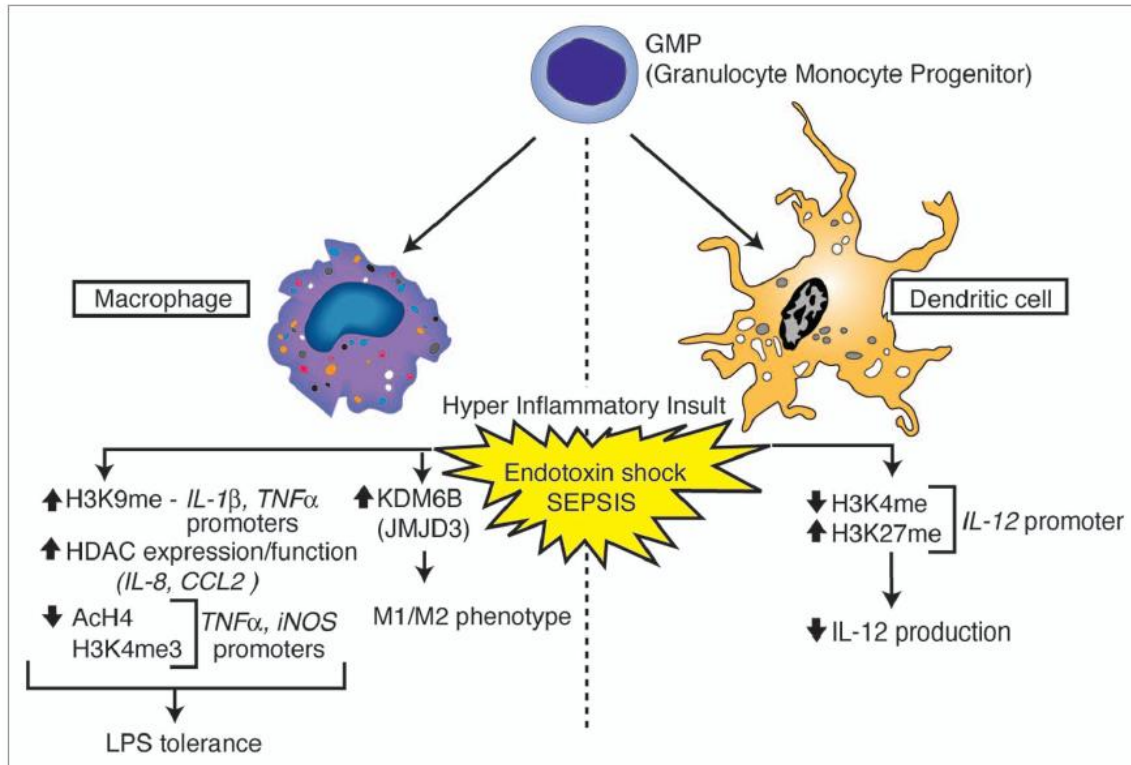


Figure 34. Epigenetic reprogramming of immune cells following sepsis

Overview of histone modifications and gene regulation events that occur in myeloid cells following endotoxic shock and sepsis. Phenotypic outcomes associated with the indicated modifications are listed below each cell type. Adapted from *Epigenetics* 6(3), 2011 [480]. Williams F Carson IV, Karen Cavassani, Yali Dou, Steven L. Kunkel, "Epigenetic regulation of immune cells functions during post-sepsis immunosuppression" pp. 273-83.

3.2 Epigenetic changes in the CNS: Roles in disease and neuroprotection

Changes in histone acetylation and methylation, as well as changes in DNA methylation, once thought to occur only in dividing cells, have been shown to occur in mature cells in the central nervous system (CNS) [389, 390]. Tellingly, these changes occur regularly and rapidly. Even a single initial episode of neural synchronization exceeding 30 seconds in the hippocampus induces DNA methylation-dependent epigenetic alterations in transcription of immediate early genes and initiates a cascade of transcription factors contributing to long-term neuronal and circuit alterations [391].

The epigenetic landscape of the brain has come under increasing scrutiny in recent years, in part due to the increasing number of techniques available for surveying the epigenome, and in part due to several seminal discoveries and 're-discoveries'. DNA methylation in particular has garnered favor, thanks in part to the 're-identification' of the sixth base of the genome, 5-hydroxymethylcytosine [419] an oxidative intermediate of DNA demethylation, and the characterization of the Tet family of proteins responsible for facilitating active DNA demethylation [420]. Shown to be integral to memory formation [421], active DNA methylation is maintained in nondividing, post-mitotic neurons via DNMTs 1 and 3a [389]. DNMT activity has also been shown to regulate synaptic plasticity in the hippocampus [422]. Subsequent work has shown that active DNA demethylation is induced by neuronal activity in mature neurons [423], leading in turn to adult neurogenesis [390]. Altered DNA methylation in the brain has also been implicated in psychiatric and neurological conditions, including epilepsy and stroke [388, 390, 392, 393].

The methylation hypothesis of epileptogenesis suggests that seizures by themselves can induce epigenetic chromatin modifications and thereby aggravate the epileptogenic condition [387]. Several lines of evidence now support the notion that epigenetic changes, including DNA methylation, histone modifications, chromatin remodeling, noncoding RNAs, and RNA editing, are pathological hallmarks of human epilepsy syndromes and intrinsically linked to the process of epileptogenesis [388]. DNA methyltransferases 1 and 3 have been found to be overexpressed in the brains of patients with temporal lobe epilepsy (TLE) [424]. Increased Reelin promoter methylation has been associated with granule cell dispersion in human TLE [392]. Genes associated with DNA methylation (e.g. MeCP2) have been shown to be elevated in human epilepsy and animal seizure models [425]. El mice, which are predisposed to develop epilepsy, are characterized by disordered feedback regulation of methyl transfer by S-adenosylhomocysteine hydrolase [491], which likely impacts DNA methylation status. Further, it has recently been discovered that several commonly used antiepileptic drugs have epigenetic effects [394, 395] which may be responsible for their efficacy. One such example is Valproic acid. Used for decades as an antiepileptic drug, Valproic acid since been shown to function as a histone deacetylase inhibitor [386, 394], and more recently as an inhibitor of DNA methylation [395, 492].

In stroke, methylation changes govern the molecular and cellular mechanisms that underlie pathogenesis and repair, including activation of the stress response and promotion of tissue regeneration and functional reorganization [388]. Alterations in gene expression, due in part to epigenetic modifications, define states of ischemic

tolerance [473, 479]. Epigenetic suppressors, such as the polycomb group of proteins and modified histone are enriched in ischemic tolerance [479]. Further, alterations to DNA methylation status can alter outcome following cerebral ischemia. Following MCAO DNA methylation levels are increased in cerebral tissue, and may be responsible for promoting cell death. Treatment of mice with the DNA methyltransferase inhibitor 5-Aza-2'-deoxycytidine reduced damage caused by transient MCAO [493], and mice deficient in DNA methyltransferase 1 in post mitotic neurons have reduced infarct volume [494]. Human patients deficient in methylenetetrahydrofolate reductase (MTHFR), involved in folate metabolism and important for the maintenance of pools of the methyl donor S-adenosylmethionine (SAM), suffer from hyperhomocysteinemia which results in an increased risk of stroke and cardiovascular disease [495, 496].

Epigenetic mechanisms are critical for neural stem cell maintenance, neurogenesis, gliogenesis, brain patterning, and synaptic plasticity and connectivity, and thus targeted therapies directed at restoring normal epigenetic programs may be highly beneficial in neurological injury (**Figure 35**). These therapies may be useful as neuroprotectants, as exemplified by preconditioning paradigms in stroke, or as regenerative treatments as modeled by adenosine augmentation therapy (AAT) in epilepsy (**Chapter 4**).

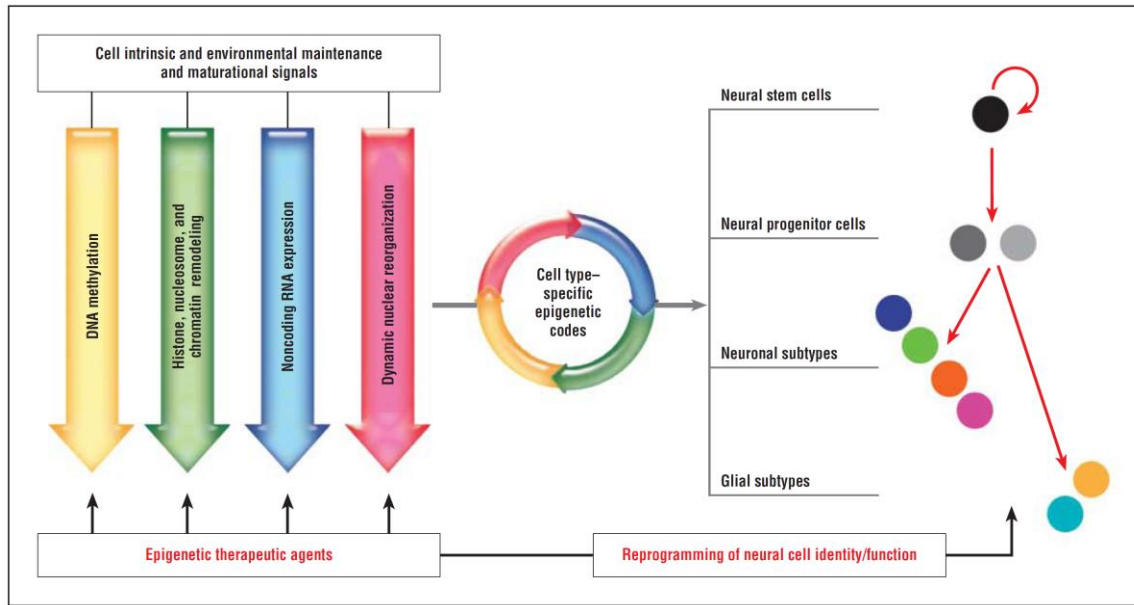


Figure 35. Epigenetic mechanisms that underlie neural stem cell maintenance and maturation

Specific epigenetic codes define neural cell identity and function. Modulation of these codes using epigenetic therapeutic agents represents a novel strategy for neural cell reprogramming and treatment of neurological disease. Adapted from *Archives of Neurology* 68(3), 2011. Ifran A Qureshi and Mark F Mehler, "The emerging role of epigenetics in stroke III. Neural stem cells biology and regenerative medicine" pp. 294-302.

3.3 Role of Adenosine as an epigenetic modifier

Acute brain injury, particularly after trauma, stroke, or seizures, is associated with a surge of the brain's endogenous neuroprotectant adenosine [363, 365], which can increase the acute neuroprotective capacity of the brain, and trigger downstream events that create a state of delayed protection that can protect the brain from subsequent injury. As increases in brain adenosine, in response to changes in ADK expression, have been shown to be both neuroprotective and antiepileptic in acute seizure models [367], ADK expression levels may also determine the degree of neuroprotection and tolerance in ischemia. Thus, the adenosine-ADK system may be a candidate as an endogenous effector of acute and delayed neuroprotection (tolerance).

Adenosine receptor dependent pathways are known to contribute to the protective role of adenosine in the delayed response to ischemic injury through its anti-inflammatory actions [375], modulation of the neuro-immune response and role in promoting angiogenesis and tissue remodeling [218]. The role of specific adenosine receptors in the context of stroke however varies with level and duration of stimulation, and is highly affected by temporal and spatial relationships. As such, the precise timing, duration and level of stimulation needed at the receptor level to provide neuroprotection is likely to be impossible to mimic pharmacologically. However, it is possible to globally manipulate adenosine tone via AAT. Interestingly, use of AAT may lead to durable changes that outlast the direct effect of adenosine on its specific receptors.

DNA methylation requires the donation of a methyl group from S-adenosylmethionine (SAM), a process that is facilitated by DNA methyltransferase enzymes (**Figure 28, Chapter 4**). The resulting product, S-adenosylhomocysteine (SAH) is then further converted into adenosine and homocysteine by SAH hydrolase. Critically, the equilibrium constant of the SAH hydrolase enzyme lies in the direction of SAH formation [397]; therefore, the reaction will only proceed when adenosine and homocysteine are constantly removed [358, 397]. If adenosine concentration is increased therapeutically (e.g. by AAT), DNA methylation, and potentially other methylation reactions, can be inhibited.

Local adenosine tone in the brain is also regulated via endogenous mechanism in disease. In the adult brain, removal of adenosine occurs largely via the astrocyte-based enzyme adenosine kinase (ADK) [220, 398]. For some time dysregulation of ADK and the resultant changes in adenosine tone have been implicated in epileptogenesis [367, 399]. Epileptogenesis may be triggered by a surge in high levels of adenosine that can result from injuries such as SE, stroke, or brain trauma [363, 365, 411]. As the current findings suggest, high levels of acute adenosine induces DNA hypomethylation, which in turn could permit the expression of early epilepsy genes that contribute to initiating epileptogenesis. Epileptogenesis in turn is associated with astrogliosis, overexpression of ADK and resulting adenosine deficiency [367, 383, 399]. Once these changes in ADK expression are established, they result in pathological hypermethylation of DNA. This in turn could lead to suppression of neurogenesis genes, perpetuating and exacerbating epileptogenesis. Alternatively, this increase in DNA methylation might occur in gene

bodies [441], leading to increased gene transcription of inflammatory or excitatory pathway intermediates.

Altered adenosine tone likely also plays a role in pathogenesis of cerebral ischemia via epigenetic mechanisms. ADK expression also decreases acutely following cerebral ischemia [364, 365], which may, as proposed in epileptogenesis, lead to hypomethylation of inflammatory gene loci at the DNA or histone level. This may result in a cascade of inflammatory mediators, worsening ischemic damage, and inhibiting repair processes. As mentioned previously, dimethylation of H3K9 has been shown to suppress TNF- α production; thus de-methylation of this same region may lead to increase TNF- α production. Longer term, ADK expression may increase in areas surrounded by glial scars, leading to further gene dysregulation via hypermethylation. Hypermethylation of genes may change the fate of neural progenitor cells, as demethylation of specific gene promoters commits these cells to either neural or glial lineage [497, 498]. Stem cell proliferation is protective in stroke, and neural progenitor cells have been shown to be a requirement for induction of tolerance [499]. Further, perturbation in the epigenetic landscape of individual cells might dysregulate cell-intrinsic properties that govern stem cell generation or formation of local circuitry. Again, use of AAT in stroke, whether alone or in combination with TLRs preceding injury to induce a neuroprotective phenotype, or following injury to induce plasticity and repair, may be beneficial (**Figure 36**).

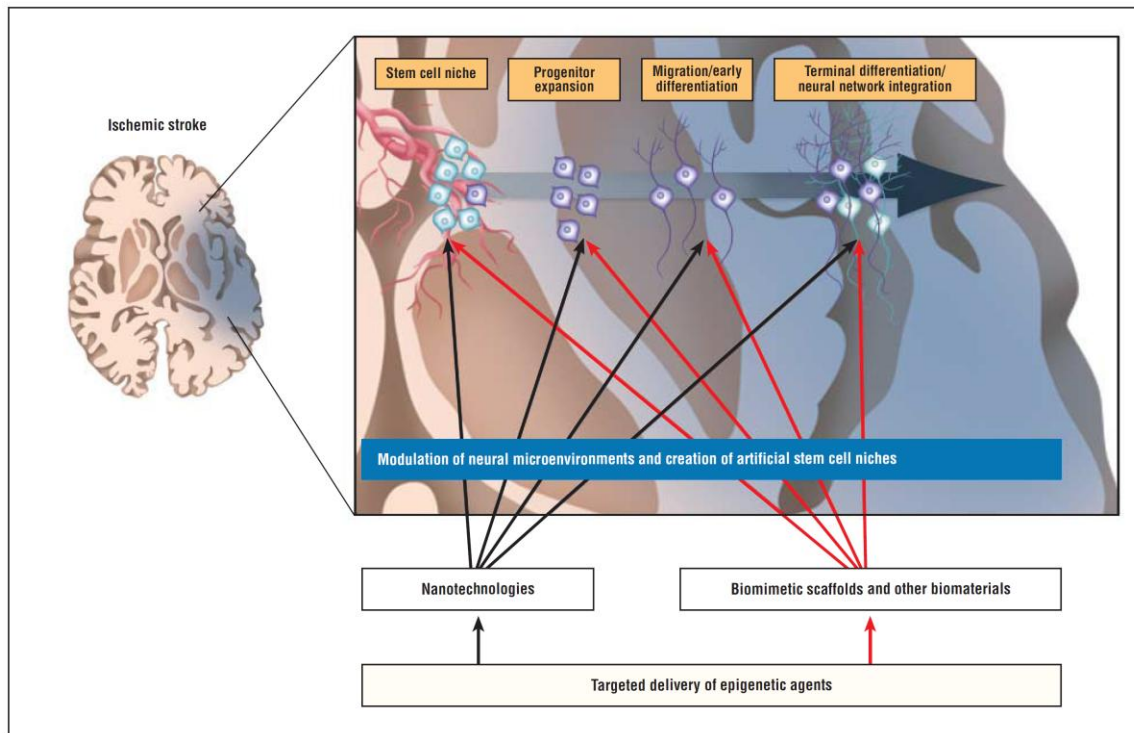


Figure 36. *Endogenous neural stem cell activation for the treatment of neurological disease*

Schematic representing emerging technological innovations, such as nanotechnologies and advanced biomaterials such as biodegradable adenosine-releasing silk polymers, for targeted delivery of epigenetic therapeutic agents to promote neural repair after neurological injury. Adapted from *Archives of Neurology* 68(3), 2011. Ifran A Qureshi and Mark F Mehler, “The emerging role of epigenetics in stroke III. Neural stem cells biology and regenerative medicine” pp. 294-302.

3.4 Long-lasting potential of epigenetic therapies

There is increasing evidence to support the idea that even a brief exposure to an epigenetic modulator may lead to long-standing changes in gene expression [430]. Recent work in cancer biology has shown that exposure to transient low doses of DNA demethylating agents can produce long-term anti-tumor effects, modulated by genome wide promoter methylation, which persist long after drug withdrawal [431]. By broadly targeting multiple intracellular pathways via genome-wide altered DNA methylation status, epigenetic reprogramming could be used to directly address a major weakness of current epilepsy treatments: inability to halt long-term disease progression [432]. Thus, it might be possible to use a transient treatment to induce durable therapeutic changes via epigenetic reprogramming.

4. Summary

CpG ODNs offer great promise as prophylactant neuroprotectants. However, they may not afford protection in all settings of neurological injury. Damage from transient ischemic stroke seems to be alleviated by CpG-induced neuroprotection, while damage from permanent occlusive stroke and seizure-induced excitotoxic cell damage do not. Fortunately, damage in these last conditions does not seem to be worsened by CpG preconditioning. However, in order maximize success of CpG ODNs in clinical trials, selection of patients should include screening to capture patients who are at risk of transient cerebral ischemic events, or should use post-hoc exclusion criteria to remove

patients that had non-transient ischemic events prior to data analysis. CpG ODNs have also not yet been tested in aged animals or in female animals, key clinical populations at risk for cerebral injury. Notably, activation of TLR9 is altered with age [500, 501], suggesting CpG ODNs may not be as effective in elderly patients. Further, animals with co-morbidities will need to be used to validate the safety of CpG ODNs. Though early suspicions that CpG ODNs would potentiate autoimmune disorders have largely proved to be unfounded, however, CpG ODNs have been shown to exacerbate lupus [502], multiple sclerosis [503], colitis [504] and arthritis [505] in mouse models; more work needs to be done to address these concerns.

Local CNS specific AAT may be highly beneficial for a variety of neurological conditions, including epilepsy and stroke. As shown here, because adenosine can act as a modulator of the epigenetic landscape in the brain, the beneficial effects of adenosine augmentation likely extend beyond the window of active receptor activation. Reversal of hypermethylated state resulting from neurological injuries such as cerebral ischemia or epileptic seizures may prove to be a universal target of neuroprotective strategies. Recent work has also shown that differential DNA methylation status define the state of epileptic tolerance following preconditioning [506]. The change in methylation status seen in a variety of neurological diseases and in neuroprotection may be commonly mediated by endogenous release of adenosine in response to injury and/or preconditioning.

Epigenetic modifications induced by adenosine likely extend beyond purely DNA methylation, and may include altered methylation of histones and other proteins. Contemporary therapeutics designed to treat neurological injuries focus on preventing cell death, inflammation, or other specific processes. Epigenetic approaches are able to exert a combinatorial effect on damaged tissue, encompassing and activating a wide range of repair systems that single action therapeutics cannot [507]. Future approaches to preventing and treating neurological diseases that manipulate the epigenetic landscape will likely have much higher rates of success in clinical disease, due to their ability to orchestrate broad changes via endogenous mechanisms .

References:

1. Brockman, J., ed. *What we believe but cannot prove*. 2006, HarperCollins Publishers: New York. 252.
2. Leonard, W.R., J.J. Snodgrass, and M.L. Robertson, *Effects of brain evolution on human nutrition and metabolism*. *Annu Rev Nutr*, 2007. **27**: p. 311-27.
3. Leonard, W.R. and M.L. Robertson, *Comparative primate energetics and hominid evolution*. *Am J Phys Anthropol*, 1997. **102**(2): p. 265-81.
4. Laughlin, S.B., R.R. de Ruyter van Steveninck, and J.C. Anderson, *The metabolic cost of neural information*. *Nat Neurosci*, 1998. **1**(1): p. 36-41.
5. Aiello, L.C., *Brains and guts in human evolution: the expensive tissue hypothesis*. *Brazilian Journal of Genetics*, 1997. **20**: p. 141-148.
6. Saver, J.L., *Time is brain--quantified*. *Stroke*, 2006. **37**(1): p. 263-6.
7. Murphy, S., J. Xu, and K. Kochanek, *Deaths: Preliminary Data for 2010*, in *National Vital Statistics Report*. 2012, Center for Disease Control and Prevention. p. 1-68.
8. CDC, *Heart disease and stroke prevention: Addressing the Nation's leading killers*, D.f.H.D.a.S. Prevention, Editor. 2011, National Center for Chronic Disease Prevention and Health Promotion. p. 1-4.
9. Hauser, W.A., J.F. Annegers, and L.T. Kurland, *Prevalence of epilepsy in Rochester, Minnesota: 1940-1980*. *Epilepsia*, 1991. **32**(4): p. 429-45.
10. Auer, R.N., *Non-pharmacologic (physiologic) neuroprotection in the treatment of brain ischemia*. *Ann N Y Acad Sci*, 2001. **939**: p. 271-82.

11. Doyle, K.P., R.P. Simon, and M.P. Stenzel-Poore, *Mechanisms of ischemic brain damage*. Neuropharmacology, 2008. **55**(3): p. 310-8.
12. Gonzalez, R., et al., *Acute ischemic stroke: Imaging and intervention*. 2006: Springer.
13. Olney, J.W., *Brain lesions, obesity, and other disturbances in mice treated with monosodium glutamate*. Science, 1969. **164**(3880): p. 719-21.
14. Gunter, T.E. and K.K. Gunter, *Uptake of calcium by mitochondria: transport and possible function*. IUBMB Life, 2001. **52**(3-5): p. 197-204.
15. Khodorov, B., *Glutamate-induced deregulation of calcium homeostasis and mitochondrial dysfunction in mammalian central neurones*. Prog Biophys Mol Biol, 2004. **86**(2): p. 279-351.
16. Gogvadze, V. and S. Orrenius, *Mitochondrial regulation of apoptotic cell death*. Chem Biol Interact, 2006. **163**(1-2): p. 4-14.
17. White, R.J. and I.J. Reynolds, *Mitochondrial depolarization in glutamate-stimulated neurons: an early signal specific to excitotoxin exposure*. J Neurosci, 1996. **16**(18): p. 5688-97.
18. Starkov, A.A., C. Chinopoulos, and G. Fiskum, *Mitochondrial calcium and oxidative stress as mediators of ischemic brain injury*. Cell Calcium, 2004. **36**(3-4): p. 257-64.
19. Edvinsson, L. and D.N. Krause, *Cerebral blood flow and metabolism*. 2nd ed. 2002: Lipincott, Williams and Wilkins.
20. Coyle, J. and P. Puttfarcken, *Oxidative stress, glutamate, and neurodegenerative disorders*. Science, 1993. **262**: p. 689-695.

21. Halliwell, B., *Free radicals, antioxidants, and human disease: curiosity, cause, or consequence?* Lancet, 1994. **344**(8924): p. 721-4.
22. Sugawara, T. and P.H. Chan, *Reactive oxygen radicals and pathogenesis of neuronal death after cerebral ischemia.* Antioxid Redox Signal, 2003. **5**(5): p. 597-607.
23. Huang, J., U.M. Upadhyay, and R.J. Tamargo, *Inflammation in stroke and focal cerebral ischemia.* Surg Neurol, 2006. **66**(3): p. 232-45.
24. Yamasaki, Y., et al., *New therapeutic possibility of blocking cytokine-induced neutrophil chemoattractant on transient ischemic brain damage in rats.* Brain Res, 1997. **759**(1): p. 103-11.
25. Garau, A., et al., *Neuroprotection with the CXCL8 inhibitor repertaxin in transient brain ischemia.* Cytokine, 2005. **30**(3): p. 125-31.
26. Hurn, P.D., et al., *T- and B-cell-deficient mice with experimental stroke have reduced lesion size and inflammation.* J Cereb Blood Flow Metab, 2007. **27**(11): p. 1798-805.
27. Rodrigues, S.F. and D.N. Granger, *Role of blood cells in ischaemia-reperfusion induced endothelial barrier failure.* Cardiovasc Res, 2010. **87**(2): p. 291-9.
28. Jain, K.K., *The Handbook of Neuroprotection.* 1st edition ed. 2011: Humana Press. 547.
29. Reis, D.J., et al., *Central neurogenic neuroprotection: central neural systems that protect the brain from hypoxia and ischemia.* Ann N Y Acad Sci, 1997. **835**: p. 168-86.

30. Folkow, A.B.B., *Cardiovascular adjustments to diving in mammals and birds*, in *The Cardiovascular System*, E.M.R.C.C. Michel, Editor. 1983, American Physiological Society: Bethesda, MD. p. 917-945.
31. Wolf, S., *Sudden death and the oxygen-conserving reflex*. Am Heart J, 1966. **71**(6): p. 840-1.
32. Golanov, E.V. and D.J. Reis, *Contribution of oxygen-sensitive neurons of the rostral ventrolateral medulla to hypoxic cerebral vasodilatation in the rat*. J Physiol, 1996. **495 (Pt 1)**: p. 201-16.
33. Zhou, F., et al., *Hibernation, a model of neuroprotection*. Am J Pathol, 2001. **158**(6): p. 2145-51.
34. Heldmaier, G., S. Ortmann, and R. Elvert, *Natural hypometabolism during hibernation and daily torpor in mammals*. Respir Physiol Neurobiol, 2004. **141**(3): p. 317-29.
35. Barnes, B.M., *Freeze avoidance in a mammal: body temperatures below 0 degree C in an Arctic hibernator*. Science, 1989. **244**(4912): p. 1593-5.
36. Buck, C.L. and B.M. Barnes, *Effects of ambient temperature on metabolic rate, respiratory quotient, and torpor in an arctic hibernator*. Am J Physiol Regul Integr Comp Physiol, 2000. **279**(1): p. R255-62.
37. Frerichs, K.U., et al., *Local cerebral blood flow during hibernation, a model of natural tolerance to "cerebral ischemia"*. J Cereb Blood Flow Metab, 1994. **14**(2): p. 193-205.
38. Nathaniel, T.I., *Brain-regulated metabolic suppression during hibernation: a neuroprotective mechanism for perinatal hypoxia-ischemia*. Int J Stroke, 2008. **3**(2): p. 98-104.

39. Drew, K.L., et al., *Hypoxia tolerance in mammalian heterotherms*. J Exp Biol, 2004. **207**(Pt 18): p. 3155-62.
40. Drew, K.L., et al., *Neuroprotective adaptations in hibernation: therapeutic implications for ischemia-reperfusion, traumatic brain injury and neurodegenerative diseases*. Free Radic Biol Med, 2001. **31**(5): p. 563-73.
41. Hiestand, W.A., et al., *The comparative hypoxic resistance of hibernators and nonhibernators*. Physiol Zool, 1950. **23**(3): p. 264-8.
42. Frerichs, K.U. and J.M. Hallenbeck, *Hibernation in ground squirrels induces state and species-specific tolerance to hypoxia and aglycemia: an in vitro study in hippocampal slices*. J Cereb Blood Flow Metab, 1998. **18**(2): p. 168-75.
43. Ghai, H.S. and L.T. Buck, *Acute reduction in whole cell conductance in anoxic turtle brain*. Am J Physiol, 1999. **277**(3 Pt 2): p. R887-93.
44. Hochachka, P.W., *Defense strategies against hypoxia and hypothermia*. Science, 1986. **231**(4735): p. 234-41.
45. Perez-Pinzon, M.A., et al., *Downregulation of sodium channels during anoxia: a putative survival strategy of turtle brain*. Am J Physiol, 1992. **262**(4 Pt 2): p. R712-5.
46. Popov, V.I. and L.S. Bocharova, *Hibernation-induced structural changes in synaptic contacts between mossy fibres and hippocampal pyramidal neurons*. Neuroscience, 1992. **48**(1): p. 53-62.
47. Toien, O., et al., *Ascorbate dynamics and oxygen consumption during arousal from hibernation in Arctic ground squirrels*. Am J Physiol Regul Integr Comp Physiol, 2001. **281**(2): p. R572-83.

48. Drew, K.L., et al., *Ascorbate and glutathione regulation in hibernating ground squirrels*. Brain Res, 1999. **851**(1-2): p. 1-8.
49. Buzadzic, B., et al., *Seasonal variation in the antioxidant defense system of the brain of the ground squirrel (Citellus citellus) and response to low temperature compared with rat*. Comp Biochem Physiol C Pharmacol Toxicol Endocrinol, 1997. **117**(2): p. 141-9.
50. Buzadzic, B., et al., *Antioxidant defenses in the ground squirrel Citellus citellus. 1. A comparison with the rat*. Free Radic Biol Med, 1990. **9**(5): p. 401-6.
51. Buzadzic, B., et al., *Antioxidant defenses in the ground squirrel Citellus citellus. 2. The effect of hibernation*. Free Radic Biol Med, 1990. **9**(5): p. 407-13.
52. Svihla, A., H. Bowman, and R. Pearson, *Prolongation of Blood Clotting Time in the Dormant Hamster*. Science, 1952. **115**(2984): p. 272.
53. Svihla, A., H.R. Bowman, and R. Ritenour, *Prolongation of clotting time in dormant estivating mammals*. Science, 1951. **114**(2960): p. 298-9.
54. Pivorun, E.B. and W.B. Sinnamon, *Blood coagulation studies in normothermic, hibernating, and aroused Spermophilus franklini*. Cryobiology, 1981. **18**(5): p. 515-20.
55. Lyman, C.P. and P.O. Chatfield, *Physiology of hibernation in mammals*. Physiol Rev, 1955. **35**(2): p. 403-25.
56. Sidky, Y.A., J.S. Hayward, and R.F. Ruth, *Seasonal variations of the immune response of ground squirrels kept at 22-24 degrees C*. Can J Physiol Pharmacol, 1972. **50**(3): p. 203-6.

57. Spurrier, W.A. and A.R. Dawe, *Several blood and circulatory changes in the hibernation of the 13-lined ground squirrel, Citellus tridecemlineatus*. *Comp Biochem Physiol A Comp Physiol*, 1973. **44**(2): p. 267-82.
58. Hoff, J.T., et al., *Barbiturate protection from cerebral infarction in primates*. *Stroke*, 1975. **6**(1): p. 28-33.
59. Michenfelder, J.D., J.H. Milde, and T.M. Sundt, Jr., *Cerebral protection by barbiturate anesthesia. Use after middle cerebral artery occlusion in Java monkeys*. *Arch Neurol*, 1976. **33**(5): p. 345-50.
60. Michenfelder, J.D. and R.A. Theye, *Cerebral protection by thiopental during hypoxia*. *Anesthesiology*, 1973. **39**(5): p. 510-7.
61. Secher, O. and B. Wilhjelm, *The protective action of anaesthetics against hypoxia*. *Can Anaesth Soc J*, 1968. **15**(5): p. 423-40.
62. Goldstein, A., Jr., B.A. Wells, and A.S. Keats, *Increased tolerance to cerebral anoxia by pentobarbital*. *Arch Int Pharmacodyn Ther*, 1966. **161**(1): p. 138-43.
63. Hippocrates, *De Vetere Medicina*, in *Hippocrates Volume II*, L.C. Library, Editor. 460-375 BC, Harvard University Press. p. 416.
64. Celcus, A., *De Medicina*, in *Celus AD*, L.C. Library, Editor. 1st century AD, Harvard University Press.
65. Galaeus, C., *Galaenus: On the natural faculties*, L.C. Library, Editor. 129-199 AD, Harvard University Press.
66. Sanchez, G.M. and A.L. Burrige, *Decision making in head injury management in the Edwin Smith Papyrus*. *Neurosurg Focus*, 2007. **23**(1): p. E5.
67. Feldman, R.P. and J.T. Goodrich, *The Edwin Smith Surgical Papyrus*. *Childs Nerv Syst*, 1999. **15**(6-7): p. 281-4.

68. Breasted, J.H., *The Edwin Surgical Papyrus: published in facsimile and hieroglyphic transliteration with translation and commentary in two volumes*. Vol. 3-4. 1991, Chicago: University of Chicago Oriental Institute Publications.
69. Dimopoulos, V.G., et al., *Head injury management algorithm as described in Hippocrates' "peri ton en cephalo traumaton"*. *Neurosurgery*, 2005. **57**(6): p. 1303-5; discussion 1303-5.
70. Kshetry, V.R., S.A. Mindea, and H.H. Batjer, *The management of cranial injuries in antiquity and beyond*. *Neurosurg Focus*, 2007. **23**(1): p. E8.
71. Rose, F.C., *The history of head injuries: an overview*. *J Hist Neurosci*, 1997. **6**(2): p. 154-80.
72. Fay, T., *Early experiences with local and general refrigeration of the human brain*. *Journal of Neurosurgery*, 1959. **16**: p. 22.
73. Fay, T., *Observations on generalized refrigeration in cases of severe cerebral trauma*. *Proceedings of the Association for Research of Nervous and Mental Diseases*, 1943. **24**: p. 611-619.
74. Polderman, K.H., *Application of therapeutic hypothermia in the ICU: opportunities and pitfalls of a promising treatment modality. Part 1: Indications and evidence*. *Intensive Care Med*, 2004. **30**(4): p. 556-75.
75. Froehler, M.T. and R.G. Geocadin, *Hypothermia for neuroprotection after cardiac arrest: mechanisms, clinical trials and patient care*. *J Neurol Sci*, 2007. **261**(1-2): p. 118-26.
76. Milde, L.N., *Clinical use of mild hypothermia for brain protection: a dream revisited*. *J Neurosurg Anesthesiol*, 1992. **4**(3): p. 211-5.

77. Small, D.L., P. Morley, and A.M. Buchan, *Biology of ischemic cerebral cell death*. Prog Cardiovasc Dis, 1999. **42**(3): p. 185-207.
78. Botterell, E.H., et al., *Hypothermia in the surgical treatment of ruptured intracranial aneurysms*. J Neurosurg, 1958. **15**(1): p. 4-18.
79. Bigelow, W.G., W.K. Lindsay, and W.F. Greenwood, *Hypothermia; its possible role in cardiac surgery: an investigation of factors governing survival in dogs at low body temperatures*. Ann Surg, 1950. **132**(5): p. 849-66.
80. Bigelow, W.C., *Methods for inducing hypothermia and rewarming*. Ann N Y Acad Sci, 1959. **80**: p. 522-32.
81. Rosomoff, H.L., *Protective effects of hypothermia against pathological processes of the nervous system*. Ann N Y Acad Sci, 1959. **80**: p. 475-86.
82. Rosomoff, H.L., *Experimental brain injury during hypothermia*. J Neurosurg, 1959. **16**(2): p. 177-87.
83. Rosomoff, H.L. and P. Safar, *Management of the comatose patient*. Clin Anesth, 1965. **1**: p. 244-58.
84. Lazorthes, G. and L. Campan, *Moderate hypothermia in the treatment of head injuries*. Clin Neurosurg, 1964. **12**: p. 293-9.
85. Hamby, W.B., *Intracranial Surgery for Aneurysm: Effect of Hypothermia Upon Survival*. J Neurosurg, 1963. **20**: p. 41-5.
86. Hegnauer, A.H. and H.E. D'Amato, *Oxygen consumption and cardiac output in the hypothermic dog*. Am J Physiol, 1954. **178**(1): p. 138-42.
87. Ames, A., 3rd, et al., *Cerebral ischemia. II. The no-reflow phenomenon*. Am J Pathol, 1968. **52**(2): p. 437-53.

88. Symon, L., *The concept of threshold of ischemia in relation to brain structures and function*. Journal of Clinical Pathology, 1976. **11**(Supplement): p. 149-154.
89. Steen, P.A. and J.D. Michenfelder, *Barbiturate protection in tolerant and nontolerant hypoxic mice: comparison with hypothermic protection*. Anesthesiology, 1979. **50**(5): p. 404-8.
90. Steen, P.A. and J.D. Michenfelder, *Cerebral protection with barbiturates: relation to anesthetic effect*. Stroke, 1978. **9**(2): p. 140-2.
91. Benveniste, H., et al., *Elevation of the extracellular concentrations of glutamate and aspartate in rat hippocampus during transient cerebral ischemia monitored by intracerebral microdialysis*. J Neurochem, 1984. **43**(5): p. 1369-74.
92. Jorgensen, M.B. and N.H. Diemer, *Selective neuron loss after cerebral ischemia in the rat: possible role of transmitter glutamate*. Acta Neurol Scand, 1982. **66**(5): p. 536-46.
93. Schwarcz, R. and B. Meldrum, *Excitatory amino acid antagonists provide a therapeutic approach to neurological disorders*. Lancet, 1985. **2**(8447): p. 140-3.
94. Rothman, S., *Synaptic release of excitatory amino acid neurotransmitter mediates anoxic neuronal death*. J Neurosci, 1984. **4**(7): p. 1884-91.
95. Simon, R.P., et al., *Blockade of N-methyl-D-aspartate receptors may protect against ischemic damage in the brain*. Science, 1984. **226**(4676): p. 850-2.
96. Gill, R., A.C. Foster, and G.N. Woodruff, *Systemic administration of MK-801 protects against ischemia-induced hippocampal neurodegeneration in the gerbil*. J Neurosci, 1987. **7**(10): p. 3343-9.
97. Dahl, N.A. and W.M. Balfour, *Prolonged Anoxic Survival Due to Anoxia Pre-Exposure: Brain Atp, Lactate, and Pyruvate*. Am J Physiol, 1964. **207**: p. 452-6.

98. Murry, C.E., R.B. Jennings, and K.A. Reimer, *Preconditioning with ischemia: a delay of lethal cell injury in ischemic myocardium*. *Circulation*, 1986. **74**(5): p. 1124-36.
99. Shiki, K. and D.J. Hearse, *Preconditioning of ischemic myocardium: reperfusion-induced arrhythmias*. *Am J Physiol*, 1987. **253**(6 Pt 2): p. H1470-6.
100. Miyazaki, T., H.P. Pride, and D.P. Zipes, *Modulation of cardiac autonomic neurotransmission by epicardial superfusion. Effects of hexamethonium and tetrodotoxin*. *Circ Res*, 1989. **65**(5): p. 1212-9.
101. Kitagawa, K., et al., *'Ischemic tolerance' phenomenon found in the brain*. *Brain Res*, 1990. **528**(1): p. 21-4.
102. Kitagawa, K., et al., *'Ischemic tolerance' phenomenon detected in various brain regions*. *Brain Res*, 1991. **561**(2): p. 203-11.
103. Chopp, M., et al., *Transient hyperthermia protects against subsequent forebrain ischemic cell damage in the rat*. *Neurology*, 1989. **39**(10): p. 1396-8.
104. Kitagawa, K., et al., *Hyperthermia-induced neuronal protection against ischemic injury in gerbils*. *J Cereb Blood Flow Metab*, 1991. **11**(3): p. 449-52.
105. Liu, Y., et al., *Protection of rat hippocampus against ischemic neuronal damage by pretreatment with sublethal ischemia*. *Brain Res*, 1992. **586**(1): p. 121-4.
106. Li, G.C. and Z. Werb, *Correlation between synthesis of heat shock proteins and development of thermotolerance in Chinese hamster fibroblasts*. *Proc Natl Acad Sci U S A*, 1982. **79**(10): p. 3218-22.
107. Nowak, G., et al., *Swim stress increases the potency of glycine at the N-methyl-D-aspartate receptor complex*. *J Neurochem*, 1995. **64**(2): p. 925-7.

108. Brown, I.R., S. Rush, and G.O. Ivy, *Induction of a heat shock gene at the site of tissue injury in the rat brain*. *Neuron*, 1989. **2**(6): p. 1559-64.
109. Lindquist, S., *The heat-shock response*. *Annu Rev Biochem*, 1986. **55**: p. 1151-91.
110. Lowenstein, D.H., R.P. Simon, and F.R. Sharp, *The pattern of 72-kDa heat shock protein-like immunoreactivity in the rat brain following flurothyl-induced status epilepticus*. *Brain Res*, 1990. **531**(1-2): p. 173-82.
111. Feder, M.E. and G.E. Hofmann, *Heat-shock proteins, molecular chaperones, and the stress response: evolutionary and ecological physiology*. *Annu Rev Physiol*, 1999. **61**: p. 243-82.
112. Li, G.C. and G.M. Hahn, *A proposed operational model of thermotolerance based on effects of nutrients and the initial treatment temperature*. *Cancer Res*, 1980. **40**(12): p. 4501-8.
113. Henle, K.J. and L.A. Dethlefsen, *Heat fractionation and thermotolerance: a review*. *Cancer Res*, 1978. **38**(7): p. 1843-51.
114. Rothman, S.M. and J.W. Olney, *Glutamate and the pathophysiology of hypoxic--ischemic brain damage*. *Ann Neurol*, 1986. **19**(2): p. 105-11.
115. Siesjo, B.K. and F. Bengtsson, *Calcium fluxes, calcium antagonists, and calcium-related pathology in brain ischemia, hypoglycemia, and spreading depression: a unifying hypothesis*. *J Cereb Blood Flow Metab*, 1989. **9**(2): p. 127-40.
116. Flamm, E.S., et al., *Free radicals in cerebral ischemia*. *Stroke*, 1978. **9**(5): p. 445-7.
117. Hallenbeck, J.M., et al., *Polymorphonuclear leukocyte accumulation in brain regions with low blood flow during the early postischemic period*. *Stroke*, 1986. **17**(2): p. 246-53.

118. Gaudet, R.J., I. Alam, and L. Levine, *Accumulation of cyclooxygenase products of arachidonic acid metabolism in gerbil brain during reperfusion after bilateral common carotid artery occlusion*. J Neurochem, 1980. **35**(3): p. 653-8.
119. Gaudet, R.J. and L. Levine, *Effect of unilateral common carotid artery occlusion on levels of prostaglandins D2, F2 alpha and 6-keto-prostaglandin F1 alpha in gerbil brain*. Stroke, 1980. **11**(6): p. 648-52.
120. Stagliano, N.E., et al., *Focal ischemic preconditioning induces rapid tolerance to middle cerebral artery occlusion in mice*. J Cereb Blood Flow Metab, 1999. **19**(7): p. 757-61.
121. Prass, K., et al., *Hyperbaric oxygenation induced tolerance against focal cerebral ischemia in mice is strain dependent*. Brain Res, 2000. **871**(1): p. 146-50.
122. Kobayashi, S., V.A. Harris, and F.A. Welsh, *Spreading depression induces tolerance of cortical neurons to ischemia in rat brain*. J Cereb Blood Flow Metab, 1995. **15**(5): p. 721-7.
123. Nishio, S., et al., *Ischemic tolerance in the rat neocortex following hypothermic preconditioning*. J Neurosurg, 2000. **93**(5): p. 845-51.
124. Galea, E., et al., *Cerebellar stimulation reduces inducible nitric oxide synthase expression and protects brain from ischemia*. Am J Physiol, 1998. **274**(6 Pt 2): p. H2035-45.
125. Wiegand, F., et al., *Respiratory chain inhibition induces tolerance to focal cerebral ischemia*. J Cereb Blood Flow Metab, 1999. **19**(11): p. 1229-37.
126. Tasaki, K., et al., *Lipopolysaccharide pre-treatment induces resistance against subsequent focal cerebral ischemic damage in spontaneously hypertensive rats*. Brain Res, 1997. **748**(1-2): p. 267-70.

127. Zimmermann, C., et al., *Lipopolysaccharide-induced ischemic tolerance is associated with increased levels of ceramide in brain and in plasma*. Brain Res, 2001. **895**(1-2): p. 59-65.
128. Perez-Pinzon, M.A., et al., *Rapid preconditioning protects rats against ischemic neuronal damage after 3 but not 7 days of reperfusion following global cerebral ischemia*. J Cereb Blood Flow Metab, 1997. **17**(2): p. 175-82.
129. Schurr, A., et al., *Adaptation of adult brain tissue to anoxia and hypoxia in vitro*. Brain Res, 1986. **374**(2): p. 244-8.
130. Stenzel-Poore, M.P., et al., *Effect of ischaemic preconditioning on genomic response to cerebral ischaemia: similarity to neuroprotective strategies in hibernation and hypoxia-tolerant states*. Lancet, 2003. **362**(9389): p. 1028-37.
131. Dirnagl, U., R.P. Simon, and J.M. Hallenbeck, *Ischemic tolerance and endogenous neuroprotection*. Trends Neurosci, 2003. **26**(5): p. 248-54.
132. Stenzel-Poore, M.P., et al., *Preconditioning reprograms the response to ischemic injury and primes the emergence of unique endogenous neuroprotective phenotypes: a speculative synthesis*. Stroke, 2007. **38**(2 Suppl): p. 680-5.
133. Heemann, U., et al., *Lipopolysaccharide pretreatment protects from renal ischemia/reperfusion injury : possible connection to an interleukin-6-dependent pathway*. Am J Pathol, 2000. **156**(1): p. 287-93.
134. Eising, G.P., et al., *Effects of induced tolerance to bacterial lipopolysaccharide on myocardial infarct size in rats*. Cardiovasc Res, 1996. **31**(1): p. 73-81.
135. Medzhitov, R., P. Preston-Hurlburt, and C.A. Janeway, Jr., *A human homologue of the Drosophila Toll protein signals activation of adaptive immunity*. Nature, 1997. **388**(6640): p. 394-7.

136. Marsh, B.J., R.L. Williams-Karnesky, and M.P. Stenzel-Poore, *Toll-like receptor signaling in endogenous neuroprotection and stroke*. Neuroscience, 2009. **158**(3): p. 1007-20.
137. Bsibsi, M., et al., *Broad expression of Toll-like receptors in the human central nervous system*. J Neuropathol Exp Neurol, 2002. **61**(11): p. 1013-21.
138. Singh, A.K. and Y. Jiang, *How does peripheral lipopolysaccharide induce gene expression in the brain of rats?* Toxicology, 2004. **201**(1-3): p. 197-207.
139. Jack, C.S., et al., *TLR signaling tailors innate immune responses in human microglia and astrocytes*. J Immunol, 2005. **175**(7): p. 4320-30.
140. Bsibsi, M., et al., *Toll-like receptor 3 on adult human astrocytes triggers production of neuroprotective mediators*. Glia, 2006. **53**(7): p. 688-95.
141. Vogel, S.N., K.A. Fitzgerald, and M.J. Fenton, *TLRs: differential adapter utilization by toll-like receptors mediates TLR-specific patterns of gene expression*. Mol Interv, 2003. **3**(8): p. 466-77.
142. Takeda, K. and S. Akira, *Toll-like receptors in innate immunity*. Int Immunol, 2005. **17**(1): p. 1-14.
143. Laflamme, N. and S. Rivest, *Toll-like receptor 4: the missing link of the cerebral innate immune response triggered by circulating gram-negative bacterial cell wall components*. FASEB J, 2001. **15**(1): p. 155-163.
144. Laflamme, N., G. Soucy, and S. Rivest, *Circulating cell wall components derived from gram-negative, not gram-positive, bacteria cause a profound induction of the gene-encoding Toll-like receptor 2 in the CNS*. J Neurochem, 2001. **79**(3): p. 648-57.

145. Chakravarty, S. and M. Herkenham, *Toll-like receptor 4 on nonhematopoietic cells sustains CNS inflammation during endotoxemia, independent of systemic cytokines*. J Neurosci, 2005. **25**(7): p. 1788-96.
146. Olson, J.K. and S.D. Miller, *Microglia initiate central nervous system innate and adaptive immune responses through multiple TLRs*. J Immunol, 2004. **173**(6): p. 3916-24.
147. Carpentier, P.A., et al., *Differential activation of astrocytes by innate and adaptive immune stimuli*. Glia, 2005. **49**(3): p. 360-74.
148. McKimmie, C.S. and J.K. Fazakerley, *In response to pathogens, glial cells dynamically and differentially regulate Toll-like receptor gene expression*. J Neuroimmunol, 2005. **169**(1-2): p. 116-25.
149. Kagan, J.C., et al., *TRAM couples endocytosis of Toll-like receptor 4 to the induction of interferon-beta*. Nat Immunol, 2008. **9**(4): p. 361-8.
150. Constantin, D., et al., *Neisseria meningitidis-induced death of cerebrovascular endothelium: mechanisms triggering transcriptional activation of inducible nitric oxide synthase*. J Neurochem, 2004. **89**(5): p. 1166-74.
151. Zhou, M.L., et al., *Expression of Toll-like receptor 4 in the brain in a rabbit experimental subarachnoid haemorrhage model*. Inflamm Res, 2007. **56**(3): p. 93-7.
152. Ziegler, G., et al., *TLR2 has a detrimental role in mouse transient focal cerebral ischemia*. Biochem Biophys Res Commun, 2007. **359**(3): p. 574-9.
153. Lloyd-Jones, K.L., M.M. Kelly, and P. Kubes, *Varying importance of soluble and membrane CD14 in endothelial detection of lipopolysaccharide*. J Immunol, 2008. **181**(2): p. 1446-53.

154. Lafon, M., et al., *The innate immune facet of brain: human neurons express TLR-3 and sense viral dsRNA*. J Mol Neurosci, 2006. **29**(3): p. 185-94.
155. Ma, Y., et al., *Toll-like receptor 8 functions as a negative regulator of neurite outgrowth and inducer of neuronal apoptosis*. J Cell Biol, 2006. **175**(2): p. 209-15.
156. Rolls, A., et al., *Toll-like receptors modulate adult hippocampal neurogenesis*. Nat Cell Biol, 2007. **9**(9): p. 1081-8.
157. Shishido, T., et al., *Toll-like receptor-2 modulates ventricular remodeling after myocardial infarction*. Circulation, 2003. **108**(23): p. 2905-10.
158. Ha, T., et al., *Reduced cardiac hypertrophy in toll-like receptor 4-deficient mice following pressure overload*. Cardiovasc Res, 2005. **68**(2): p. 224-34.
159. Tobias, P.S. and L.K. Curtiss, *Toll-like receptors in atherosclerosis*. Biochem Soc Trans, 2007. **35**(Pt 6): p. 1453-5.
160. Tsukumo, D.M., et al., *Loss-of-function mutation in Toll-like receptor 4 prevents diet-induced obesity and insulin resistance*. Diabetes, 2007. **56**(8): p. 1986-98.
161. Davis, J.E., et al., *Tlr-4 deficiency selectively protects against obesity induced by diets high in saturated fat*. Obesity (Silver Spring), 2008. **16**(6): p. 1248-55.
162. Jiang, D., et al., *The role of Toll-like receptors in non-infectious lung injury*. Cell Res, 2006. **16**(8): p. 693-701.
163. Zhang, X., et al., *Toll-like receptor 4 deficiency causes pulmonary emphysema*. J Clin Invest, 2006. **116**(11): p. 3050-9.
164. Relton, J.K., et al., *Peripheral administration of Interleukin-1 Receptor antagonist inhibits brain damage after focal cerebral ischemia in the rat*. Exp Neurol, 1996. **138**(2): p. 206-13.

165. Hara, H., et al., *Inhibition of interleukin 1beta converting enzyme family proteases reduces ischemic and excitotoxic neuronal damage*. Proc Natl Acad Sci U S A, 1997. **94**(5): p. 2007-12.
166. Spera, P.A., et al., *IL-10 reduces rat brain injury following focal stroke*. Neurosci Lett, 1998. **251**(3): p. 189-92.
167. Zarembek, K.A. and P.J. Godowski, *Tissue expression of human Toll-like receptors and differential regulation of Toll-like receptor mRNAs in leukocytes in response to microbes, their products, and cytokines*. J Immunol, 2002. **168**(2): p. 554-61.
168. Oyama, J., et al., *Reduced myocardial ischemia-reperfusion injury in toll-like receptor 4-deficient mice*. Circulation, 2004. **109**(6): p. 784-9.
169. Sakata, Y., et al., *Toll-like receptor 2 modulates left ventricular function following ischemia-reperfusion injury*. Am J Physiol Heart Circ Physiol, 2007. **292**(1): p. H503-9.
170. Shigeoka, A.A., et al., *TLR2 is constitutively expressed within the kidney and participates in ischemic renal injury through both MyD88-dependent and -independent pathways*. J Immunol, 2007. **178**(10): p. 6252-8.
171. Zhai, Y., et al., *Cutting edge: TLR4 activation mediates liver ischemia/reperfusion inflammatory response via IFN regulatory factor 3-dependent MyD88-independent pathway*. J Immunol, 2004. **173**(12): p. 7115-9.
172. Shen, X.D., et al., *Toll-like receptor and heme oxygenase-1 signaling in hepatic ischemia/reperfusion injury*. Am J Transplant, 2005. **5**(8): p. 1793-800.
173. Cao, C.X., et al., *Reduced cerebral ischemia-reperfusion injury in Toll-like receptor 4 deficient mice*. Biochem Biophys Res Commun, 2007. **353**(2): p. 509-14.

174. Lehnardt, S., et al., *Toll-like receptor 2 mediates CNS injury in focal cerebral ischemia*. J Neuroimmunol, 2007. **190**(1-2): p. 28-33.
175. Caso, J.R., et al., *Toll-like receptor 4 is involved in brain damage and inflammation after experimental stroke*. Circulation, 2007. **115**(12): p. 1599-608.
176. Hua, F., et al., *Activation of Toll-like receptor 4 signaling contributes to hippocampal neuronal death following global cerebral ischemia/reperfusion*. J Neuroimmunol, 2007. **190**(1-2): p. 101-11.
177. Kinouchi, H., et al., *Induction of 70-kDa heat shock protein and hsp70 mRNA following transient focal cerebral ischemia in the rat*. J Cereb Blood Flow Metab, 1993. **13**(1): p. 105-15.
178. Faraco, G., et al., *High mobility group box 1 protein is released by neural cells upon different stresses and worsens ischemic neurodegeneration in vitro and in vivo*. J Neurochem, 2007. **103**(2): p. 590-603.
179. Lehnardt, S., et al., *A vicious cycle involving release of heat shock protein 60 from injured cells and activation of toll-like receptor 4 mediates neurodegeneration in the CNS*. J Neurosci, 2008. **28**(10): p. 2320-31.
180. Rosenzweig, H.L., et al., *Endotoxin preconditioning prevents cellular inflammatory response during ischemic neuroprotection in mice*. Stroke, 2004. **35**(11): p. 2576-81.
181. Hickey, E.J., et al., *Lipopolysaccharide preconditioning induces robust protection against brain injury resulting from deep hypothermic circulatory arrest*. J Thorac Cardiovasc Surg, 2007. **133**(6): p. 1588-96.
182. Rosenzweig, H.L., et al., *Endotoxin preconditioning protects against the cytotoxic effects of TNFalpha after stroke: a novel role for TNFalpha in LPS-ischemic tolerance*. J Cereb Blood Flow Metab, 2007. **27**(10): p. 1663-74.

183. Ahmed, S.H., et al., *Effects of lipopolysaccharide priming on acute ischemic brain injury*. Stroke, 2000. **31**(1): p. 193-9.
184. Bordet, R., et al., *Increase in endogenous brain superoxide dismutase as a potential mechanism of lipopolysaccharide-induced brain ischemic tolerance*. J Cereb Blood Flow Metab, 2000. **20**(8): p. 1190-6.
185. Furuya, K., et al., *Differences in infarct evolution between lipopolysaccharide-induced tolerant and nontolerant conditions to focal cerebral ischemia*. J Neurosurg, 2005. **103**(4): p. 715-23.
186. Kunz, A., et al., *Neurovascular protection by ischemic tolerance: role of nitric oxide and reactive oxygen species*. J Neurosci, 2007. **27**(27): p. 7083-93.
187. Bastide, M., et al., *Delayed cerebrovascular protective effect of lipopolysaccharide in parallel to brain ischemic tolerance*. J Cereb Blood Flow Metab, 2003. **23**(4): p. 399-405.
188. Dawson, D.A., et al., *Cerebrovascular hemodynamics and ischemic tolerance: lipopolysaccharide-induced resistance to focal cerebral ischemia is not due to changes in severity of the initial ischemic insult, but is associated with preservation of microvascular perfusion*. J Cereb Blood Flow Metab, 1999. **19**(6): p. 616-23.
189. Ginis, I., et al., *TNF-alpha pretreatment prevents subsequent activation of cultured brain cells with TNF-alpha and hypoxia via ceramide*. Am J Physiol, 1999. **276**(5 Pt 1): p. C1171-83.
190. Stevens, S.L., et al., *Toll-like receptor 9: a new target of ischemic preconditioning in the brain*. J Cereb Blood Flow Metab, 2008. **28**(5): p. 1040-7.

191. Bahjat, F.R., et al., *Proof of concept: pharmacological preconditioning with a Toll-like receptor agonist protects against cerebrovascular injury in a primate model of stroke*. *J Cereb Blood Flow Metab*, 2011. **31**(5): p. 1229-42.
192. Medvedev, A.E., et al., *Dysregulation of LPS-induced Toll-like receptor 4-MyD88 complex formation and IL-1 receptor-associated kinase 1 activation in endotoxin-tolerant cells*. *J Immunol*, 2002. **169**(9): p. 5209-16.
193. Kobayashi, K., et al., *IRAK-M is a negative regulator of Toll-like receptor signaling*. *Cell*, 2002. **110**(2): p. 191-202.
194. Sly, L.M., et al., *LPS-induced upregulation of SHIP is essential for endotoxin tolerance*. *Immunity*, 2004. **21**(2): p. 227-39.
195. Shi, M., et al., *TRIM30 alpha negatively regulates TLR-mediated NF-kappa B activation by targeting TAB2 and TAB3 for degradation*. *Nat Immunol*, 2008. **9**(4): p. 369-77.
196. Broad, A., J.A. Kirby, and D.E. Jones, *Toll-like receptor interactions: tolerance of MyD88-dependent cytokines but enhancement of MyD88-independent interferon-beta production*. *Immunology*, 2007. **120**(1): p. 103-11.
197. Dalpke, A.H., et al., *Differential effects of CpG-DNA in Toll-like receptor-2/-4/-9 tolerance and cross-tolerance*. *Immunology*, 2005. **116**(2): p. 203-12.
198. Bagchi, A., et al., *MyD88-dependent and MyD88-independent pathways in synergy, priming, and tolerance between TLR agonists*. *J Immunol*, 2007. **178**(2): p. 1164-71.
199. Schneider, A., et al., *NF-kappaB is activated and promotes cell death in focal cerebral ischemia*. *Nat Med*, 1999. **5**(5): p. 554-9.

200. Liu, H., et al., *Interferon-beta administration confers a beneficial outcome in a rabbit model of thromboembolic cerebral ischemia*. Neurosci Lett, 2002. **327**(2): p. 146-8.
201. Veldhuis, W.B., et al., *Interferon-beta blocks infiltration of inflammatory cells and reduces infarct volume after ischemic stroke in the rat*. J Cereb Blood Flow Metab, 2003. **23**(9): p. 1029-39.
202. Veldhuis, W.B., et al., *Interferon-beta prevents cytokine-induced neutrophil infiltration and attenuates blood-brain barrier disruption*. J Cereb Blood Flow Metab, 2003. **23**(9): p. 1060-9.
203. Kraus, J., et al., *Interferon-beta stabilizes barrier characteristics of brain endothelial cells in vitro*. Ann Neurol, 2004. **56**(2): p. 192-205.
204. Liuzzi, G.M., et al., *Interferon-beta inhibits the expression of metalloproteinases in rat glial cell cultures: implications for multiple sclerosis pathogenesis and treatment*. Mult Scler, 2004. **10**(3): p. 290-7.
205. Seguin, R., et al., *Human brain endothelial cells supply support for monocyte immunoregulatory functions*. J Neuroimmunol, 2003. **135**(1-2): p. 96-106.
206. Lopez-Collazo, E., et al., *Triggering of peritoneal macrophages with IFN-alpha/beta attenuates the expression of inducible nitric oxide synthase through a decrease in NF-kappaB activation*. J Immunol, 1998. **160**(6): p. 2889-95.
207. Stewart, V.C., et al., *Pretreatment of astrocytes with interferon-alpha/beta prevents neuronal mitochondrial respiratory chain damage*. J Neurochem, 1998. **70**(1): p. 432-4.
208. Hua, L.L., et al., *Modulation of astrocyte inducible nitric oxide synthase and cytokine expression by interferon beta is associated with induction and inhibition*

- of interferon gamma-activated sequence binding activity.* J Neurochem, 2002. **83**(5): p. 1120-8.
209. Bosca, L., et al., *Anti-inflammatory action of type I interferons deduced from mice expressing interferon beta.* Gene Ther, 2000. **7**(10): p. 817-25.
210. Palmer, G., et al., *Interferon beta stimulates interleukin 1 receptor antagonist production in human articular chondrocytes and synovial fibroblasts.* Ann Rheum Dis, 2004. **63**(1): p. 43-9.
211. Boutros, T., E. Croze, and V.W. Yong, *Interferon-beta is a potent promoter of nerve growth factor production by astrocytes.* J Neurochem, 1997. **69**(3): p. 939-46.
212. Jin, S., et al., *Interferon-beta is neuroprotective against the toxicity induced by activated microglia.* Brain Res, 2007. **1179**: p. 140-6.
213. Yeh, H.J., et al., *Upregulation of pleiotrophin gene expression in developing microvasculature, macrophages, and astrocytes after acute ischemic brain injury.* J Neurosci, 1998. **18**(10): p. 3699-707.
214. Endres, M., et al., *Ischemic brain damage in mice after selectively modifying BDNF or NT4 gene expression.* J Cereb Blood Flow Metab, 2000. **20**(1): p. 139-44.
215. Zhang, W., et al., *Neuronal activation of NF-kappaB contributes to cell death in cerebral ischemia.* J Cereb Blood Flow Metab, 2005. **25**(1): p. 30-40.
216. Nhu, Q.M., N. Cuesta, and S.N. Vogel, *Transcriptional regulation of lipopolysaccharide (LPS)-induced Toll-like receptor (TLR) expression in murine macrophages: role of interferon regulatory factors 1 (IRF-1) and 2 (IRF-2).* J Endotoxin Res, 2006. **12**(5): p. 285-95.

217. von Lubitz, D.K., *Adenosine and cerebral ischemia: therapeutic future or death of a brave concept?* Eur J Pharmacol, 1999. **371**(1): p. 85-102.
218. Hasko, G., et al., *Adenosine receptor signaling in the brain immune system.* Trends Pharmacol Sci, 2005. **26**(10): p. 511-6.
219. Cunha, R.A., *Neuroprotection by adenosine in the brain: From A(1) receptor activation to A (2A) receptor blockade.* Purinergic Signal, 2005. **1**(2): p. 111-34.
220. Boison, D., *Adenosine kinase, epilepsy and stroke: mechanisms and therapies.* Trends Pharmacol Sci, 2006. **27**(12): p. 652-8.
221. Dunwiddie, T.V. and S.A. Masino, *The role and regulation of adenosine in the central nervous system.* Annu Rev Neurosci, 2001. **24**: p. 31-55.
222. Pearson, T., et al., *Sustained elevation of extracellular adenosine and activation of A1 receptors underlie the post-ischaemic inhibition of neuronal function in rat hippocampus in vitro.* J Neurochem, 2006. **97**(5): p. 1357-68.
223. Kobayashi, T., T. Yamada, and Y. Okada, *The levels of adenosine and its metabolites in the guinea pig and rat brain during complete ischemia-in vivo study.* Brain Res, 1998. **787**(2): p. 211-9.
224. Laghi Pasini, F., et al., *Increase in plasma adenosine during brain ischemia in man: a study during transient ischemic attacks, and stroke.* Brain Res Bull, 2000. **51**(4): p. 327-30.
225. Cunha, F.Q., et al., *Differential induction of nitric oxide synthase in various organs of the mouse during endotoxaemia: role of TNF-alpha and IL-1-beta.* Immunology, 1994. **81**(2): p. 211-5.
226. Fredholm, B.B., *Adenosine and neuroprotection.* Int Rev Neurobiol, 1997. **40**: p. 259-80.

227. Ribeiro, J.A., *What can adenosine neuromodulation do for neuroprotection?* *Curr Drug Targets CNS Neurol Disord*, 2005. **4**(4): p. 325-9.
228. Kitagawa, H., et al., *Intracerebral adenosine infusion improves neurological outcome after transient focal ischemia in rats.* *Neurol Res*, 2002. **24**(3): p. 317-23.
229. Pignataro, G., R.P. Simon, and D. Boison, *Transgenic overexpression of adenosine kinase aggravates cell death in ischemia.* *J Cereb Blood Flow Metab*, 2007. **27**(1): p. 1-5.
230. Picano, E. and M.P. Abbracchio, *Adenosine, the imperfect endogenous anti-ischemic cardio-neuroprotector.* *Brain Res Bull*, 2000. **52**(2): p. 75-82.
231. Faulds, D., P. Chrisp, and M.M. Buckley, *Adenosine. An evaluation of its use in cardiac diagnostic procedures, and in the treatment of paroxysmal supraventricular tachycardia.* *Drugs*, 1991. **41**(4): p. 596-624.
232. Pardridge, W.M., et al., *Blood-brain barrier transport and brain metabolism of adenosine and adenosine analogs.* *J Pharmacol Exp Ther*, 1994. **268**(1): p. 14-8.
233. Bjorklund, O., et al., *Adenosine A1 and A3 receptors protect astrocytes from hypoxic damage.* *Eur J Pharmacol*, 2008. **596**(1-3): p. 6-13.
234. Tatlisumak, T., et al., *Delayed treatment with an adenosine kinase inhibitor, GP683, attenuates infarct size in rats with temporary middle cerebral artery occlusion.* *Stroke*, 1998. **29**(9): p. 1952-8.
235. Azzimondi, G., et al., *Variables associated with hospital arrival time after stroke: effect of delay on the clinical efficiency of early treatment.* *Stroke*, 1997. **28**(3): p. 537-42.

236. Chen, G.J., et al., *Activation of adenosine A3 receptors reduces ischemic brain injury in rodents*. J Neurosci Res, 2006. **84**(8): p. 1848-55.
237. Sebastiao, A.M., et al., *Activation of synaptic NMDA receptors by action potential-dependent release of transmitter during hypoxia impairs recovery of synaptic transmission on reoxygenation*. J Neurosci, 2001. **21**(21): p. 8564-71.
238. Olsson, T., et al., *Deletion of the adenosine A1 receptor gene does not alter neuronal damage following ischaemia in vivo or in vitro*. Eur J Neurosci, 2004. **20**(5): p. 1197-204.
239. Gao, Y. and J.W. Phillis, *CGS 15943, an adenosine A2 receptor antagonist, reduces cerebral ischemic injury in the Mongolian gerbil*. Life Sci, 1994. **55**(3): p. PL61-5.
240. Melani, A., et al., *The selective A2A receptor antagonist SCH 58261 reduces striatal transmitter outflow, turning behavior and ischemic brain damage induced by permanent focal ischemia in the rat*. Brain Res, 2003. **959**(2): p. 243-50.
241. Monopoli, A., et al., *Blockade of adenosine A2A receptors by SCH 58261 results in neuroprotective effects in cerebral ischaemia in rats*. Neuroreport, 1998. **9**(17): p. 3955-9.
242. Phillis, J.W., *Adenosine and adenine nucleotides as regulators of cerebral blood flow: roles of acidosis, cell swelling, and KATP channels*. Crit Rev Neurobiol, 2004. **16**(4): p. 237-70.
243. Von Lubitz, D.K., R.C. Lin, and K.A. Jacobson, *Cerebral ischemia in gerbils: effects of acute and chronic treatment with adenosine A2A receptor agonist and antagonist*. Eur J Pharmacol, 1995. **287**(3): p. 295-302.

244. Chen, J.F., et al., *A(2A) adenosine receptor deficiency attenuates brain injury induced by transient focal ischemia in mice*. J Neurosci, 1999. **19**(21): p. 9192-200.
245. Trincavelli, M.L., et al., *Regulation of A(2A) adenosine receptor expression and functioning following permanent focal ischemia in rat brain*. J Neurochem, 2008. **104**(2): p. 479-90.
246. Cassada, D.C., et al., *Adenosine A2A analogue improves neurologic outcome after spinal cord trauma in the rabbit*. J Trauma, 2002. **53**(2): p. 225-9; discussion 229-31.
247. Reece, T.B., et al., *Comparison of systemic and retrograde delivery of adenosine A2A agonist for attenuation of spinal cord injury after thoracic aortic cross-clamping*. Ann Thorac Surg, 2006. **81**(3): p. 902-9.
248. Mayne, M., et al., *Adenosine A2A receptor activation reduces proinflammatory events and decreases cell death following intracerebral hemorrhage*. Ann Neurol, 2001. **49**(6): p. 727-35.
249. Bshesh, K., et al., *The A2A receptor mediates an endogenous regulatory pathway of cytokine expression in THP-1 cells*. J Leukoc Biol, 2002. **72**(5): p. 1027-36.
250. Link, A.A., et al., *Ligand-activation of the adenosine A2a receptors inhibits IL-12 production by human monocytes*. J Immunol, 2000. **164**(1): p. 436-42.
251. Li, Y., et al., *Mouse spinal cord compression injury is reduced by either activation of the adenosine A2A receptor on bone marrow-derived cells or deletion of the A2A receptor on non-bone marrow-derived cells*. Neuroscience, 2006. **141**(4): p. 2029-39.

252. Fiebich, B.L., et al., *Adenosine A2b receptors mediate an increase in interleukin (IL)-6 mRNA and IL-6 protein synthesis in human astroglioma cells*. J Neurochem, 1996. **66**(4): p. 1426-31.
253. Kalaria, R.N. and S.I. Harik, *Adenosine receptors of cerebral microvessels and choroid plexus*. J Cereb Blood Flow Metab, 1986. **6**(4): p. 463-70.
254. Klinger, M., M. Freissmuth, and C. Nanoff, *Adenosine receptors: G protein-mediated signalling and the role of accessory proteins*. Cell Signal, 2002. **14**(2): p. 99-108.
255. Ribeiro, J.A., A.M. Sebastiao, and A. de Mendonca, *Participation of adenosine receptors in neuroprotection*. Drug News Perspect, 2003. **16**(2): p. 80-6.
256. Yamagata, K., et al., *Adenosine induces expression of glial cell line-derived neurotrophic factor (GDNF) in primary rat astrocytes*. Neurosci Res, 2007. **59**(4): p. 467-74.
257. Hermann, D.M., et al., *Adenovirus-mediated GDNF and CNTF pretreatment protects against striatal injury following transient middle cerebral artery occlusion in mice*. Neurobiol Dis, 2001. **8**(4): p. 655-66.
258. Kitagawa, H., et al., *Adenovirus-mediated gene transfer of glial cell line-derived neurotrophic factor prevents ischemic brain injury after transient middle cerebral artery occlusion in rats*. J Cereb Blood Flow Metab, 1999. **19**(12): p. 1336-44.
259. Kobayashi, T., et al., *Intracerebral infusion of glial cell line-derived neurotrophic factor promotes striatal neurogenesis after stroke in adult rats*. Stroke, 2006. **37**(9): p. 2361-7.
260. Eckle, T., et al., *A2B adenosine receptor dampens hypoxia-induced vascular leak*. Blood, 2008. **111**(4): p. 2024-35.

261. Yang, D., et al., *The A2B adenosine receptor protects against inflammation and excessive vascular adhesion*. J Clin Invest, 2006. **116**(7): p. 1913-23.
262. von Lubitz, D.K., et al., *Stimulation of adenosine A3 receptors in cerebral ischemia. Neuronal death, recovery, or both?* Ann N Y Acad Sci, 1999. **890**: p. 93-106.
263. Abbracchio, M.P. and F. Cattabeni, *Brain adenosine receptors as targets for therapeutic intervention in neurodegenerative diseases*. Ann N Y Acad Sci, 1999. **890**: p. 79-92.
264. Von Lubitz, D.K., et al., *Adenosine A3 receptor stimulation and cerebral ischemia*. Eur J Pharmacol, 1994. **263**(1-2): p. 59-67.
265. Pugliese, A.M., et al., *Role of adenosine A3 receptors on CA1 hippocampal neurotransmission during oxygen-glucose deprivation episodes of different duration*. Biochem Pharmacol, 2007. **74**(5): p. 768-79.
266. Palmer, T.M., J.L. Benovic, and G.L. Stiles, *Agonist-dependent phosphorylation and desensitization of the rat A3 adenosine receptor. Evidence for a G-protein-coupled receptor kinase-mediated mechanism*. J Biol Chem, 1995. **270**(49): p. 29607-13.
267. Trincavelli, M.L., et al., *A3 adenosine receptors in human astrocytoma cells: agonist-mediated desensitization, internalization, and down-regulation*. Mol Pharmacol, 2002. **62**(6): p. 1373-84.
268. Boison, D., *Adenosine and epilepsy: from therapeutic rationale to new therapeutic strategies*. Neuroscientist, 2005. **11**(1): p. 25-36.
269. Wilz, A., et al., *Silk polymer-based adenosine release: therapeutic potential for epilepsy*. Biomaterials, 2008. **29**(26): p. 3609-16.

270. Farina, C., F. Aloisi, and E. Meinl, *Astrocytes are active players in cerebral innate immunity*. Trends Immunol, 2007. **28**(3): p. 138-45.
271. Hauwel, M., et al., *Innate (inherent) control of brain infection, brain inflammation and brain repair: the role of microglia, astrocytes, "protective" glial stem cells and stromal ependymal cells*. Brain Res Brain Res Rev, 2005. **48**(2): p. 220-33.
272. Abbruscato, T.J. and T.P. Davis, *Combination of hypoxia/aglycemia compromises in vitro blood-brain barrier integrity*. J Pharmacol Exp Ther, 1999. **289**(2): p. 668-75.
273. Betz, A.L., et al., *Blood-brain barrier permeability and brain concentration of sodium, potassium, and chloride during focal ischemia*. J Cereb Blood Flow Metab, 1994. **14**(1): p. 29-37.
274. Barone, F.C., et al., *Tumor necrosis factor-alpha. A mediator of focal ischemic brain injury*. Stroke, 1997. **28**(6): p. 1233-44.
275. Hosomi, N., et al., *Tumor necrosis factor-alpha neutralization reduced cerebral edema through inhibition of matrix metalloproteinase production after transient focal cerebral ischemia*. J Cereb Blood Flow Metab, 2005. **25**(8): p. 959-67.
276. Cassada, D.C., et al., *Adenosine A2A analogue ATL-146e reduces systemic tumor necrosing factor-alpha and spinal cord capillary platelet-endothelial cell adhesion molecule-1 expression after spinal cord ischemia*. J Vasc Surg, 2002. **35**(5): p. 994-8.
277. Williams-Karnesky, R.L. and M.P. Stenzel-Poore, *Adenosine and stroke: maximizing the therapeutic potential of adenosine as a prophylactic and acute neuroprotectant*. Curr Neuropharmacol, 2009. **7**(3): p. 217-27.
278. Fischer, D., et al., *A role for adenosine deaminase in human monocyte maturation*. J Clin Invest, 1976. **58**(2): p. 399-407.

279. Hasko, G., et al., *Shaping of monocyte and macrophage function by adenosine receptors*. *Pharmacol Ther*, 2007. **113**(2): p. 264-75.
280. Hasko, G., et al., *Adenosine receptors: therapeutic aspects for inflammatory and immune diseases*. *Nat Rev Drug Discov*, 2008. **7**(9): p. 759-70.
281. Chen, H., et al., *Activation of the macrophage A2b adenosine receptor regulates tumor necrosis factor-alpha levels following vascular injury*. *Exp Hematol*, 2009. **37**(5): p. 533-8.
282. Merrill, J.T., et al., *Adenosine A1 receptor promotion of multinucleated giant cell formation by human monocytes: a mechanism for methotrexate-induced nodulosis in rheumatoid arthritis*. *Arthritis Rheum*, 1997. **40**(7): p. 1308-15.
283. Clark, A.N., et al., *A1 adenosine receptor activation promotes angiogenesis and release of VEGF from monocytes*. *Circ Res*, 2007. **101**(11): p. 1130-8.
284. Streitova, D., et al., *Adenosine A(1), A(2a), A(2b), and A(3) receptors in hematopoiesis. 2. Expression of receptor mRNA in resting and lipopolysaccharide-activated mouse RAW 264.7 macrophages*. *Physiol Res*, 2010. **59**(1): p. 139-44.
285. Gessi, S., et al., *Adenosine and lymphocyte regulation*. *Purinergic Signal*, 2007. **3**(1-2): p. 109-16.
286. Hoskin, D.W., et al., *Inhibition of T cell and natural killer cell function by adenosine and its contribution to immune evasion by tumor cells (Review)*. *Int J Oncol*, 2008. **32**(3): p. 527-35.
287. Zarek, P.E., et al., *A2A receptor signaling promotes peripheral tolerance by inducing T-cell anergy and the generation of adaptive regulatory T cells*. *Blood*, 2008. **111**(1): p. 251-9.

288. Deaglio, S., et al., *Adenosine generation catalyzed by CD39 and CD73 expressed on regulatory T cells mediates immune suppression*. J Exp Med, 2007. **204**(6): p. 1257-65.
289. Takahashi, H.K., et al., *Effect of adenosine receptor subtypes stimulation on mixed lymphocyte reaction*. Eur J Pharmacol, 2007. **564**(1-3): p. 204-10.
290. Witko-Sarsat, V., et al., *Neutrophils: molecules, functions and pathophysiological aspects*. Lab Invest, 2000. **80**(5): p. 617-53.
291. Welbourn, C.R., et al., *Pathophysiology of ischaemia reperfusion injury: central role of the neutrophil*. Br J Surg, 1991. **78**(6): p. 651-5.
292. Chen, Y., et al., *ATP release guides neutrophil chemotaxis via P2Y2 and A3 receptors*. Science, 2006. **314**(5806): p. 1792-5.
293. Rose, F.R., et al., *Adenosine promotes neutrophil chemotaxis*. J Exp Med, 1988. **167**(3): p. 1186-94.
294. Bouma, M.G., et al., *Adenosine inhibits neutrophil degranulation in activated human whole blood: involvement of adenosine A2 and A3 receptors*. J Immunol, 1997. **158**(11): p. 5400-8.
295. Fortin, A., et al., *Differential expression of adenosine receptors in human neutrophils: up-regulation by specific Th1 cytokines and lipopolysaccharide*. J Leukoc Biol, 2006. **79**(3): p. 574-85.
296. Akaiwa, K., et al., *Moderate cerebral venous congestion induces rapid cerebral protection via adenosine A1 receptor activation*. Brain Res, 2006. **1122**(1): p. 47-55.

297. Nakamura, M., et al., *Rapid tolerance to focal cerebral ischemia in rats is attenuated by adenosine A1 receptor antagonist*. J Cereb Blood Flow Metab, 2002. **22**(2): p. 161-70.
298. Liu, Y., et al., *Isoflurane tolerance against focal cerebral ischemia is attenuated by adenosine A1 receptor antagonists*. Can J Anaesth, 2006. **53**(2): p. 194-201.
299. Heurteaux, C., et al., *Essential role of adenosine, adenosine A1 receptors, and ATP-sensitive K⁺ channels in cerebral ischemic preconditioning*. Proc Natl Acad Sci U S A, 1995. **92**(10): p. 4666-70.
300. Yoshida, M., et al., *Adenosine A(1) receptor antagonist and mitochondrial ATP-sensitive potassium channel blocker attenuate the tolerance to focal cerebral ischemia in rats*. J Cereb Blood Flow Metab, 2004. **24**(7): p. 771-9.
301. Biber, K., et al., *Interleukin-6 enhances expression of adenosine A(1) receptor mRNA and signaling in cultured rat cortical astrocytes and brain slices*. Neuropsychopharmacology, 2001. **24**(1): p. 86-96.
302. Morello, S., et al., *IL-1 beta and TNF-alpha regulation of the adenosine receptor (A2A) expression: differential requirement for NF-kappa B binding to the proximal promoter*. J Immunol, 2006. **177**(10): p. 7173-83.
303. St Hilaire, C., et al., *TNF-alpha upregulates the A2B adenosine receptor gene: The role of NAD(P)H oxidase 4*. Biochem Biophys Res Commun, 2008. **375**(3): p. 292-6.
304. Bouma, M.G., F.A. van den Wildenberg, and W.A. Buurman, *Adenosine inhibits cytokine release and expression of adhesion molecules by activated human endothelial cells*. Am J Physiol, 1996. **270**(2 Pt 1): p. C522-9.
305. Pober, J.S. and W.C. Sessa, *Evolving functions of endothelial cells in inflammation*. Nat Rev Immunol, 2007. **7**(10): p. 803-15.

306. Feoktistov, I., et al., *Differential expression of adenosine receptors in human endothelial cells: role of A2B receptors in angiogenic factor regulation*. *Circ Res*, 2002. **90**(5): p. 531-8.
307. Khoa, N.D., et al., *Inflammatory cytokines regulate function and expression of adenosine A(2A) receptors in human monocytic THP-1 cells*. *J Immunol*, 2001. **167**(7): p. 4026-32.
308. Hamano, R., et al., *Stimulation of adenosine A2A receptor inhibits LPS-induced expression of intercellular adhesion molecule 1 and production of TNF-alpha in human peripheral blood mononuclear cells*. *Shock*, 2008. **29**(2): p. 154-9.
309. Marsh, B., et al., *Systemic lipopolysaccharide protects the brain from ischemic injury by reprogramming the response of the brain to stroke: a critical role for IRF3*. *J Neurosci*, 2009. **29**(31): p. 9839-49.
310. Macedo, L., et al., *Wound healing is impaired in MyD88-deficient mice: a role for MyD88 in the regulation of wound healing by adenosine A2A receptors*. *Am J Pathol*, 2007. **171**(6): p. 1774-88.
311. Olah, M.E. and C.C. Caldwell, *Adenosine receptors and mammalian toll-like receptors: synergism in macrophages*. *Mol Interv*, 2003. **3**(7): p. 370-4.
312. Ramakers, B.P., et al., *The effect of adenosine receptor agonists on cytokine release by human mononuclear cells depends on the specific Toll-like receptor subtype used for stimulation*. *Cytokine*, 2006. **35**(1-2): p. 95-9.
313. Gourine, A.V., et al., *Release of ATP in the central nervous system during systemic inflammation: real-time measurement in the hypothalamus of conscious rabbits*. *J Physiol*, 2007. **585**(Pt 1): p. 305-16.

314. Braeuninger, S. and C. Kleinschnitz, *Rodent models of focal cerebral ischemia: procedural pitfalls and translational problems*. *Exp Transl Stroke Med*, 2009. **1**: p. 8.
315. STAIR, *Recommendations for standards regarding preclinical neuroprotective and restorative drug development*. *Stroke*, 1999. **30**: p. 2752-8.
316. Fukuda, S. and G.J. del Zoppo, *Models of focal cerebral ischemia in the nonhuman primate*. *ILAR J*, 2003. **44**(2): p. 96-104.
317. Bihel, E., et al., *Permanent or transient chronic ischemic stroke in the non-human primate: behavioral, neuroimaging, histological, and immunohistochemical investigations*. *J Cereb Blood Flow Metab*, 2010. **30**(2): p. 273-85.
318. Furuichi, Y., et al., *Therapeutic time window of tacrolimus (FK506) in a nonhuman primate stroke model: comparison with tissue plasminogen activator*. *Exp Neurol*, 2007. **204**(1): p. 138-46.
319. Mack, W.J., et al., *Serial magnetic resonance imaging in experimental primate stroke: validation of MRI for pre-clinical cerebroprotective trials*. *Neurol Res*, 2003. **25**(8): p. 846-52.
320. Baron, J.C., *Perfusion thresholds in human cerebral ischemia: historical perspective and therapeutic implications*. *Cerebrovasc Dis*, 2001. **11 Suppl 1**: p. 2-8.
321. Jones, T.H., et al., *Thresholds of focal cerebral ischemia in awake monkeys*. *J Neurosurg*, 1981. **54**(6): p. 773-82.
322. Arakawa, S., et al., *Ischemic thresholds for gray and white matter: a diffusion and perfusion magnetic resonance study*. *Stroke*, 2006. **37**(5): p. 1211-6.

323. Sawada, H., et al., *MRI demonstration of cortical laminar necrosis and delayed white matter injury in anoxic encephalopathy*. *Neuroradiology*, 1990. **32**(4): p. 319-21.
324. West, G.A., et al., *A new model of cortical stroke in the rhesus macaque*. *J Cereb Blood Flow Metab*, 2009. **29**(6): p. 1175-86.
325. Barber, P.A., et al., *Cerebral ischemic lesions on diffusion-weighted imaging are associated with neurocognitive decline after cardiac surgery*. *Stroke*, 2008. **39**(5): p. 1427-33.
326. Kariko, K., D. Weissman, and F.A. Welsh, *Inhibition of toll-like receptor and cytokine signaling--a unifying theme in ischemic tolerance*. *J Cereb Blood Flow Metab*, 2004. **24**(11): p. 1288-304.
327. Leung, P.Y., A.E. Packard, and M.P. Stenzel-Poore, *It's all in the family: multiple Toll-like receptors offer promise as novel therapeutic targets for stroke neuroprotection*. *Future Neurol*, 2009. **4**(2): p. 201-208.
328. Hua, F., et al., *Preconditioning with a TLR2 specific ligand increases resistance to cerebral ischemia/reperfusion injury*. *J Neuroimmunol*, 2008. **199**(1-2): p. 75-82.
329. Krieg, A.M., *Therapeutic potential of Toll-like receptor 9 activation*. *Nat Rev Drug Discov*, 2006. **5**(6): p. 471-84.
330. Leifer, C.A., D. Verthelyi, and D.M. Klinman, *Heterogeneity in the human response to immunostimulatory CpG oligodeoxynucleotides*. *J Immunother*, 2003. **26**(4): p. 313-9.
331. Clark, W.M., et al., *Monofilament intraluminal middle cerebral artery occlusion in the mouse*. *Neurol Res*, 1997. **19**(6): p. 641-8.

332. Swanson, R.A., et al., *A semiautomated method for measuring brain infarct volume*. J Cereb Blood Flow Metab, 1990. **10**(2): p. 290-3.
333. Spetzler, R.F., et al., *Chronic reversible cerebral ischemia: evaluation of a new baboon model*. Neurosurgery, 1980. **7**(3): p. 257-61.
334. Verthelyi, D., et al., *CpG oligodeoxynucleotides as vaccine adjuvants in primates*. J Immunol, 2002. **168**(4): p. 1659-63.
335. Benedek, A., et al., *Use of TTC staining for the evaluation of tissue injury in the early phases of reperfusion after focal cerebral ischemia in rats*. Brain Res, 2006. **1116**(1): p. 159-65.
336. Vogelgesang, A., et al., *Analysis of lymphocyte subsets in patients with stroke and their influence on infection after stroke*. Stroke, 2008. **39**(1): p. 237-41.
337. Buck, B.H., et al., *Early neutrophilia is associated with volume of ischemic tissue in acute stroke*. Stroke, 2008. **39**(2): p. 355-60.
338. Smith, C.J., et al., *Peak plasma interleukin-6 and other peripheral markers of inflammation in the first week of ischaemic stroke correlate with brain infarct volume, stroke severity and long-term outcome*. BMC Neurol, 2004. **4**: p. 2.
339. Fisher, M., et al., *Update of the stroke therapy academic industry roundtable preclinical recommendations*. Stroke, 2009. **40**(6): p. 2244-50.
340. Chang, Z.L., *Important aspects of Toll-like receptors, ligands and their signaling pathways*. Inflamm Res, 2010. **59**(10): p. 791-808.
341. Sloane, J.A., et al., *A clear and present danger: endogenous ligands of Toll-like receptors*. Neuromolecular Med, 2010. **12**(2): p. 149-63.
342. Hua, F., et al., *Differential roles of TLR2 and TLR4 in acute focal cerebral ischemia/reperfusion injury in mice*. Brain Res, 2009. **1262**: p. 100-8.

343. Wagner, I., et al., *Repeated peripheral administrations of CpG oligodeoxynucleotides lead to sustained CNS immune activation*. Immunopharmacol Immunotoxicol, 2007. **29**(3-4): p. 413-24.
344. Agrawal, S., J. Temsamani, and J.Y. Tang, *Pharmacokinetics, biodistribution, and stability of oligodeoxynucleotide phosphorothioates in mice*. Proc Natl Acad Sci U S A, 1991. **88**(17): p. 7595-9.
345. Banks, W.A., et al., *Delivery across the blood-brain barrier of antisense directed against amyloid beta: reversal of learning and memory deficits in mice overexpressing amyloid precursor protein*. J Pharmacol Exp Ther, 2001. **297**(3): p. 1113-21.
346. Cossum, P.A., et al., *Disposition of the 14C-labeled phosphorothioate oligonucleotide ISIS 2105 after intravenous administration to rats*. J Pharmacol Exp Ther, 1993. **267**(3): p. 1181-90.
347. Takamatsu, H., et al., *Detection of reperfusion injury using PET in a monkey model of cerebral ischemia*. J Nucl Med, 2000. **41**(8): p. 1409-16.
348. Gunzer, M., et al., *Systemic administration of a TLR7 ligand leads to transient immune incompetence due to peripheral-blood leukocyte depletion*. Blood, 2005. **106**(7): p. 2424-32.
349. Akopov, S.E., N.A. Simonian, and G.S. Grigorian, *Dynamics of polymorphonuclear leukocyte accumulation in acute cerebral infarction and their correlation with brain tissue damage*. Stroke, 1996. **27**(10): p. 1739-43.
350. Ember, J.A., et al., *Polymorphonuclear leukocyte behavior in a nonhuman primate focal ischemia model*. J Cereb Blood Flow Metab, 1994. **14**(6): p. 1046-54.

351. Emerich, D.F., R.L. Dean, 3rd, and R.T. Bartus, *The role of leukocytes following cerebral ischemia: pathogenic variable or bystander reaction to emerging infarct?* Exp Neurol, 2002. **173**(1): p. 168-81.
352. Shenhar-Tsarfaty, S., et al., *Interleukin-6 as an early predictor for one-year survival following an ischaemic stroke/transient ischaemic attack.* Int J Stroke. **5**(1): p. 16-20.
353. Song, I.U., et al., *Relationship between high-sensitivity C-reactive protein and clinical functional outcome after acute ischemic stroke in a Korean population.* Cerebrovasc Dis, 2009. **28**(6): p. 545-50.
354. Shen, H.Y., et al., *Adenosine kinase determines the degree of brain injury after ischemic stroke in mice.* J Cereb Blood Flow Metab, 2011. **31**(7): p. 1648-59.
355. Wahlgren, N.G. and N. Ahmed, *Neuroprotection in cerebral ischaemia: facts and fancies--the need for new approaches.* Cerebrovasc Dis, 2004. **17 Suppl 1**: p. 153-66.
356. Dirnagl, U., K. Becker, and A. Meisel, *Preconditioning and tolerance against cerebral ischaemia: from experimental strategies to clinical use.* Lancet Neurol, 2009. **8**(4): p. 398-412.
357. Dhodda, V.K., et al., *Putative endogenous mediators of preconditioning-induced ischemic tolerance in rat brain identified by genomic and proteomic analysis.* J Neurochem, 2004. **89**(1): p. 73-89.
358. Boison, D., et al., *Neonatal hepatic steatosis by disruption of the adenosine kinase gene.* Proc Natl Acad Sci U S A, 2002. **99**(10): p. 6985-90.
359. Fredholm, B.B., *Adenosine, an endogenous distress signal, modulates tissue damage and repair.* Cell Death Differ, 2007. **14**(7): p. 1315-23.

360. Newby, A.C., Y. Worku, and C.A. Holmquist, *Adenosine formation. Evidence for a direct biochemical link with energy metabolism*. *Adv Myocardiol*, 1985. **6**: p. 273-84.
361. Stone, T.W., S. Ceruti, and M.P. Abbracchio, *Adenosine receptors and neurological disease: neuroprotection and neurodegeneration*. *Handb Exp Pharmacol*, 2009(193): p. 535-87.
362. Boison, D., J.F. Chen, and B.B. Fredholm, *Adenosine signaling and function in glial cells*. *Cell Death Differ*. **17**(7): p. 1071-82.
363. Clark, R.S., et al., *Cerebrospinal fluid adenosine concentration and uncoupling of cerebral blood flow and oxidative metabolism after severe head injury in humans*. *Neurosurgery*, 1997. **41**(6): p. 1284-92; discussion 1292-3.
364. Melani, A., et al., *Striatal outflow of adenosine, excitatory amino acids, gamma-aminobutyric acid, and taurine in awake freely moving rats after middle cerebral artery occlusion: correlations with neurological deficit and histopathological damage*. *Stroke*, 1999. **30**(11): p. 2448-54; discussion 2455.
365. Pignataro, G., et al., *Downregulation of hippocampal adenosine kinase after focal ischemia as potential endogenous neuroprotective mechanism*. *J Cereb Blood Flow Metab*, 2008. **28**(1): p. 17-23.
366. Li, T., et al., *Adenosine kinase is a target for the prediction and prevention of epileptogenesis in mice*. *J Clin Invest*, 2008. **118**(2): p. 571-582.
367. Li, T., et al., *Adenosine kinase is a target for the prediction and prevention of epileptogenesis in mice*. *J Clin Invest*, 2008. **118**(2): p. 571-82.
368. Theofilas, P., et al., *Adenosine kinase as a target for therapeutic antisense strategies in epilepsy*. *Epilepsia*, 2011. *in press*.

369. Lee, Y., et al., *GFAP promoter elements required for region-specific and astrocyte-specific expression*. *Glia*, 2008. **56**(5): p. 481-93.
370. Studer, F.E., et al., *Shift of adenosine kinase expression from neurons to astrocytes during postnatal development suggests dual functionality of the enzyme*. *Neuroscience*, 2006. **142**(1): p. 125-37.
371. Theofilas, P., et al., *Adenosine kinase as a target for therapeutic antisense strategies in epilepsy*. *Epilepsia*, 2011. **52**(3): p. 589-601.
372. Etherington, L.A., et al., *Astrocytic adenosine kinase regulates basal synaptic adenosine levels and seizure activity but not activity-dependent adenosine release in the hippocampus*. *Neuropharmacology*, 2009. **56**(2): p. 429-437.
373. Dale, N., et al., *Listening to the brain: microelectrode biosensors for neurochemicals*. *Trends Biotechnol*, 2005. **23**(8): p. 420-8.
374. Delaney, S.M. and J.D. Geiger, *Brain regional levels of adenosine and adenosine nucleotides in rats killed by high-energy focused microwave irradiation*. *J Neurosci Methods*, 1996. **64**(2): p. 151-6.
375. Yu, L., et al., *Selective inactivation or reconstitution of adenosine A2A receptors in bone marrow cells reveals their significant contribution to the development of ischemic brain injury*. *Nat Med*, 2004. **10**(10): p. 1081-7.
376. Dragunow, M. and R.L. Faull, *Neuroprotective effects of adenosine*. *Trends Pharmacol Sci*, 1988. **9**(6): p. 193-4.
377. Fredholm, B.B., et al., *Adenosine and brain function*. *Int Rev Neurobiol*, 2005. **63**: p. 191-270.

378. Sommerschild, H.T. and K.A. Kirkeboen, *Adenosine and cardioprotection during ischaemia and reperfusion--an overview*. Acta Anaesthesiol Scand, 2000. **44**(9): p. 1038-55.
379. Li, W., et al., *Genetic inactivation of adenosine A2A receptors attenuates acute traumatic brain injury in the mouse cortical impact model*. Exp Neurol, 2009. **215**(1): p. 69-76.
380. von Lubitz, D.K., et al., *Adenosine: a prototherapeutic concept in neurodegeneration*. Ann N Y Acad Sci, 1995. **765**: p. 163-78; discussion 196-7.
381. Boison, D., *Adenosine augmentation therapies (AATs) for epilepsy: prospect of cell and gene therapies*. Epilepsy Res, 2009. **85**(2-3): p. 131-41.
382. Kossoff, E.H., B.A. Zupec-Kania, and J.M. Rho, *Ketogenic diets: an update for child neurologists*. J Child Neurol, 2009. **24**(8): p. 979-88.
383. Masino, S.A., et al., *A ketogenic diet suppresses seizures in mice through adenosine A(1) receptors*. J Clin Invest, 2011. **121**(7): p. 2679-83.
384. Loscher, W. and C. Brandt, *Prevention or modification of epileptogenesis after brain insults: experimental approaches and translational research*. Pharmacol Rev, 2010. **62**(4): p. 668-700.
385. Dudek, F.E., et al., *The course of cellular alterations associated with the development of spontaneous seizures after status epilepticus*. Prog Brain Res, 2002. **135**: p. 53-65.
386. Fukuchi, M., et al., *Valproic acid induces up- or down-regulation of gene expression responsible for the neuronal excitation and inhibition in rat cortical neurons through its epigenetic actions*. Neurosci Res, 2009. **65**(1): p. 35-43.

387. Kobow, K. and I. Blumcke, *The methylation hypothesis: do epigenetic chromatin modifications play a role in epileptogenesis?* *Epilepsia*, 2011. **52 Suppl 4**: p. 15-9.
388. Qureshi, I.A. and M.F. Mehler, *Epigenetic mechanisms underlying human epileptic disorders and the process of epileptogenesis*. *Neurobiol Dis*, 2010. **39(1)**: p. 53-60.
389. Feng, J., et al., *Dnmt1 and Dnmt3a maintain DNA methylation and regulate synaptic function in adult forebrain neurons*. *Nat Neurosci*, 2010. **13(4)**: p. 423-30.
390. Ma, D.K., et al., *Neuronal activity-induced Gadd45b promotes epigenetic DNA demethylation and adult neurogenesis*. *Science*, 2009. **323(5917)**: p. 1074-7.
391. Nelson, E.D., E.T. Kavalali, and L.M. Monteggia, *Activity-dependent suppression of miniature neurotransmission through the regulation of DNA methylation*. *J Neurosci*, 2008. **28(2)**: p. 395-406.
392. Kobow, K., et al., *Increased reelin promoter methylation is associated with granule cell dispersion in human temporal lobe epilepsy*. *J Neuropathol Exp Neurol*, 2009. **68(4)**: p. 356-64.
393. Veldic, M., et al., *In psychosis, cortical interneurons overexpress DNA-methyltransferase 1*. *Proc Natl Acad Sci U S A*, 2005. **102(6)**: p. 2152-7.
394. Gottlicher, M., *Valproic acid: an old drug newly discovered as inhibitor of histone deacetylases*. *Ann Hematol*, 2004. **83 Suppl 1**: p. S91-2.
395. Milutinovic, S., et al., *Valproate induces widespread epigenetic reprogramming which involves demethylation of specific genes*. *Carcinogenesis*, 2007. **28(3)**: p. 560-71.

396. Lubin, F.D., *Epileptogenesis: can the science of epigenetics give us answers?* *Epilepsy Curr*, 2012. **12**(3): p. 105-10.
397. Kredich, N.M. and D.V. Martin, Jr., *Role of S-adenosylhomocysteine in adenosinemediated toxicity in cultured mouse T lymphoma cells.* *Cell*, 1977. **12**(4): p. 931-8.
398. Fredholm, B.B., *Rethinking the purinergic neuron-glia connection.* *Proc Natl Acad Sci U S A*, 2012. **109**(16): p. 5913-4.
399. Aronica, E., et al., *Upregulation of adenosine kinase in astrocytes in experimental and human temporal lobe epilepsy.* *Epilepsia*. **52**(9): p. 1645-55.
400. Boison, D., *Adenosine dysfunction in epilepsy.* *Glia*, 2012. **60**(8): p. 1234-43.
401. Dunwiddie, T.V., *Endogenously released adenosine regulates excitability in the in vitro hippocampus.* *Epilepsia*, 1980. **21**(5): p. 541-8.
402. Fedele, D.E., et al., *Adenosine A1 receptors are crucial in keeping an epileptic focus localized.* *Exp Neurol*, 2006. **200**(1): p. 184-90.
403. Johansson, B., et al., *Hyperalgesia, anxiety, and decreased hypoxic neuroprotection in mice lacking the adenosine A1 receptor.* *Proc Natl Acad Sci U S A*, 2001. **98**(16): p. 9407-12.
404. Lovatt, D., et al., *Neuronal adenosine release, and not astrocytic ATP release, mediates feedback inhibition of excitatory activity.* *Proc Natl Acad Sci U S A*, 2012. **109**(16): p. 6265-70.
405. Huber, A., et al., *Grafts of adenosine-releasing cells suppress seizures in kindling epilepsy.* *Proc Natl Acad Sci U S A*, 2001. **98**(13): p. 7611-6.

406. Stohr, T., et al., *Lacosamide, a novel anti-convulsant drug, shows efficacy with a wide safety margin in rodent models for epilepsy*. *Epilepsy Res*, 2007. **74**(2-3): p. 147-54.
407. White, H.S., et al., *The National Institutes of Health Anticonvulsant Drug Development Program: screening for efficacy*. *Adv Neurol*, 1998. **76**: p. 29-39.
408. Racine, R., *Kindling: the first decade*. *Neurosurgery*, 1978. **3**(2): p. 234-52.
409. Ndode-Ekane, X.E., et al., *Vascular changes in epilepsy: functional consequences and association with network plasticity in pilocarpine-induced experimental epilepsy*. *Neuroscience*, 2010. **166**(1): p. 312-32.
410. Cavazos, J.E., G. Golarai, and T.P. Sutula, *Mossy fiber synaptic reorganization induced by kindling: time course of development, progression, and permanence*. *J Neurosci*, 1991. **11**(9): p. 2795-803.
411. Gouder, N., et al., *Overexpression of adenosine kinase in epileptic hippocampus contributes to epileptogenesis*. *J Neurosci*, 2004. **24**(3): p. 692-701.
412. Szybala, C., et al., *Antiepileptic effects of silk-polymer based adenosine release in kindled rats*. *Exp Neurol*, 2009. **219**(1): p. 126-35.
413. Boison, D., et al., *Seizure suppression by adenosine-releasing cells is independent of seizure frequency*. *Epilepsia*, 2002. **43**(8): p. 788-96.
414. Cui, X.A., et al., *Subcellular localization of adenosine kinase in mammalian cells: The long isoform of AdK is localized in the nucleus*. *Biochem Biophys Res Commun*, 2009. **388**(1): p. 46-50.
415. Williams, P.A., et al., *Development of spontaneous recurrent seizures after kainate-induced status epilepticus*. *J Neurosci*, 2009. **29**(7): p. 2103-12.

416. Pitkanen, A. and K. Lukasiuk, *Mechanisms of epileptogenesis and potential treatment targets*. *Lancet Neurol*, 2011. **10**(2): p. 173-86.
417. Dudek, F.E. and K.J. Staley, *The time course of acquired epilepsy: implications for therapeutic intervention to suppress epileptogenesis*. *Neurosci Lett*, 2011. **497**(3): p. 240-6.
418. Dudek, F.E. and T.P. Sutula, *Epileptogenesis in the dentate gyrus: a critical perspective*. *Prog Brain Res*, 2007. **163**: p. 755-73.
419. Kriaucionis, S. and N. Heintz, *The nuclear DNA base 5-hydroxymethylcytosine is present in Purkinje neurons and the brain*. *Science*, 2009. **324**(5929): p. 929-30.
420. Tahiliani, M., et al., *Conversion of 5-methylcytosine to 5-hydroxymethylcytosine in mammalian DNA by MLL partner TET1*. *Science*, 2009. **324**(5929): p. 930-5.
421. Miller, C.A. and J.D. Sweatt, *Covalent modification of DNA regulates memory formation*. *Neuron*, 2007. **53**(6): p. 857-69.
422. Levenson, J.M., et al., *Evidence that DNA (cytosine-5) methyltransferase regulates synaptic plasticity in the hippocampus*. *J Biol Chem*, 2006. **281**(23): p. 15763-73.
423. Guo, J.U., et al., *Neuronal activity modifies the DNA methylation landscape in the adult brain*. *Nat Neurosci*, 2011. **14**(10): p. 1345-51.
424. Zhu, Q., et al., *Increased expression of DNA methyltransferase 1 and 3a in human temporal lobe epilepsy*. *J Mol Neurosci*, 2002. **46**(2): p. 420-6.
425. Tao, S., et al., *Up-Regulated Methyl CpG Binding Protein-2 in Intractable Temporal Lobe Epilepsy Patients and a Rat Model*. *Neurochem Res*, 2012.

426. Gore, S.D., *New ways to use DNA methyltransferase inhibitors for the treatment of myelodysplastic syndrome*. Hematology Am Soc Hematol Educ Program, 2011. **2011**: p. 550-5.
427. Momparler, R.L., et al., *Pilot phase I-II study on 5-aza-2'-deoxycytidine (Decitabine) in patients with metastatic lung cancer*. Anticancer Drugs, 1997. **8**(4): p. 358-68.
428. Lado, F.A. and S.L. Moshe, *How do seizures stop?* Epilepsia, 2008. **49**(10): p. 1651-64.
429. Fuks, F., *DNA methylation and histone modifications: teaming up to silence genes*. Curr Opin Genet Dev, 2005. **15**(5): p. 490-5.
430. Csoka, A.B. and M. Szyf, *Epigenetic side-effects of common pharmaceuticals: a potential new field in medicine and pharmacology*. Med Hypotheses, 2009. **73**(5): p. 770-80.
431. Tsai, H.C., et al., *Transient low doses of DNA-demethylating agents exert durable antitumor effects on hematological and epithelial tumor cells*. Cancer Cell, 2012. **21**(3): p. 430-46.
432. Loscher, W. and D. Schmidt, *Modern antiepileptic drug development has failed to deliver: ways out of the current dilemma*. Epilepsia, 2011. **52**(4): p. 657-78.
433. Cibula, J.E. and R.L. Gilmore, *Secondary epileptogenesis in humans*. J Clin Neurophysiol, 1997. **14**(2): p. 111-27.
434. de Tisi, J., et al., *The long-term outcome of adult epilepsy surgery, patterns of seizure remission, and relapse: a cohort study*. Lancet, 2011. **378**(9800): p. 1388-95.

435. Urdinguio, R.G., J.V. Sanchez-Mut, and M. Esteller, *Epigenetic mechanisms in neurological diseases: genes, syndromes, and therapies*. *Lancet Neurol*, 2009. **8**(11): p. 1056-72.
436. Yan, J., J.R. Zierath, and R. Barres, *Evidence for non-CpG methylation in mammals*. *Exp Cell Res*, 2011. **317**(18): p. 2555-61.
437. Fuchikami, M., et al., *DNA methylation profiles of the brain-derived neurotrophic factor (BDNF) gene as a potent diagnostic biomarker in major depression*. *PLoS One*, 2011. **6**(8): p. e23881.
438. Brooks-Kayal, A.R., Y.H. Raol, and S.J. Russek, *Alteration of epileptogenesis genes*. *Neurotherapeutics*, 2009. **6**(2): p. 312-8.
439. Paradiso, B., et al., *Localized overexpression of FGF-2 and BDNF in hippocampus reduces mossy fiber sprouting and spontaneous seizures up to 4 weeks after pilocarpine-induced status epilepticus*. *Epilepsia*, 2011. **52**(3): p. 572-8.
440. Boison, D., *The adenosine kinase hypothesis of epileptogenesis*. *Prog Neurobiol*, 2008. **84**(3): p. 249-62.
441. Jones, P.A., *Functions of DNA methylation: islands, start sites, gene bodies and beyond*. *Nat Rev Genet*, 2012. **13**(7): p. 484-92.
442. Baldwin, S.A., et al., *The equilibrative nucleoside transporter family, SLC29*. *Pflugers Arch*, 2004. **447**(5): p. 735-43.
443. Gray, J.H., R.P. Owen, and K.M. Giacomini, *The concentrative nucleoside transporter family, SLC28*. *Pflugers Arch*, 2004. **447**(5): p. 728-34.
444. Zhang, D., et al., *Expression of human equilibrative nucleoside transporter 1 in mouse neurons regulates adenosine levels in physiological and hypoxic-ischemic conditions*. *J Neurochem*, 2011. **118**(1): p. 4-11.

445. Shakespeare, W., *As you like it*, E.C. Black, Editor. 1906, Ginn and Company. p. 152.
446. NIGMS, *Sepsis Fact Sheet*. 2012, National Institutes of Health.
447. Leung, P.Y., et al., *Toll-like receptor 7 preconditioning induces robust neuroprotection against stroke by a novel type I interferon-mediated mechanism*. *Stroke*, 2012. **43**(5): p. 1383-9.
448. Packard, A.E., et al., *Poly-IC preconditioning protects against cerebral and renal ischemia-reperfusion injury*. *J Cereb Blood Flow Metab*, 2012. **32**(2): p. 242-7.
449. Song, W., B.L. Furman, and J.R. Parratt, *Delayed protection against ischaemia-induced ventricular arrhythmias and infarct size limitation by the prior administration of Escherichia coli endotoxin*. *Br J Pharmacol*, 1996. **118**(8): p. 2157-63.
450. Wang, Y.P., et al., *Lipopolysaccharide triggers late preconditioning against myocardial infarction via inducible nitric oxide synthase*. *Cardiovasc Res*, 2002. **56**(1): p. 33-42.
451. Rowland, R.T., et al., *LPS-induced delayed myocardial adaptation enhances acute preconditioning to optimize postischemic cardiac function*. *Am J Physiol*, 1997. **272**(6 Pt 2): p. H2708-15.
452. Merry, H.E., et al., *Lipopolysaccharide pre-conditioning is protective in lung ischemia-reperfusion injury*. *J Heart Lung Transplant*, 2010. **29**(4): p. 471-8.
453. Sano, T., et al., *Hepatic preconditioning using lipopolysaccharide: association with specific negative regulators of the Toll-like receptor 4 signaling pathway*. *Transplantation*, 2011. **91**(10): p. 1082-9.

454. Colletti, L.M., D.G. Remick, and D.A. Campbell, Jr., *LPS pretreatment protects from hepatic ischemia/reperfusion*. J Surg Res, 1994. **57**(3): p. 337-43.
455. Longhi, L., et al., *Long-lasting protection in brain trauma by endotoxin preconditioning*. J Cereb Blood Flow Metab, 2011. **31**(9): p. 1919-29.
456. Dmowska, M., et al., *Behavioural and histological effects of preconditioning with lipopolysaccharide in epileptic rats*. Neurochem Res, 2010. **35**(2): p. 262-72.
457. Mirrione, M.M., et al., *Microglial ablation and lipopolysaccharide preconditioning affects pilocarpine-induced seizures in mice*. Neurobiol Dis, 2010. **39**(1): p. 85-97.
458. Hurley, J.C., *Endotoxemia: methods of detection and clinical correlates*. Clin Microbiol Rev, 1995. **8**(2): p. 268-92.
459. Krieg, A.M., et al., *CpG motifs in bacterial DNA trigger direct B-cell activation*. Nature, 1995. **374**(6522): p. 546-9.
460. Asselin-Paturel, C., et al., *Type I interferon dependence of plasmacytoid dendritic cell activation and migration*. J Exp Med, 2005. **201**(7): p. 1157-67.
461. Jung, J., et al., *Distinct response of human B cell subpopulations in recognition of an innate immune signal, CpG DNA*. J Immunol, 2002. **169**(5): p. 2368-73.
462. Krieg, A.M., *CpG motifs in bacterial DNA and their immune effects*. Annu Rev Immunol, 2002. **20**: p. 709-60.
463. Krieg, A.M., et al., *Induction of systemic TH1-like innate immunity in normal volunteers following subcutaneous but not intravenous administration of CPG 7909, a synthetic B-class CpG oligodeoxynucleotide TLR9 agonist*. J Immunother, 2004. **27**(6): p. 460-71.

464. Klinman, D.M., et al., *CpG motifs present in bacteria DNA rapidly induce lymphocytes to secrete interleukin 6, interleukin 12, and interferon gamma*. Proc Natl Acad Sci U S A, 1996. **93**(7): p. 2879-83.
465. Zhu, Q., et al., *Toll-like receptor ligands synergize through distinct dendritic cell pathways to induce T cell responses: implications for vaccines*. Proc Natl Acad Sci U S A, 2008. **105**(42): p. 16260-5.
466. Auer, R.N. and B.K. Siesjo, *Biological differences between ischemia, hypoglycemia, and epilepsy*. Ann Neurol, 1988. **24**(6): p. 699-707.
467. Bowman, C.C., et al., *Cultured astrocytes express toll-like receptors for bacterial products*. Glia, 2003. **43**(3): p. 281-91.
468. Tang, S.C., et al., *Pivotal role for neuronal Toll-like receptors in ischemic brain injury and functional deficits*. Proc Natl Acad Sci U S A, 2007. **104**(34): p. 13798-803.
469. Iliev, A.I., et al., *Neuronal injury mediated via stimulation of microglial toll-like receptor-9 (TLR9)*. FASEB J, 2004. **18**(2): p. 412-4.
470. Yu, Z.F. and M.P. Mattson, *Dietary restriction and 2-deoxyglucose administration reduce focal ischemic brain damage and improve behavioral outcome: evidence for a preconditioning mechanism*. J Neurosci Res, 1999. **57**(6): p. 830-9.
471. Hsu, J.C., et al., *Sleep deprivation prior to transient global cerebral ischemia attenuates glial reaction in the rat hippocampal formation*. Brain Res, 2003. **984**(1-2): p. 170-81.
472. Plamondon, H., et al., *Mutually protective actions of kainic acid epileptic preconditioning and sublethal global ischemia on hippocampal neuronal death: involvement of adenosine A1 receptors and K(ATP) channels*. J Cereb Blood Flow Metab, 1999. **19**(12): p. 1296-308.

473. Simon, R.P., et al., *Can genes modify stroke outcome and by what mechanisms?* Stroke, 2012. **43**(1): p. 286-91.
474. Stenzel-Poore, M.P., S.L. Stevens, and R.P. Simon, *Genomics of preconditioning.* Stroke, 2004. **35**(11 Suppl 1): p. 2683-6.
475. Bernaudin, M., et al., *Brain genomic response following hypoxia and re-oxygenation in the neonatal rat. Identification of genes that might contribute to hypoxia-induced ischemic tolerance.* J Biol Chem, 2002. **277**(42): p. 39728-38.
476. Tang, Y., et al., *Effect of hypoxic preconditioning on brain genomic response before and following ischemia in the adult mouse: identification of potential neuroprotective candidates for stroke.* Neurobiol Dis, 2006. **21**(1): p. 18-28.
477. Hatazaki, S., et al., *Microarray profile of seizure damage-refractory hippocampal CA3 in a mouse model of epileptic preconditioning.* Neuroscience, 2007. **150**(2): p. 467-77.
478. Jimenez-Mateos, E.M., et al., *Hippocampal transcriptome after status epilepticus in mice rendered seizure damage-tolerant by epileptic preconditioning features suppressed calcium and neuronal excitability pathways.* Neurobiol Dis, 2008. **32**(3): p. 442-53.
479. Stapels, M., et al., *Polycomb group proteins as epigenetic mediators of neuroprotection in ischemic tolerance.* Sci Signal, 2010. **3**(111): p. ra15.
480. Carson, W.F., et al., *Epigenetic regulation of immune cell functions during post-septic immunosuppression.* Epigenetics, 2011. **6**(3): p. 273-83.
481. Ward, N.S., B. Casserly, and A. Ayala, *The compensatory anti-inflammatory response syndrome (CARS) in critically ill patients.* Clin Chest Med, 2008. **29**(4): p. 617-25, viii.

482. Reddy, R.C., et al., *Alveolar macrophage deactivation in murine septic peritonitis: role of interleukin 10*. *Infect Immun*, 2001. **69**(3): p. 1394-401.
483. Reddy, R.C., et al., *Sepsis-induced immunosuppression: from bad to worse*. *Immunol Res*, 2001. **24**(3): p. 273-87.
484. Chan, C., et al., *Endotoxin tolerance disrupts chromatin remodeling and NF-kappaB transactivation at the IL-1beta promoter*. *J Immunol*, 2005. **175**(1): p. 461-8.
485. De Santa, F., et al., *The histone H3 lysine-27 demethylase Jmjd3 links inflammation to inhibition of polycomb-mediated gene silencing*. *Cell*, 2007. **130**(6): p. 1083-94.
486. El Gazzar, M., et al., *G9a and HP1 couple histone and DNA methylation to TNFalpha transcription silencing during endotoxin tolerance*. *J Biol Chem*, 2008. **283**(47): p. 32198-208.
487. Tsaprouni, L.G., et al., *Suppression of lipopolysaccharide- and tumour necrosis factor-alpha-induced interleukin (IL)-8 expression by glucocorticoids involves changes in IL-8 promoter acetylation*. *Clin Exp Immunol*, 2007. **150**(1): p. 151-7.
488. El Gazzar, M. and C.E. McCall, *MicroRNAs distinguish translational from transcriptional silencing during endotoxin tolerance*. *J Biol Chem*, 2010. **285**(27): p. 20940-51.
489. Lal, G. and J.S. Bromberg, *Epigenetic mechanisms of regulation of Foxp3 expression*. *Blood*, 2009. **114**(18): p. 3727-35.
490. Lal, G., et al., *Epigenetic regulation of Foxp3 expression in regulatory T cells by DNA methylation*. *J Immunol*, 2009. **182**(1): p. 259-73.

491. Ohmori, O., et al., *Down-regulation of S-adenosylhomocysteine hydrolase in the active methyl transfer system in the brain of genetically epileptic El mice.* Neurochem Res, 1996. **21**(10): p. 1173-80.
492. Detich, N., V. Bovenzi, and M. Szyf, *Valproate induces replication-independent active DNA demethylation.* J Biol Chem, 2003. **278**(30): p. 27586-92.
493. Endres, M., et al., *DNA methyltransferase contributes to delayed ischemic brain injury.* J Neurosci, 2000. **20**(9): p. 3175-81.
494. Endres, M., et al., *Effects of cerebral ischemia in mice lacking DNA methyltransferase 1 in post-mitotic neurons.* Neuroreport, 2001. **12**(17): p. 3763-6.
495. Kelly, P.J., et al., *Homocysteine, MTHFR 677C-->T polymorphism, and risk of ischemic stroke: results of a meta-analysis.* Neurology, 2002. **59**(4): p. 529-36.
496. Casas, J.P., et al., *Meta-analysis of genetic studies in ischemic stroke: thirty-two genes involving approximately 18,000 cases and 58,000 controls.* Arch Neurol, 2004. **61**(11): p. 1652-61.
497. Setoguchi, H., et al., *Methyl-CpG binding proteins are involved in restricting differentiation plasticity in neurons.* J Neurosci Res, 2006. **84**(5): p. 969-79.
498. Wu, Z., et al., *Dnmt3a regulates both proliferation and differentiation of mouse neural stem cells.* J Neurosci Res, 2012.
499. Maysami, S., et al., *Proliferating progenitor cells: a required cellular element for induction of ischemic tolerance in the brain.* J Cereb Blood Flow Metab, 2008. **28**(6): p. 1104-13.

500. Kawabata, T., et al., *Functional alterations of liver innate immunity of mice with aging in response to CpG-oligodeoxynucleotide*. *Hepatology*, 2008. **48**(5): p. 1586-97.
501. Stout-Delgado, H.W., et al., *Aging impairs IFN regulatory factor 7 up-regulation in plasmacytoid dendritic cells during TLR9 activation*. *J Immunol*, 2008. **181**(10): p. 6747-56.
502. Hasegawa, K. and T. Hayashi, *Synthetic CpG oligodeoxynucleotides accelerate the development of lupus nephritis during preactive phase in NZB x NZWF1 mice*. *Lupus*, 2003. **12**(11): p. 838-45.
503. Ichikawa, H.T., L.P. Williams, and B.M. Segal, *Activation of APCs through CD40 or Toll-like receptor 9 overcomes tolerance and precipitates autoimmune disease*. *J Immunol*, 2002. **169**(5): p. 2781-7.
504. Obermeier, F., et al., *CpG motifs of bacterial DNA exacerbate colitis of dextran sulfate sodium-treated mice*. *Eur J Immunol*, 2002. **32**(7): p. 2084-92.
505. Ronaghy, A., et al., *Immunostimulatory DNA sequences influence the course of adjuvant arthritis*. *J Immunol*, 2002. **168**(1): p. 51-6.
506. Miller-Delaney, S.F., et al., *Differential DNA methylation patterns define status epilepticus and epileptic tolerance*. *J Neurosci*, 2012. **32**(5): p. 1577-88.
507. Szyf, M., *Epigenetics, DNA methylation, and chromatin modifying drugs*. *Annu Rev Pharmacol Toxicol*, 2009. **49**: p. 243-63.
508. Vartanian, K.B., et al., *LPS preconditioning redirects TLR signaling following stroke: TRIF-IRF3 plays a seminal role in mediating tolerance to ischemic injury*. *J Neuroinflammation*, 2011. **8**: p. 140.

509. Stevens, S.L., Leung, P.Y., Vartanian, K.B., Gopalan, B., Yang, T., Simon, R.P., and Stenzel-Poore, M.P., *Multiple Preconditioning Paradigms Converge on Interferon Regulatory Factor-Dependent Signaling to Promote Tolerance to Ischemic Brain Injury*. The Journal of Neuroscience, 2011. **31**(23): p. 8456-8463.
510. Xiao, G., et al., *Alternative pathways of NF-kappaB activation: a double-edged sword in health and disease*. Cytokine Growth Factor Rev, 2006. **17**(4): p. 281-93.
511. Medzhitov, R., *Toll-like receptors and innate immunity*. Nat Rev Immunol, 2001. **1**(2): p. 135-45.
512. Kastenbauer, S. and H.W. Ziegler-Heitbrock, *NF-kappaB1 (p50) is upregulated in lipopolysaccharide tolerance and can block tumor necrosis factor gene expression*. Infect Immun, 1999. **67**(4): p. 1553-9.
513. Naumann, M., F.G. Wulczyn, and C. Scheidereit, *The NF-kappa B precursor p105 and the proto-oncogene product Bcl-3 are I kappa B molecules and control nuclear translocation of NF-kappa B*. Embo J, 1993. **12**(1): p. 213-22.
514. Driessler, F., et al., *Molecular mechanisms of interleukin-10-mediated inhibition of NF-kappaB activity: a role for p50*. Clin Exp Immunol, 2004. **135**(1): p. 64-73.
515. Carmody, R.J., et al., *Negative regulation of toll-like receptor signaling by NF-kappaB p50 ubiquitination blockade*. Science, 2007. **317**(5838): p. 675-8.
516. Stevens, S.L., et al., *The use of flow cytometry to evaluate temporal changes in inflammation*. Brain Res, 2002. **932**: p. 110-119.
517. Meller, R., et al., *Neuroprotection by Osteopontin in Stroke*. J Cereb. Blood Flow & Metab, 2005. **25**: p. 217-225.
518. Offner, H., et al., *Experimental stroke induces massive, rapid activation of the peripheral immune system*. J Cereb Blood Flow Metab, 2006. **26**(5): p. 654-65.

519. Ferrarese, C., et al., *Increased cytokine release from peripheral blood cells after acute stroke*. J Cereb Blood Flow Metab, 1999. **19**(9): p. 1004-9.
520. Genin, P., et al., *Regulation of RANTES chemokine gene expression requires cooperativity between NF-kappa B and IFN-regulatory factor transcription factors*. J Immunol, 2000. **164**(10): p. 5352-61.
521. Hatada, E.N., M. Naumann, and C. Scheidereit, *Common structural constituents confer I kappa B activity to NF-kappa B p105 and I kappa B/MAD-3*. Embo J, 1993. **12**(7): p. 2781-8.
522. Nijboer, C.H., et al., *Strong neuroprotection by inhibition of NF-kappaB after neonatal hypoxia-ischemia involves apoptotic mechanisms but is independent of cytokines*. Stroke, 2008. **39**(7): p. 2129-37.
523. Nijboer, C.H., et al., *Alternate pathways preserve tumor necrosis factor-alpha production after nuclear factor-kappaB inhibition in neonatal cerebral hypoxia-ischemia*. Stroke, 2009. **40**(10): p. 3362-8.
524. Harari, O.A. and J.K. Liao, *NF-kappaB and innate immunity in ischemic stroke*. Ann N Y Acad Sci. **1207**: p. 32-40.
525. Bhakar, A.L., et al., *Constitutive nuclear factor-kappa B activity is required for central neuron survival*. J Neurosci, 2002. **22**(19): p. 8466-75.
526. Dvorianchikova, G., et al., *Inactivation of astroglial NF-kappa B promotes survival of retinal neurons following ischemic injury*. Eur J Neurosci, 2009. **30**(2): p. 175-85.
527. Ceulemans, A.G., et al., *The dual role of the neuroinflammatory response after ischemic stroke: modulatory effects of hypothermia*. J Neuroinflammation. **7**: p. 74.

528. Suzuki, S., K. Tanaka, and N. Suzuki, *Ambivalent aspects of interleukin-6 in cerebral ischemia: inflammatory versus neurotrophic aspects*. J Cereb Blood Flow Metab, 2009. **29**(3): p. 464-79.
529. Loddick, S.A., A.V. Turnbull, and N.J. Rothwell, *Cerebral interleukin-6 is neuroprotective during permanent focal cerebral ischemia in the rat*. J Cereb Blood Flow Metab, 1998. **18**(2): p. 176-9.
530. Rothwell, N., *Interleukin-1 and neuronal injury: mechanisms, modification, and therapeutic potential*. Brain Behav Immun, 2003. **17**(3): p. 152-7.
531. Bartee, E., M.R. Mohamed, and G. McFadden, *Tumor necrosis factor and interferon: cytokines in harmony*. Curr Opin Microbiol, 2008. **11**(4): p. 378-83.
532. Nayak, A.R., et al., *Evaluation of the inflammatory response in sera from acute ischemic stroke patients by measurement of IL-2 and IL-10*. Inflamm Res, 2009. **58**(10): p. 687-91.
533. Gros, E. and N. Novak, *Cutaneous dendritic cells in allergic inflammation*. Clin Exp Allergy, 2012. **42**(8): p. 1161-75.
534. Shinoda, S., et al., *Bim regulation may determine hippocampal vulnerability after injurious seizures and in temporal lobe epilepsy*. J Clin Invest, 2004. **113**(7): p. 1059-68.
535. Elkins, K.L., et al., *Bacterial DNA containing CpG motifs stimulates lymphocyte-dependent protection of mice against lethal infection with intracellular bacteria*. J Immunol, 1999. **162**(4): p. 2291-8.
536. Jhaveri, K.A., et al., *Reduced basal and lipopolysaccharide-stimulated adenosine A1 receptor expression in the brain of nuclear factor-kappaB p50^{-/-} mice*. Neuroscience, 2007. **146**(1): p. 415-26.

537. Bischofberger, N., K.A. Jacobson, and D.K. von Lubitz, *Adenosine A1 receptor agonists as clinically viable agents for treatment of ischemic brain disorders*. Ann N Y Acad Sci, 1997. **825**: p. 23-9.
538. von Lubitz, D.K., et al., *Cyclohexyl adenosine protects against neuronal death following ischemia in the CA1 region of gerbil hippocampus*. Stroke, 1988. **19**(9): p. 1133-9.
539. Rudolphi, K.A., M. Keil, and H.J. Hinze, *Effect of theophylline on ischemically induced hippocampal damage in Mongolian gerbils: a behavioral and histopathological study*. J Cereb Blood Flow Metab, 1987. **7**(1): p. 74-81.
540. Tureyen, K., et al., *Exacerbated brain damage, edema and inflammation in type-2 diabetic mice subjected to focal ischemia*. J Neurochem, 2011. **116**(4): p. 499-507.
541. Ritter, L., et al., *Exaggerated neutrophil-mediated reperfusion injury after ischemic stroke in a rodent model of type 2 diabetes*. Microcirculation, 2011. **18**(7): p. 552-61.
542. Ritter, L.S., et al., *Leukocyte accumulation and hemodynamic changes in the cerebral microcirculation during early reperfusion after stroke*. Stroke, 2000. **31**(5): p. 1153-61.
543. Hartmann, G. and A.M. Krieg, *Mechanism and function of a newly identified CpG DNA motif in human primary B cells*. J Immunol, 2000. **164**(2): p. 944-53.
544. Verthelyi, D., et al., *Human peripheral blood cells differentially recognize and respond to two distinct CPG motifs*. J Immunol, 2001. **166**(4): p. 2372-7.
545. Blaeser, A., K. McGlauchlen, and L.A. Vogel, *Aged B lymphocytes retain their ability to express surface markers but are dysfunctional in their proliferative capability during early activation events*. Immun Ageing, 2008. **5**: p. 15.

546. CDC, *Prevalence and most common causes on disability among adults - United States, 2005*. MMWR, 2009. **58**: p. 421-426.
547. De Haan, R., et al., *A comparison of five stroke scales with measures of disability, handicap, and quality of life*. Stroke, 1993. **24**(8): p. 1178-81.
548. Cheung, V.H., L. Gray, and M. Karunanithi, *Review of accelerometry for determining daily activity among elderly patients*. Arch Phys Med Rehabil, 2011. **92**(6): p. 998-1014.
549. Gebruers, N., et al., *Monitoring of physical activity after stroke: a systematic review of accelerometry-based measures*. Arch Phys Med Rehabil, 2010. **91**(2): p. 288-97.
550. Haley, G.E., et al., *Circadian activity associated with spatial learning and memory in aging rhesus monkeys*. Exp Neurol, 2009. **217**(1): p. 55-62.
551. Mann, T.M., et al., *A novel method for activity monitoring in small non-human primates*. Lab Anim, 2005. **39**(2): p. 169-77.
552. Papailiou, A., E. Sullivan, and J.L. Cameron, *Behaviors in rhesus monkeys (Macaca mulatta) associated with activity counts measured by accelerometer*. Am J Primatol, 2008. **70**(2): p. 185-90.
553. Urbanski, H.F., *Circadian variation in the physiology and behavior of humans and non-human primates*, in *Animal Models of Behavior Analysis*, J. Raber, Editor. 2011, Springer: New York. p. 217-235.
554. Masuda, K. and I.V. Zhdanova, *Intrinsic activity rhythms in Macaca mulatta: their entrainment to light and melatonin*. J Biol Rhythms, 2010. **25**(5): p. 361-71.
555. Williams, L. and I. Bernstein, *Non-human primates in biomedical research: Biology and management*. 1995, San Diego: Academic Press.

556. Gebruers, N., et al., *Is activity loss predictive for development of upper limb oedema after stroke?* J Rehabil Med, 2011. **43**(5): p. 398-403.
557. Yoneyama, K., et al., *Effects of indeloxazine hydrochloride on activities of daily living in cerebrovascular disease: Evaluation by accelerometer.* Current Therapeutic Research 1993. **54**: p. 413-419.
558. Reiterer, V., et al., *Actigraphy--a useful tool for motor activity monitoring in stroke patients.* Eur Neurol, 2008. **60**(6): p. 285-91.
559. Sullivan, E.L., F.H. Koegler, and J.L. Cameron, *Energy expenditure resulting from physical activity is similar in femal rhesus monkeys (Macaca mulatta) house as a group in pens vs. single cages.*, in *Proceedings of the 28th Annual Meeting of the American Society of Primatologists.* 2005: Seattle, WA.
560. Baecke, J.A., W.A. van Staveren, and J. Burema, *Food consumption, habitual physical activity, and body fatness in young Dutch adults.* Am J Clin Nutr, 1983. **37**(2): p. 278-86.
561. Levin, B.E., *Spontaneous motor activity during the development and maintenance of diet-induced obesity in the rat.* Physiol Behav, 1991. **50**(3): p. 573-81.
562. Sullivan, E.L., F.H. Koegler, and J.L. Cameron, *Individual differences in physical activity are closely associated with changes in body weight in adult female rhesus monkeys (Macaca mulatta).* Am J Physiol Regul Integr Comp Physiol, 2006. **291**(3): p. R633-42.
563. Mehlman, P.T., et al., *CSF 5-HIAA and nighttime activity in free-ranging primates.* Neuropsychopharmacology, 2000. **22**(2): p. 210-8.
564. Cohen-Zion, M. and S. Ancoli-Israel, *Sleep in children with attention-deficit hyperactivity disorder (ADHD): a review of naturalistic and stimulant intervention studies.* Sleep Med Rev, 2004. **8**(5): p. 379-402.

565. Rowland, T.W., *The biological basis of physical activity*. Med Sci Sports Exerc, 1998. **30**(3): p. 392-9.
566. Wade, G.N., *Gonadal hormones and behavioral regulation of body weight*. Physiol Behav, 1972. **8**(3): p. 523-34.
567. Kiwaki, K., et al., *Orexin A (hypocretin 1) injected into hypothalamic paraventricular nucleus and spontaneous physical activity in rats*. Am J Physiol Endocrinol Metab, 2004. **286**(4): p. E551-9.
568. Verheyden, G., et al., *Clinical tools to measure trunk performance after stroke: a systematic review of the literature*. Clin Rehabil, 2007. **21**(5): p. 387-94.
569. Magalhaes, I., et al., *High content cellular immune profiling reveals differences between rhesus monkeys and men*. Immunology, 2010. **131**(1): p. 128-40.
570. Chamorro, A., X. Urra, and A.M. Planas, *Infection after acute ischemic stroke: a manifestation of brain-induced immunodepression*. Stroke, 2007. **38**(3): p. 1097-103.
571. Felten, D.L., et al., *Noradrenergic and peptidergic innervation of lymphoid tissue*. J Immunol, 1985. **135**(2 Suppl): p. 755s-765s.
572. Bellavance, M.A. and S. Rivest, *The neuroendocrine control of the innate immune system in health and brain diseases*. Immunol Rev, 2012. **248**(1): p. 36-55.
573. Webster, J.I., L. Tonelli, and E.M. Sternberg, *Neuroendocrine regulation of immunity*. Annu Rev Immunol, 2002. **20**: p. 125-63.
574. Prass, K., et al., *Stroke-induced immunodeficiency promotes spontaneous bacterial infections and is mediated by sympathetic activation reversal by poststroke T helper cell type 1-like immunostimulation*. J Exp Med, 2003. **198**(5): p. 725-36.

575. Czlonkowska, A., B. Cyrta, and J. Korlak, *Immunological observations on patients with acute cerebral vascular disease*. J Neurol Sci, 1979. **43**(3): p. 455-64.
576. Vogelgesang, A., et al., *Functional status of peripheral blood T-cells in ischemic stroke patients*. PLoS One, 2010. **5**(1): p. e8718.
577. Emsley, H.C., et al., *An early and sustained peripheral inflammatory response in acute ischaemic stroke: relationships with infection and atherosclerosis*. J Neuroimmunol, 2003. **139**(1-2): p. 93-101.
578. Emsley, H.C., C.J. Smith, and S.J. Hopkins, *Infection and brain-induced immunodepression after acute ischemic stroke*. Stroke, 2008. **39**(1): p. e7; author reply e8.
579. Urra, X., et al., *Harms and benefits of lymphocyte subpopulations in patients with acute stroke*. Neuroscience, 2009. **158**(3): p. 1174-83.
580. Chen, H., et al., *Changes in humoral immunological function and their clinical significance in patients with cerebral hemorrhage*. Zhongguo Wei Zhong Bing Ji Jiu Yi Xue, 2005. **17**(3): p. 177-9.
581. Segel, G.B., M.W. Halterman, and M.A. Lichtman, *The paradox of the neutrophil's role in tissue injury*. J Leukoc Biol. **89**(3): p. 359-72.
582. Schurer, L., et al., *Leucocyte depletion does not affect post-ischaemic nerve cell damage in the rat*. Acta Neurochir (Wien), 1991. **111**(1-2): p. 54-60.
583. Strecker, J.K., et al., *Effects of G-CSF treatment on neutrophil mobilization and neurological outcome after transient focal ischemia*. Exp Neurol, 2010. **222**(1): p. 108-13.
584. Schabitz, W.R., et al., *AXIS: a trial of intravenous granulocyte colony-stimulating factor in acute ischemic stroke*. Stroke, 2010. **41**(11): p. 2545-51.

585. Urra, X., et al., *Monocytes are major players in the prognosis and risk of infection after acute stroke*. *Stroke*, 2009. **40**(4): p. 1262-8.
586. Yang, Q.W., et al., *Upregulated expression of toll-like receptor 4 in monocytes correlates with severity of acute cerebral infarction*. *J Cereb Blood Flow Metab*, 2008. **28**(9): p. 1588-96.
587. Yan, J., et al., *Immune activation in the peripheral blood of patients with acute ischemic stroke*. *J Neuroimmunol*, 2009. **206**(1-2): p. 112-7.
588. Tarkowski, E., P. Ekelund, and A. Tarkowski, *Increased systemic T-lymphocyte reactivity in patients with established stroke*. *J Clin Lab Immunol*, 1991. **35**(4): p. 171-6.
589. Tarkowski, E., et al., *Lateralization of T-lymphocyte responses in patients with stroke. Effect of sympathetic dysfunction?* *Stroke*, 1995. **26**(1): p. 57-62.

APPENDIX

APPENDIX A

Studies exploring the role of the non-canonical NFκB1 (p105/p50) signaling pathway in lipopolysaccharide-mediated ischemic tolerance in the brain.

Data presented in Appendix A contains material modified from the original paper “LPS preconditioning redirects TLR signaling following stroke: TRIF-IRF3 plays a seminal role in mediating tolerance to ischemic injury”, by Vartanian KB, Stevens SL, Marsh BJ, **Williams-Karnesky RL**, Lessov NS and Stenzel-Poore MP, published in the *Journal of Neuroinflammation* October 14th, 2011 [508].

Background

Emerging evidence suggests that TLR-induced neuroprotection occurs by reprogramming the genomic response to the danger associated molecular patterns (DAMPs), which are produced in response to ischemic injury. In this reprogrammed state, the resultant pathway activation of TLR4 signaling preferentially leads to IRF-mediated gene expression [309, 509]. However, whether TLR preconditioning affects NFκB activity and pro-inflammatory signaling is unknown.

The nuclear factor kappa B (NFκB) proteins are a family of transcriptional regulators, including: RelA (p65), NFκB1 (p105/p50), NFκB2 (p100/p52), RelB and c-Rel. These subunits exist either as heterodimers or homodimers, though p65, RelB and c-Rel are the only NFκB proteins which contain a transactivation domain [510]. In their inactive state, NFκB dimers are sequestered in the cytosol of the cell bound to an inhibitor kappa B (IκB) protein. When activated by I Kappa B kinase (IKK), which phosphorylates IκB and targets it for degradation in the proteasome, a DNA binding domain is exposed on the NFκB dimer causing it to translocate to the nucleus. In the nucleus, the NFκB dimer binds DNA and acts as either an activator or inhibitor of gene transcription, depending on its component subunits. NFκB proteins have been shown to be activated via inflammatory signaling through the toll-like and other receptors [511].

Members of the NFκB family of proteins have been shown to play a central role in toll-like receptor-mediated ischemic preconditioning [508]. The emphasis in preconditioning research to date has been on the role of transcriptionally active

members of the NFκB family of proteins, including NFκB p65/p65 homodimers and p50/p65 heterodimers. Consequently, little is known about the potential role inhibitory NFκB proteins, such as p105 and p50/p50 homodimers, play in ischemic preconditioning. Past work has shown that NFκB levels of p50/50 homodimers are increased in LPS tolerant cells, and are specifically increased in the nuclei of these cells [512]. Research has shown that these NFκB p50 homodimers may bind to DNA and block expression of the TNF-α gene [512]. TNF-α is required for endotoxin tolerance and ischemic preconditioning [182]. Finally, macrophages from NFκB p50 -/- mice do not become tolerant to LPS. In 1992, Hatada et al demonstrated that NFκB p105 binds NFκB p65 in an IκB-like fashion. By binding NFκB p65, NFκB p105 prevents its nuclear translocation and binding of DNA [513]. This could serve to limit the transcription of pro-inflammatory genes mediated by NFκB p65.

Further, the role of the anti-inflammatory cytokine IL-10 in ischemic tolerance is unclear. In endotoxin tolerance, IL-10 has been shown to induce nuclear translocation of NFκB p50, induce binding of p50/50 homodimers to DNA, and inhibit binding of p65/50 heterodimers to DNA [514]. IL-10 acts through Bcl-3, which stabilizes NFκB p50/50, increased that half life of NFκB p50, and increases NFκB p50/50 targeting to the nucleus [515]. Carmody et al have also shown that Bcl-3 -/- mice and macrophages do not become LPS tolerant. Data from cytokine assays show an increase in IL-10 following LPS administration in the serum of animals undergoing preconditioning [508]. RNA microarray data also shows changed in expression of Bcl-3 following stroke in the blood and brain tissue of LPS preconditioned animals (Stenzel-Poore lab, unpublished data).

Thus, the following studies sought to build a better understanding of the non-canonical NF κ B1 (p105/p50) pathway using lipopolysaccharide (LPS)-mediated ischemic tolerance in the brain.

Materials and Methods

Animals

C57BL/6 mice (male, 8-12 weeks) were purchased from Jackson Laboratories (West Sacramento, CA). All mice were housed in an American Association for Laboratory Animal Care-approved facility. Procedures were conducted according to Oregon Health & Science University, Institutional Animal Care and Use Committee, and National Institutes of Health guidelines.

Middle Cerebral Artery Occlusion (MCAO)

Mice were preconditioned with LPS (0.2-0.8 mg/kg, *Escherichia coli* serotype 0111:B4; Sigma) or saline 72 hr prior to MCAO. Mice were anesthetized with isoflurane (1.5-2%) and subjected to MCAO using the monofilament suture method described previously [516]. Briefly, a silicone-coated 7-0 monofilament nylon surgical suture was threaded through the external carotid artery to the internal carotid artery to block the middle cerebral artery, and maintained intraluminally for 40 to 60 min. The suture was then removed to restore blood flow. Cerebral blood flow (CBF) was monitored

throughout surgery by laser doppler flowmetry. Any mouse that did not maintain a CBF during occlusion of <25% of baseline was excluded from the study. Body temperature was monitored and maintained at 37°C with a thermostat-controlled heating pad. Infarct measurements were made using TTC staining of 1 mm coronal brain sections.

Western Blot

Protein extraction was performed as described previously [517] with some modifications. Briefly, tissue samples were dissected from the ipsilateral cortex and lysed in a buffer containing a protease inhibitor cocktail (Roche). Protein concentrations were determined using the BCA method (Pierce-Endogen). Protein samples (50 µg) were denatured in a gel-loading buffer (Bio-Rad Laboratories) at 100°C for 5 min and then loaded onto 12% Bis-Tris polyacrylamide gels (Bio-Rad Laboratories). Following electrophoresis, proteins were transferred to polyvinylodene difluoride membranes (Bio-Rad Laboratories) and incubated with primary antibodies for Ship-1 (Santa Cruz, sc8425), Tollip (AbCam, Ab37155), p105 (Santa Cruz, sc7178), or β-Actin (Santa Cruz, sc1616R) at 4°C overnight. Membranes were then incubated with horseradish peroxidase conjugated anti-rabbit, anti-goat, or anti-mouse antibody (Santa Cruz Biotechnology) and detected by chemiluminescence (NEN Life Science Products) and exposure to Kodak film (Biomax). Images were captured using an Epson scanner and the

densitometry of the gel bands, including β -Actin loading control, was analyzed using ImageJ.

Cytokine Analysis

Heparinized blood was collected 72 hr post injection and 3 or 24 hr post MCAO and centrifuged at 5000xg for 20 min. The plasma layer was collected and stored at -80°C. Cytokine/chemokine analysis for IL1 β , IL1 α , MIP-1 α , MCP-1, RANTES, and IL-10 was performed using a multiplex ELISA (Quansys). An IFN β ELISA (PBL Interferon Source) was used to measure plasma levels of IFN β .

Electrophoretic Mobility Shift Assay

Nuclear protein extracts were prepared from tissue dissected from the ipsilateral cortex. Homogenized tissue was incubated in Buffer A (10mM HEPES-KOH pH7.9, 60mM KCl, 1mM EDTA, 1mM DTT, 1mM PMSF) for 5 min on ice, centrifuged at 3000 rpm for 5 min at 4°C. The supernatant was saved and stored as cytoplasmic extract. The pellets were washed in Buffer B (10mM HEPES-KOH pH7.9, 60mM KCl, 1mM EDTA, 0.5% NP-40, 1mM DTT, 1mM PMSF), resuspended in Buffer C (250mM Tris pH7.8, 60mM KCl, 1mM DTT, 1mM PMSF), and freeze-thawed 3 times in liquid nitrogen. All buffers contained a protease inhibitor cocktail (Roche). After centrifuging at 10,000 rpm for 10 min at 4°C, the supernatant was stored as nuclear extract at -80°C. Nuclear protein concentrations were determined using the BCA method (Pierce-Endogen). Electrophoretic mobility shift

assays were performed using the Promega Gel Shift Assay System according to the manufacturer's instructions. Briefly, 15 µg of nuclear protein was incubated with ³²P-labeled NFκB consensus oligonucleotide (Promega), either with or without unlabeled competitor oligonucleotide, unlabeled noncompetitor oligonucleotide, or anti-p65 antibody (Santa Cruz). Samples were electrophoresed on a 4% acrylamide gel, dried and exposed to phosphorimager overnight. The densitometry of the gel bands was analyzed using scanning integrated optical density software (ImageJ).

Statistical Analysis

Data is represented as mean ± SEM. The n for each experiment is greater than or equal to 3, as specified in each figure. Statistical analysis was performed using GraphPad Prism5 software. Two-way ANOVA with Bonferroni post hoc test and Student's T-test were utilized as specified. Significance was determined as p<0.05.

Results

Blood cytokine/chemokine levels in the blood

Evidence indicates that stroke alters the cytokine profile in the plasma [518, 519]. To determine whether LPS preconditioning changes the balance of pro- and anti-inflammatory cytokines and chemokines in the plasma we examined the levels of seven inflammatory molecules using ELISAs. The results indicate that the level of pro-

inflammatory cytokines, such as IL-6, IL1 β , and MCP-1, are increased in both LPS and saline preconditioned mice (**Figure 37**). The inflammatory cytokines MIP-1 α and IL1 β were not detected in the serum (data not shown). The anti-inflammatory cytokine IL-10 was significantly increased only in the plasma of LPS preconditioned mice and was undetectable in saline preconditioned mice (**Figure 37**). RANTES, which is a chemokine associated with IRF3 and IRF7 activity [520], was present in the blood of LPS-preconditioned mice at significantly greater levels than saline preconditioned mice (**Figure 37**). IFN β was not detectable in the blood of LPS or saline preconditioned animals following stroke (data not shown).

NF κ B activity is suppressed in the brains of LPS-preconditioned animals 24 hr post MCAO

NF κ B activity is associated with damage and inflammation in the brain that occurs in response to stroke. We used EMSA to evaluate the activity of the NF κ B subunit p65 in the brain following stroke. The results indicated that LPS and saline preconditioned mice have comparable NF κ B activity at 3 hr post MCAO (**Figure 38 A**). However, at 24 hr post MCAO, LPS-preconditioned animals have significantly suppressed NF κ B activity compared to saline preconditioned mice (**Figure 38 A**).

Ship1 and Tollip are cytosolic molecules that inhibit TLR signaling, which leads to the suppression of NF κ B activity. We found that Ship1 and Tollip mRNA and protein are significantly enhanced in the brain of LPS-preconditioned mice compared to saline at 24 hr post MCAO (**Figure 38 B & C**). Additionally, the p50 precursor protein p105, which

inhibits NFκB activity by acting like an IκB molecule by sequestering NFκB in the cytosol [513, 521], was significantly upregulated 24 hr post stroke in LPS preconditioned mice compared to saline (**Figure 38 D**). Thus, despite the upregulation of inflammatory genes, the activity of NFκB is suppressed in the late-phase of the neuroprotective response of LPS-preconditioned mice.

Conclusions

These results demonstrate that NFκB activity is suppressed and that the cytosolic inhibitors of NFκB, Ship1, Tollip, and p105 are present 24 hr post MCAO although pro-inflammatory gene expression is unaffected (diagrammed in **Figure 39**). Interestingly, there is evidence that suppression of NFκB can promote protection against cerebral ischemia without influencing pro-inflammatory cytokine production [522, 523]. In particular, administration of the NFκB inhibitor Tat-Nemo provided protection against hypoxia-ischemia in neonatal rats without affecting TNF-α or IL1β production [522]. Furthermore, TLR4 deficient mice have smaller infarcts in response to MCAO, yet the production of TNF-α and IL1β was unaffected [175]. This suggests that reduced ischemic injury can be achieved in the presence of pro-inflammatory cytokines and that TLR4 signaling is not the sole source of these pro-inflammatory cytokines in response to ischemic injury.

NFκB is the major mediator of inflammatory gene expression. While NFκB is known to be induced acutely in response to ischemic injury, investigation into the role

of NF κ B activity has revealed conflicting results [524]. For instance, NF κ B is constitutively active in neurons, a requirement for their survival, while the surrounding glial cells have inducible NF κ B activity [525]. In response to ischemic challenge, NF κ B activity in astrocytes is responsible for detrimental inflammation [526]. This concept of pleotropic roles also applies to many of the inflammatory genes expressed in the brain in the setting of stroke [527, 528]. For example, intracerebroventricular injection of recombinant IL-6 significantly decreased the infarct size in rats 24 hr post MCAO [529]. IL-1 β is a potent inducer of IL-1 receptor antagonist (IL-1rn), which significantly reduces damage in response to stroke [530] and, notably, is also upregulated in microarray data (not shown). TNF- α is considered to play multiple roles in stroke injury mediating many neuroprotective and injurious effects [527]. Furthermore, in response to viral challenge, the simultaneous presence of inflammatory cytokines, such as TNF- α , and type I IFNs can alter their effects and synergize to promote a more protective state [531]. Thus, alterations in the environment in which NF κ B is activated and inflammatory genes are present may affect the roles pro-inflammatory mediators play in injury and may even contribute to the protective phenotype.

Overall, inflammatory cytokine protein levels were similarly induced in LPS and saline preconditioned mice following stroke. However, we have previously published that TNF- α is significantly reduced in the plasma of LPS-preconditioned mice following MCAO [182]. The anti-inflammatory and type I IFN-induced cytokines and chemokines measured in the blood were enhanced in LPS preconditioned mice compared to saline. In particular, IL-10 was significantly upregulated in the blood following MCAO in LPS

preconditioned mice. Importantly, in humans, upregulation of IL-10 in the blood has been correlated with improved outcome in stroke [532]. While IL-10 mRNA was not detectable in the brain (data not shown), IL-10 can be induced by IRF3 activity and therefore is indicative of the same redirected response seen in the brain. The redirected signaling in the blood may stem from the brain's response to injury by leaking proteins into the peripheral circulation; however, this is not considered a major source of plasma cytokines at these early timepoints following stroke [519]. Alternately, because LPS administration occurs by a systemic route, target cells in the periphery may become tolerant to activation by the secondary stimuli resulting from ischemic injury. Although our data does not distinguish between these possibilities, it is clear that LPS preconditioning alters the response to injury in the brain and the blood in a manner that promotes a protective phenotype.

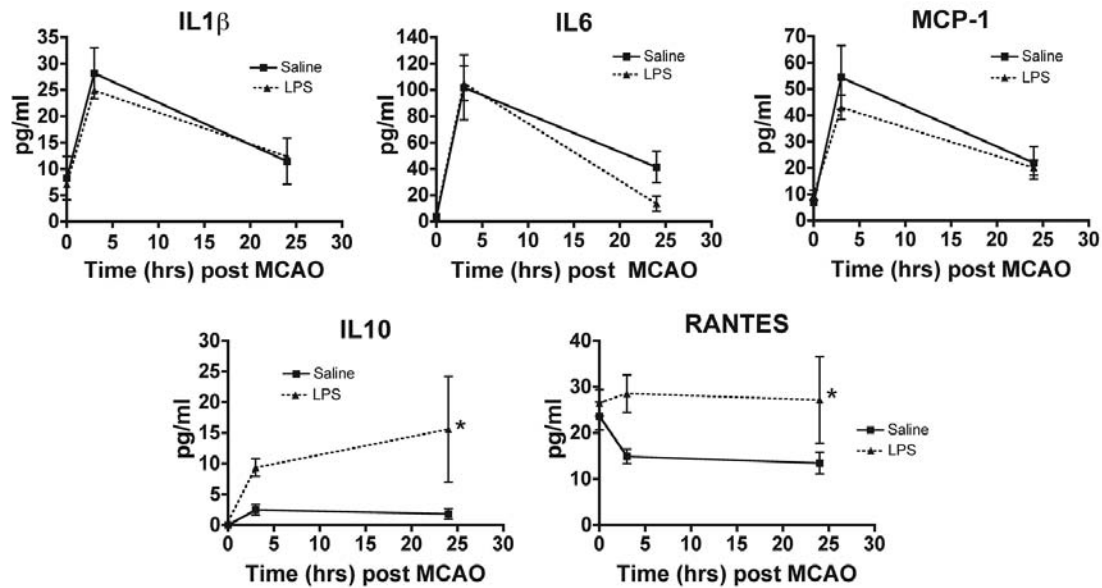


Figure 37. Blood cytokine/chemokine profile following *i.p.* LPS administration

Plasma collected from saline or LPS preconditioned mice at the time of or following MCAO was examined using a multikine ELISA (Quansys). Results indicated that pro-inflammatory cytokines IL-1 β , IL-6 and MCP-1 are similar in saline and LPS preconditioned mice. In contrast, LPS-preconditioned mice have significantly enhanced levels of the anti-inflammatory/type I IFN-associated cytokines and chemokines IL-10 and Rantes compared to saline following MCAO. Two-way ANOVA, * $p < 0.05$ LPS vs. Saline, $n \geq 4$ per treatment.

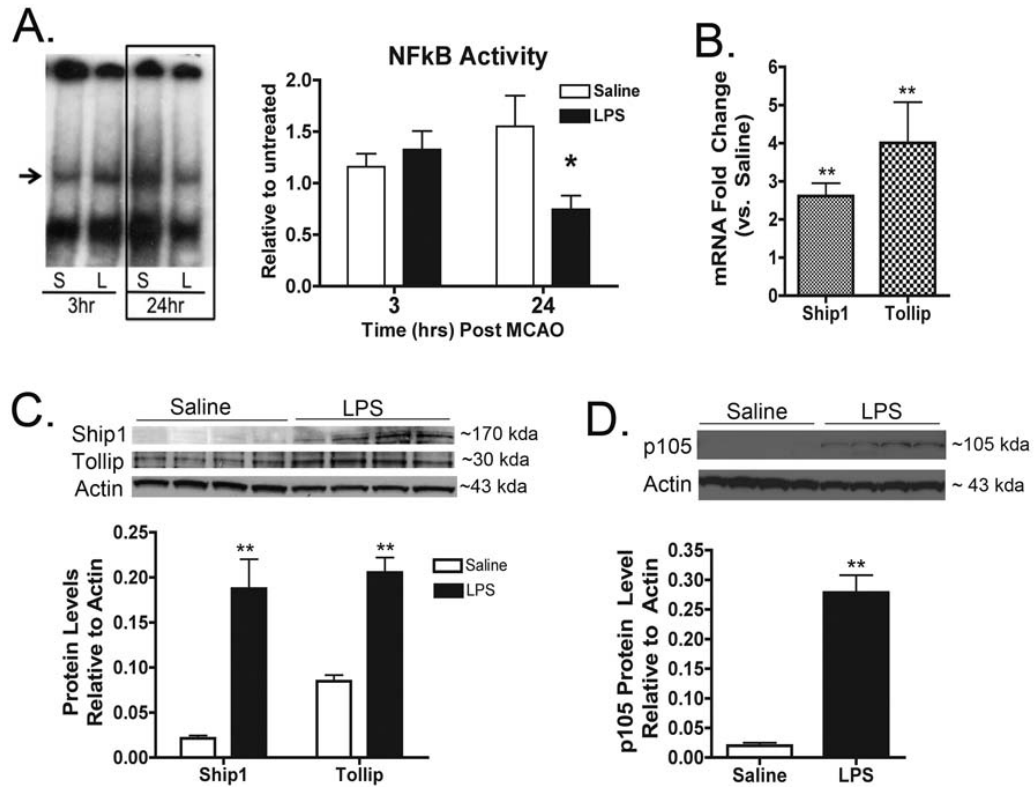


Figure 38. *NFκB Suppression following MCAO in LPS preconditioned animals*

(A) Nuclear protein obtained from ipsilateral cortices was used to measure p65 activity by EMSA analysis. EMSA gel of pooled samples (n=4) following MCAO for saline and LPS preconditioned mice (Left side). Quantification of band intensity of individual mice following MCAO (Right side). NFκB is significantly decreased in LPS preconditioned mice 24 hr post MCAO compared to saline. **(B)** Ship1 and Tollip mRNA are significantly upregulated 24 hr post MCAO in LPS-preconditioned mice compared to saline. **(C)** Western blot for Ship1 and Tollip and relative band quantification showing significant upregulation of Ship1 and Tollip protein 24 hr post MCAO in LPS-preconditioned mice, **(D)** Western blot and relative band quantification for p105, 24 hr post stroke show significant upregulation in LPS-preconditioned mice. Supershift assay confirmed specificity for p65 oligos (data not shown). **(A)** Two-Way ANOVA, Boneferroni Post Hoc, *p<0.05, n≥4 per treatment. **(B-D)** Student's T-test, vs. Saline, **p<0.01, n≥4 per treatment.

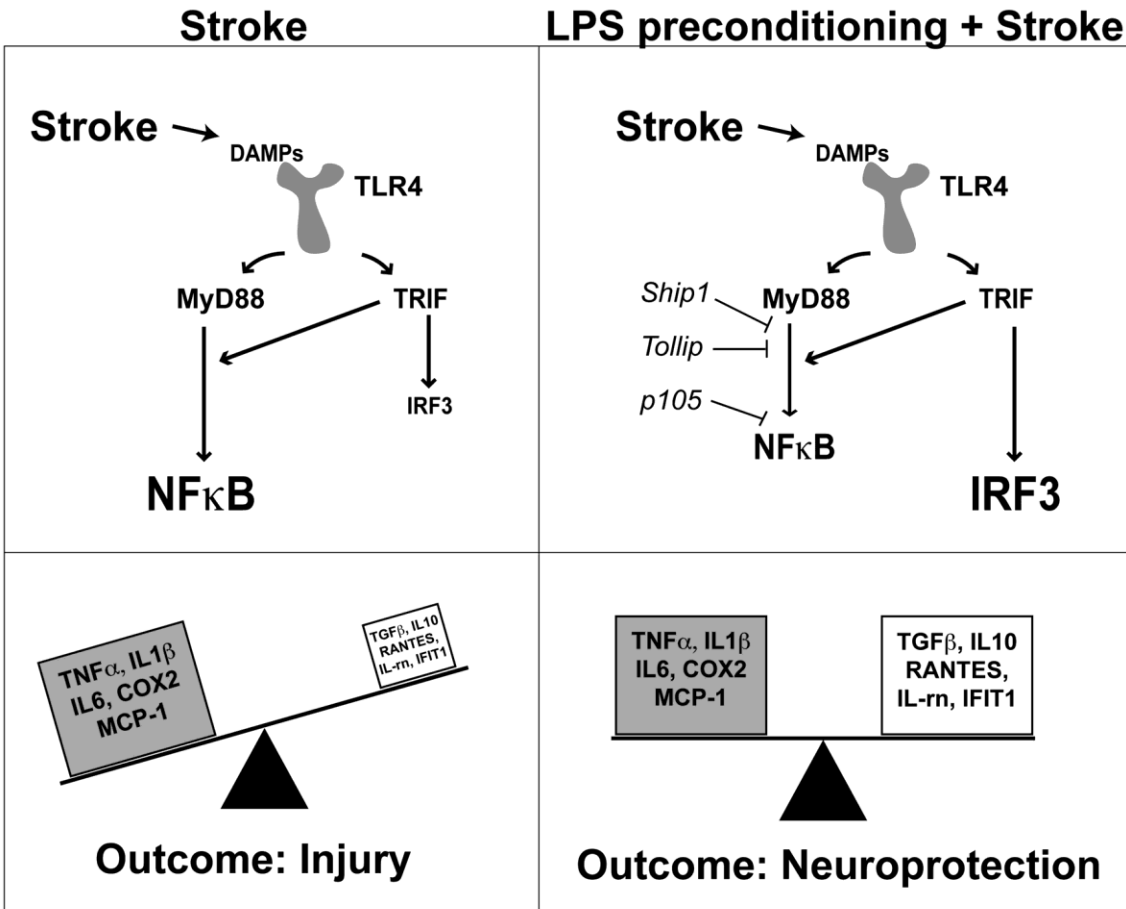


Figure 39. Reprogramming of TLR4 signaling and gene expression following stroke in LPS preconditioned animals

(Top row) TLR4 signaling cascades following stroke. In the absence of LPS preconditioning, stroke leads to NFκB activation without IRF3 activation. LPS-preconditioning prior to stroke leads to robust activation of IRF3 and suppressed NFκB activity compared to stroke alone. **(Bottom row)** Gene expression 24 hr post stroke. Stroke alone dramatically upregulates pro-inflammatory genes. LPS-preconditioning prior to stroke dramatically upregulates anti-inflammatory/Type I IFN genes, many of which are associated with IRF3, while still maintaining a pro-inflammatory response.

APPENDIX B

Studies on effectiveness of CpG ODNs via multiple routes of administration

Background

When designing therapeutics for translation to clinical use, it is highly desirable to be able to take advantage of multiple effective routes of administration. While intraperitoneal administration is feasible in rodents, it is less desirable in a clinical setting especially for a repeatedly administered compound. Here the efficacy of CPG preconditioning was assessed using two additional routes of administration: subcutaneous and intranasal. Reduction in infarct was then compared to traditional delivery of CpG ODNs via intraperitoneal administration.

Material and Methods

Animals

All animal procedures were conducted in a facility accredited by the Association for Assessment and Accreditation of Laboratory Animal Care (AAALAC) in accordance with protocols approved by the Legacy Institutional Animal Care and Use Committee (IACUC) and the principles outlined by the National Institute of Health (NIH). Male C57BL/6 wild-type (WT) mice (Charles River, Wilmington, MA, USA) weighing 25 to 30 g were housed under diurnal lighting conditions (12 h/12 h cycle).

Middle Cerebral Artery Occlusion (MCAO)

Mice were preconditioned with CpG ODNs 1826 (Invivogen) or saline 72 hr prior to MCAO as previously reported [190]. Mice were anesthetized with isoflurane (1.5-2%) and subjected to MCAO using the monofilament suture method described previously [516]. Briefly, a silicone-coated 7-0 monofilament nylon surgical suture was threaded through the external carotid artery to the internal carotid artery to block the middle cerebral artery, and maintained intraluminally for 60 min. The suture was then removed to restore blood flow. Cerebral blood flow (CBF) was monitored throughout surgery by laser doppler flowmetry. Any mouse that did not maintain a CBF during occlusion of <25% of baseline was excluded from the study. Body temperature was monitored and maintained at 37°C with a thermostat-controlled heating pad. Infarct measurements were made using TTC staining of 1 mm coronal brain sections.

Results

Administering CpG ODNs via the intraperitoneal, intranasal and subcutaneous routes results in approximately equivalent levels of protection to cerebral ischemia (**Figure 40**). Traditional administration of 20 μ g CpG ODNs via the intraperitoneal route resulted in a 65% percent reduction in infarct volume when compared to saline treated controls. Intranasal administration of a higher concentration (80 μ g) of CpG ODNs afforded slightly less protection, but was still highly significant, reduce infarct by 46%. Subcutaneous administration of CpG ODNs produced the most dramatic reduction in infarct volume (72%).

Conclusions

The ability of CpG ODNs to be administered via several routes increases their translational potential. Intranasal administration in particular would be highly desirable, as this could be an easily self-administered treatment on a regular basis by high risk patients (e.g. recent TIA). The increase in CpG ODN efficacy seen following subcutaneous administration may be explained by the large number of resident dendritic cells (DCs) in the skin [533]. These resident DCs may quickly sense, process, becoming activated by, and traffic CpG to lymph nodes, inducing a robust response in lymphocytes [463]. In other routes of administration, CpG ODNs must drain to the lymph node and then be sensed and presented by DCs. DCs are a key mediator of peripheral immune modulation via CpG ODNs [465], and subcutaneous administration

may increase the likelihood that these cells are able to “see” and respond to preconditioning CpG ODNs.

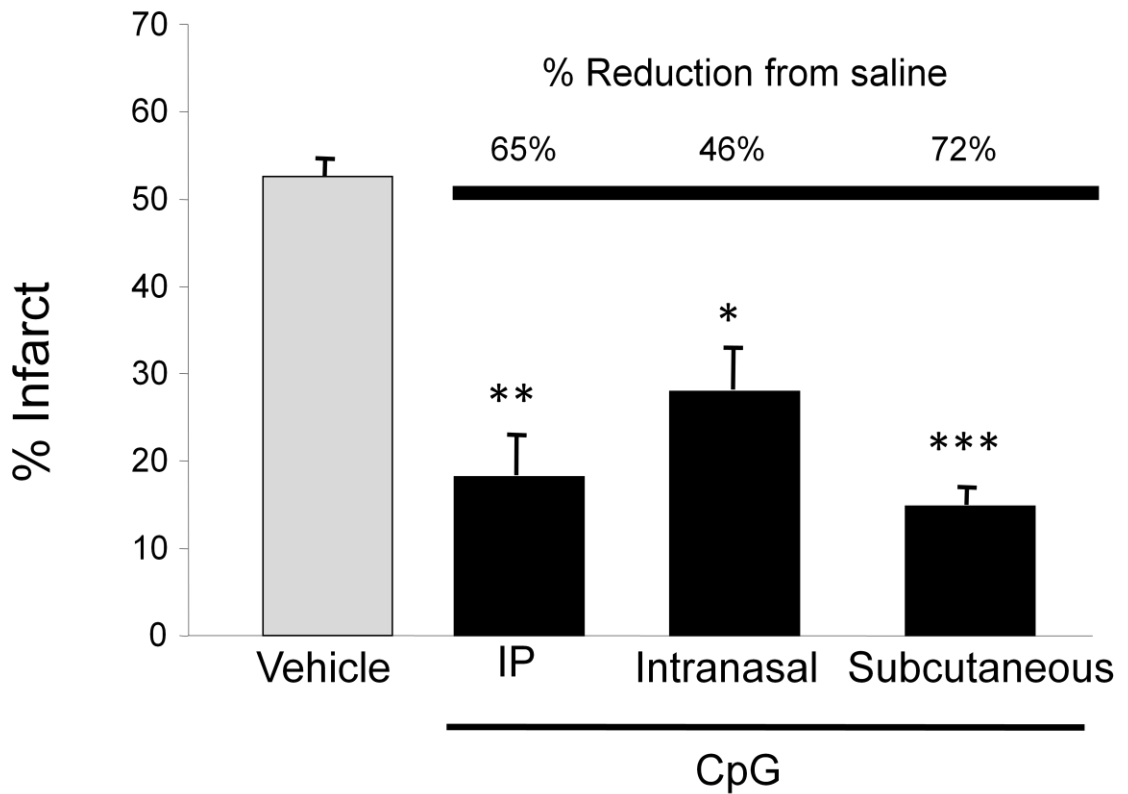


Figure 40. *Prophylactic CpG ODNs can induce neuroprotection via multiple routes of administration*

CpG ODN or saline control was administered via intranasal (80ug), intraperitoneal (i.p., 20ug), or subcutaneous (20ug) delivery 72 hours prior to 60 minutes of MCAO. Infarct was quantified after 24 hours of reperfusion. Values are displayed as means \pm SEM; (intranasal CpG n=8, i.p. CpG n=6, s.c. CpG n=8); * p< 0.05, **p<0.005, ***p<0.00001.

APPENDIX C

Studies of the effectiveness of CpG preconditioning in epilepsy and permanent MCAO

Background

Using multiple injury models when testing a novel neuroprotectant can be helpful for evaluating probable efficacy and translational potential, and can also give insight into the mechanism by which the therapeutic acts. For instance, the relative contribution of peripheral versus central mediators of damage and/or protection may be separable, and it may be possible to observe temporal dynamics in one system better than another. The need for testing of therapeutics in multiple injury models has been highlighted by the Stroke Therapy Academic Industry Roundtable [315], as part of the strategic approach to addressing the fact that many therapeutic prove efficacious in animals but do not translate successfully to clinical use.

CpG ODNs have been shown to provide robust protection from transient ischemic stroke in both rodent [190] and non-human primate models [191]. Here, the efficacy of CpG ODN-induced preconditioning was tested in a model of permanent ischemic stroke and a model of kainic acid-induced excitotoxic cell death.

Material and Methods

Animals

C57BL/6 mice (male, 8-12 weeks) were purchased from Jackson Laboratories (West Sacramento, CA). All mice were housed in an American Association for Laboratory Animal Care-approved facility. Procedures were conducted in an Association for the Assessment and Accreditation of Laboratory Animal Care accredited facility according to Institutional Animal Care and Use Committee, and National Institutes of Health guidelines.

Epileptogenesis model

Mice were preconditioned with CpG ODNs 1826 (20 μ g, Invivogen) or saline 72 hr prior to seizure induction as previously reported [190]. Seizures were induced in adult male wild-type mice weighing 25–30 g by unilateral stereotaxic microinjection of KA into the basolateral amygdala nucleus based on stereotaxic coordinates relative to bregma: AP, –0.94 mm; ML, –2.85 mm; and DV, –3.75 mm (AP, anterior- posterior; ML, medio-lateral; DV, dorso-ventral) as previously described [534]. Briefly, under anesthesia with 68.5% N₂O, 30% O₂, and 1.5% isoflurane, mice were affixed with 3 recording electrodes (Plastics One Inc.) and a 26-gauge steel guide cannula over the intact dura using dental cement. To perform the subsequent EEG recordings and drug injections in awake animals, the mice were placed into a plexiglass restrainer. Anesthesia was discontinued and EEG recordings commenced, and then a 31-gauge internal cannula was inserted into

the lumen of the guide to inject 0.3 µg KA in a volume of 0.2 µl PBS, pH 7.4, into the amygdala. The EEG was monitored for 30 min using a Nervus video-EEG recording device until lorazepam (6 mg/kg) was administered i.v. to terminate seizures. The EEG was further monitored for up to 30 min to ensure seizure cessation. An observer unaware of the experimental treatment performed quantification of EEG records, and the duration of type IV seizure activity was calculated.

Histology

Brains were collected 24 h following KA injection were immediately frozen in 2-methylbutane (−30°C) and sectioned at 12 µm on a cryostat. Coronal sections at the level of bregma −1.7 mm were air dried, postfixed in 10% formalin (15 min), washed twice in PBS, and then processed for histopathology (cresyl violet staining) or for detection of DNA fragmentation (TUNEL) as previously described [534].

Middle Cerebral Artery Occlusion (MCAO)

Mice were preconditioned with CpG ODNs 1826 (20µg, Invivogen) or saline 72 hr prior to MCAO as previously reported [190]. Mice were anesthetized with isoflurane (1.5-2%) and subjected to MCAO using the monofilament suture method described previously [516]. Briefly, a silicone-coated 7-0 monofilament nylon surgical suture was threaded through the external carotid artery to the internal carotid artery to block the middle cerebral artery and, in the case of permanent occlusion, secured via a suture

around the vessel. In the case of transient occlusion, the suture was withdrawn after 60 minutes. Cerebral blood flow (CBF) was monitored throughout surgery by laser doppler flowmetry. Any mouse that did not achieve a post-occlusion CBF of <25% of baseline was excluded from the study. Body temperature was monitored and maintained at 37°C with a thermostat-controlled heating pad. Infarct measurements were made using TTC staining of 1 mm coronal brain sections.

Results

Prophylactic administration of CpG ODNs does not protect against kainic acid induced injury in mice (**Figure 41**). Mice were given an i.p. injection of CpG ODNs prior to intra-amygdala injection of KA. KA induced seizures were stopped after 30 minute, and brains were collected 24 hours after. There was no difference in number of TUNEL positive cells in the hippocampal CA3 following intra-amygdala administration of KA.

Despite conferring robust neuroprotection in a transient MCAO (tMCAO) model, prophylactic CpG ODNs do not reduce infarct volume in a model of permanent MCAO (pMCAO) (**Figure 42**). Mice were given an i.p. dose of CpG ODNs prior to permanent unilateral MCAO. Following 24 hours of reperfusion, brains were collected and stained with TTC. No difference was seen between CpG-treated and non-CpG-treated pMCAO animals, while CpG-treated animals subjected to tMCAO had significantly reduced infarct volume when compared to their saline treated counterparts.

Conclusions

Comparing the effectiveness of potential neuroprotective compounds across multiple injury models can give insight into their mechanism of action. In the present study, prophylactic administration of CpG ODNs failed to afford protection in a model seizure induced damage in the hippocampus, and a model of permanent occlusive stroke. TLR-mediated preconditioning occurs via reprogramming the endogenous response to the danger-associated molecular patterns (DAMPs) released during ischemic injury away from release of pro-inflammatory cytokines towards release of anti-inflammatory cytokines [132, 136]. This switch appears to be mediated via TNF- α , in both LPS and CpG preconditioning in mice as TNF- α levels increase acutely following LPS or CpG administration and TNF- α deficient mice cannot be preconditioned with LPS or CpG ODNs [182, 190]. However, the blood levels of TNF- α seen after administration of CpG ODNs are nearly 100 fold lower than those seen following LPS administration (**Figure 43**). Further, humans and non-human primates do not secrete high levels of TNF- α following administration [463], but NHPs can be robustly protected from transient cerebral ischemia by CpG ODNs [191]. Thus, CpG and LPS may induce protection via slightly different mechanisms; because it induces such a large release of TNF- α , LPS might induce protection via TNF- α -mediated reprogramming of resident cells in the CNS, while CpG might induce more potent changes to peripheral immune cells, and may have a smaller effect on resident CNS cells.

Since the peripheral immune response is an important contributor to infarct volume after transient ischemia [26, 27], reprogramming of peripheral immune cells to an anti-inflammatory phenotype could significantly reduce damage following ischemic/reperfusion injury. CpG ODNs may act in just such a manner. By trafficking to draining lymph nodes, CpG ODNs could be sensed by dendritic cells (DCs), which could then activate passing immune cells. CpG ODNs have been shown to induce protection from otherwise lethal doses of bacteria in mice in a B-lymphocyte-dependent manner [535].

Indeed, CpG ODNs have been shown to induce B, T and Natural Killer cells to secrete cytokines more readily than LPS [464]. Further, CpG ODNs have been shown to induce DCs to establish unidirectional intracellular cross-talk to induce T cell responses [465]. In DCs this process occurs via a MyD88-dependent, c-Jun N-terminal kinase (JNK)-amplified mechanism, resulting in MyD88-dependent cytokine production [465]. This MyD88-dependent cytokine amplification may then be self-controlled through production of regulatory cytokines such as IL-10. Hence, when injury occurs after preconditioning with CpG ODNs, lymphocytes may be reprogrammed to produce anti-inflammatory cytokines. Thus, CpG ODNs may fail to offer protection in models of neurological injury where damage is less-dependent on extravasion of peripheral immune cells into the brain parenchyma, such as seizure or permanent occlusion [466].

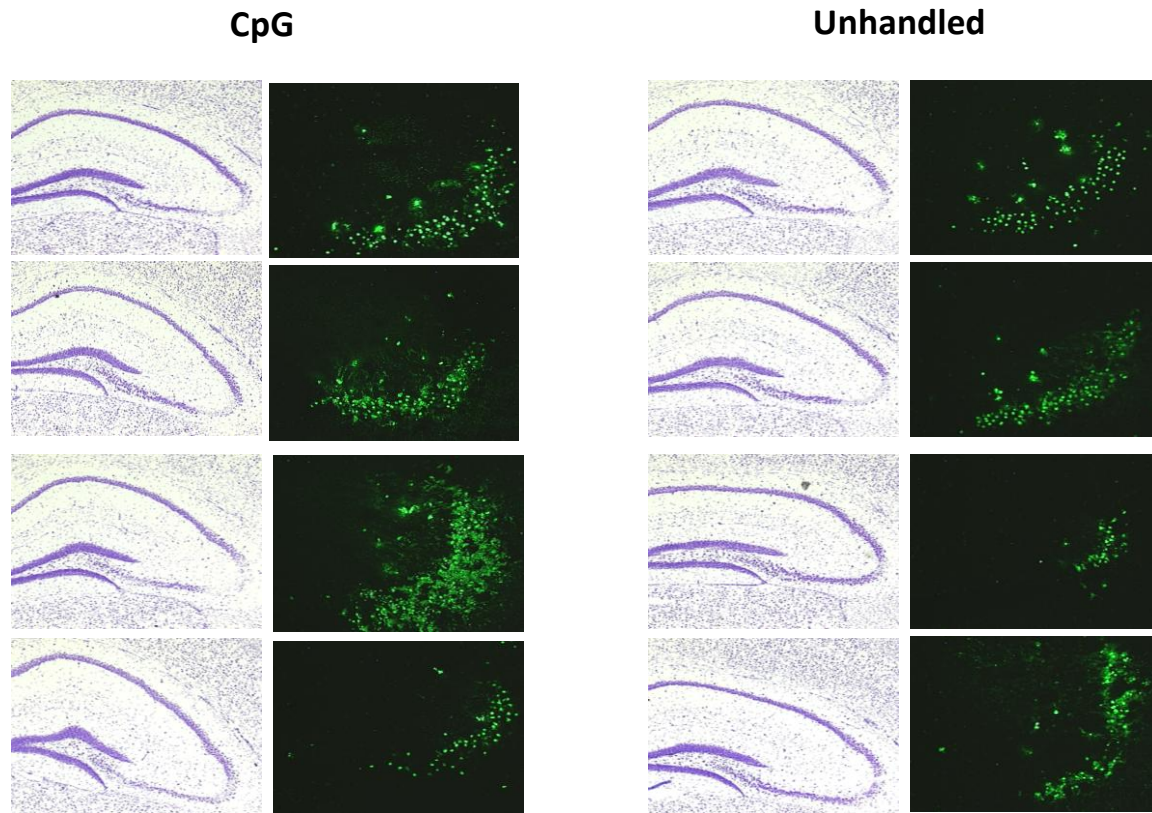


Figure 41. *CpG preconditioning does not protect in a KA-induced model of excitotoxic cell death*

Mice treated with CpG ODNs 72 hours prior to intra-amygdala kainic acid-induced seizure were not protected from injury when compared to saline treated controls. Representative Nissl and TUNEL staining from n=4 animals per group. Levels of cell death in the hippocampal CA3 were equivalent 24 hours after seizure cessation.

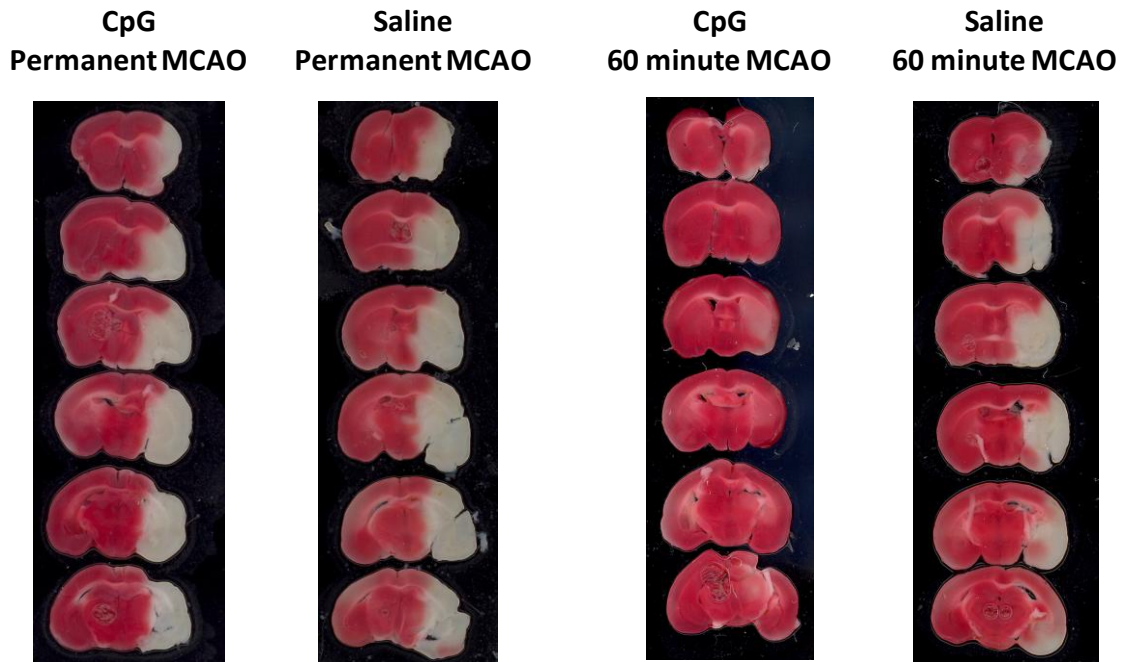


Figure 42. *CpG preconditioning does not reduce infarct volume in a model of permanent MCAO*

Pre-exposure to CpG ODNs 72 hours prior to permanent MCA occlusion did not reduce infarct volume in mice. Representative serial TTC stained coronal brain sections taken from four mice, left to right: CpG pMCAO, saline pMCAO, CpG tMCAO and saline tMCAO (n=1 per condition). Prophylactic CpG ODNs did protect in a parallel group of animals subjected to transient (60 minute) MCAO.

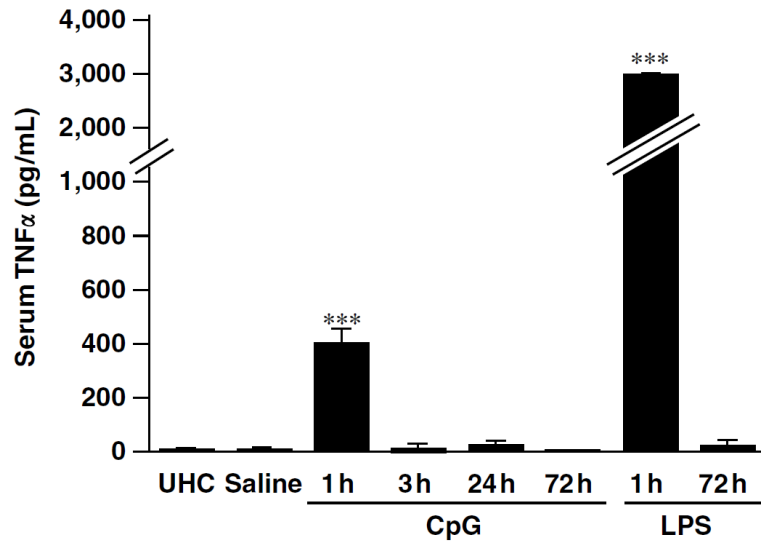


Figure 43. Levels of serum TNF- α increase acutely following administration of CpG ODNs or LPS

Serum TNF- α levels significantly increased 1 h after CpG treatment. Mice (n=4/time point) were administered CpG 1826 (20 mg, intraperitoneally) and blood was collected at 1, 3, 24, or 72 h after injection. Blood was allowed to clot for 2 h at room temperature and the serum was collected. Tumor necrosis factor α levels (pg/mL blood) were measured with a TNF- α ELISA (R&D Systems). Values denote group means \pm SEM.;

***P<0.001 by two-way ANOVA followed by Bonferroni's multiple comparison test. LPS (5 mg, intraperitoneally)-treated mice were included in the same experiment for comparison. Adapted from *Journal of Cerebral Blood Flow and Metabolism* 28(5), 2008 [190]. Susan L Stevens, Thomas M Ciesielski, Brenda J Marsh, Tao Yang, Delfina S Homen, Jo-lynn L Boule, Nicola S Lessov, Roger P Simon, Mary P Stenzel-Poore. "Toll-like receptor 9: A new target of ischemic preconditioning in the brain" pp. 1040-7.

APPENDIX D

Studies of the effectiveness of CpG preconditioning in ADK transgenic animals

Background

Although effective in blunting the deleterious effects of a stroke, the underlying mechanisms of ischemic preconditioning are only partly understood. Epigenetic mechanisms might be involved in this phenomenon [130], as direct neuroprotective mediators have been identified by genomic and proteomic analyses [357]. Importantly, adenosine serves as a regulator of transmethylation reactions [358], and thus changes in adenosine tone may affect gene expression via modification of DNA or histone methylation patterns. Adenosine plays a role in LPS-induced preconditioning, and is diminished in mice overexpressing adenosine kinase (ADK), the key adenosine metabolizing enzyme in the brain [354]. It was therefore hypothesized that CpG-induced preconditioning would be abrogated under conditions of increased adenosine clearance, such as ADK overexpression, as an acute surge of adenosine may serve as a key initiator

of delayed ischemic tolerance. It was also hypothesized that increased adenosine tone in the forebrain would have no effect of CpG induced preconditioning.

Material and Methods

Animals

All animal procedures were conducted in a facility accredited by the Association for Assessment and Accreditation of Laboratory Animal Care (AAALAC) in accordance with protocols approved by the Legacy Institutional Animal Care and Use Committee (IACUC) and the principles outlined by the National Institute of Health (NIH). Male C57BL/6 wild-type (WT) mice (Charles River, Wilmington, MA, USA) and fb-Adk-def and Adk-tg mutants of the same genetic background weighing 25 to 30 g were housed under diurnal lighting conditions (12 h/12 h cycle). The fb-Adk-def mutant line was recently created by cross-breeding *Emx1-Cre-Tg3* mice expressing Cre-recombinase in neurons and astrocytes of the telencephalon with ADK transgenic mice (“Adk-tg mice”) carrying a *loxP*-flanked ADK transgene (*Adktm1^{-/-}:TgUbiAdk*) in an otherwise lethal ADK knockout (*Adktm1^{-/-}*) background [366]. The resulting *Adktm1^{-/-}:Tg(UbiAdk):Emx1-Cre-Tg3* mice (referred to as “fb-Adk-def mice”) are triple mutants homozygous for the deletion of the endogenous *Adk* gene, homozygous for the *Adk*-transgene, and heterozygous for Cre. These animals have a forebrain-selective reduction of ADK in cortical and hippocampal regions, while ADK continues to be overexpressed in striatum in analogy with the Adk-tg

mice. Mutant animals for this study were generated by breeding Adk-tg mice with fb-Adk-def mice, resulting in both genotypes as littermates in a 1:1 ratio.

Middle Cerebral Artery Occlusion (MCAO)

Mice were preconditioned with CpG ODNs 1826 (20µg, Invivogen) or saline 72 hr prior to MCAO as previously reported [190]. Mice were anesthetized with isoflurane (1.5-2%) and subjected to MCAO using the monofilament suture method described previously [516]. Briefly, a silicone-coated 7-0 monofilament nylon surgical suture was threaded through the external carotid artery to the internal carotid artery to block the middle cerebral artery, and maintained intraluminally for 40 minutes. The suture was then removed to restore blood flow. Cerebral blood flow (CBF) was monitored throughout surgery by laser doppler flowmetry. Any mouse that did not maintain a CBF during occlusion of <25% of baseline was excluded from the study. Body temperature was monitored and maintained at 37°C with a thermostat-controlled heating pad. Infarct measurements were made using TTC staining of 1 mm coronal brain sections.

Results

Surprisingly, despite the fact that they have a decreased protective response to prophylactic LPS administration, mice overexpressing ADK can be successfully

preconditioned via prophylactic administration of CpG ODNs (**Figure 44**). Pretreatment with CpG ODNs 72 hours prior to MCAO decreased indirect infarct volume in Adk-tg mice from ~40% to ~20% of contralateral hemisphere. This is commensurate with the reduction seen in wild type animals, from ~27% to ~10% of contralateral hemisphere. Thus, CpG preconditioning is not dependent on adenosine tone in the brain for inducing protection.

Additionally, mice lacking ADK in the forebrain, and thus having increased adenosine tone, can be preconditioned with CpG ODNs (**Figure 45**). Peripheral administration of CpG ODNs 72 hours prior to induction of MCAO resulted in a decrease in indirect infarct volume from ~50% to ~22% in Fb-Adk-def mice. This surpasses the reduction in infarct seen in wild type mice, which was decreased from ~25% to ~12%. As hypothesized, increased adenosine tone in the forebrain does not negatively impact CpG-mediated preconditioning.

Conclusions

Considered in the light of recent publications on the role of adenosine in mediating TLR-induced neuroprotection [354], the results from the present study indicate that LPS-induced preconditioning is more dependent on the central effects of adenosine than CpG-induced preconditioning. Peripheral administration of low-dose LPS has been shown to increase adenosine tone in the CNS acutely, a response which may be required for the central reprogramming of the genomic response to future ischemia

[354]. LPS preconditioning may rely more heavily on reprogramming of resident CNS cells, whereas CpG preconditioning may rely predominantly on the response of the peripheral immune system for efficacy. This can be seen when the regulation of genes in the blood and brain compartments are compared following preconditioning with either CpG or LPS, or after subsequent ischemia in preconditioned animals (**Figure 46**). Three hours following systemic administration of LPS, approximately 273 gene change expression in the brain. This is nearly three times the 87 genes that change expression in the brain following CpG administration. This may indicate that central genomic changes play a more important role in LPS preconditioning than in CpG preconditioning.

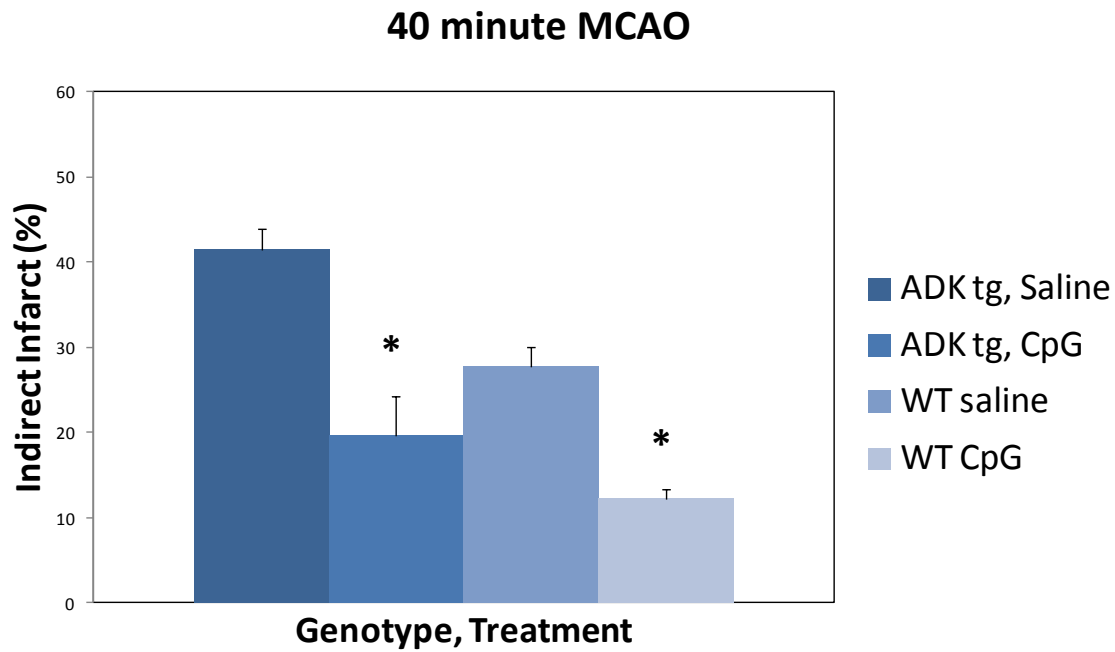


Figure 44. *Mice with decreased adenosine tone in the brain can be preconditioned with CpG ODNs*

CpG ODNs or saline control was administered in a final volume of 200µl via intraperitoneal injection 72 hours prior to the onset of surgical occlusion. All animals were subjected to 40 minutes of MCA occlusion and infarct volumes were measured 72 hours following reperfusion. Data are displayed as mean ± SEM. * indicates $p < 0.05$.

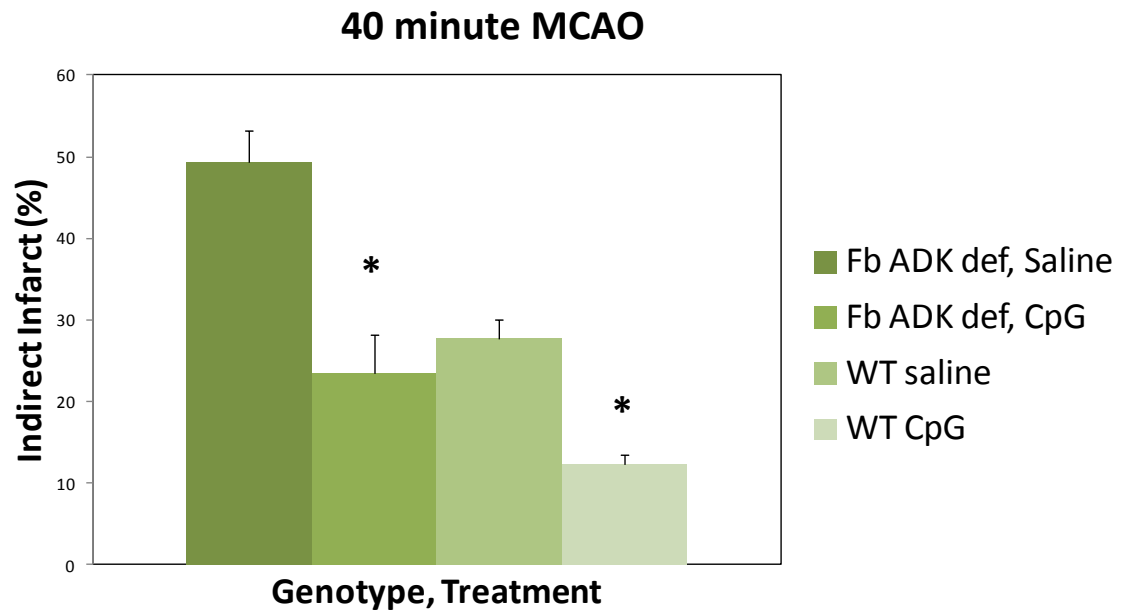
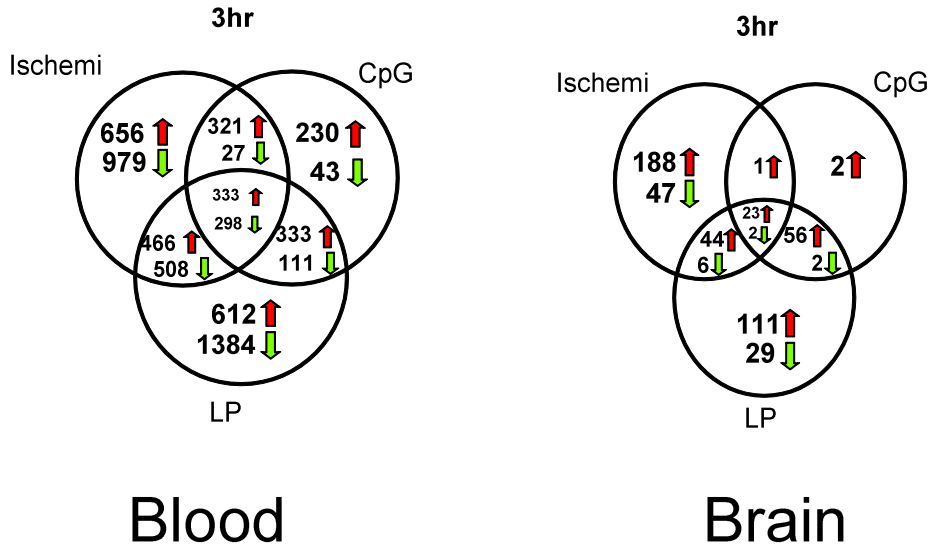


Figure 45. *Mice with increased adenosine tone in the forebrain can be preconditioned with CpG ODNs*

CpG ODNs or saline control was administered in a final volume of 200µl via intraperitoneal injection 72 hours prior to the onset of surgical occlusion. All animals were subjected to 40 minutes of MCA occlusion and infarct volumes were measured 72 hours following reperfusion. Data are displayed as mean ± SEM. * indicates $p < 0.05$.

Genomic profile following preconditioning



≥ 2 fold change compared to unhandled

Genomic profile following stroke

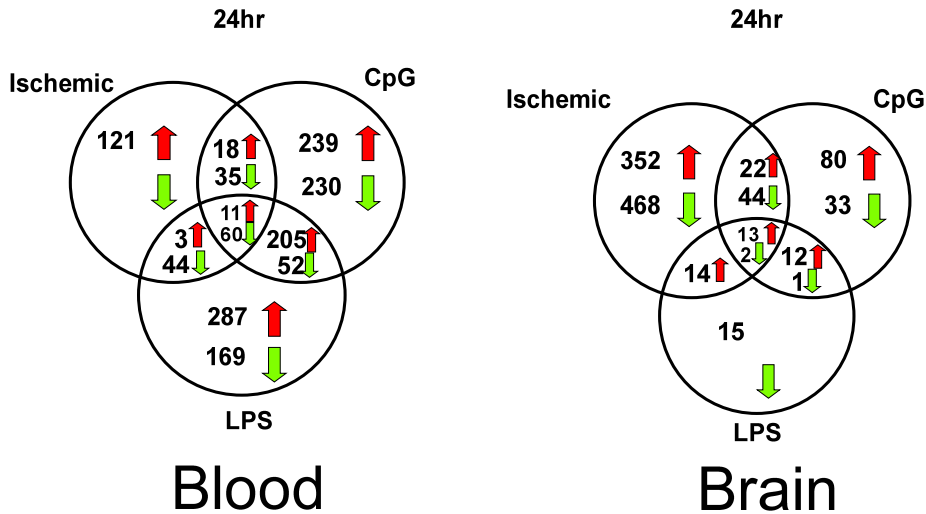


Figure 46. Differential genomic response in blood and brain following preconditioning with ischemic, CpG or LPS

Venn diagrams showing the number of transcripts regulated in the blood at 3 hr following CpG, LPS or ischemic preconditioning (top panel) and 24 hr following stroke (MCAO; bottom panel). Numbers in bottom panel do not include genes shared with stroke alone. Criteria for regulation:

fdr adjusted $p < 0.05$ and ≥ 1.5 fold regulation compared to non-stroked mice. Red arrows indicate upregulated transcripts, green arrows indicate down regulated transcripts.

APPENDIX E

Studies on the role of adenosine A₁ receptors on TLR-mediated preconditioning and infarct volume following MCAO

Background

Following peripheral administration of a preconditioning dose of lipopolysaccharide (LPS) there is an NF κ B-dependent upregulation of adenosine A₁ receptors (A₁Rs) in the brain [536]. Similarly, peripheral administration of a preconditioning dose of CpG ODNs leads to regulation of adenosine receptors mRNA in blood and brain *in vivo* (Stenzel-Poore lab, unpublished observation). Activation of NF κ B is also well established mediator of TLR-mediated preconditioning [508]. Since A₁Rs serve to decrease excitatory amino acid release, hyperpolarize neurons and decrease

neuronal firing, this increased A₁R expression following preconditioning with TLR-ligands may serve to protect the brain from ischemic injury during middle cerebral artery occlusion (MCAO). To test this hypothesis, mice lacking A₁Rs (A₁R KO) were preconditioned with CpG ODNs and then subjected to transient MCAO. Infarct volume was assessed and compared to that of wild-type mice.

Material and Methods

Animals

C57BL/6 mice (male, 8-12 weeks) were purchased from Jackson Laboratories (West Sacramento, CA). A₁R^{-/-} mice lack both A₁R alleles [403], and were maintained on a C57BL/6 background. All mice were housed in an American Association for Laboratory Animal Care-approved facility. Procedures were conducted in an Association for the Assessment and Accreditation of Laboratory Animal Care accredited facility according to Institutional Animal Care and Use Committee, and National Institutes of Health guidelines.

Middle Cerebral Artery Occlusion (MCAO)

Mice were preconditioned with CpG ODNs 1826 (20µg, Invivogen) or saline 72 hr prior to MCAO as previously reported [190]. Mice were anesthetized with isoflurane (1.5-2%) and subjected to MCAO using the monofilament suture method described previously [516]. Briefly, a silicone-coated 7-0 monofilament nylon surgical suture was

threaded through the external carotid artery to the internal carotid artery to block the middle cerebral artery, and maintained intraluminally for 40 to 60 min. The suture was then removed to restore blood flow. Cerebral blood flow (CBF) was monitored throughout surgery by laser doppler flowmetry. Any mouse that did not maintain a CBF during occlusion of <25% of baseline was excluded from the study. Body temperature was monitored and maintained at 37°C with a thermostat-controlled heating pad. Infarct measurements were made using TTC staining of 1 mm coronal brain sections.

Results

Surprisingly, following 40 minutes of MCAO, A₁R KO mice were significantly protected from ischemic injury (**Figure 47**). Indirect infarct volume in wild-type animals following 72 hours of reperfusion was approximately 28% of contralateral hemisphere, while indirect infarct volume in A₁R deficient mice was only approximately 8%. Thus, in the context of transient ischemia/reperfusion, A₁Rs may increase cerebral injury.

A₁R KO mice are not able to be preconditioned via prophylactic administration of CpG ODNs (**Figure 48**). Infarct volume after 40 minutes of MCAO was not significantly changed in A₁R mice following pretreatment with CpG ODNs. Thus, CpG-mediated preconditioning may require upregulation of A₁Rs to induce the preconditioned phenotype. However, the infarcts seen in non-preconditioned A₁R mice were extremely small, thus the protective effects of CpG preconditioning may not be quantifiable. The

duration of ischemia should be increased such that level of ischemic damage in A₁R KO mice is commensurate with what is seen in wild-type animals prior to preconditioning for these results to be meaningful.

Conclusions

Extracellular adenosine is increased dramatically following induction of ischemic *in vivo*, serving as an endogenous neuroprotective response. It has been thought that this protective effect is largely mediated via activation of A₁Rs [537-539], though this conclusion has been challenged [238]. When administered prior to or immediately after 5 minutes of global ischemic in gerbils, the A₁R agonist adenosine amine cogener (ADAC) has been shown to increase the number of surviving neurons [537]. Similarly, administration of the A₁R agonist N⁶-cyclohexyladenosine (CHA) mitigated damage to CA1 neurons in gerbils following 30 minutes of bilateral carotid artery occlusion [538]. Administration of the A₁R antagonist theophylline ten minute prior to 5 minutes of bilateral carotid artery occlusion has been shown to aggravate neuronal loss in the CA1 region of the hippocampus [539]. Contrary to this previous finding, Olsson *et al* saw no significant change in percent of dead neurons in the hippocampal CA1, the cortex or the striatum following 12 minutes of global ischemia in A₁R KO mice [238]. Further, A₁R KO mice have been shown to have increased susceptibility to excitotoxic cell death in a model of intrahippocampal kainic acid-induced epileptogenesis [402].

Surprisingly, we found mice lacking A₁Rs to be robustly protected from 40 minutes of transient MCAO. To explain the discrepancy seen between these studies, it is

important to consider the contribution of peripheral immune activation to damage following ischemic/reperfusion injury [26, 27]. Adenosine receptors are not only present on cells within the CNS, but also on cells throughout the periphery, including on immune cells (**Figure 15**). Following stroke, adenosine levels increase not only in the CNS [223], but throughout the body [224]. Increased extravasation of neutrophils has been shown to increase infarct volume following ischemia/reperfusion injury [27, 290, 291, 540-542]. Stimulation of A₁Rs on neutrophils increases migration of these cells [292, 293]; thus, A₁R KO mice may have decreased extravasation of neutrophils into the brain parenchyma, decreasing damage following reperfusion.

In line with the hypothesis that A₁R KO mice could not upregulate A₁Rs following systemic administration of a preconditioning dose of a TLR-agonist, and thus would not be protected from subsequent ischemia, A₁R KO mice are not protected from ischemic injury in an MCAO model following CpG ODN preconditioning. However, the infarct volume seen in A₁R KO following 40 minutes of MCAO was so small that there may not have been enough salvageable tissue to appreciate a protective effect. Thus, more studies with an increased duration of MCAO to make initial injury approximate that seen in wild-type animals is needed.

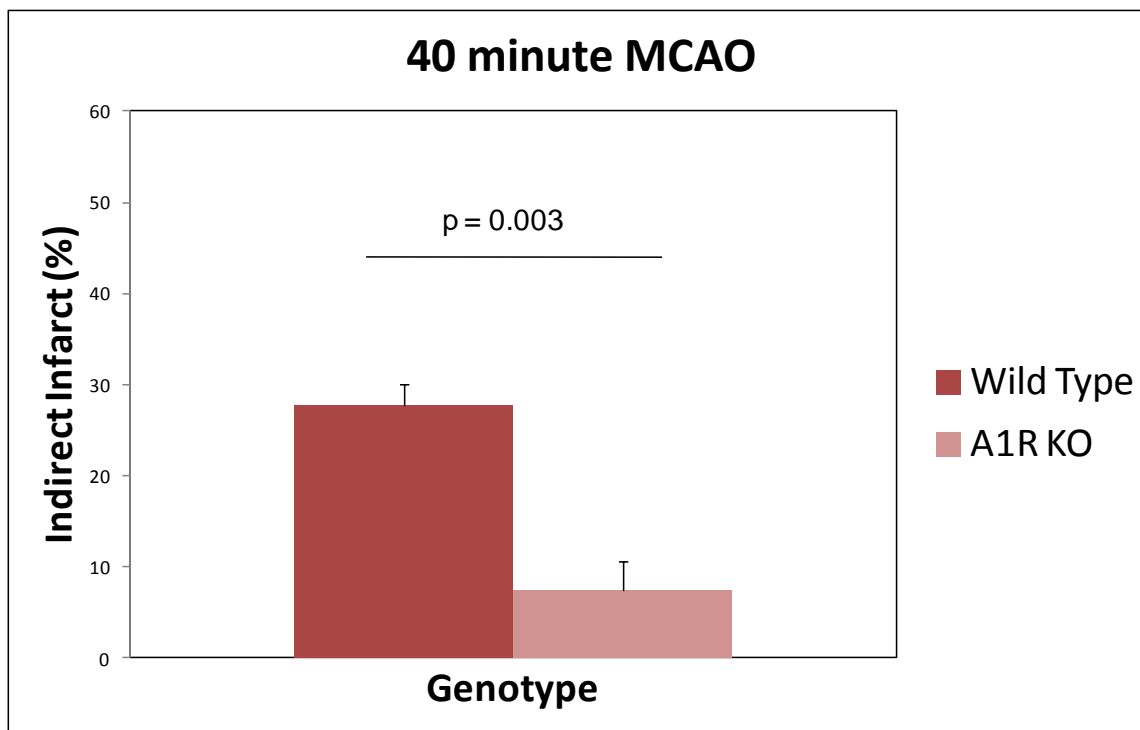


Figure 47. *A₁R knockout mice have reduced infarct volume following transient MCAO*

Mice lacking adenosine A₁ receptors have significantly decreased infarct volume following 40 minutes of transient middle cerebral artery occlusion (MCAO). Infarct volume was measured 72 hours post-reperfusion. Data is displayed as mean \pm SEM.

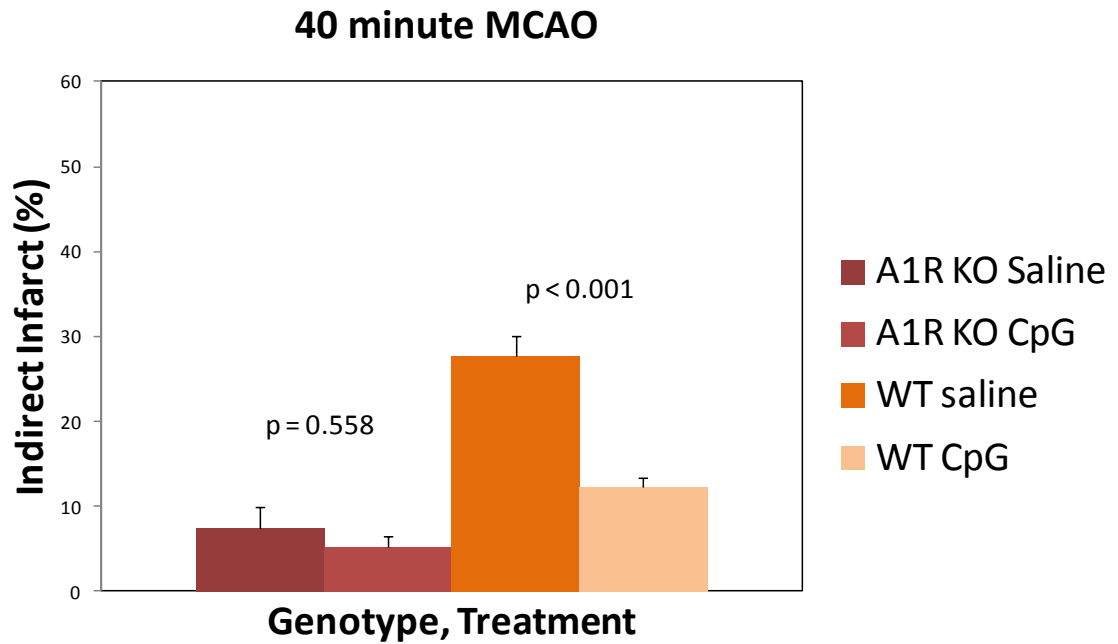


Figure 48. *A₁R* mice cannot be preconditioned with CpG ODNs

CpG ODNs or saline control was administered in a final volume of 200µl via intraperitoneal injection 72 hours prior to the onset of surgical occlusion. All animals were subjected to 40 minutes of MCA occlusion and infarct volumes were measured 72 hours following reperfusion. Data are displayed as mean ± SEM.

APPENDIX F

Development of an *in vitro* prescreening assay for assessing CpG response in non-human primates using peripheral mononuclear blood cells

Background

Due to polymorphisms in the Toll-like receptors, not all humans respond to CpG ODNs [330, 543, 544]. If CpG ODNs are to be advanced to therapeutic use, development of a prescreen test to assess efficacy on an individual basis is highly desirable. Similarly, not all non-human primates respond to CpG ODNs, so creating a test to exclude non-responders from preliminary testing in order to obtain an accurate reflection of efficacy is needed. Kmix CpG ODNs were developed in order to optimize responsivity [330], but validation of response is still needed. In order to assess responsivity to Kmix CpG ODNs, an *in vitro* assay utilizing peripheral blood mononuclear cells (PBMCs) was developed, and 26 Chinese-origin rhesus macaques were screened for response to Kmix CpG ODNs and LPS.

Material and Methods

Blood samples

Animals had an average age of 8.8 ± 2.3 years and an average body weight of 8.4 ± 1.7 kg. Animals were single-housed indoors in double cages on a 12h:12h light/dark cycle, with lights-on from 0700 to 1900h, and at a constant temperature of $24 \pm 2^\circ\text{C}$. Laboratory diet was provided bi-daily (Lab Diet 5047, PMI Nutrition International, Richmond, IN) supplemented with fresh fruits and vegetables, and drinking water was provided *ad libitum*. The animal care program is compliant with federal and local regulations regarding the care and use of research animals and is Association for Assessment and Accreditation of Laboratory Animal Care (AAALAC)-accredited. All animal experiments were subject to approval by the Institutional Animal Care and Use Committee (IACUC) at the Oregon National Primate Research Center. Peripheral blood was obtained from 26 male rhesus macaques (*Macaca mulatta*) of Chinese origin via femoral blood draw. PBMCs were isolated from the freshly obtained, heparinized peripheral blood by Ficoll-Hypaque density gradient centrifugation.

Reagents

Kmix CpG ODN, a 1:1:1 mixture of 3 human specific phosphorothioate K type ODNs (K3: ATC GAC TCT CGA GCG TTC TC; K23: TCG AGC GTT CTC; K123: TCG TTC GTT CTC), [330]

was obtained from Oligos Etc. (Wilsonville, OR, USA) for NHP studies. LPS (*Escherichia coli* serotype 0111:B4) was obtained from Sigma.

Multiparametric flow cytometry

PBMCs (1×10^6 per well) in 6-well tissue culture plates at 37°C were incubated with CpG ODN (50µg, ~3mM), LPS (50µg) or saline for 16 hours in 1mL RPMI 1640 media supplemented with 10% heat-inactivated FBS. After incubation, cells were washed with HBSS and then incubated in cell staining buffer (1x PBS, 1% BSA, 0.1% NaN₃, pH7.4) for 1 hour at 4°C with the following fluorochrome conjugated antibodies: Pacific Blue-conjugated anti-CD3 (BD Bioscience), allophycocyanin (APC)-eFluor 780-conjugated anti-CD20 (eBioscience), fluorescein isothiocyanate (FITC)-conjugated anti-CD56 (BD Bioscience), fluorescein isothiocyanate (FITC)-conjugated anti-CD16 (BD Bioscience), Phycoerythrin (PE)-conjugated anti-CD69 (BD Bioscience). Samples were analyzed immediately after staining using a BD LSR II flow cytometer (Becton Dickenson, Franklin Lakes, NJ). A minimum of 500,000 events were collected. Data was analyzed using FlowJo software (Treestar Inc., Ashland, OR).

Results

Following 16 hours of *in vitro* treatment with 50µg Kmix CpG ODNs, there was a significant increase in CD69+ CD3-CD20+ PBMCs (**Figure 50**). This response was seen in

all but two individual primates (**Table 6**). PBMCs in all blood samples tested showed increased expression of CD69 in response to LPS, indicating that all samples tested were able to respond to TLR stimulation. Using CD69 upregulation as a measure of response, Chinese-origin Rhesus macaques show >90% responsiveness to *in vitro* stimulation with Kmix CpG ODNs.

Conclusions

While individual CpG ODN sequences are capable of eliciting robust responses in a given inbred rodent strain, outbred populations, such as non-human primates and humans, show more highly variable and even absent immune responses with a given CpG ODN. Further, structural differences between various classes of CpG ODNs have been shown to selectively stimulate distinct cell populations, allowing these compounds to be used selectively to achieve specific therapeutic goals. K-type (also called B-type) ODNs predominantly stimulate B cells to proliferate and produce IgM and IL-6, while D-type (also called A-type) CpG ODNs predominantly elicit plasmacytoid dendritic cell production of type I IFNs and NK cell production of IFN- γ [334]. Kmix CpG ODNs represent a mixture of three CpG DNA sequences, shown to optimally stimulate peripheral blood mononuclear cells (PBMC) from a heterogeneous human population [330]. This mixture of K-type ODNs was shown to have similar broad stimulatory activity in PBMC from rhesus macaques [334]. However, not all individuals respond to Kmix CpG ODNs, so a prescreening assay to determine individual response is highly desirable.

In order to assess individual responsiveness to Kmix CpG ODNs, PBMCs were isolated from peripheral blood and stimulated *in vitro* with CpG ODNs, LPS (positive control) or saline (negative control). Activation of B cells (CD3-CD20+) was assessed 16 hours later by looking at expression of the early activation marker CD69 [545]. Blood samples from 26 adult male rhesus macaques were used in this study, and only 3 animals failed to upregulate CD69 in response to Kmix CpG ODNs (**Table 6**). Of these three animals, one animal did upregulate CD69 when tested a second time one month later. All animals upregulated CD69 following stimulation with LPS, showing the cells were able to respond to TLR-mediated stimulation. Overall, assessment of CD69 expression on CD3-CD20+ PBMCs following *in vitro* stimulation with Kmix CpG ODNs appears to be a good screening assay for detecting non-responding individuals.

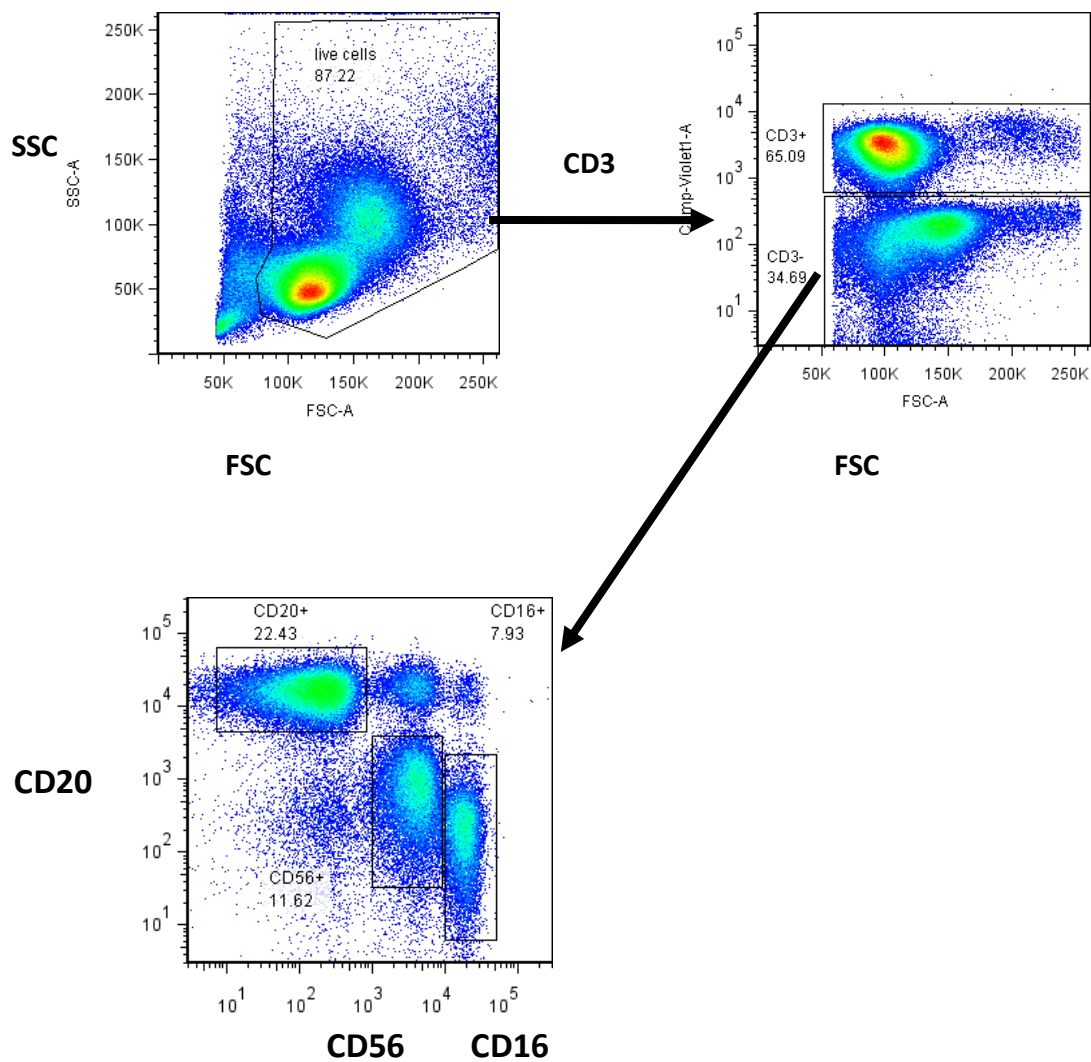


Figure 49. Gating strategy used to identify CD3-CD20+ cells

Live cells were gated based on FSC and SSC, then further identified as CD3+ or CD3-. CD3- cells were then sorted into CD20+, CD56+ or CD16+ populations.

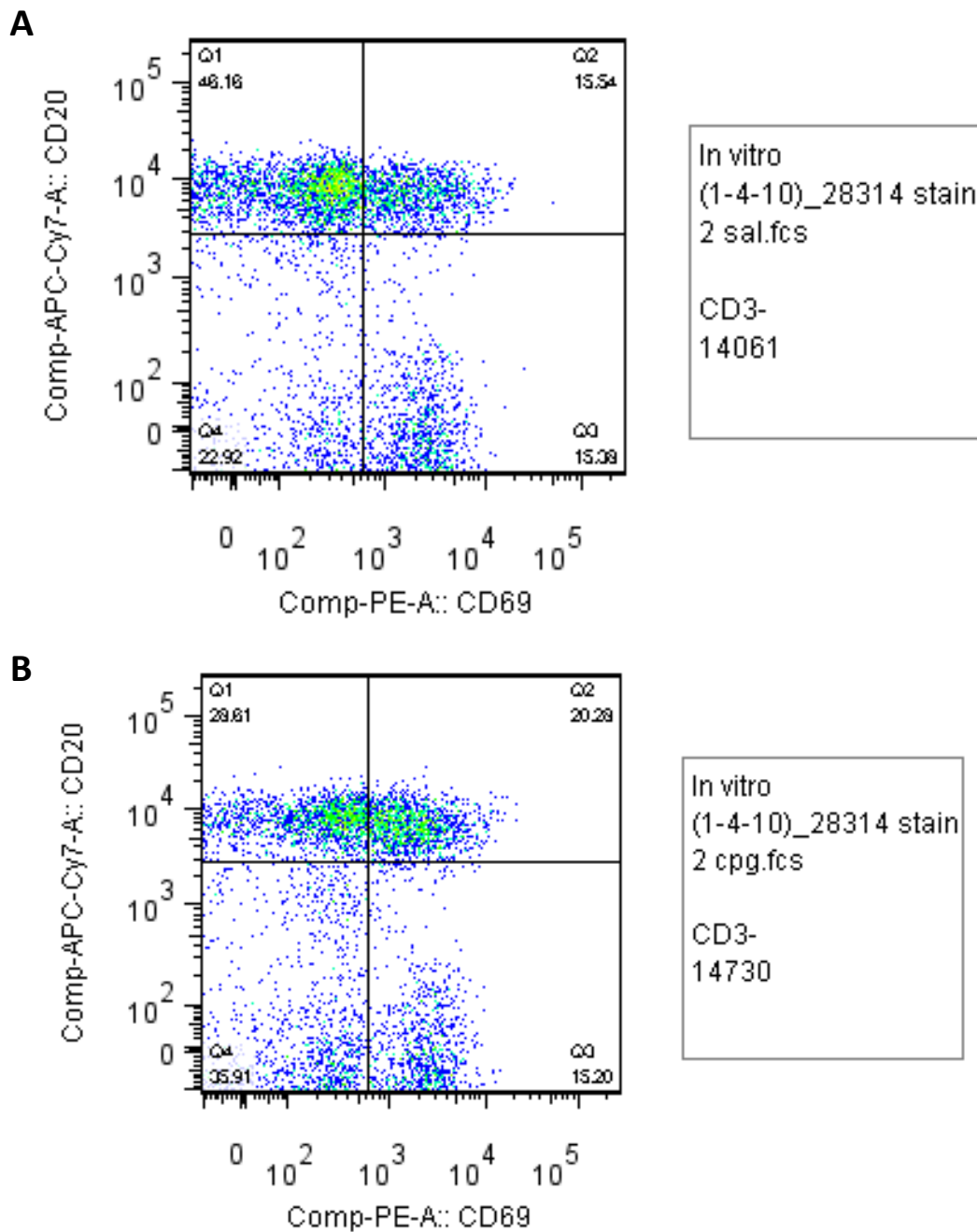


Figure 50. Gating strategy to identify $CD20+CD69^{hi}$ cells following stimulation with CpG ODNs

(A) $CD20+CD69^{low}$ cells from peripheral blood mononuclear cell isolates prior to stimulation with CpG ODNs. **(B)** Increase in $CD20+CD69^{hi}$ cells from peripheral blood mononuclear cell isolates following 16 hour incubation with $50\mu\text{g}$ CpG ODNs *in vitro*.

Table 6. Response of peripheral blood mononuclear cells from individual non-human primates to CpG ODNs or LPS

Animal number	Stimulus		LPS	Kmix Summary	
	Kmix CpG				
28303	+	+	+	Tested	26
28308	-	+	+	Responders	21
28310	+	+	+	Non-responders	2
28314	+		+	Unclear	2
28325	-		+	Excluded	1 poor staining
28311	+	+	+	Multiple tests?	4 28308: one neg one pos; 28303: both pos; 28310: both pos; 28311: both weakly positive
28326	+		+		
28492	+		+	Positive: +	
28516	+		+	Negative: -	
28527	+		+	No test: (blank)	
28504	+		+	unclear	
28514	+		+		
28515	+		+		
28503	+		+		
28649	+		+		
28656	-		+		
28640	+		+		
28645	+		+		
28325	+		+		
28657	+		+		
28658	+		+		
28659	+		+		
28680	+		+		
28314	+		+		
28513	+		+		
28518	+		+		
28526	+		+		
28502	+		+		
28490	+		+		

APPENDIX G

Comparative assessment of three neurological scales for predicting function recovery between days 2 and 7 post-stroke in non-human primates

Background

Pilot testing of Kmix CpG ODNs in a NHP model of stroke showed a non-significant improvement in neurological function despite the fact that animals preconditioned with CpG ODNs had significantly reducing infarct volume [191]. Development of an improved, more species specific neurological scoring system might improve the sensitive of neurological testing and enable detection of spared neurological functions by CpG-induce preconditioning in future studies. Here, three separate neurological scales were used to assess neurological function at 2 and 7 days post ACA/MCAO. One scale has previously been published for use in non-human primate stroke models [333], but was developed in baboons. The second two neurological scales were modified from the Spetzler scale specifically for use in rhesus macaques. Seven day predictive value of 2 day neurological score as determined by each scale was also assessed.

Material and Methods

Two-vessel Occlusion Protocol in NHP

Two weeks before surgery, animals were screened for general health, endemic disease, and neurological disorders. The right middle cerebral artery (distal to the orbitofrontal branch) and both anterior cerebral arteries were exposed and occluded with vascular clips, as previously described [324]. Surgical procedures were conducted by a single surgeon. Briefly, anesthesia was induced with ketamine (~10 mg/kg, intramuscular injection) and animals were then intubated and maintained under general anesthesia using 0.8% to 1.3% isoflurane vaporized in 100% oxygen. A blood sample was taken and a venous line was placed for fluid replacement. An arterial line was established for blood pressure monitoring throughout surgery to maintain a mean arterial blood pressure of 60 to 80mmHg. End-tidal CO₂ and arterial blood gases were continuously monitored to titrate ventilation to achieve a goal PaCO₂ of 35 to 40 mm Hg. The surgery was performed as described previously [324]. Post-operative analgesia consisted of intramuscular hydromorphone HCl and buprenorphine.

Infarct measurement

Measurement of infarct volume was performed using T₂-weighted magnetic resonance images taken after 48 hours of reperfusion [324]. All scans were performed on a Siemen's 3T Trio system, housed near the surgical suite at ONPRC. Because of the small filling capacity of the rhesus macaque head, an extremity coil was used to achieve

better image quality of the brain. Anesthesia was induced initially with ketamine (10mg/kg intramuscular injection) and a blood sample was obtained. The animals were then intubated and administered 1% isoflurane vaporized in 100% oxygen for anesthesia maintenance. Animals were scanned in the supine position 2 days after surgery, and most animals also received baseline scans before surgery. Animals were monitored for physiologic signs, including pulse-oximetry, end-tidal CO₂, and respiration rate. All animals received anatomical MRI scans, which included T₁- and T₂-weighted, high-resolution time of flight scans, and a diffusion-weighted scan. The T₁ scan was an MPRAGE protocol, with TR=2500ms, TE=4.38ms, number of averages=1 and the flip angle=12°. Full brain coverage was attained at a resolution of 0.5mm isovoxel. The T₂ scan was a turbo spin-echo experiment, with TR=5280ms, TE=57ms, number of averages=4, an echo train length of 5, and a refocusing pulse flip angle of 120°. The entire brain was imaged with a 0.5x0.5 mm in-plane resolution and a slice thickness of 1mm. For visualization of the region of infarction, sections were immediately placed in 1.5% 2,3,5-triphenyl tetrazolium chloride (TTC, Sigma) in 0.9% phosphate-buffered saline and stained for 15-45 mins at 37°C, as appropriate. Images from T2-weighted MRIs and TTC stained sections were examined for the location of infarction, and the total affected area measured using ImageJ, as previously described [324]. Each of the techniques (MRI, TTC) analyzed comparable anatomical regions and sampled approximately 15 slices (4mm each). Measurements of infarct volume as a percentage of the ipsilateral hemisphere or cortex were made using the following formula: (area damaged/total area)x100%.

Neurologic Assessment in NHP

Neurologic assessments were performed by a single observer daily for 7 days post-stroke. The Spetzler, Simon and Lessov neurological scales were scored in parallel.

Results

All three neurological scales had good correlation with infarct volume as assessed by T2 MRI at 48 hour and 7 days post ischemia (**Figures 51, 53 and 55**). The Spetzler and Lessov had strongest correlations at both time points. The predictive value of the 48 hours neurological exam was also high for all scales (**Figures 52, 54, 56**), with the Simon scale having the lowest predictive value. All three scales are suitable for use in the rhesus macaques two vessel occlusion model of cerebral ischemia. However, additional neurological information can be acquired with the Spetzler and Lessov neurological scales that cannot be seen with the Simon neurological scale.

Conclusions

The Spetzler neurological scale was developed for evaluation of baboons following permanent and reversible middle cerebral artery occlusion (**Table 6**) [333]. Development of a more specific neurological scale was needed for assessment of animals following the newly developed dual artery occlusion model developed in rhesus

macaques [324], as the Spetzler neurological scale failed to reflect the reduction in infarct volumes seen in pilot studies of CpG-induced neuroprotection [191]. Thus two additional neurological scales were independently developed by established clinical neurologists, Dr. Roger P. Simon and Dr. Nicola S. Lessov. These scales were specifically tailored to the rhesus macaque dual vessel occlusion model of cerebral ischemia.

Unlike the Spetzler scale, the Simon scale focuses exclusively on motor deficits in the upper and lower extremities (**Table 7**). Behavior and alertness are excluded from this scale as the infarct induced by the dual-vessel occlusion model primarily affects the motor cortex. Further, behavior and alertness scoring can be confounded by post-surgical medication regimen, are more subject to interpretation by the evaluator. In contrast to the Simon neurological scale, the Lessov neurological scale uses additional behavioral assessments, including evaluation of posture prior to the entrance of the evaluator into the animal room (**Table 8**). The Lessov neurological scale also incorporates responsiveness to external stimuli, including both negative (e.g. a loud noise such as made by clapping) and positive (e.g. presentation of a treat) stimuli created by the evaluator. The assessment of motor function by the Lessov scale is also more nuanced than in either the Simon or Spetzler scales, include assessment of response to tactile (e.g. light touch) as well as noxious (e.g. light pinch) stimuli.

Interestingly, all three neurological scales correlated highly to infarct volume as assessed by T2 MRI. Despite the Lessov scale incorporating evaluation of an increased number of parameters, the Spetzler scale still had the highest correlation with infarct

volume at 48 hours ($R^2=0.85$ versus $R^2=0.91$, respectively). However, the Lessov scale had a slightly higher correlation with infarct volume at one week post-infarct ($R^2=0.82$ versus $R^2=0.81$). This improvement in the Lessov scale may be attributable to the fact that at 48 hours post-surgery animals are still on medication for pain control. Thus, they may not respond as robustly to the tactile and noxious stimuli. Similarly behavior and alertness is more difficult to assess accurately at this timepoint. The Simon scale had the lowest correlation with infarct volume at both 48 hours and 7 days ($R^2=0.79$ and $R^2=0.75$, respectively). Predictive value for all neurological scales was good; that is, 48 hour post-injury neurological score could be used to predict neurological score at 7 days post injury. Again, the motor-only Simon neurological scale had a lower predictive value than either the Spetzler or Lessov scales ($R^2=0.78$, $R^2=0.965$ and $R^2=0.934$, respectively). These results indicate that motor assessment alone may miss some defining details scoring of behavior and alertness can capture.

Table 7. Elaborated Spetzler neurological scale

Spetzler		
Motor Function (1-75)		
Extremities:		
Paralysis	1	Paralysis: No movement of limb at all. <i>Upper extremity is an obstacle to movement; cannot be repositioned except with great effort involving entire body.</i>
Severe hemiparesis	10	Severe hemiparesis: Very little to no movement of hand or leg. Cannot lift or grip using this limb. When hand is lifted with bar or pole and removed, the hand/arm falls limp. Will not reach for treats or support with this hand. <i>Function of shoulder is intact. Animal can reposition arm, but with effort and may require extra trunk movement.</i>
Mild hemiparesis	25	Mild hemiparesis: Limited movement and dexterity of arm, leg or hand. When hand is lifted with bar or pole, the hand may grip slightly and when removed, the hand/arm does not fall limp. Most likely will not reach for treats or support with this hand. <i>Function of shoulder and elbow are intact. Animal will hold arm bend at elbow across chest when ambulating. May reach towards treats with affect limb, but is unable to move hand.</i>
Favors normal side	55	Favors normal side: Decreased dexterity in affected limb. When moving, the affected side may do little work. When reaching for treats, even on affected side, the animal will consistently use its normal hand. <i>Function of shoulder, elbow and wrist/hand are intact. For a score of 55, an animal must be able to take treats or grab cage or bar with its affected limb – hand must be functional (at least to a limited extent). Dexterity may be poor, grip may be weak, and it may take coaxing to get the animal to use this limb.</i>
Normal	70	Normal: Supports its self with both limbs and reaches for treats with both sides equally as often.
Face:		
Normal or one sided paralysis	1	Normal or one sided paralysis: Paralysis of affected side of face – seen in the corner of the mouth dropping on that side. <i>If any sign of facial paralysis is seen, such as drooling, uneven chewing, forcing food out of pocket on affected side with limb, the animal is scored as a 1. No interpolation of score used.</i>
Normal facial movement	5	Normal: No paralysis.

Behavior and alertness (0-20)		
Comatose	1	Comatose: Laying on side, most likely with eyes closed. If eyes are open they do not move. Nonreactive to your entrance, approach, or auditory stimulation. Animal may be reclined on chest or back, non-responsive to physical contact and pain. This is an animal that may have extensive edema, and veterinary staff should be notified. If pupils are non-responsive to light, animal may be brain dead.
Aware but inactive	5	Aware but inactive: May be laying on healthy side but doesn't move much. Will look at you but with little movement in response to your presence. May only move away slightly when pushed. Animal is reclined. Responds to physical contact, but only briefly in a limited way (i.e. eyes open then close). Does not track well. Shows no interest in treats. May not drink from ORT bottle when offered.
Aware but medium inactive	10	Aware with only medium activity: May be sitting. Acknowledges your entrance/presence by looking at you. May also not pay attention to you or react to auditory stimulus. Unafraid of your presence. Animal may be reclined but can reposition to partially or unstable fully erect position when you enter the room or approach. May not track well, shows limited interest in treats. May take a treat but not finish chewing it. Spontaneous movements such as scratching are rare, require effort and lack dexterity.
Aware but less active	15	Aware but less active: Full range of movement but moves slowly. Not very afraid but moves away from stimulus like poking with bar. May be standing. Animal may be leaning against cage wall, but can sit unaided. Movements are slow, and direct stimuli may be needed to elicit ambulation. Diminished spontaneous movements such as scratching.
Normal	20	Normal: Full movement, fear of you, vocalization, etc.
Visual field deficit (1-5)		
Field deficit present	1	Deficit present: Lack of peripheral vision on one side. When a treat is offered, or fingers are wiggled, outside of direct line of vision animal does not turn head to look. Over time, peripheral vision may improve from initial tunnel vision; however if any deficit remains animal is scored as a 1. No interpolation of score used.
Field deficit absent	5	Deficit absent: Normal peripheral vision.

The Spetzler neurological scale focuses primarily on evaluation of the upper extremity. Though the leg is mentioned, the emphasis is on the upper limb.

Table 8. Elaborated Simon neurological scale

Simon		
Front Limbs (upper extremity)		
Normal	50	Both upper extremities participate with equal speed, strength, and dexterity in spontaneous or provoked motion.
Distal weakness	40	Able to take food with the left hand but with less distal dexterity and often prefers the contralateral limb. Function of shoulder, elbow and wrist/hand are intact. For a score of 40, an animal must be able to take treats or grab cage or bar with its affected limb – hand must be functional (at least to a limited extent). Dexterity may be poor, grip may be weak, and it may take coaxing to get the animal to use this limb.
Mild paresis	25	Not able to take food with distal left upper extremity. Still capable of supporting body with proximal left arm muscle of shoulder and elbow. Function of shoulder and elbow are intact. Animal will hold arm bend at elbow across chest when ambulating. May reach towards treats with affect limb, but is unable to move hand.
Distal plegia	10	No spontaneous movement in left hand; some shoulder movement preserved. Function of shoulder is intact. Animal can reposition arm, but with effort and may require extra trunk movement.
Plegic	0	With excessive general neurological impairments, a precise assessment of front limb function may not be possible. Upper extremity is an obstacle to movement; cannot be repositioned except with great effort involving entire body. Also given to an animal that is consistently recline and cannot be encouraged to move freely enough to allow thorough examination.

Rear Limbs (lower extremity)		
Normal	25	Both limbs participate with equal speed, strength, and dexterity in motion or static position. Left limb is weaker. Limping may be detectable. Will prefer to take a new position beginning with the right leg. Function of hip, knee, and limited ankle/foot are intact.
Mild paresis	20	Animal may be unsteady when standing fully erect and trying to reach for a treat held above its head. Will likely use non-affected foot to step on to perch.
Severe paresis	15	Limping is present. Left leg unable to maintain position on top of cage bars and often slips through. Function of hip, and limited knee are intact. Animal can pull leg under itself or retract. Animal will not use limb to scratch.
Paralysis	5	No movement in left leg. Cannot correct position of the left leg. Animal will circle towards unaffected side. With great effort, some correction of hip may be possible, leg generally lies straight.
No Assessment Possible	0	Because of excessive general neurological impairments, a precise assessment of rear limb function is not possible. Lower extremity is an obstacle to movement; cannot be repositioned except with great effort involving entire body (i.e. limb will be dragging). An animal with this level of impairment but some arm function may be able to pull self up, but if both limbs are impaired, animal will likely remain supine. This score will also be given to an animal who is non-responsive or continually recline.

The Simon Neurological scale is a purely motor assessment. Deficit is judged from proximal to distal (shoulder to hand, or hip to foot), as proximal function will return first (distal function will be the last to be regained). The arm is essentially divided into three segments: shoulder, elbow, wrist/hand. Similarly function of the leg is assessed in three segments: hip, knee, ankle/foot.

Table 9. Elaborated Lesson neurological scale

Lessov		
Object Evaluated	Score	Description of signs
General Neurological Signs:		
Consciousness		
Normal	0	Alert, swiftly tracks changes in surroundings.
Obnubilation (Clouding of consciousness)	1	Alert but quiet, calm, tired. Eye slowly checks and follows changes in the surroundings. <i>Animal may be leaning against cage wall, but can sit unaided. Movements are slow, and direct stimuli may be needed to elicit ambulation. Diminished spontaneous movements such as scratching or repositioning.</i>
Somnolent	2	Appears aware but inert, drowsy, sleepy. Sluggishly check for changes in surroundings but does not track them. <i>Animal may be reclined but can reposition to partially or unstable fully erect position when you enter the room or approach. May not track well, shows limited interest in treats. May take a treat but not finish chewing it. May appear drowsy. Spontaneous movements such as scratching are rare, require effort and lack dexterity.</i>
Stupor	3	Appears conscious but deeply inert, lethargic; unaware and unresponsive to surroundings. <i>Animal is reclined. Responds to physical contact, but only briefly in a limited way (i.e. eyes open then close). Does not track well. Shows no interest in treats. May not drink from ORT bottle when offered.</i>
Coma	4	Not alert or aware. The eye, if open, does not move at all. <i>Animal may be reclined on chest or back, non-responsive to physical contact and pain. This is an animal that may have extensive edema, and veterinary staff should be notified. If pupils are non-responsive to light, animal may be brain dead.</i>

Posture		
Normal	0	Stable, erect sitting; quickly and effortlessly changes position from seated to upright. <i>Animal will likely be seated on perch, or move to perch when observer enters room. If animal is prone when observer enters room, animal will most likely right itself.</i>
Abnormal active	1	Unstable, erect sitting; leans on the wall; able to change position but slowly and with effort. <i>Animal may be reclined but can reposition to partially or unstable fully erect position when you enter the room or approach.</i>
Reclined active	2	Reclines in prone position. With big effort, the animal is capable of moving into a partially erect sitting position. <i>Often due to severe hemiparesis. Even with direct stimulus (such as poking with a bar) animal is not able to achieve or maintain fully erect posture.</i>
Consistently reclined	3	Reclines in prone or side position. Cannot move into sitting or standing. Able to raise only the head or head and upper chest on stimuli or spontaneously. Shifting of the whole body is not possible.
Passive	4	Lies on side with no spontaneous or provoked posture changes.
Motor Activity		
Spontaneous		
Normal	0	Vigorously and fluidly moves/jumps in cage from wall to wall, at full speed. <i>Animal will scratch, grab food or reposition freely. May ambulate in cage when observer enters room. More vigorous movements may not appear until stimulus is applied.</i>
Diminished	1	Spontaneous movements are with slower speed and less dexterity. <i>May appear drowsy. Spontaneous movements such as scratching are rare, require effort and lack dexterity.</i>
Limited spontaneous	2	Moves rarely only to change position of the body or limbs, or to scratch itself.
Ceased	3	No spontaneous movements.
Provoked		
Positive Stimuli:		<i>Handing the animal a treat.</i>
Normal	0	Approaches and takes treat fast, chews and swallows at normal rate.
Diminished	1	Takes and chews treat slowly often loses part of the treat.
Limited	2	Acknowledges the treat but does not attempt to take it.
No Response	3	No acknowledgement or reaction.

Negative stimuli:		
<i>Indirect (distant)</i> <i>Stimuli:</i>		<p><i>Staring, fast, aggressive movements or sudden noise from investigator.</i></p> <p>This test can be administered by: the investigator making a threatening facial display at the animal, clapping, or quickly pulling on the cage back to elicit the sound made when an animal is going to be squeezed. The cage back movement is identifiable by the animals and generally provokes movement in a healthy animal.</p>
Normal	0	Threatening, aggressive facial and body displays lasting more than 5 seconds.
Diminished	1	Short, 3-5sec., mainly facial displays.
Limited Response	2	Perceives the stimuli but does not react.
N.A.P.	3	No assessment possible because of excessive general neurological impairments.*
<i>Direct (tactile)</i> <i>Stimuli:</i>		<p><i>Touch or light poke.</i></p> <p>This test is administered by gently poking of the animal with the end of the feeding bar.</p>
Normal	0	Immediately retreats to a safe distance and vigorously removes the irritating object.
Diminished	1	Short facial threatening display and withdraws at a slower speed.
Limited Response	2	No threatening display, withdraws sluggishly after multiple irritation.
No Response	3	No motor response on tactile stimuli.

Noxious (pain) stimuli:		<p><i>Needle stick or pinch</i></p> <p>This test was formulated when animals were only survived to 48h and as such had much more severe deficits than can be allowed for animals surviving to 7 days. As such, though this test was initially administered as a whole-body exam (i.e. animals may not have responded to pain on non-affect side due to excessive neurological impairment), this should be divided in to upper and lower extremity on the affected side only. Pain response is tested with a light needle stick, or pinching. The most distal part of the extremity (hand or foot) will be the last to recover feeling.</p>
Normal	0	Not possible to apply due to rapid and constant movements or fast, immediate and complete withdrawal.
Diminished reaction	1	Withdrawal after some delay.
Limited reaction	2	Sluggish or weak withdrawal after multiple (3-5) stimuli. <i>Unclear if animal responds to first application of stimuli.</i>
Attempted reaction	3	Attempt to withdraw is not accomplished with real movement away from stimuli.
No reaction	4	No motor response on pain stimuli.
<i>Focal Neurological Signs:</i>		
Front Limbs		
Normal	0	Both limbs participate with equal speed, strength, and dexterity in spontaneous or provoked motion (reaching for handed treat, removing irritating stimuli).
Mild paresis	1	Able to take food with the left hand but with less dexterity and often prefers the right one.
Severe paresis	2	Not able to take food with left hand. Still capable of supporting the body with left arm.
Paralysis	3	Left hand and arm not active at all; it is an obstacle to movement.
NAP (No Assessment Possible)	4	Because of excessive general neurological impairments, a precise assessment of front limb symmetry is not possible.*

Rear Limbs		
Normal	0	Both limbs participate with equal speed, strength, and dexterity in motion or static position.
Mild paresis	1	Left limb is weaker. Limping may be detectable. Will prefer to take a new position beginning with the right leg.
Severe paresis	2	Limping is present. Left leg unable to maintain position on top of cage bars and often slips through.
Paralysis	3	No movement in left leg. Cannot correct position of the left leg.
NAP (No Assessment Possible)	4	Because of excessive general neurological impairments, a precise assessment of rear limb symmetry is not possible.*
Facial Symmetry		
Normal	0	Signs of facial paralysis may include drooling, uneven chewing, and forcing food out of pocket on affected side with limb. Facial asymmetries can also be detected during facial displays if animal does not take a treat. Symmetrical engagement of sides when chewing, swallowing, and showing teeth.
Mild Paresis (asymmetry)	1	Left corner of mouth is slightly less engaged in chewing process, slight but not constant leek of saliva from left part of mouth. Left submandibular pocket is slightly full (size of a walnut) Animal may force food out of pocket on affected side. Food may fall into pocket on affected side due to mild paralysis.
Severe Paresis	2	As in score of 1 plus: constant leek of saliva (when chewing). Submandibular pocket much bigger (size of an apple or orange).
NAP	3	Because of excessive general neurological impairments, a precise assessment of rear limb symmetry is not possible.*

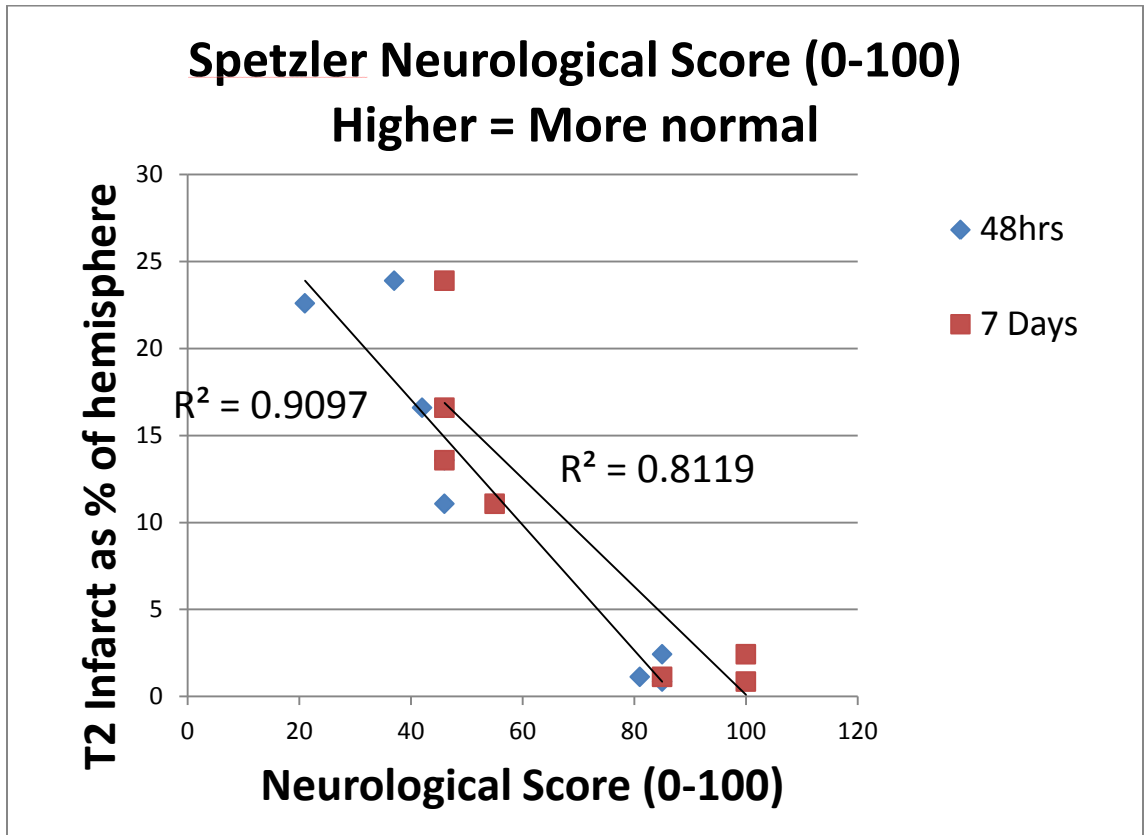


Figure 51. *Spetzler neurological score correlates with infarct volume*

Neurological score at 48 hours (blue diamonds) and 7 days (red squares) post-injury versus infarct volume as assessed by T2 MRI. For the Spetzler neurological scale, a higher score indicates improved neurological function. N=7, data points represent individual animals. R^2 value based on linear regression analysis.

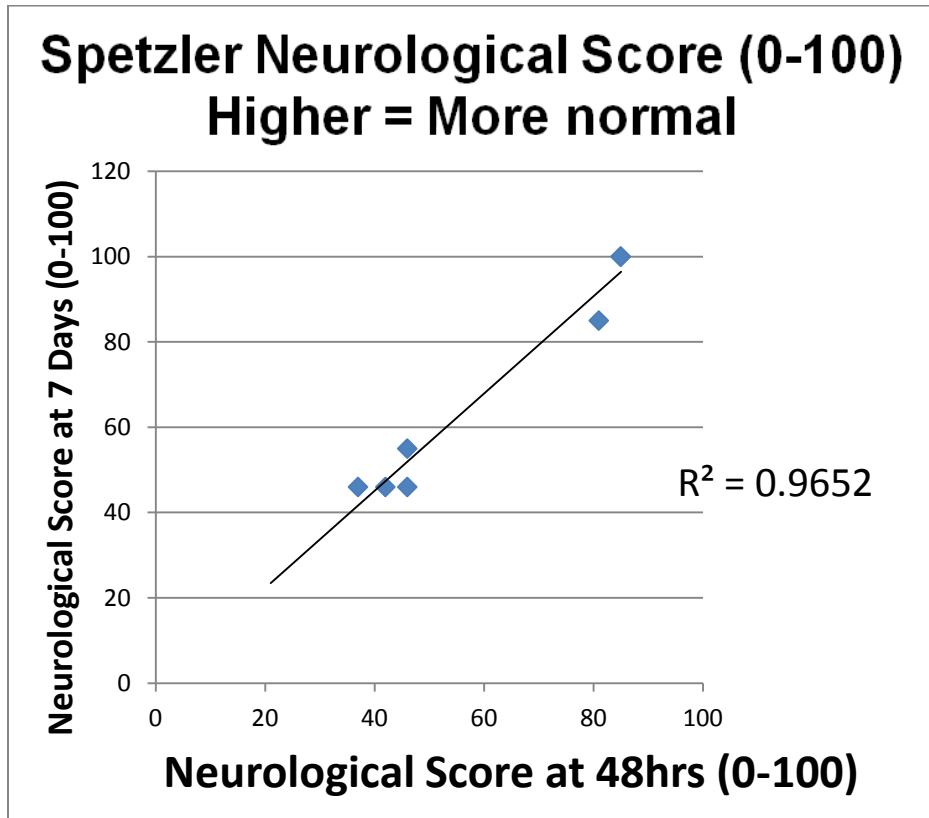


Figure 52. 7 day predictive value of day 2 Spetzler neurological score

Spetzler neurological score at 48 hours post-injury versus Spetzler neurological score at 7 days post-injury. N=7, data points represent individual animals. R^2 value based on linear regression analysis.

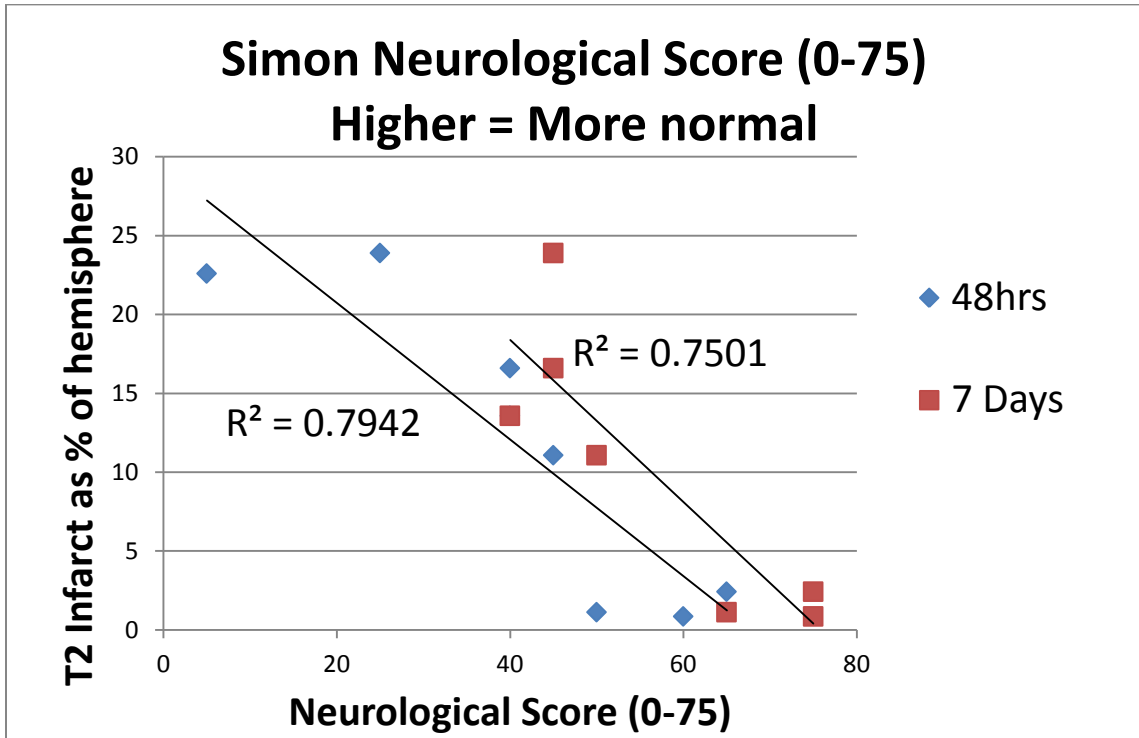


Figure 53. Simon neurological score correlates with infarct volume

Neurological score at 48 hours (blue diamonds) and 7 days (red squares) post-injury versus infarct volume as assessed by T2 MRI. For the Simon neurological scale, a higher score indicates improved neurological function. N=7, data points represent individual animals. R^2 value based on linear regression analysis.

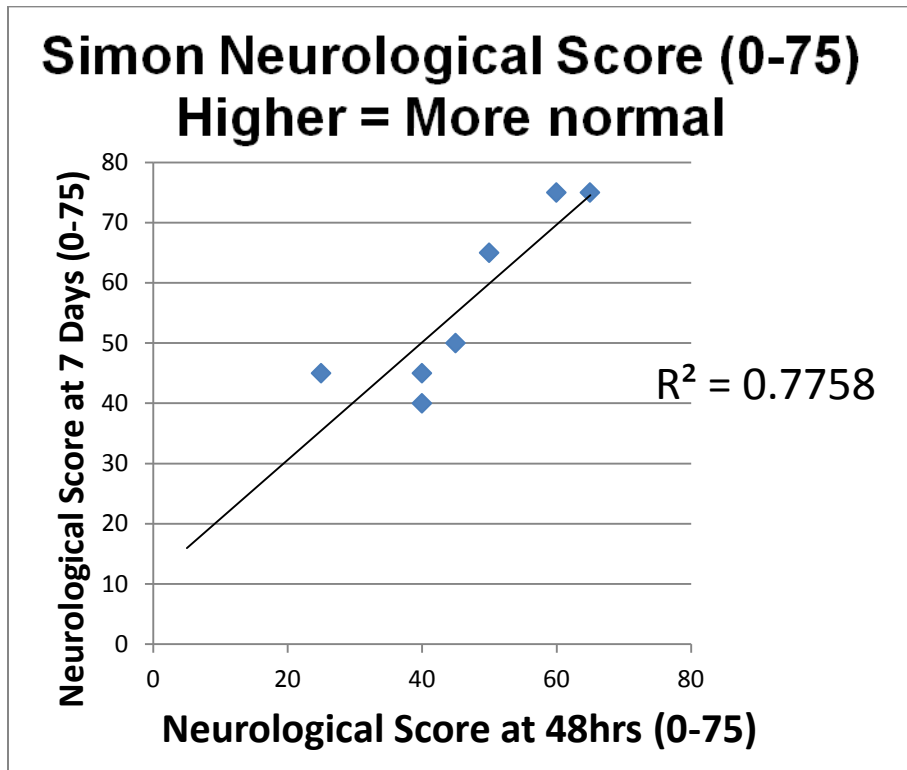


Figure 54. 7 day predictive value of day 2 Simon neurological score

Simon neurological score at 48 hours post-injury versus Simon neurological score at 7 days post-injury. N=7, data points represent individual animals. R^2 value based on linear regression analysis.

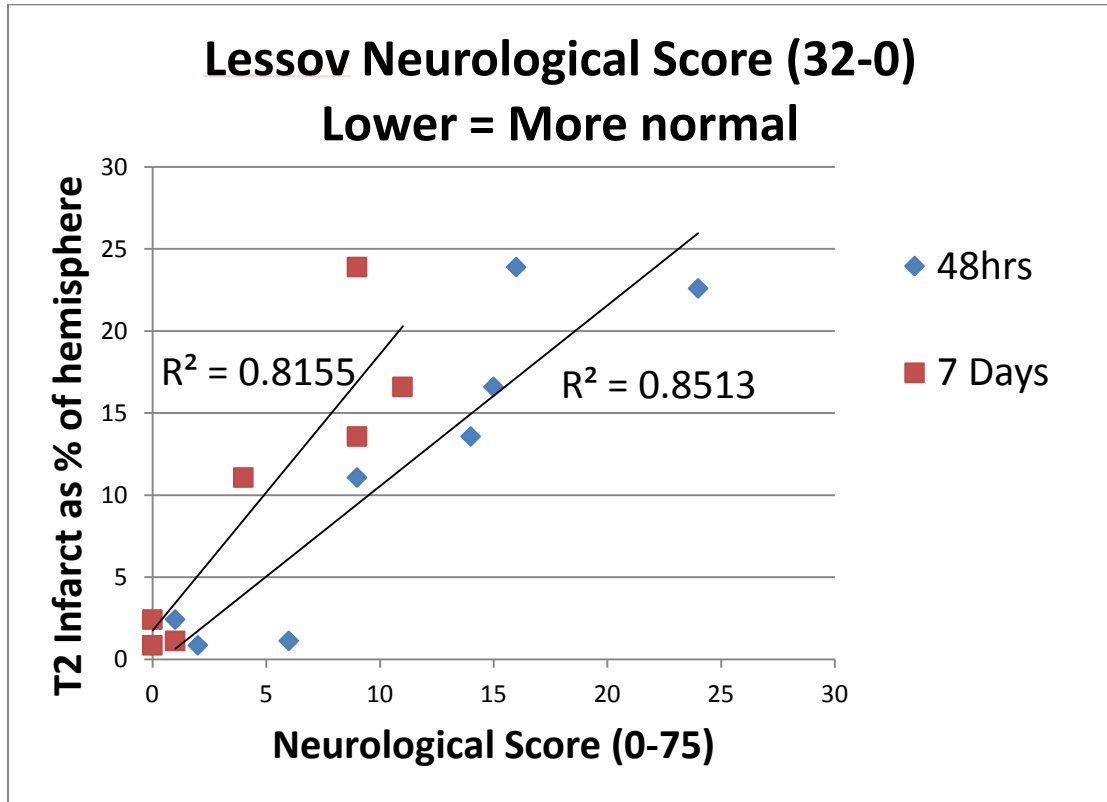


Figure 55. *Lessov neurological score correlates with infarct volume*

Neurological score at 48 hours (blue diamonds) and 7 days (red squares) post-injury versus infarct volume as assessed by T2 MRI. For the Lessov neurological scale, a higher score indicates worse neurological function. N=7-8, data points represent individual animals. R^2 value based on linear regression analysis.

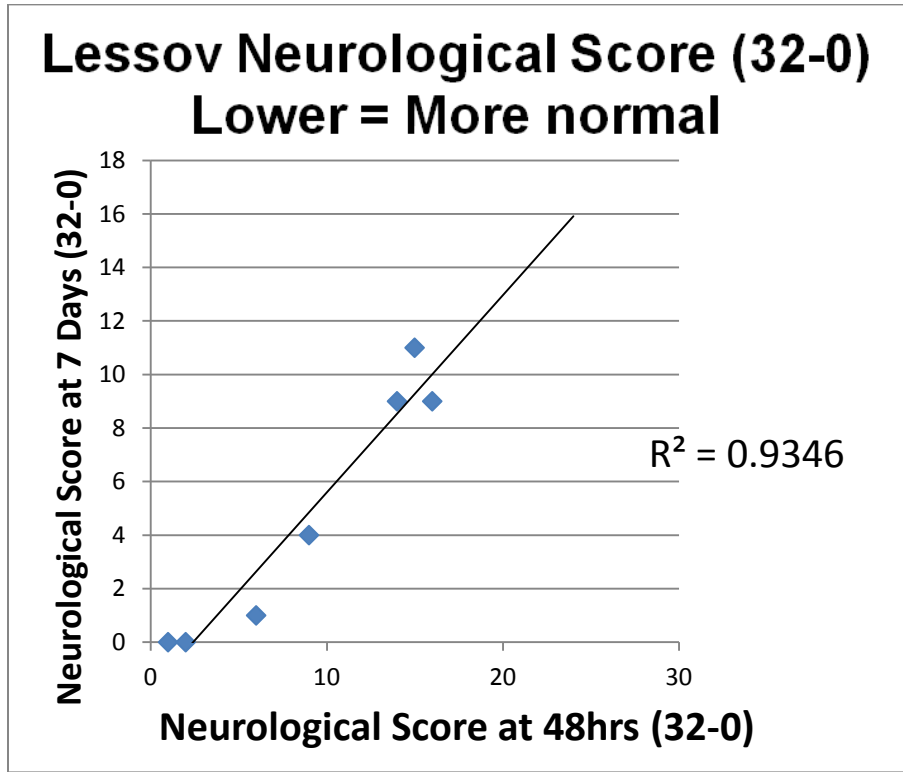


Figure 56. 7 day predictive value of day 2 Lessov neurological score

Lessov neurological score at 48 hours post-injury versus Lessov neurological score at 7 days post-injury. N=7, data points represent individual animals. R^2 value based on linear regression analysis.

APPENDIX H

Manuscript #4

Changes in spontaneous activity assessed by accelerometry correlate with extent of cerebral ischemia-reperfusion injury in the nonhuman primate.

Henryk F. Urbanski^{1,2}, Steven G. Kohama¹, G. Alexander West³, Christine Glynn⁴,
Rebecca L. Williams-Karnesky⁴, Eric Earl⁵, Martha N. Neuringer¹, Lauren Renner¹, Alison
Weiss¹, Mary Stenzel-Poore⁴, Frances Rena Bahjat⁴

¹Division of Neuroscience, Oregon National Primate Research Center, Beaverton, Oregon, USA; ²Department of Behavioral Neuroscience, Oregon Health & Science University, Portland, Oregon, USA; ³Colorado Brain & Spine Institute, Neurotrauma Research Laboratory, Swedish Medical Center, Englewood, Colorado, USA; ⁴Department of Molecular Microbiology and Immunology, Oregon Health & Science University, Portland, Oregon, USA; ⁵Advanced Imaging Research Center, Oregon Health & Science University, Portland, Oregon, USA.

Appendix C is modified from the original paper published in *Translational Stroke Research* March 23, 2012.

Abstract

The use of accelerometry to monitor activity in human stroke patients has revealed strong correlations between objective activity measurements and subjective neurological findings. The goal of our study was to assess the applicability of accelerometry-based measurements in experimental animals subject to surgically-induced cerebral ischemia. Using a nonhuman primate cortical stroke model, we demonstrate for the first time that monitoring locomotor activity prior to and following cerebrovascular ischemic injury using an accelerometer is feasible in adult male rhesus macaques and that the measured activity outcomes significantly correlate with severity of brain injury. The use of accelerometry as an unobtrusive, objective preclinical efficacy determinant could complement standard practices involving subjective neurological scoring and magnetic resonance imaging in nonhuman primates. Similar activity monitoring devices to those employed in this study are currently in use in human clinical trials, underscoring the feasibility of this approach for assessing the clinical potential of novel treatments for cerebral ischemia.

Introduction

Impaired physical activity following stroke has a negative impact on the quality of life of not only stroke patients, but also their families. Approximately 700,000 people suffer from stroke each year in the United States. Of the 4.8 million Americans currently diagnosed with stroke, over one million are reported to have ongoing problems carrying out activities related to daily living [546]. Stroke often results in a profound impairment in motor activity with the degree of disability following stroke dependent upon the area and extent of the brain that is affected. Hemiparesis and hemiplegia are common neurological impairments following stroke, although a wide-range of other motor deficits can also be seen in both humans and experimental animals. Quantification of the extent of motor deficits following stroke can therefore be problematic and has been historically limited to the use of subjective neurological scales [547]. While these sophisticated neurological scoring systems have great value, they have obvious limitations in that they provide a discontinuous view of the status of motor paresis of the subject and require significant expertise to implement. Additionally, neurological scales differ in their emphases on specific deficits and often are insensitive to subtle changes in motor function [547]. The aforementioned limitations are particularly problematic for preclinical studies examining novel therapeutic strategies in a research laboratory setting. In a preclinical setting, establishing unbiased, quantitative and reliable measures of drug efficacy is essential to successful drug development.

In the search for reliable and objective measurements of motor activity, lightweight miniaturized accelerometer devices offer great promise. The major advantage of accelerometer activity monitoring is that it enables the continuous objective evaluation of motor activity using a non-invasive, safe, and convenient method. Data derived from miniaturized accelerometers have recently been validated for use as objective measures of total physical activity [548] and to evaluate the extent of motor impairment and quantitatively assess post-stroke rehabilitation and recovery outcomes in humans [549]. We postulate that these devices could also be used in preclinical development to quantitatively assess neurological outcomes in nonhuman primate (NHP) models of stroke.

Nonhuman primates are useful for modeling human pathologies since they exhibit a range of activities more similar to humans when compared to other experimental animals. A novel NHP model of stroke using a two-vessel occlusion model was recently developed by our laboratory [324]. In this model, quantitative information about the degree of brain infarction and location of injury is obtained by magnetic resonance imaging (MRI) [324]. In addition, motor function is assessed subjectively using complex neurological scales reflective of human stroke scales [333]. Although functional outcomes are a desired measure for preclinical studies testing novel therapeutics for stroke, subjective measurements of neurological deficits using traditional clinical scoring methods are difficult to apply to NHP due to an inability to accurately detect cognitive or motor impairments. Furthermore, implementation of neurological scoring systems in NHP studies is labor intensive and requires sufficient

knowledge of typical NHP behavior, as well as clinical neurology. In contrast, application of accelerometer-based activity monitoring to NHP stroke models, whereby one monitors activity in a non-invasive and unbiased fashion, could provide a more practical, continuous and reproducible measure of the neurological deficits resulting from stroke.

Although application of this technology to experimental animal stroke models has not previously been reported, activity monitoring has been applied to behavior and physiology studies in the rhesus macaque by attaching accelerometers to lightweight neck collars [550-553]. Studies by Papailiou *et al.* [552] support the hypothesis that collar-mounted activity monitors allow effective quantification of activity in rhesus macaques. These studies showed that omnidirectional accelerometers attached to collars measure whole body movements (i.e., movement of body over distance, continuous repetitive movement, jumping), whereas other behaviors (i.e., chewing, grooming, toy manipulation, and arm movement) do not significantly influence overall activity levels. These data suggested that recording whole body movement using this approach could provide a surrogate measure of motor function in rhesus macaques. Collar worn accelerometers that detect total movement provide a continuous quantitative measure of locomotor activity and may be a valuable parameter for NHP stroke models. More importantly, activity monitoring could be of significant value as a more objective measure for the evaluation of novel clinical therapeutics, and could provide a means to more effectively compare results from multiple studies from different laboratories.

The purpose of this study was to determine if the monitoring of physical activity over 24-hour activity-rest cycles by means of an Actiwatch recording device could be implemented as an additional objective measure to quantify changes in spontaneous motor activity in a rhesus macaque stroke model. Importantly, we sought to determine in this NHP cerebral ischemic injury model 1) whether quantitative results from continuous activity monitoring correlate with the extent of brain damage measured by MR imaging, 2) whether activity results correlate with subjective neurological scoring parameters and 3) whether differences in the temporal distribution of activity over a 24-hour activity-rest cycle could be discerned. The importance of this work is that by using these methods it may be possible to simplify neurological assessments in an experimental stroke model and simultaneously improve the quality of motor function data using a non-invasive approach with less potential bias.

Materials and Methods

Animal husbandry

Adult male Chinese rhesus macaques (*Macaca mulatta*, n=23) were cared for by the Division of Animal Resources at the Oregon National Primate Research Center (ONPRC) in accordance with the National Research Council's Guide for the Care and Use of Laboratory Animals. The animal care program is compliant with federal and local regulations regarding the care and use of research animals and is Association for Assessment and Accreditation of Laboratory Animal Care (AAALAC)-accredited. All

procedures were approved by the Institutional Animal Care and Use Committee (IACUC). The animals were housed indoors under controlled conditions at a constant temperature of $24 \pm 2^{\circ}\text{C}$, 12L:12D photoperiods, and regular meals at 0830 h and 1500 h (Purina High Protein Monkey Chow, Purina Mills, Inc., St. Louis, MO) supplemented with juice, fresh fruit, vegetables and candy treats; fresh drinking water was available *ad libitum* (**Figure 57**) during acclimation period. Animals received a variety pan of food post-stroke to stimulate appetite and were given treats during neurological assessments. Adult male rhesus macaques between six and twelve years of age were housed individually in a double cage within a single room. Room lights (~300 lux) were set to a 12-hour light/dark cycle starting at 0700 h and ending at 1900 h daily. Animals were subject to morning observations between 0730 h and 0800 h, and received enrichments between 1300 h and 1400 h. In addition, room washing was performed daily between 1000 h and 1100 h, except for the days following surgically-induced stroke.

Animal selection and acclimation

Approximately 3 weeks prior to stroke surgery, adult male rhesus macaques were examined for general health by the attending veterinarian and then moved to their study cages for acclimation. At this time an Actiwatch activity monitor was attached to each animal's collar and a blood sample was collected to help identify potential health concerns. Animals were selected based on normal results from a

physical examination and/or normal clinical laboratory findings. Exclusion criteria included: 1) abnormal hematology and/or clinical chemistry values outside of 2SD from mean of our historical ranges in adult male Chinese rhesus macaques (data from >60 individual age/sex-matched controls), 2) recent invasive procedures (e.g., dental cleaning or tooth extraction), 3) presence of serum cytokines or other indicators of inflammation or infection (e.g., tooth abscess, high c-reactive protein levels, visible injury, chronic diarrhea), 4) neurological disorders evident by abnormal motor or cognitive abilities, or 5) stress-associated behaviors.

Surgical protocol

Cerebral ischemia was induced using procedures previously described [191] for the purpose of testing the efficacy of novel therapies for stroke. Briefly, up to four weeks before surgery, animals were screened for general health, endemic disease, and neurological disorders. Animals were given ketamine (~10mg/kg, intramuscular injection) and then intubated and maintained under general anesthesia using 0.8% to 1.3% isoflurane vaporized in 100% oxygen. A blood sample was taken and a venous line was placed for fluid replacement. An arterial line was established for blood pressure monitoring throughout surgery and to maintain a mean arterial blood pressure of 60-80 mm Hg. End-tidal CO₂ and arterial blood gases were continuously monitored to titrate ventilation to achieve a goal PaCO₂ of 35-40 mm Hg. The right middle cerebral artery (distal to the orbitofrontal branch) and both anterior cerebral arteries were exposed and

occluded with vascular clips for 60 minutes, as previously described [191, 324]. Surgical procedures were conducted by a single surgeon. Post-operative analgesia was given on Days 1 and 2 post-op consisting of intramuscular hydromorphone HCl and buprenorphine. Animals were monitored closely for the 7 study days following stroke.

Infarct volume measurements

Infarct volume was measured from T2-weighted magnetic resonance images taken after 2 days of reperfusion [324]. All scans were performed on a Siemen's 3T Trio system, housed on-campus near the surgical suite at ONPRC. Because of the small filling capacity of the rhesus macaque head, a human extremity coil was used to achieve better image quality of the brain. Animals were given ketamine (10 mg/kg intramuscularly) and a blood sample collected. Animals were then intubated and administered 1% isoflurane vaporized in 100% oxygen for anesthesia maintenance. All animals received numerous anatomical MRI scans. The T2 scan was a turbo spin-echo protocol, with TR=5280 ms, TE=57 ms, number of averages=4, an echo train length of 5, and a refocusing pulse flip angle of 120°. The entire brain was imaged with a 0.5 x 0.5 mm in-plane resolution and a slice thickness of 1 mm. Images from T2-weighted MRIs were examined for the location of infarction, and the total affected area measured using ImageJ, as previously described [324] by sampling approximately 15 slices (4 mm each). Measurements of infarct volume as a percentage of the ipsilateral hemisphere were

made using the following formula: (volume of infarcted tissue of the ipsilateral hemisphere / total volume of the ipsilateral hemisphere) x100%.

Neurological assessments in NHP

Neurological assessments were performed by a single observer as previously described for this model [191] using a scoring system adapted from that previously described [333]. Our scale evaluates motor function and behavior (mental status) with higher scores representing better functional outcomes (100=normal). Motor function is scored from 1 to 70, according to severity of hemiparesis in the left extremities. A score of 10=severe hemiparesis, 25=moderate hemiparesis, 40= slight hemiparesis, 55=favors normal side, or 70=normal ability. Behavior and alertness are scored ranging from 1 to 20, with 1=unresponsive, 5=aware but inactive, 15=aware but less active, and 20=normal. Facial deficit was scored as 1=one-sided paralysis or 5=normal facial movement. Visual deficit was scored as 1=present and 5=absent.

Actiwatch device

The Actiwatch activity monitor consists of a piezoelectric accelerometer with 64 kilobytes of memory capacity [550], which records the integration of intensity, amount, and duration of movement in all directions with a force sensitivity of 0.05 g and a maximum sampling frequency of 32 Hz. Each animal was fitted with an Actiwatch

(Philips-Respironics, Bend, OR, USA; part number U198-0301-00) placed inside a protective case (Philips-Respironics; part number 198-0232-00 M) and then attached to a lightweight loose-fitting aluminum collar (Primate Products, Inc., Immokalee, FL) approximately 3-4 weeks prior to surgery, as described previously [553]. Continuous recordings were made approximately 21 days prior to surgery and up to 8 days after surgery. Devices were programmed to collect data in 60-second epochs and data were downloaded using a dedicated reader (Philips-Respironics; part number 198-0150-00). Data were interpreted and actograms drawn using Actiware-Sleep version 3.4 software (Cambridge Neurotechnology Ltd, Cambridge, United Kingdom). The mean daytime activity (defined as activity during the period between 0700 h and 1859 h) and mean nocturnal activity (activity between 1900 h and 0659 h) were calculated. In addition, the mean total daily activity defined as the sum of the daytime and nocturnal activity, as well as the ratio of day to nocturnal activity defined as the daytime activity divided by the nocturnal activity, were tabulated prior to stroke and after stroke (**Table 10**). Individual daily activities from the 4 consecutive days the week prior to surgery (**Figure 58**) were tabulated generating a mean baseline value according to the following: mean baseline activity = $(A_{\text{Day-7}} + A_{\text{Day-6}} + A_{\text{Day-5}} + A_{\text{Day-4}}) / 4$; where A=activity. The activities of Days 3 thru 6 post-surgery (comprised of days following the cessation of post-surgical drug administration) were used to determine post-stroke changes in activity. The percent change from mean baseline value was calculated for each of the four days using the following equation: % change = $(\text{post-stroke activity}_{(\text{Day } x)} / \text{mean baseline activity}) * 100$. The mean % change post-stroke was then calculated. Animals sacrificed

prior to Days 3-6 post-stroke were assigned a value of 100% as a mean reduction in activity.

Data exclusions

Data show that rhesus macaques typically demonstrate stable daily circadian rhythms of motor activity [554]. As an *a priori* exclusion criterion for this analysis, we retrospectively evaluated this parameter for each animal in our study. Day-to-day changes in total activity were determined for each animal by examining Days -7 to -4 from the week prior to surgery for individual animals according to the following equation: mean % change in day-to-day activity = (% change in activity_{Day-7 to -6} + % change in activity_{Day -6 to -5} + % change in activity_{Day -5 to -4}) / 3. The mean (\pm SEM) change in day-to-day activity was 14% \pm 3% for the entire cohort (n=21). A single animal demonstrated 53% mean change in activity level day-to-day and as such was excluded from all analyses as a significant outlier for baseline activity (>2.5 SD from the mean of the group). The reason for unstable baseline activity levels in this animal was unclear.

Data and statistical analyses

Data described in the text reflect mean \pm SD unless otherwise noted. All statistical analyses were performed using Prism 5.0 software (GraphPad Software, La Jolla, CA). Correlations between parameters were determined using Pearson's

correlation. Differences were considered statistically significant when two-tailed $p < 0.05$. It was necessary to terminate five animals with large infarcts at two days following surgical occlusion. For analysis of neurological data, rather than assigning a value of zero for days following termination, the last measured observation was carried forward (LOCF) for subsequent days when animals were terminated prior to the end of the study. The LOCF method is often used for clinical data to handle attrition or incomplete longitudinal data. We justify the decision to use this method by examining our historical data, which shows that little if any improvement occurs in severely affected animals beyond day 3. Rather than analyzing only study completers or assigning a zero value, the LOCF method in our case offers less bias as the final measured carried forward likely underestimates severity of neurological deficits for days following termination rather than overestimating it. For data analysis of activity data, animals were assigned a value of 100% decrease in activity level due to early termination. We justify this analysis approach since animals with severe infarcts (>25%) surviving to the end of the study had >80% reduction in activity levels for all but nocturnal activity and activity levels, like neurological scores, do not typically show improvement over this 7 day time period in this stroke model. LOCF method could not be used in this case since activity measurements taken at day 2 prior to termination were compromised by the administration of post-stroke analgesics. Statistical analyses of these data were performed with both the inclusion and the exclusion of these early terminated animals. We found that the statistical significance of correlations between infarct or neurological score and activity parameters were independent of data from these animals ($p < 0.05$ for

all correlations), with the exception of nocturnal activity ($p=0.97$ versus infarct and $p=0.32$ versus neurological score) which did not achieve statistical significance without these data.

Results

Locomotor Activity Levels Change Following Cerebral Ischemic Injury

Following cerebral ischemic injury induced by two-vessel surgical occlusion, adult male rhesus macaques demonstrated a range of responses spanning from mild hemiparesis (reduced movement) to paralysis (no movement) of upper and/or lower limbs. Facial paresis was also commonly observed, as demonstrated by an asymmetrical grimace and difficulty chewing on the affected side. Distal plegia of the upper limb (hand) was more commonly present while lower limb deficits were seen rarely and varied in severity, although when present, mild paresis of distal lower limb was most commonly observed. Behavioral changes were varied but the majority of affected animals generally were alert and responsive with good mentation, although decreased aggression and fear responses were sometimes observed. Following stroke, the animals demonstrated reduced activity levels, a phenotype that has not previously been quantified in NHP stroke models and our study specifically aimed to quantify these changes.

In general, total activity levels dramatically decreased (~80%) following stroke. Furthermore, decreases in daytime activity predominated and were related to severity of injury. In contrast, nocturnal activity was generally decreased following stroke irrespective of infarct size (~28% mean reduction compared to baseline) although a few animals showed increased activity (~30% increase) compared to their baseline values. A representative actogram showing activity count patterns from a single animal illustrates the total daily activity measured prior to (**Figure 59**, baseline) and following stroke (**Figure 59**, recovery). These images of the raw activity data depict a substantial decrease in activity typically observed following stroke in this model, as compared to activity recorded prior to stroke.

Changes in Activity Levels Correlate with the Extent of Brain Injury

The extent of cerebral ischemic injury following surgical occlusion can be measured using an MRI approach that derives infarct volumes as a percent of hemisphere (**Figure 60**). Infarct volumes in this study ranged from 0 to 37% of ipsilateral hemisphere at 2 days following occlusion. We hypothesized that the resulting infarct volume would be proportional to the change in activity level, in that animals with larger infarcts would demonstrate greater decreases in activity after stroke as compared to their baseline values. As predicted, the percent change in post-stroke total daily activity (**Figure 61 A**) and daytime activity (**Figure 61 B**) compared to baseline values significantly correlated with infarct volume. These data reinforce the notion that a

dramatic decrease (~80%) in the magnitude of post-stroke activity occurs in animals with severe brain injury.

Nocturnal activity levels in rhesus macaques at baseline compared to values determined after stroke were not substantially different, although a nearly significant correlation between infarct volume and nocturnal activity was observed (**Figure 61 C**; $p=0.05$). Mean daily nocturnal activity prior to stroke ranged from 8.6 to 89 counts in all male rhesus macaque animals tested (10-fold range), with a mean nocturnal activity value of 29 ± 16 counts per day for the entire cohort. Similarly, mean daily nocturnal activity after stroke ranged from 11.4 to 54.5 mean daily counts (~5-fold range) with a mean nocturnal activity of 25 ± 12 counts per day for the entire cohort. Although mean nocturnal activity did not change dramatically following stroke, we did note a proportional increase in nocturnal activity compared to daytime activity. Nocturnal activity accounted for 3-15% of total activity at baseline prior to stroke and 16-39% after stroke in our study cohort. The reason for a perceived proportional increase in nocturnal activity is primarily due to a concomitant decrease in daytime activity. Therefore, an overall decrease in total activity occurred, mostly comprised of decreased daytime activity, which lead to a concomitant decrease in day:night activity ratio. The ratio of day:night activity correlated significantly with infarct volume (**Figure 61 D**).

We hypothesized that the surgical model itself or the stress involved in the manipulation of the animals would result in measurable changes in activity levels that were unrelated to the severity of stroke. To address this hypothesis, baseline changes in

day-to-day activity prior to stroke were determined for each animal and these changes were compared to mean changes in activity among animals demonstrating only minor brain injury defined as infarct volume $\leq 3\%$ of ipsilateral hemisphere. Overall, most animals had stable daily motor activity prior to stroke, as demonstrated by minimal individual variation in total daily activity levels during the acclimation period prior to stroke. Data from the 22 animals included in this analysis revealed that the mean change in baseline day-to-day activity prior to stroke over a prescribed 4-day period was $11\% \pm 6.5\%$ (**Figure 62**), with individual values ranging from 2 to 25%. In contrast, animals that had very minimal stroke outcomes ranging from 0-3% of hemisphere (n=4; $1.8 \pm 1.3\%$ infarct) demonstrated a mean decrease of 51% in total daily activity level (**Figure 62**), as well as mean decreases of 57% in daytime activity and day:night activity ratio compared to baseline values. Mean change in baseline day-to-day activity prior to stroke was only 9% for this minor stroke outcome group with individual baseline changes ranged from 3-17%. These data suggest that the experimental protocol may result in substantial activity changes irrespective of infarct volume. Importantly though, activity changes in animals with severe stroke outcomes $>3\%$ hemispheric infarct (n=18; mean infarct of $23 \pm 2\%$) showed even greater mean decreases in total daily activity (83%; **Figure 59**), daytime activity (86%), and nocturnal activity (35%) compared to their changes in day-to-day baseline activity prior to stroke ($13 \pm 3\%$ mean total daily activity change). These results argue that the experimental protocol contributes to significant activity changes ($\sim 51\%$), although correlation analyses (**Figure 61**) show that activity changes beyond that level were indeed correlated with infarct severity.

Changes in Activity Levels Correlate with Neurobehavioral Outcomes

Given the proper training and experience, subjective measurement of neurological deficits using traditional clinical scaling methods can be difficult, though not impossible, to apply to NHP. In our study, daily neurological assessments of rhesus macaques following surgical occlusion revealed that the extent of motor deficits compared to baseline values were related to infarct severity quantified by MRI at 48 hours (**Figure 63**). As we previously reported for adult male Indian rhesus macaques [324], infarct volumes in adult male Chinese rhesus macaques correlated with the cumulative neurological scores ($p < 0.001$; **Figure 63**). Animals having small 0-3% hemispheric infarct had a range of 592-696 cumulative neurological score (score of 700=no deficit) with a group mean score 648 ± 50 , whereas animals with >3% hemispheric infarct had greater functional neurological deficits with a mean cumulative score of only 203 ± 139 .

While these data validate the use of subjective scoring, these methods are not easily transferred between laboratories and much training is required to implement our scoring paradigm. Therefore, we aimed to determine if objective activity measures were related to subjective neurological scores by performing correlation analyses. Indeed, we found that the changes observed in total daily activity levels (**Figure 64 A**), daytime activity levels (**Figure 64 B**), nocturnal activity (**Figure 64 C**) and day:night activity ratio (**Figure 64 D**) correlated with the level of cumulative neurological deficits measured by

subjective neurological scores. Of all of the activity parameters measured in this study, nocturnal activity was least affected by infarct severity. In the absence of data points reflective of animals terminated early (100% reduction), nocturnal activity data did not significantly correlate with neurological score ($p=0.3$). All other activity parameters correlated with neurological score irrespective of the inclusion of data from these animals. This suggests that nocturnal activity may not be significantly affected by extent of infarct or neurological function.

Discussion

Neurological behavior scoring in a nonhuman primate model of experimental stroke requires personnel with special behavioral training, and is a time consuming process. For example, understanding of the typical behavior patterns of individual monkeys and their reactions to certain stimuli allows for a better interpretation of changing behaviors after the onset of brain damage. However, monkeys often mask signs of weakness or physical deficits, an inherent behavior arising from the fear of predation [555]. Thus, assessing motor dysfunction requires astute observation of each animal by a skilled observer. Once a study has begun, it is ideal to have a single “blind” observer perform the neurological scoring. However, large stroke studies may span for several years and thus observer consistency cannot always be guaranteed. These, as well as other factors, highlight the obvious complexities involved in subjective analysis of neurological deficits in nonhuman primates, as well as the need for additional

methods to consistently and objectively evaluate functional neurological deficits both within and between laboratories.

Clinical studies employ accelerometer devices worn by patients following stroke, allowing for quantitative comparisons between affected and unaffected limbs [549, 556, 557]. In one such study actigraphic recordings of total motor activity were lower on the impaired arm versus non-impaired arm. These data revealed a significant positive correlation between motor activity and neurological scores including the Scandinavian Stroke scale, the Barthel Index, and the Rankin Scale Score during the 1st week post-stroke, corresponding to the time when neurological deficits were most pronounced [558]. While not able to directly assess affected limbs in monkeys, we now show that measuring total body activity using neck collars correlates with outcome in our stroke model. Similarly, we show that actigraphy can be used to evaluate changes in activity occurring in singly-caged nonhuman primates following strokes. Studies in adult female rhesus macaques showed that similar activity (measured by accelerometer or energy expenditure due to physical activity measured by indirect calorimetry) was observed between monkeys housed in single cages versus monkeys housed in group pens [559]. The most active monkeys tended to rank as more active regardless of the type of housing conditions. These findings argue that level of activity may be inherent to an individual and changes in patterns of activity can be accurately assessed even in the context of caged housing conditions.

In general, we show that activity in the rhesus macaque was dramatically reduced following stroke in a manner related to the infarct volume and neurological outcomes using a validated neurological stroke scale. Notably, all animals on this study showed a decrease in activity following the surgical occlusion procedure regardless of infarct volume or extent of neurological deficit. In our study animals showing minimal to no infarct and minimal neurological deficits demonstrated an approximate 51% reduction in total activity after the stroke procedure versus their baseline activity. In comparison, a less than 10% baseline daily change in activity was observed at baseline prior to surgical manipulation of these animals. These data suggest that the experimental protocol results in a reduction in total activity regardless of the severity of clinical outcome. These data could also argue that some damage is unidentifiable by MRI, but may contribute to a decline in activity; therefore, a detailed histological examination may be warranted as gross examination of the brain tissue from these animals did not appear noticeably infarcted by day 7 following stroke (data not shown). Importantly though, animals with larger strokes demonstrated much larger decreases in activity which correlated with infarct severity suggesting that an appropriate dynamic range still exists for this outcome variable. Therefore, activity parameters measured by actigraphy may indeed be useful as an outcome variable in preclinical studies testing novel drug candidates.

Individual differences in daily pattern and level of activity have been readily observed in humans [560] and experimental animals [561, 562]. In general, animals with higher daytime activity tend to have higher nocturnal activity as well. Therefore, using

day:night activity ratio values for each animal can serve to normalize activity levels among individuals and more reliably explore changes in patterns of activity. Nocturnal activity varied significantly between individual animals in our study. This finding was anticipated because several published studies note a similar 10-fold range in the duration and level of nocturnal activity in both free-ranging male [563] and cage-housed female rhesus monkeys [562]. One study showed that nocturnal activity was correlated with daytime activity, suggesting that similar mechanisms are operating at both times of day and similar variability exists. This positive correlation between day and nighttime activity is also reinforced by studies in humans [564].

The mechanisms that regulate physical activity are poorly understood although studies show that several neurotransmitters (e.g. serotonin, dopamine, norepinephrine [565]), as well as estrogens [566], have all been shown to regulate physical activity. Moreover, certain brain regions may be involved in activity regulation [565]. Studies of lesioned areas of the basal forebrain, ventromedial hypothalamus, paraventricular nucleus, amygdala, and thalamus suggest that these structures may play a role in regulating activity [565], although these are not areas commonly affected in our model. Mechanisms that appear to regulate nocturnal activity include orexin A [567]. Moreover, recent data show that orexin A injected into the paraventricular nucleus increases both daytime and nocturnal activity in rats suggesting that orexin A may play a role in global activity regulation [567]. Another worthy goal of future studies would be to evaluate the status of neurotransmitters, hormones, and orexin A in the context of

stroke in the rhesus macaque and to correlate these values with changes in activity level.

Activity changes due to stroke pathology are but one aspect of this technology. Accelerometry was also recently used as an outcome measure in a human clinical study in patients with stroke. The effects of indeloxazine hydrochloride and ticlopidine hydrochloride was evaluated in 17 patients with stroke [557]. These data showed that both groups of patients treated with drugs improved significantly after an 8-week administration period compared to the improvement seen in the control group. Our data show that actigraphy may similarly be a useful surrogate marker of efficacy in preclinical stroke studies in nonhuman primates, such that improvement in activity measures could be indicative of improvement in neurological function and a reduced infarct volume, and ultimately drug efficacy. Moreover, temporal changes are often not adequately discerned by subjective neurological scoring performed at limited or prescribed time points, whereas actigraphy could allow for such continuous analysis. This method also provides an inexpensive means to follow neurological improvement or decline with minimal expert staff or imaging needs over long periods of time. There could be significant value in the assessment of clinical improvement over time, which may be a component of efficacy with some stroke therapeutic strategies. Human studies evaluating motor and functional recovery patterns after stroke have confirmed the importance of the first month for recovery [568], which is a timeframe easily monitored by these devices.

In this study, we confirm that changes in activity occur following stroke and these changes correlate with severity of stroke measured by infarct volume or neurological score in a rhesus macaque model of cerebral ischemic injury. These data show that objective activity measures can be used to support neurological findings lending to the rapid adaptation of these methods among many laboratories. Additionally, the use of such devices for the preclinical evaluation of therapeutics in a monkey model of stroke has the potential to provide a more extensive assessment of changes in global activity. Studies to validate the use of actigraphy in a preclinical setting by testing the efficacy of novel therapeutics in this rhesus macaque stroke model are underway. These studies should provide more insight as to the benefits of this technology for stroke drug development.



Figure 57. *Daily schedule*

Animals received visitors according to daily schedule where light gray circle indicates morning clinical observations, star indicates times of food administration, black dot denotes enrichment time, and square indicates room washing. Timeline reflects 12 hour light-dark cycle wherein black denotes periods of lights out (nighttime or nocturnal activity) between 0700 h and 1859 h and white denotes periods of lights on (daytime activity) between 1900 h and 0659 h.

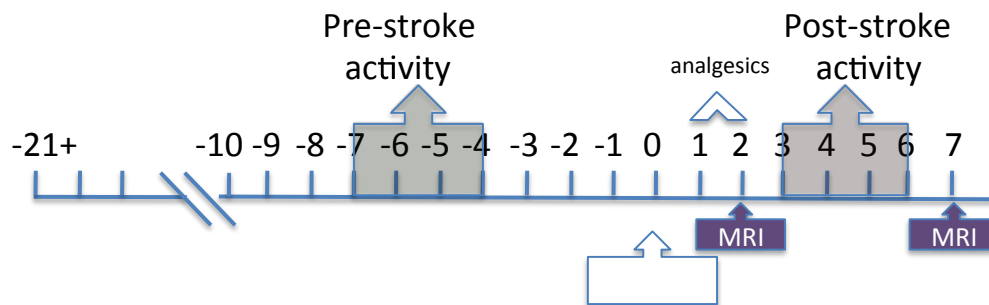


Figure 58. Study timeline

Animals are acclimated for three weeks prior to stroke. At baseline prior to stroke activity levels from Days -7 to -4 were used to derive a mean baseline activity level for each animal for each parameter. Following stroke, activity levels from Days 3 to 6 of the study were used to derive individual post-stroke mean activity levels. Post-stroke values were then compared to baseline mean activity values and the percent change in activity post-stroke was determined for each activity parameter for each animal.

Table 10. *Activity parameters*

Parameter	Definition
Total daily activity	Activity between 0 and 2400 h
Daytime activity (D)	Activity between 0700 h and 1859 h
Nocturnal activity (N)	Activity between 1900 h and 0659 h
Day:Night activity ratio	Equal to D/N

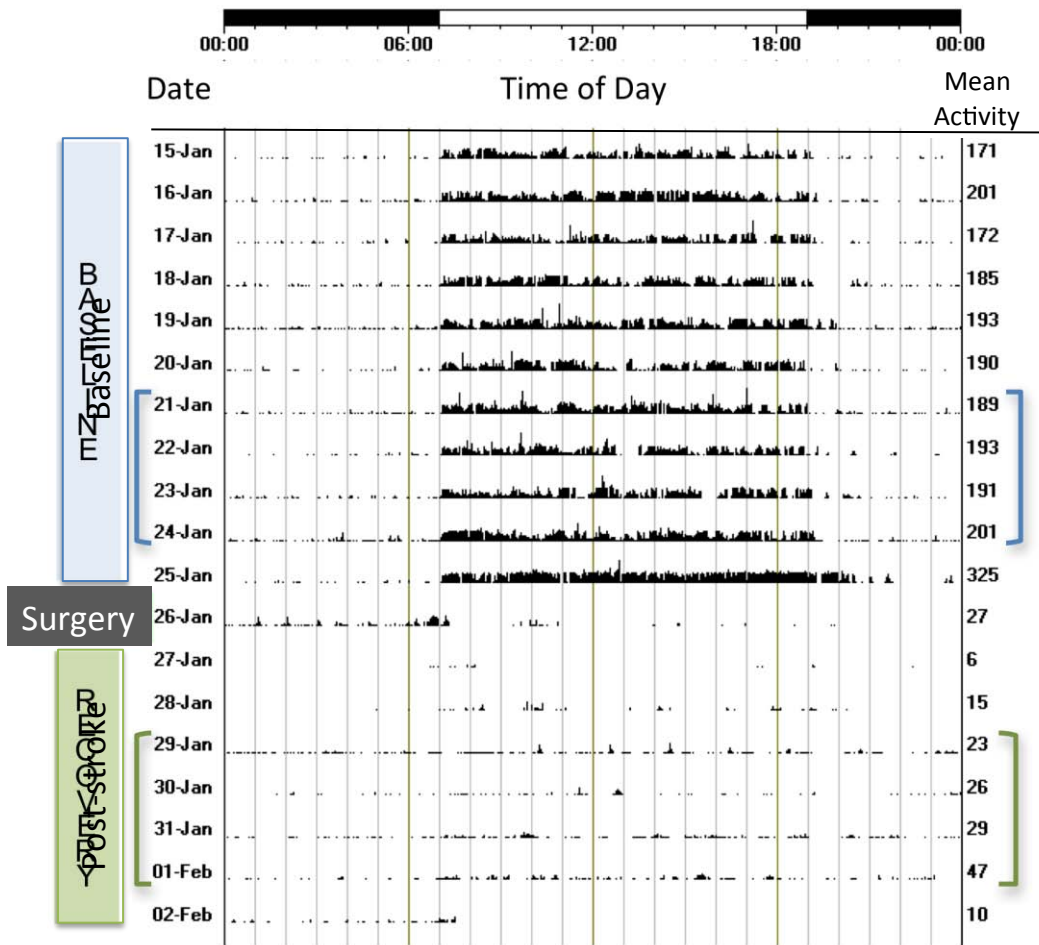


Figure 59. Actogram representing a subset of continuous recordings made prior to and following stroke in a representative animal with a measured infarct volume of 26% by MRI method

The time of day is depicted at the top with the black bar representing lights off (from 1900 h to 0659 h, nocturnal activity) and white section depicting the period when lights are on (from 0700 h to 1859 h, daytime activity). The days used for calculating percent changes are denoted in blue and green brackets on right and left of actogram within the baseline and post-stroke timeframes.

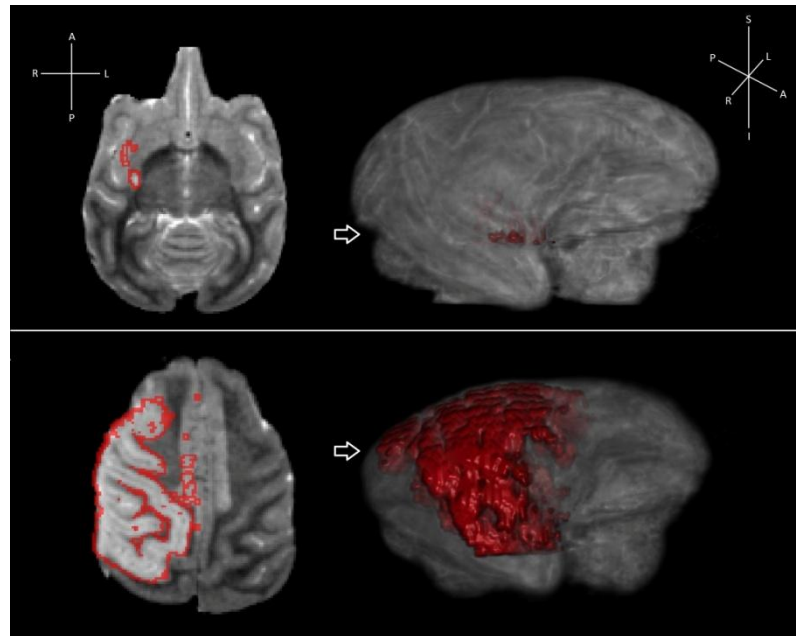


Figure 60. Representative brain images showing infarct regions determined by T2-weighted MRI

Data reflect representative MR images of an animal with a 3% stroke volume (top panel) and 26% stroke volume (bottom panel). The figures on the left of each panel are of a single axial slice collected at the level of the arrow seen on a 3-D representation of each brain (right). Areas of infarct are hyperintense, circumscribed on the axial slices and denoted in red on the 3-D reconstruction. Lines represent the anterior (A)-posterior (P), left (L)-right (R) and inferior (I)-superior (S) axes.

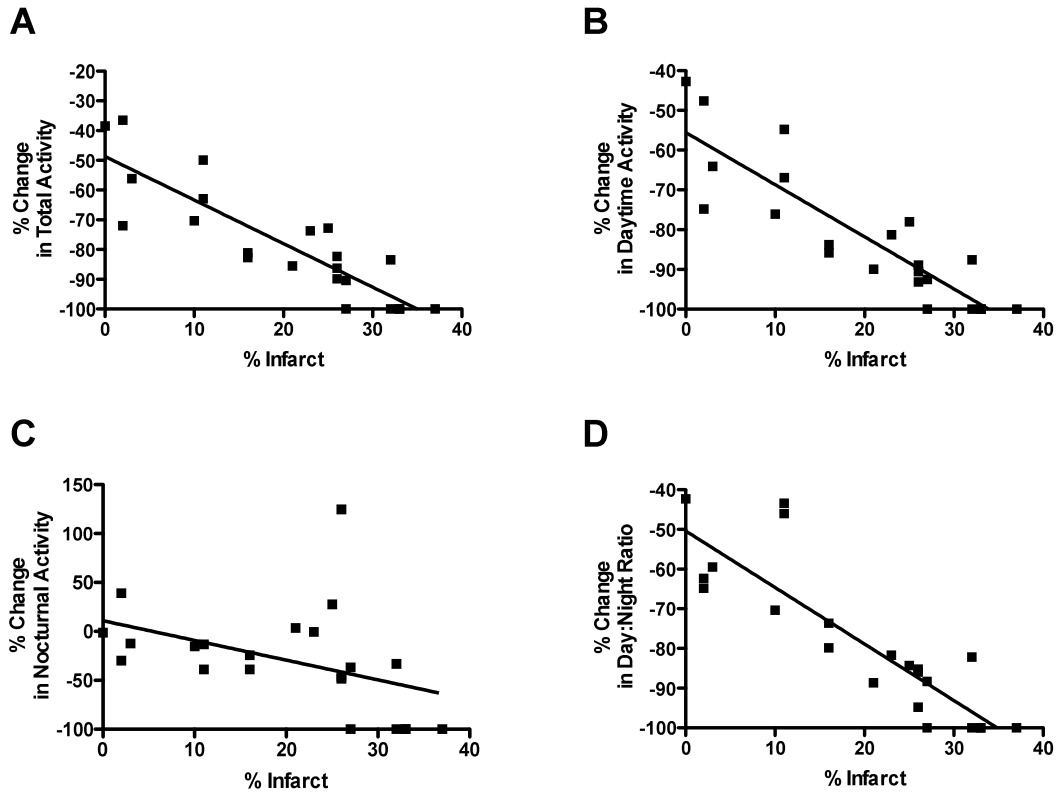


Figure 61. Correlation between mean activity values versus infarct volume

Pearson's correlation was performed using (A) total activity ($p < 0.0001$), (B) daytime activity ($p < 0.0001$), (C) nocturnal activity ($p = 0.05$) or (D) day:night activity ratio ($p = 0.05$) versus infarct volume measured at 48 hours post-stroke. Data show that all but nocturnal activity correlated with infarct volume. Baseline activity changes (not shown) were not significantly correlated to infarct volume.

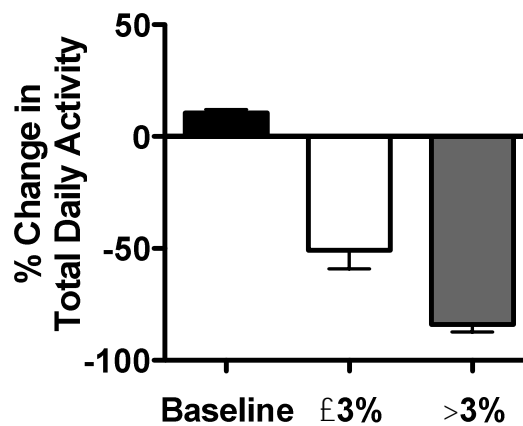


Figure 62. *Changes in total daily activity were related to the experimental procedure and infarct volume*

At a fixed timepoint ~1 week prior to stroke following ~2 weeks of acclimation in home cages, the mean change in day-to-day activity over 4 consecutive days was determined for each animal (Baseline). Mean change in total daily activity including animals with infarct volumes $\leq 3\%$ of hemisphere are shown (white bar, n=4), compared to data from animals with $>3\%$ infarct (grey bar; n=18).

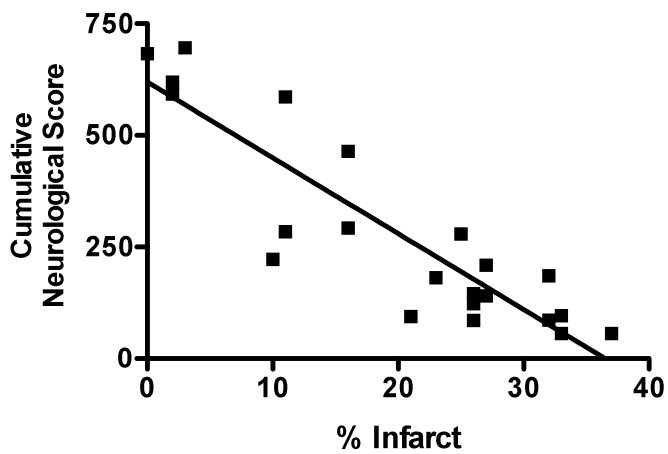


Figure 63. *Correlation between total cumulative neurological score and infarct volume*

Correlation analysis revealed statistically significant correlation between cumulative neurological score and infarct volume measured as percent of ipsilateral hemisphere ($p < 0.0001$).

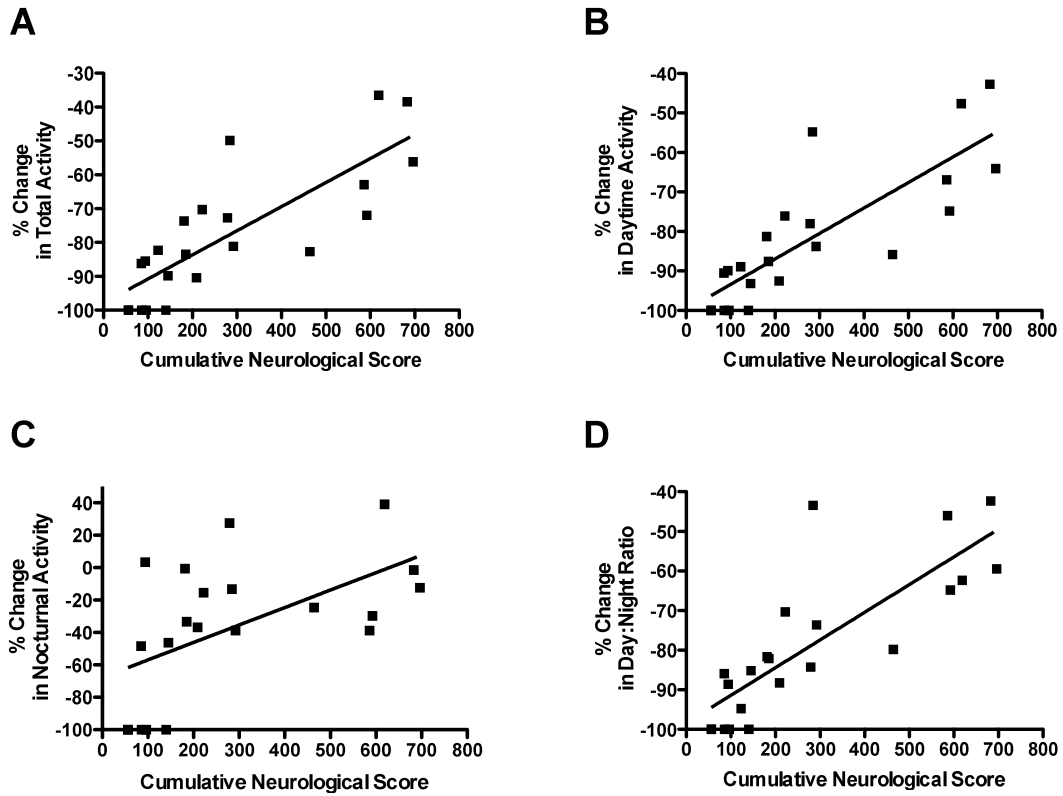


Figure 64. *Correlation between percent change in mean activity counts and cumulative neurological scores*

Pearson's correlation analysis revealed statistical significance for **(A)** total activity ($p < 0.0001$), **(B)** daytime activity ($p < 0.0001$) **(C)** nocturnal activity ($p = 0.008$) and **(D)** day:night ratio ($p < 0.0001$) versus mean cumulative neurological score. Baseline activity changes (not shown) were not significantly correlated to neurological score.

APPENDIX I

Characterization of the peripheral immune response following stroke in a non-human primate model

Background

Despite the discovery of numerous promising compounds that have been highly efficacious in rodent models of stroke, a large number of putative neuroprotective compounds have failed in clinical trials [314], and no clinical neuroprotective therapeutics exist. Recommendations from the Stroke Therapeutic Academic and Industry Roundtable (STAIR) suggest the use of non-human primate (NHP) models of stroke as translational tool to screen neuroprotective compounds in stroke prior to their advancement to clinical trials [315]. The immune response plays a key role in regulation of damage following cerebral ischemic/reperfusion injury [26, 27]. Rhesus macaques, used in the current study to model cerebral ischemic/reperfusion injury, have been shown to have similar immune responses, with some difference in subpopulation compositions [569]. If NHP models of stroke are to prove useful in vetting clinical stroke therapeutics, a better understanding of the similarities and differences between the

immunological responses to stroke between humans and NHPs is needed. This is especially true when evaluating therapies that involve modulation of the immune system prior to or after cerebral ischemia.

Material and Methods

Blood samples

Nine male rhesus macaques (*Macaca mulatta*) of Chinese origin with an average age of 8.8 ± 2.3 years and an average body weight of 8.4 ± 1.7 kg, Animals were single-housed indoors in double cages on a 12h:12h light/dark cycle, with lights-on from 0700 to 1900h, and at a constant temperature of $24 \pm 2^\circ\text{C}$. Laboratory diet was provided bi-daily (Lab Diet 5047, PMI Nutrition International, Richmond, IN) supplemented with fresh fruits and vegetables, and drinking water was provided *ad libitum*. The animal care program is compliant with federal and local regulations regarding the care and use of research animals and is Association for Assessment and Accreditation of Laboratory Animal Care (AAALAC)-accredited. All animal experiments were subject to approval by the Institutional Animal Care and Use Committee (IACUC) at the Oregon National Primate Research Center.

Peripheral blood was obtained from via femoral blood draw 4 weeks prior to surgery, at the time of surgery, 48 hours after surgery and 7 days after surgery (**Figure 62**). PBMCs were isolated from the freshly obtained, heparinized peripheral blood by

Ficoll-Hypaque density gradient centrifugation. Hematological parameters were determined from whole blood collected at the same timepoints using an ABX Pentra 60 analyzer (Horiba Medical, Irvine, CA).

Two-vessel Occlusion Protocol in NHP

Four weeks before surgery, animals were screened for general health, endemic disease, and neurological disorders. The right middle cerebral artery (distal to the orbitofrontal branch) and both anterior cerebral arteries were exposed and occluded with vascular clips, as previously described [324]. Surgical procedures were conducted by a single surgeon. Briefly, anesthesia was induced with ketamine (~10 mg/kg, intramuscular injection) and animals were then intubated and maintained under general anesthesia using 0.8% to 1.3% isoflurane vaporized in 100% oxygen. A blood sample was taken and a venous line was placed for fluid replacement. An arterial line was established for blood pressure monitoring throughout surgery to maintain a mean arterial blood pressure of 60 to 80mmHg. End-tidal CO₂ and arterial blood gases were continuously monitored to titrate ventilation to achieve a goal PaCO₂ of 35 to 40 mm Hg. The surgery was performed as described previously [324]. Post-operative analgesia consisted of intramuscular hydromorphone HCl and buprenorphine.

Infarct measurement

Measurement of infarct volume was performed using T₂-weighted magnetic resonance images taken after 48 hours of reperfusion [324]. All scans were performed on a Siemen's 3T Trio system, housed near the surgical suite at ONPRC. Because of the small filling capacity of the rhesus macaque head, an extremity coil was used to achieve better image quality of the brain. Anesthesia was induced initially with ketamine (10mg/kg intramuscular injection) and a blood sample was obtained. The animals were then intubated and administered 1% isoflurane vaporized in 100% oxygen for anesthesia maintenance. Animals were scanned in the supine position 2 days after surgery, and most animals also received baseline scans before surgery. Animals were monitored for physiologic signs, including pulse-oximetry, end-tidal CO₂, and respiration rate. All animals received anatomical MRI scans, which included T₁- and T₂-weighted, high-resolution time of flight scans, and a diffusion-weighted scan. The T₁ scan was an MPAGE protocol, with TR=2500ms, TE=4.38ms, number of averages=1 and the flip angle=12°. Full brain coverage was attained at a resolution of 0.5mm isovoxel. The T₂ scan was a turbo spin-echo experiment, with TR=5280ms, TE=57ms, number of averages=4, an echo train length of 5, and a refocusing pulse flip angle of 120°. The entire brain was imaged with a 0.5x0.5 mm in-plane resolution and a slice thickness of 1mm. For visualization of the region of infarction, sections were immediately placed in 1.5% 2,3,5-triphenyl tetrazolium chloride (TTC, Sigma) in 0.9% phosphate-buffered saline and stained for 15-45 mins at 37°C, as appropriate. Images from T₂-weighted MRIs and TTC stained sections were examined for the location of infarction, and the

total affected area measured using ImageJ, as previously described [324]. Each of the techniques (MRI, TTC) analyzed comparable anatomical regions and sampled approximately 15 slices (4mm each). Measurements of infarct volume as a percentage of the ipsilateral hemisphere or cortex were made using the following formula: (area damaged/total area)x100%. Infarct volume in the cohort of animals used for this study ranged from 10-37% of contralateral hemisphere (N=9).

Reagents

Kmix CpG ODN, a 1:1:1 mixture of 3 human specific phosphorothioate K type ODNs (K3: ATC GAC TCT CGA GCG TTC TC; K23: TCG AGC GTT CTC; K123: TCG TTC GTT CTC), [330] was obtained from Oligos Etc. (Wilsonville, OR, USA) for NHP studies. LPS (*Escherichia coli* serotype 0111:B4) was obtained from Sigma.

Multiparametric flow cytometry

Immediately after isolation, PBMCs (5×10^6) were washed with HBSS and then incubated in cell staining buffer (1x PBS, 1% BSA, 0.1% NaN₃, pH7.4) for 1 hour at 4°C with the following fluorochrome conjugated antibodies: Pacific Blue-conjugated anti-CD3 (BD Bioscience), allophycocyanin (APC)-eFluor 780-conjugated anti-CD20 (eBioscience), fluorescein isothiocyanate (FITC)-conjugated anti-CD56 (BD Bioscience), (FITC)-conjugated anti-CD16 (BD Bioscience), Peridinin chlorophyll protein (PerCP)-Cy5.5-conjugated anti-CD4 (BD Bioscience), Phycoerythrin (PE)-Cy7-conjugated anti-CD8

(eBiosciences), PE-conjugated anti-CD69 (BD Bioscience), allophycocyanin (APC)-conjugated anti-CD25 (BD Biosciences), PE-conjugated anti-CD27 (BD Bioscience), APC-conjugated anti-CD38 (BIDM), PE-conjugated anti-CD45 (BD Pharmingen), PE-conjugated anti-CD217 (Beckman Coulter), APC-conjugated anti-HLA-DR (BD Bioscience), PE-conjugated anti-CD80 (BD Bioscience), Pacific Blue-conjugated anti-CD86 (Biolegend), PE-Cy7-conjugated anti-CD11c (Biolegend), PerCP-Cy5.5-conjugated anti-CD123 (BD Bioscience), Pacific Blue-conjugated anti-FoxP3 (Biolegend) (**Table 11**). For FoxP3 staining, cells were fixed then permeabilized prior to staining with anti-FoxP3. For stimulated sample, PBMCs (1×10^6 per well) in 6-well tissue culture plates at 37°C were incubated with CpG ODN ($50\mu\text{g}$, $\sim 3\text{mM}$), LPS ($50\mu\text{g}$) or saline for 16 hours in 1mL RPMI 1640 media supplemented with 10% heat-inactivated FBS. After incubation, cells were washed with HBSS and then incubated in cell staining buffer (1x PBS, 1% BSA, 0.1% NaN_3 , pH 7.4) for 1 hour at 4°C with fluorochrome conjugated antibodies. Samples were analyzed within 6-8 hours of staining using a BD LSR II flow cytometer (Becton Dickinson, Franklin Lakes, NJ). A minimum of 1×10^6 events were collected. Data was analyzed using FlowJo software (Treestar Inc., Ashland, OR).

Results

Peripheral blood was collected from animals prior to, at the time of and 48 hours and 7 days post-surgery (**Figure 65**). PBMCs were isolated via Ficoll-Hypaque gradient centrifugation and gated to identify various subpopulations of cells (**Figure 66**).

Activation markers were identified as outline in **Table 11**. As seen in human stroke, the absolute number of white blood cells increased acutely (48 hours) after stroke, but returned to normal by 7 days post-injury (**Figure 67 A**). An increase in neutrophils accounted for the majority of this change in cell number (**Figure 67 B**). Other granulocytes, including basophils (**Figure 70 A and B**) and eosinophils (**Figure 70 C and D**) also increased following stroke. Interestingly, granulocytes increased at with the same temporal dynamics as neutrophils, while eosinophils did not increase until later (7 days post-stroke). Other hematological parameters including red blood cell count, hematocrit and hemoglobin level (**Figures 68 A, B and C**) did not change following injury, confirming there was not excessive blood loss from the surgery, and that oxygen carrying capacity of the blood did not change following stroke. As seen previously [191], C-reactive protein was elevated at 48 hours following stroke (**Figure 69**), but surprisingly returned to baseline levels as early as 7 days post-injury.

Monocytes also increase acutely following stroke (**Figure 71**) as do natural killer cells (**Figure 72**). NK cells appear to be activated early (**Figure 73**), which may contribute to worsening inflammatory tissue damage. As expected, CD4+ and CD8+ lymphocytes decrease acutely following stroke (**Figure 74, 75 and 76**). These cells have increased expression of markers of activation, including CD25 and CD69 (**Figure 75 and 76**). Interestingly, CD20+ B lymphocytes also decrease acutely after injury (**Figure 78**), but have decrease expression of activation markers. Though they have decreased expression of activation markers, B cells have increase responsiveness to TLR-induce stimulation *in vitro* (**Figure 80**), the opposite of the decreased responsiveness to TLR

ligands seen in T cells (**Figure 81**). Finally, though T lymphocytes decrease following stroke, CD25+FoxP3+ CD4+ and CD8+ T lymphocytes increase at 7 days following stroke (**Figure 79**).

For a small subset of animals (n=3, infarct volume range ~10% to ~27%), changes in immune cell markers were correlated to size of infarct volume (Figures 83 to 85).

Conclusions

The exchange of immunological information to and from the brain is bidirectional, facilitated by a rich network of connections between the innate and adaptive immune systems and the central nervous system [570]. This process is facilitated by neural pathways that innervate lymphoid organs [571], neuroendocrine glands [572], and humoral messengers such as cytokines, hormones and glucocorticoids [573] (**Figure 81**). As shown here, the extent of infarct correlates with the amount of change seen in peripheral immune cells (**Figure 83 to 85**). Interestingly, infarct volume also varies with peripheral immunological profile, as animals with low T to B cell ratios at the time of stroke have decreased infarct volume.

In humans, as well as in mice [574], the acute response to stroke is characterized by acute lymphocytopenia following ischemia [575, 576]. This loss of lymphocytes is attributed to apoptosis of these cells due to cortisol and catecholamine release [577, 578]. T cells, B cells and to some extent NK cells all follow this same pattern of acute

decrease immediately following stroke and make up an increased percentage of lymphocytes undergoing apoptosis [579]. There is further evidence that CD4+ cells comprise the majority of apoptosing T lymphocytes [576]. These changes have been shown to occur maximally immediately after or at one day post stroke [336, 579], and do not yet return to normal levels by 14 days post-injury [336]. This acute immune suppression has been associated with worsened neurological outcome, increase infarct damage and increased rates of post-stroke infection [336, 575]. Lower levels of B cells immediately following stroke have been associated with poor long-term outcome [579]. Changes in humoral (B cell) immune response in this study have also been shown to be increased in patients with higher severity of damage in hemorrhagic stroke [580]. In the current study of the peripheral immune response following stroke in non-human primates, lymphocytes also decrease acutely following injury and remain suppressed for at least 7 days (**Figure 74**). Interestingly, this decrease seems to be largely due to loss of CD20+ B cells, and not CD4+ or CD8+ T cells (**Figures 78, 75 and 76**). Though slightly different in lymphocyte subpopulations affected, rhesus macaques appear to have a similar immunosuppressive response to that of humans following cerebral ischemia.

There also appears to be a rapid increase in leukocytes and granulocytes in the circulation acutely after stroke in humans [336, 579]. The contribution of neutrophils to damage after reperfusion is controversial [541, 581, 582]; recent studies with granulocyte colony-stimulating factor (G-CSF), which induces leukocytosis and increases neutrophil count, has shown promise in rodent models of stroke [583], and does not worsen stroke outcome in human patients [584]. As in humans, the acute response to

stroke in NHPs is characterized by an increase in white blood cells, primarily neutrophils and other granulocytes (**Figures 67 and 71**).

Circulating monocytes have been shown to increase 2 and 7 days post stroke in humans [585]. These cells are characterized by decreased expression of HLA-DR, and increased expression of TLR-2 [585]. Decreased expression of HLA-DR has been associated with poor outcome [585]. Interestingly, patients who had decreased expression of TLR4 on monocytes following stroke had a more favorable outcome than patients with high or unchanged TLR4 expression [585, 586]. This would make sense, as down regulation of TLR4 following stroke would decrease the chance of monocyte activation via stroke-induced endogenous TLR ligand. Levels of circulating monocytes in rhesus macaques also increase acutely following stroke (**Figure 71**), though their expression of TLR 4 has not been characterized.

Following stroke in humans, remaining T lymphocytes appear to be activated [587], as assessed by cell surface activation markers and by function responses *in vitro* and *in vivo*. Increase in delayed-type hypersensitivity (DTH) reaction, a measure of systemic antigen specific T-cell reactivity, is seen in human patients following stroke [588, 589]. This T-cell hypersensitivity response seems to be enhanced with increased lesion volume, and also appears to be enhanced on the paretic side [589]. Stroke patients demonstrate an acute increase in HLA-DR and CD25 expression on CD4+ T cells [576, 587], as well as increased expression of CD69 on CD4+ T cells [587], indicating that stroke leads to T cell activation. These cells are able to proliferate normally and

exhibited enhanced secretion of inflammatory cytokine in response to *in vitro* stimulation [576], arguing for potential Th1 priming in T cells following stroke. Similarly, following cerebral ischemia in rhesus macaque, CD4+ cells have increased expression of CD25 and CD69 (**Figure 75**). CD8+ T cells seem to increase surface expression of CD69, but the number of CD25+ cells does not increase; instead there is an increase in CD25- cells, with no change in absolute number of CD25+ cells (**Figure 76**). After stroke, CD4+ T cells seem to have altered responsiveness to TLR ligands *in vitro* when compared to activation pre- stroke (**Figure 81**), while CD8+ T cells seem to have significantly decreased responsiveness. There is also an increase in CD4+ and CD8+ T regulatory cells (FoxP3+) at 7 days after stroke in NHPs (**Figure 79**), mirroring the increase seen in humans [579].

Stroke does not seem to enhance B-cell reactivity in humans [588]. This same phenomenon is evident in the present rhesus macaque model of stroke, as CD20+ cells appear to become deactivated, decreasing expression of CD69 and CD27, and increasing expression of CD38 (**Figure 78**). However, following stimulation with TLR ligands *in vitro* B cell have increase responsiveness, characterized by increased expression of CD69 and CD35 (**Figure 80**).

Overall, rhesus macaques appear to have a similar immune response to transient cerebral ischemia as humans. Thus, NHP models of stroke may serve as important models for assessing efficacy of potential neuroprotective compounds that rely on modulation of endogenous immune response to stroke. Further, use of NHP stroke

models may allow additional insight into the evolution and contribution of the immunological response to stroke-associated damage.

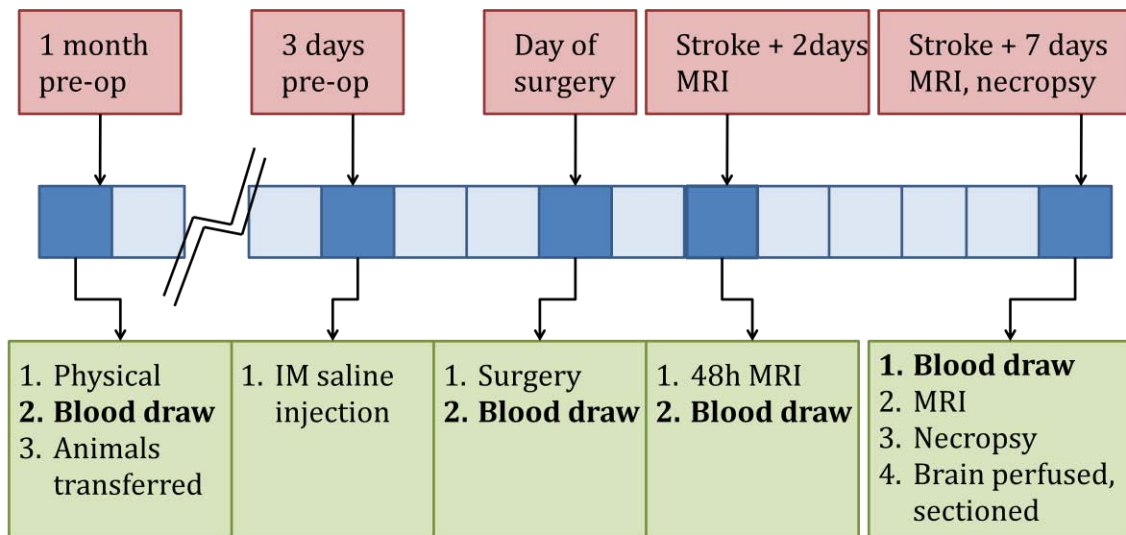


Figure 65. *Blood draw timeline*

Peripheral blood was obtained via femoral vein 4 weeks prior to surgery, at the time of surgery, 48 hours after surgery, and 7 days after surgery. Blood was collected in heparinized vacutainers, and immediately processed for flow cytometric analysis.

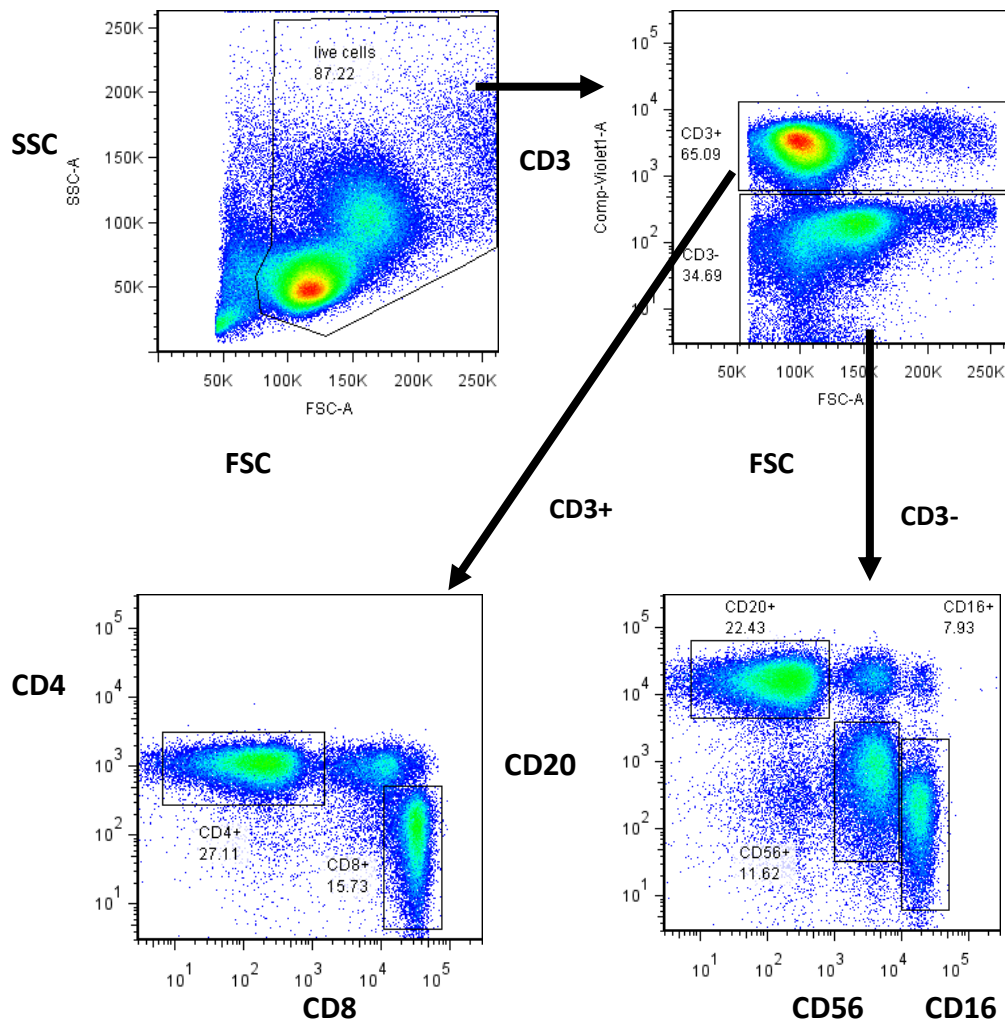


Figure 66. Gating strategy used to identifying PBMC subpopulations

Live cells were sorted based on SSC versus FSC, then further sorted into CD3+ (T lymphocyte) and CD3- populations. CD3+ cells were then sorted in to CD4+ and CD8+ T lymphocyte populations. CD3- cells were sorted into CD20+ (B lymphocyte) and CD56+ or CD16+ (natural killer cell) populations.

Table 11. Cell surface activation markers used for PBMC population identification

	Characterization markers:	Activation markers:
T lymphocytes:	<p>CD3+ All T lymphocytes</p> <p>CD4+CD3+ CD4 T cells (T helper cells)</p> <p>CD8+CD3+ CD8 T cells (cytotoxic T cells)</p> <p>CD56+CD8+ NKT cells, non-MHC-restricted</p>	<p>CD25 (IL-2 Receptor)</p> <p>CD69 early activation</p> <p>CD38 (glycoprotein - cell adhesion, signal transduction, Ca2++)</p> <p>HLA-DR (MHC class II)</p> <p>CD27 Costimulatory marker</p>
B Lymphocytes:	<p>CD20+ All B lymphocytes but plasmablasts</p> <p>CD38+CD27+ plasmablast</p> <p>CD38++CD27- transitional cells</p> <p>CD38+/-CD27+ memory B cells</p>	<p>CD27 class switched B cell, marginal zone-like B cell</p> <p>CD38 transitional B cell, naïve B cell</p> <p>CD45 lower in immature B cells than mature B cells</p> <p>CD25 (IL-2 Receptor)</p> <p>CD80 (B7.1) (cosignaling molecule for T cell activation)</p>
Natural Killer cells	<p>CD56+CD3- NK cells</p> <p>CD16+CD3- NK cells (higher cytolytic activity)</p>	<p>CD69 early activation</p> <p>CD38 (glycoprotein - cell adhesion, signal transduction, Ca2++)</p>
Dendritic Cells	<p>CD123+HLA-DR+ plasmacytoid DCs</p> <p>CD11c+HLA-DR+CD3-CD16-CD56- Myeloid DCs</p>	<p>HLA-DR (MHC class II) increased expression</p> <p>CD80 (B7.1) (cosignaling molecule for T cell activation)</p> <p>CD83 (maturation marker)</p> <p>CD86 (cosignaling molecule for T cell activation)</p>

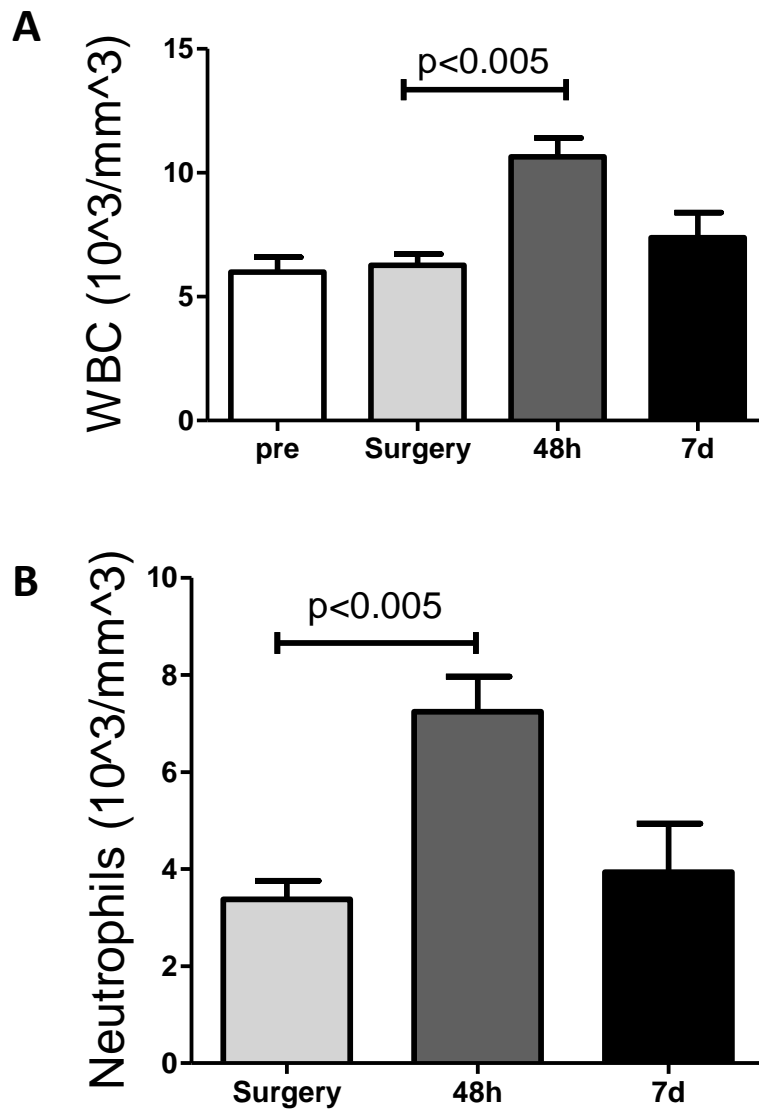


Figure 67. Increase in white blood cells 48h post-stroke in NHPs is largely due to an increase in neutrophils

(A) Absolute number of white blood cells 4 week prior to surgery, at the time of surgery, 48 hours after surgery and 7 days after surgery. **(B)** Absolute number of neutrophils at the time of surgery, 48 hours after surgery and 7 days after surgery. N=9; Data are displayed as average \pm SEM.

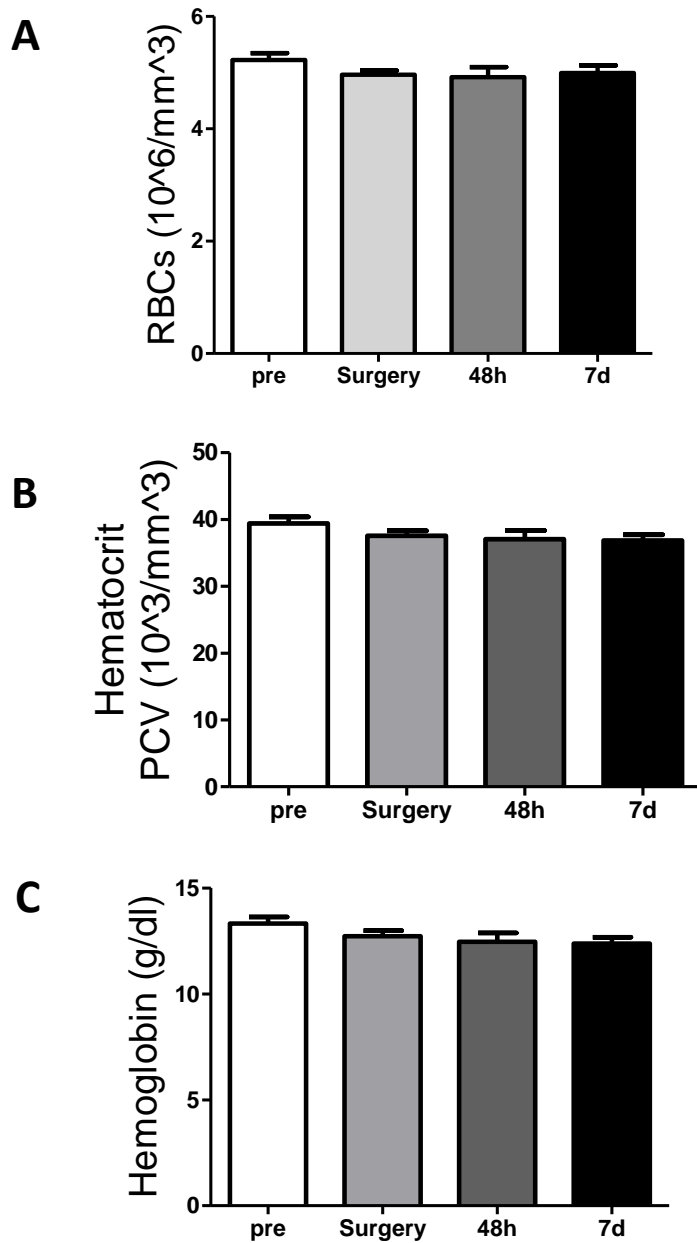


Figure 68. Red blood cell count, hematocrit and hemoglobin do not change following stroke in NHPs

(A) Absolute number of red blood cells 4 week prior to surgery, at the time of surgery, 48 hours after surgery and 7 days after surgery. **(B)** Hematocrit at the time of surgery, 48 hours after surgery and 7 days after surgery. **(C)** Hemoglobin at the time of surgery, 48 hours after surgery and 7 days after surgery N=9; Data are displayed as average \pm SEM.

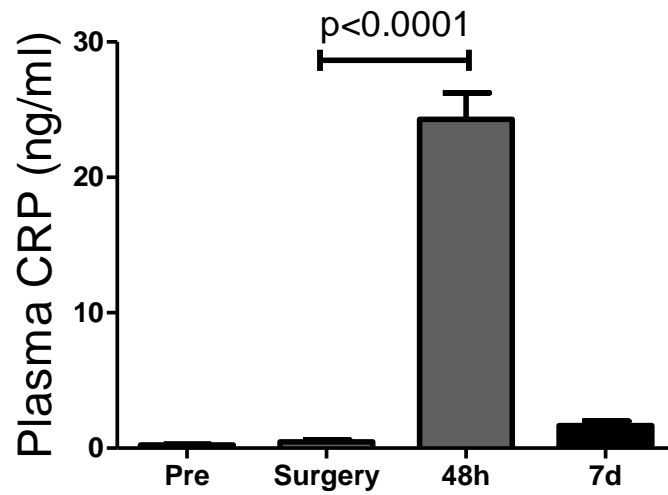


Figure 69. Plasma C-reactive protein is elevated 48 hours after stroke in NHPs

Plasma CRP measures 4 weeks prior to surgery, at the time of surgery, 48 hours after surgery and 7 days after surgery. N=9; Data are displayed as average \pm SEM.

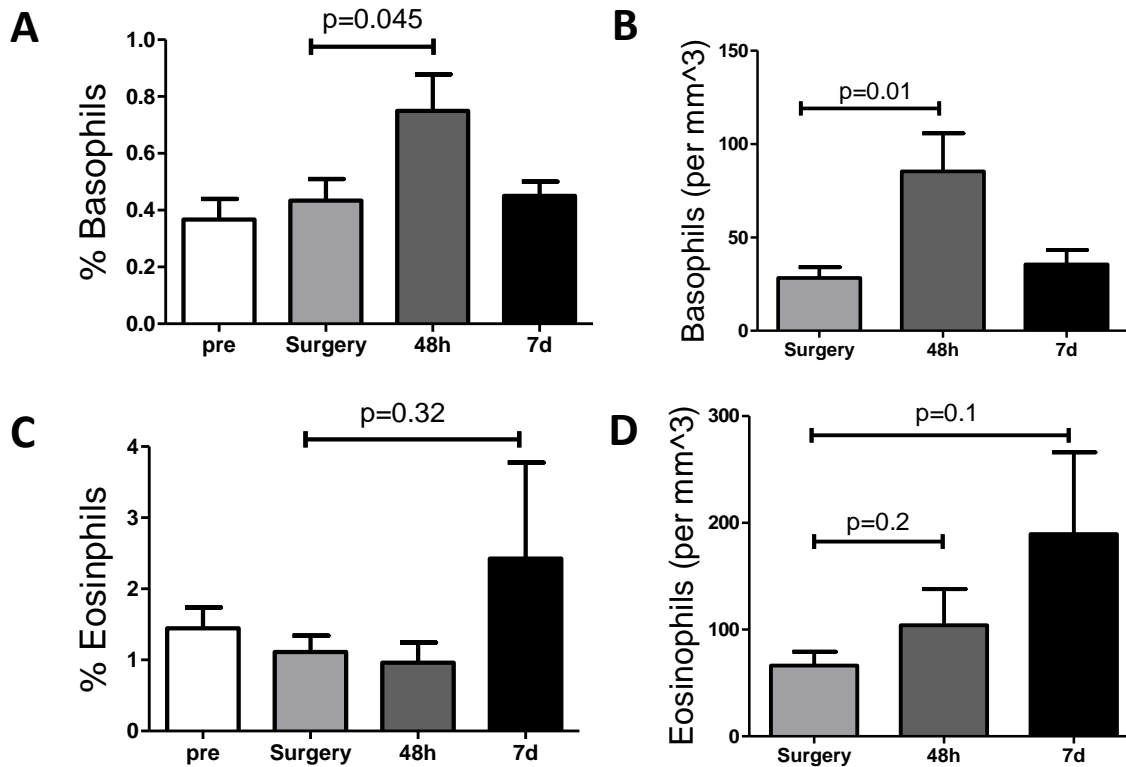


Figure 70. Granulocytes are increased following stroke in NHPs

(A) Percent basophils in peripheral blood 4 week prior to surgery, at the time of surgery, 48 hours after surgery and 7 days after surgery. **(B)** Absolute number of basophils at the time of surgery, 48 hours after surgery and 7 days after surgery. **(C)** Percent eosinophils in peripheral blood 4 week prior to surgery, at the time of surgery, 48 hours after surgery and 7 days after surgery. **(D)** Absolute number of eosinophils at the time of surgery, 48 hours after surgery and 7 days after surgery. N=9; Data are displayed as average \pm SEM.

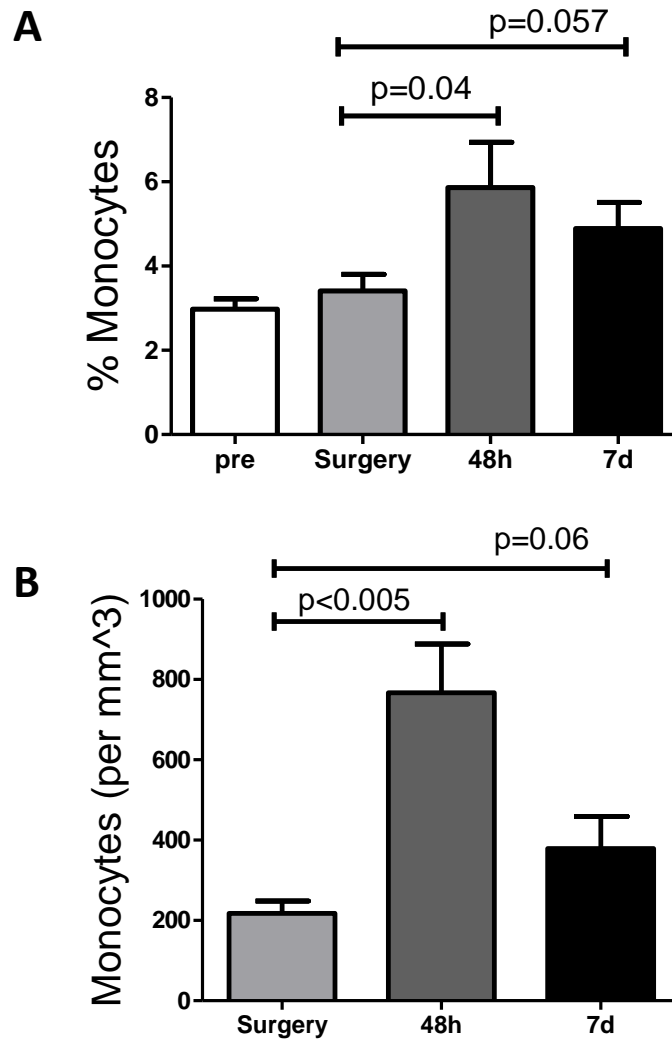


Figure 71. Monocytes are increased at 48 hours post-stroke, and remain elevated at 7 days post-infarct

(A) Percent monocytes in peripheral blood 4 week prior to surgery, at the time of surgery, 48 hours after surgery and 7 days after surgery. **(B)** Absolute number of monocytes at the time of surgery, 48 hours after surgery and 7 days after surgery. N=9; Data are displayed as average \pm SEM.

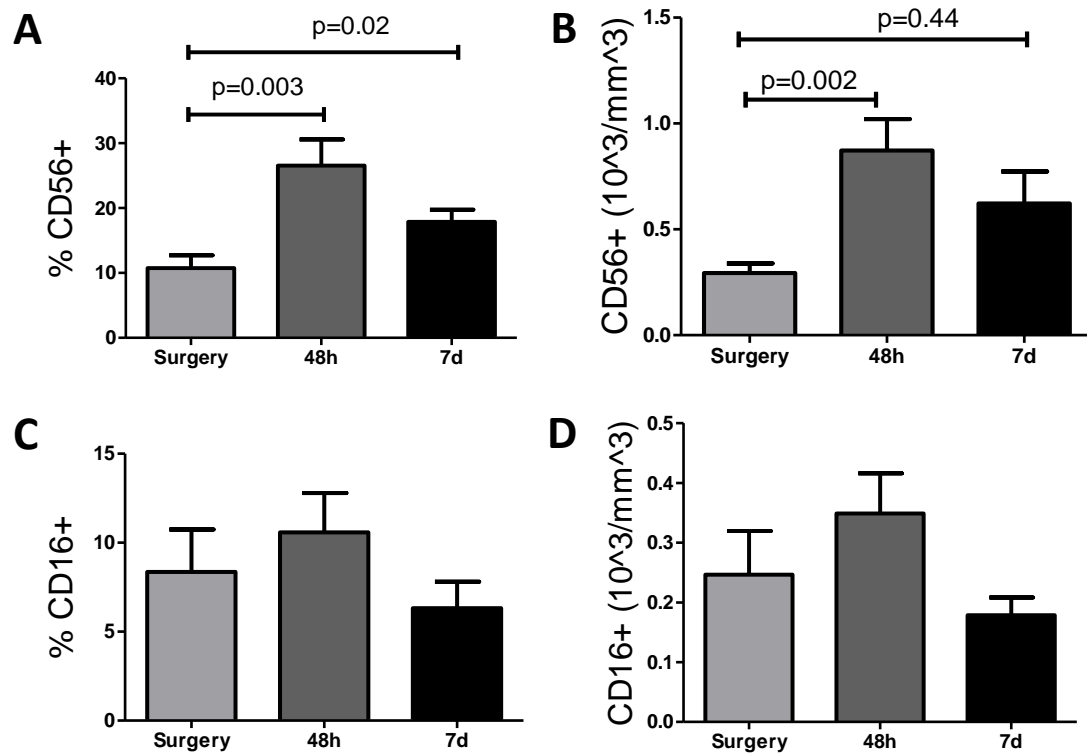


Figure 72. Number of CD56+ but not CD16+ natural killer cells increase at 48 hours post stroke in NHPs

(A) Percent CD3-CD56+ monocytes/NK cells in peripheral blood 4 week prior to surgery, at the time of surgery, 48 hours after surgery and 7 days after surgery. **(B)** Absolute number of CD56+ cells at the time of surgery, 48 hours after surgery and 7 days after surgery. **(C)** Percent CD3-CD16+ NK cells in peripheral blood 4 week prior to surgery, at the time of surgery, 48 hours after surgery and 7 days after surgery. **(D)** Absolute number of CD16+ cells at the time of surgery, 48 hours after surgery and 7 days after surgery. N=9; Data are displayed as average \pm SEM.

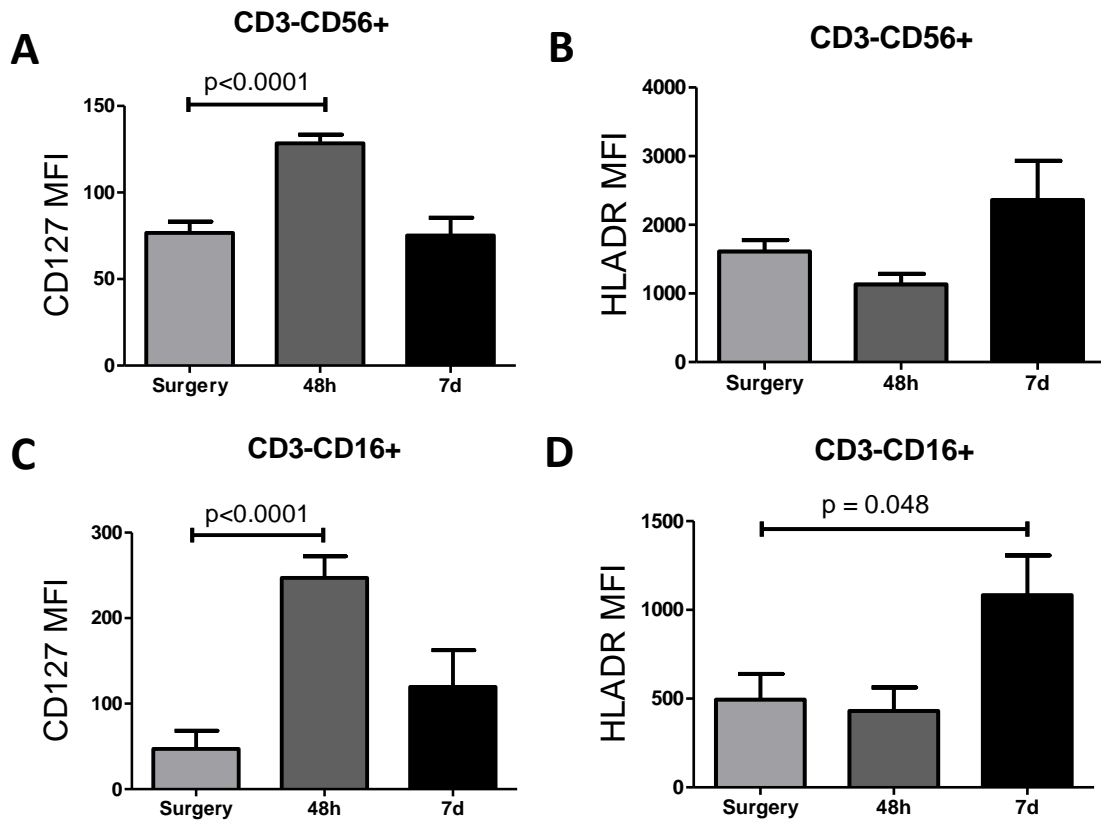


Figure 73. *Natural killer cells become activated following stroke in NHPs*

(A) Mean fluorescence intensity of CD127 on CD3-CD56+ monocytes/NK cells at the time of surgery, 48 hours after surgery and 7 days after surgery. **(B)** Mean fluorescence intensity of HLA-DR on CD56+ monocytes/NK cells at the time of surgery, 48 hours after surgery and 7 days after surgery. **(C)** Mean fluorescence intensity of CD127 on CD3-CD16+ NK cells at the time of surgery, 48 hours after surgery and 7 days after surgery. **(D)** Mean fluorescence intensity of HLA-DR on CD16+ NK cells at the time of surgery, 48 hours after surgery and 7 days after surgery. N=9; Data are displayed as average \pm SEM.

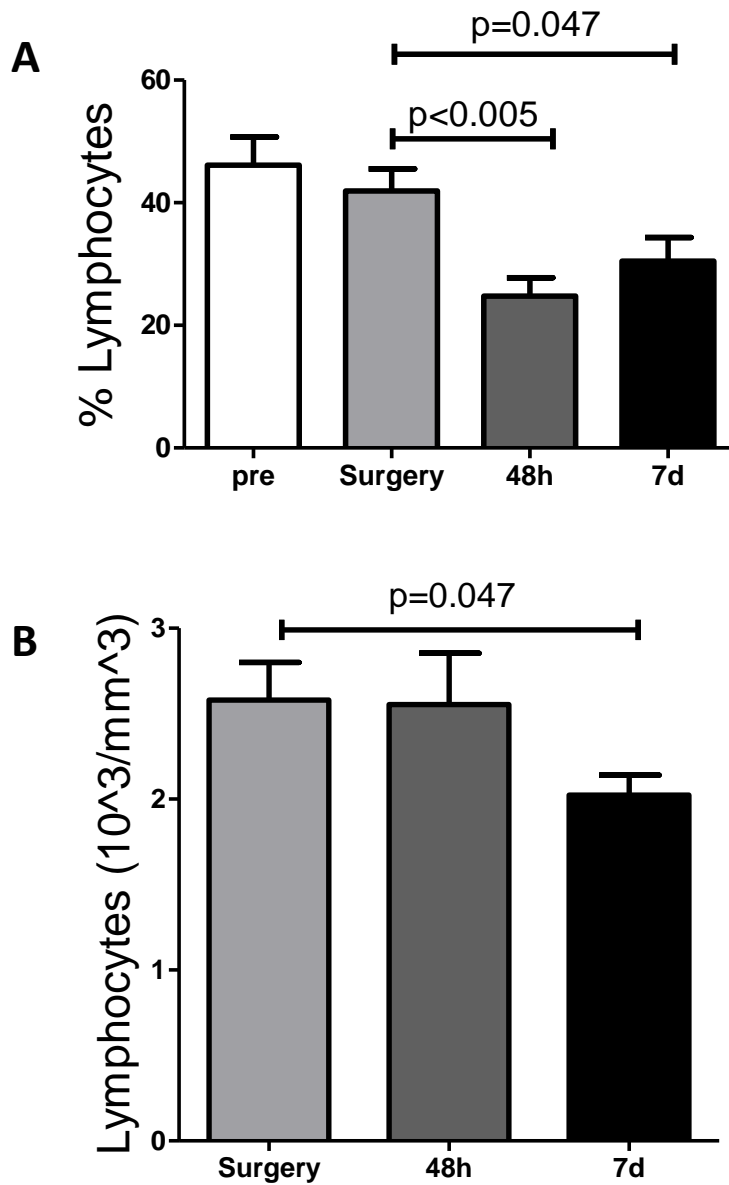


Figure 74. Lymphocytes decrease following stroke in NHPs

(A) Percent lymphocytes in peripheral blood 4 week prior to surgery, at the time of surgery, 48 hours after surgery and 7 days after surgery. **(B)** Absolute number of lymphocytes at the time of surgery, 48 hours after surgery and 7 days after surgery. N=9; Data are displayed as average \pm SEM.

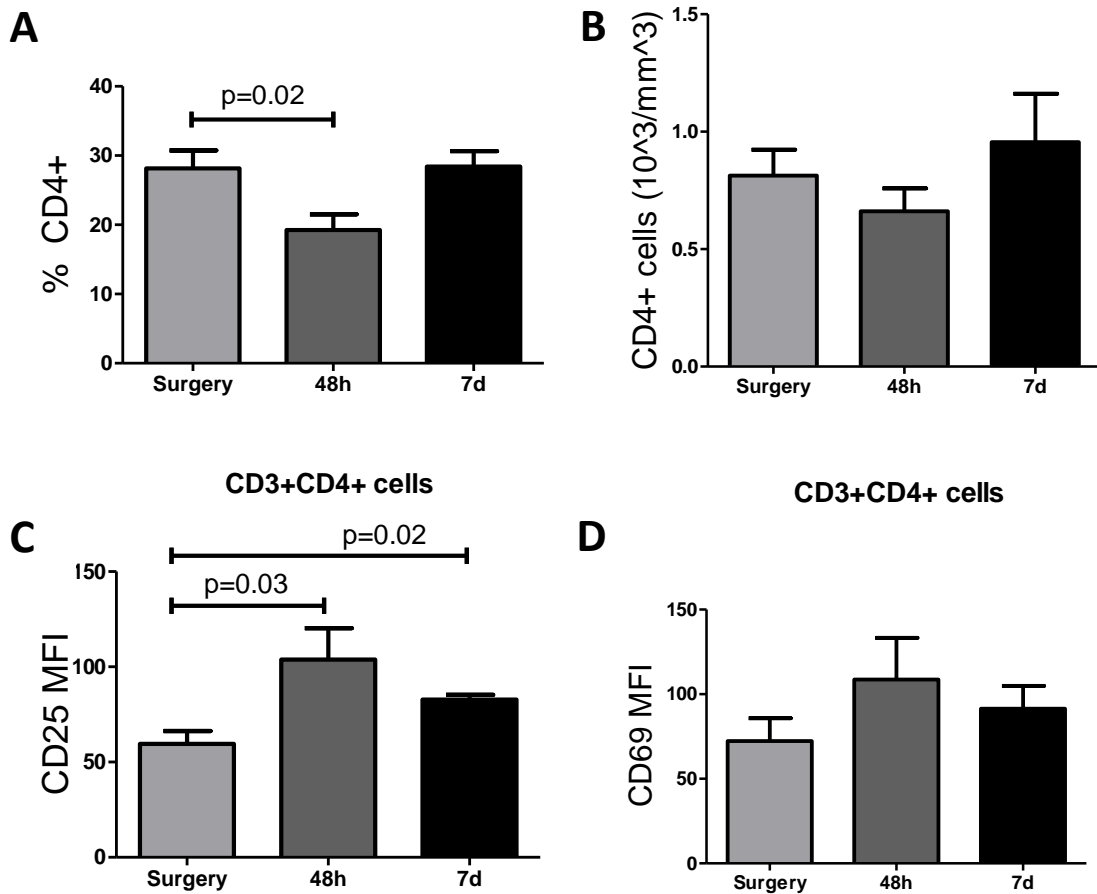


Figure 75. Slight decrease in number, but increase in activation status of CD4+ T cells following stroke in NHPs

(A) Percent CD3+CD4+ T lymphocytes in peripheral blood 4 week prior to surgery, at the time of surgery, 48 hours after surgery and 7 days after surgery. **(B)** Absolute number of CD4+ T cells at the time of surgery, 48 hours after surgery and 7 days after surgery. **(C)** Mean fluorescence intensity of CD25 on CD4+ T cells at the time of surgery, 48 hours after surgery and 7 days after surgery. **(D)** Mean fluorescence intensity of CD69 on CD4+ T cells at the time of surgery, 48 hours after surgery and 7 days after surgery. N=9; Data are displayed as average \pm SEM.

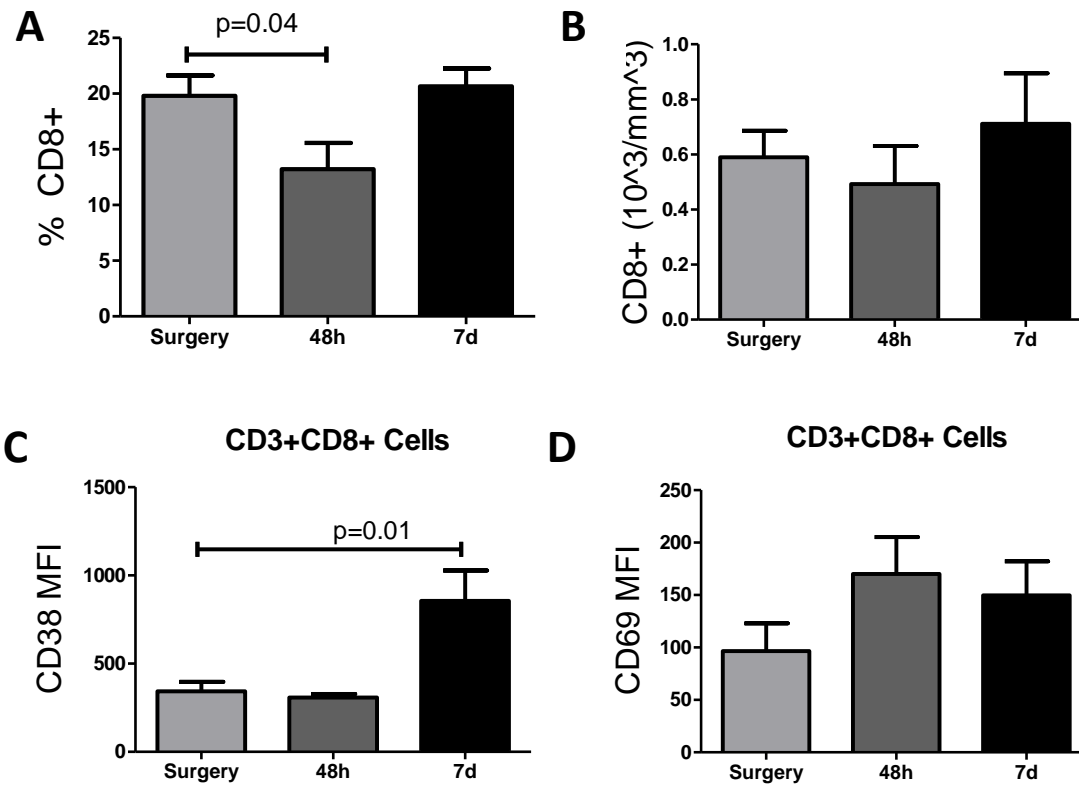


Figure 76. Slight decrease in number, but increase in activation markers on CD8+ T cells following stroke in NHPs

(A) Percent CD3+CD8+ T lymphocytes in peripheral blood 4 week prior to surgery, at the time of surgery, 48 hours after surgery and 7 days after surgery. **(B)** Absolute number of CD8+ T cells at the time of surgery, 48 hours after surgery and 7 days after surgery. **(C)** Mean fluorescence intensity of CD38 on CD8+ T cells at the time of surgery, 48 hours after surgery and 7 days after surgery. **(D)** Mean fluorescence intensity of CD69 on CD8+ T cells at the time of surgery, 48 hours after surgery and 7 days after surgery. N=9; Data are displayed as average \pm SEM.

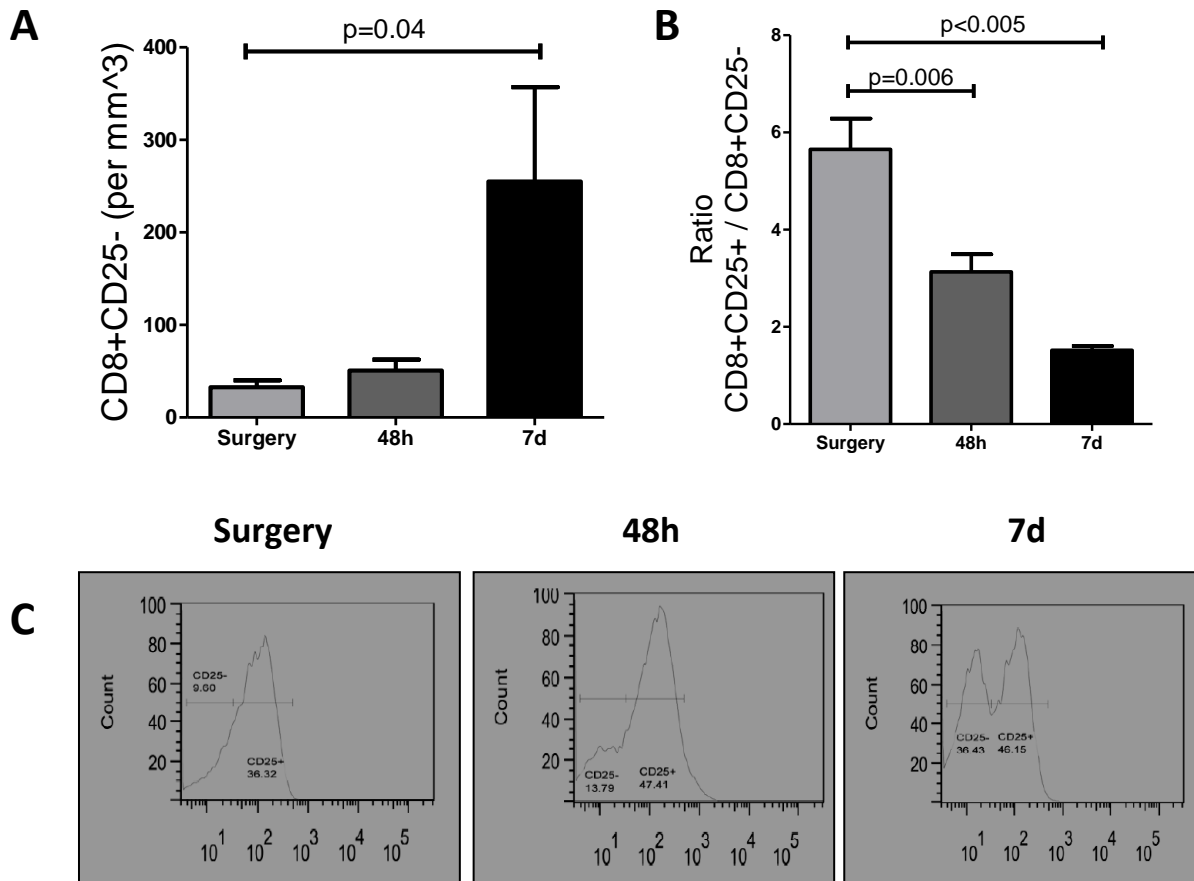


Figure 77. CD25-CD3+CD8+ cells increase following stroke in NHPs

(A) Absolute number of CD25-CD8+ T cells at the time of surgery, 48 hours after surgery and 7 days after surgery. **(B)** Ratio of CD25-/CD25+ CD8+ T cells at the time of surgery, 48 hours after surgery and 7 days after surgery. **(C)** MFI plots for CD25 at the time of surgery, 48 hours after surgery and 7 days after surgery. Note increase in CD25^{low} cell count following stroke. N=9; Data are displayed as average ± SEM.

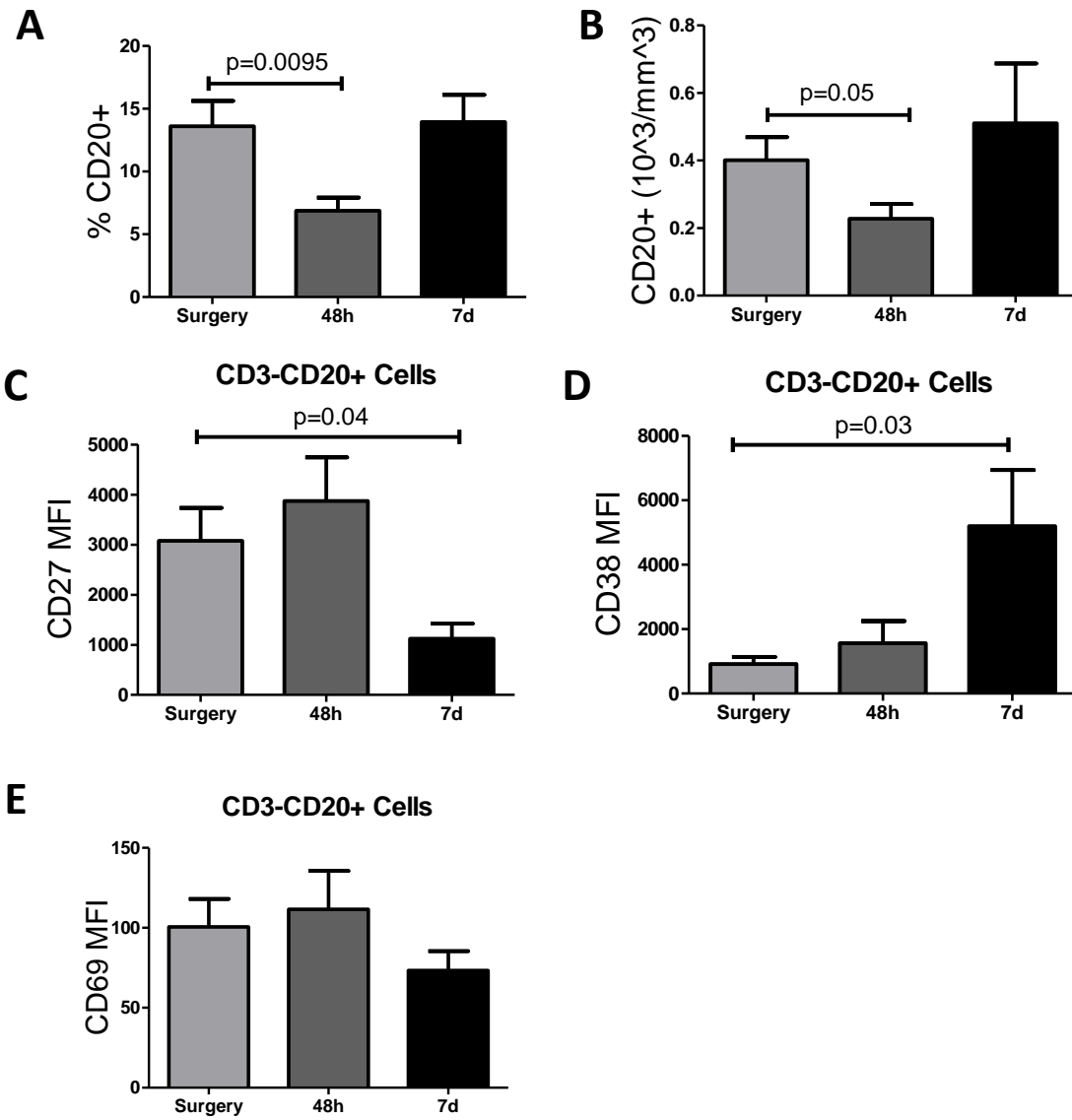


Figure 78. CD20+ B cells decrease acutely and become less activated following stroke in NHPs

(A) Percent CD3-CD20+ B lymphocytes in peripheral blood 4 week prior to surgery, at the time of surgery, 48 hours after surgery and 7 days after surgery. **(B)** Absolute number of CD20+ B cells at the time of surgery, 48 hours after surgery and 7 days after surgery. **(C)** Mean fluorescence intensity of CD27 on CD20+ B cells at the time of surgery, 48 hours after surgery and 7 days after surgery. **(D)** Mean fluorescence intensity of CD38 on CD20+ B cells at the time of surgery, 48 hours after surgery and 7 days after surgery. **(E)** Mean fluorescence intensity of CD69 on CD20+ B cells at the time of surgery, 48 hours after surgery and 7 days after surgery. N=9; Data are displayed as average \pm SEM.

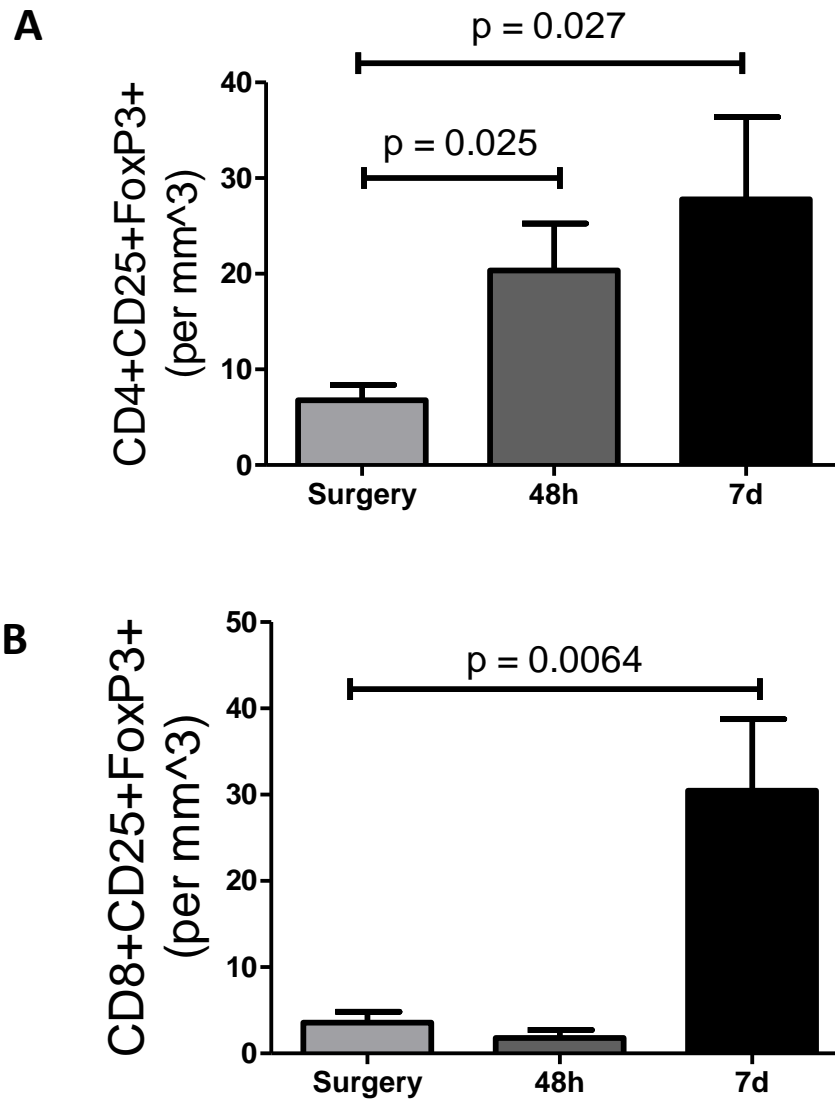
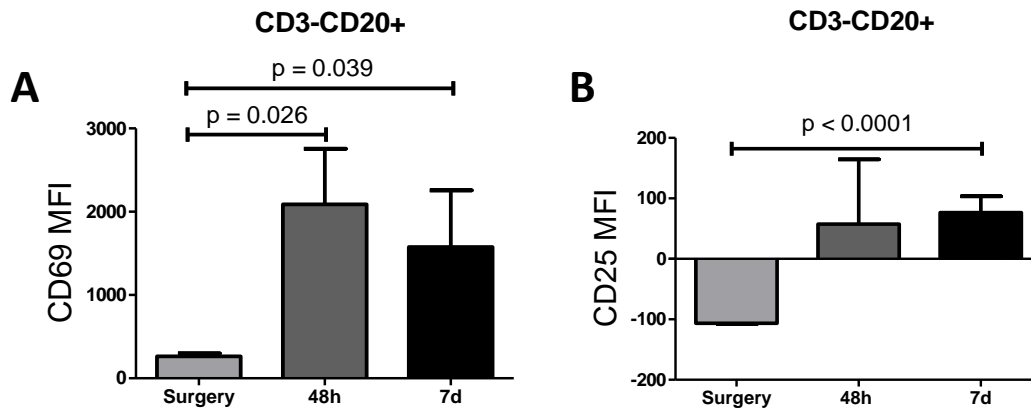


Figure 79. CD4+ and CD8+ T regulatory cells increase following stroke in NHPs

(A) Absolute number of CD3+CD4+CD25+FoxP3+ cells at the time of surgery, 48 hours after surgery and 7 days after surgery. **(B)** Absolute number of CD3+CD8+CD25+FoxP3+ cells at the time of surgery, 48 hours after surgery and 7 days after surgery. N=9; Data are displayed as average \pm SEM.

16h stimulation with CpG ODNs *in vitro*



16h stimulation with LPS *in vitro*

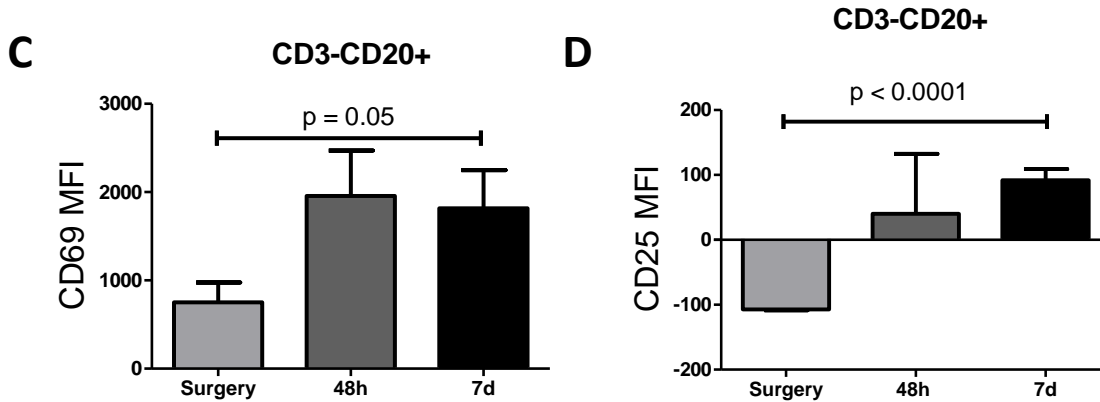


Figure 80. CD3-CD20+ B cells have increases responsiveness to Toll-like receptor ligands following stroke in NHPs

(A) Mean fluorescence intensity of CD69 on CD20+ B cells following 16 hours of stimulation with CpG ODNs *in vitro* at the time of surgery, 48 hours after surgery and 7 days after surgery. **(B)** Mean fluorescence intensity of CD25 on CD20+ B cells following 16 hours of stimulation with CpG ODNs *in vitro* at the time of surgery, 48 hours after surgery and 7 days after surgery. **(C)** Mean fluorescence intensity of CD69 on CD20+ B cells following 16 hours of stimulation with LPS *in vitro* at the time of surgery, 48 hours after surgery and 7 days after surgery. **(D)** Mean fluorescence intensity of CD25 on CD20+ B cells following 16 hours of stimulation with LPS *in vitro* at the time of surgery, 48 hours after surgery and 7 days after surgery. N=9; Data are displayed as average \pm SEM.

16h stimulation with CpG ODNs *in vitro*

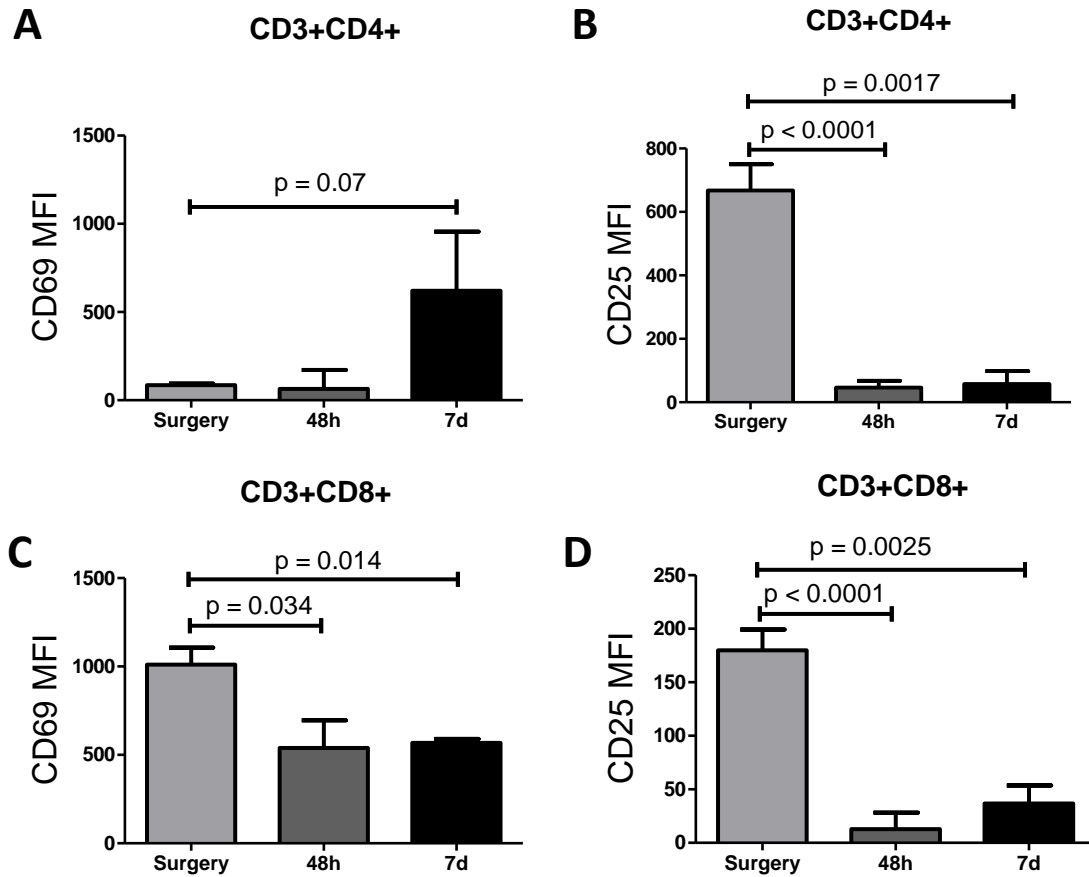


Figure 81. *CD3+CD4+* T cells and *CD3+CD8+* T cells have decreased responsiveness to Toll-like receptor ligands following stroke in NHPs

(A) Mean fluorescence intensity of CD69 on CD4+ T cells following 16 hours of stimulation with CpG ODNs *in vitro* at the time of surgery, 48 hours after surgery and 7 days after surgery. **(B)** Mean fluorescence intensity of CD25 on CD4+ T cells following 16 hours of stimulation with CpG ODNs *in vitro* at the time of surgery, 48 hours after surgery and 7 days after surgery. **(C)** Mean fluorescence intensity of CD69 on CD8+ T cells following 16 hours of stimulation with CpG ODNs *in vitro* at the time of surgery, 48 hours after surgery and 7 days after surgery. **(D)** Mean fluorescence intensity of CD25 on CD8+ T cells following 16 hours of stimulation with CpG ODNs *in vitro* at the time of surgery, 48 hours after surgery and 7 days after surgery. N=9; Data are displayed as average \pm SEM.

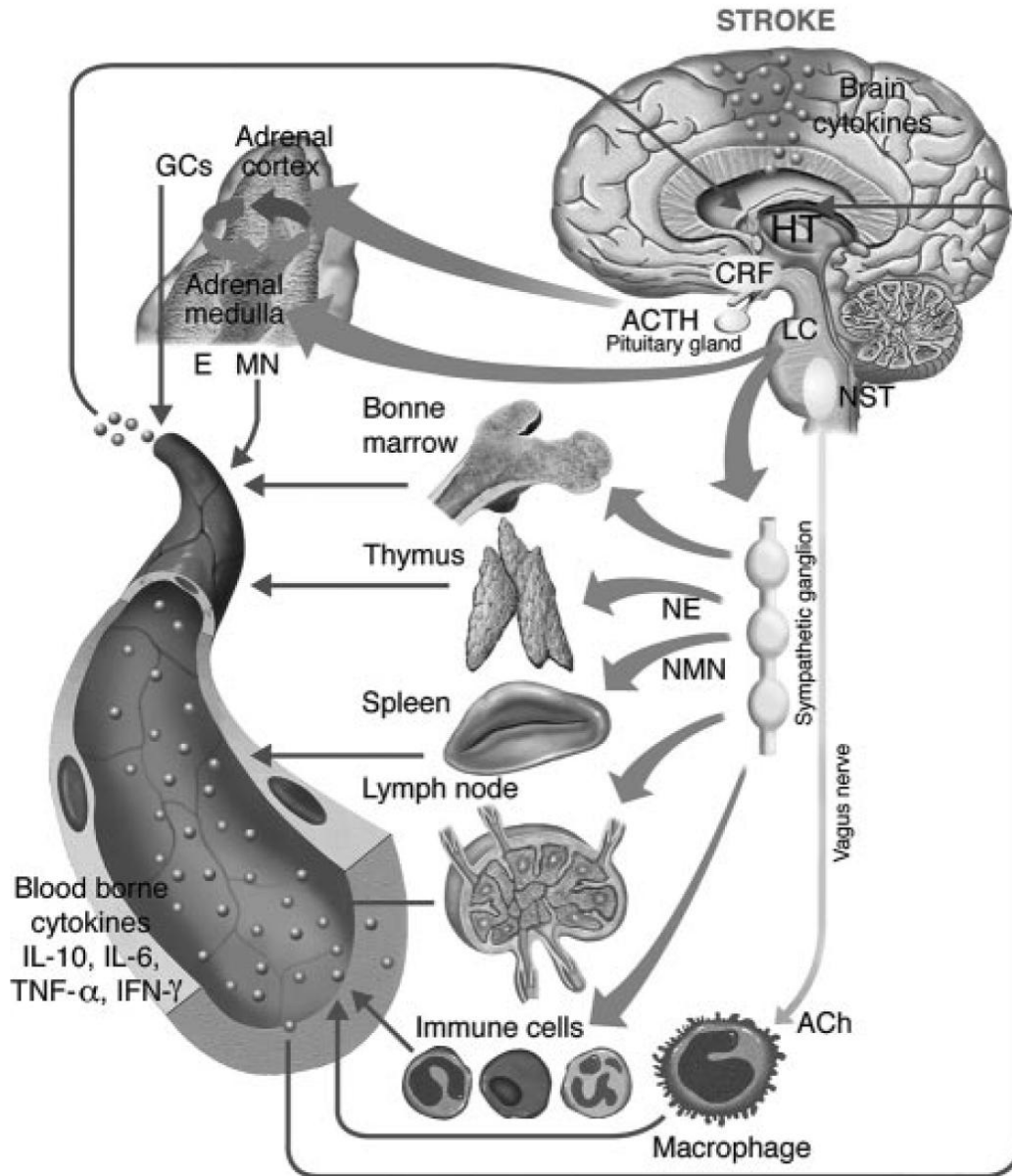


Figure 82. Schematic representation of connections from the central nervous system and the peripheral immune system

ACTH indicates adrenocorticotropic hormone, CRF is corticotropin releasing factor, E is epinephrine, GCs are glucocorticoids, HT is hypothalamus, LC is locus coeruleus, NM is metanephrine, NE is norepinephrine, NMN is normetanephrine, NST is nucleus of the solitary tract. Adapted from *Stroke* 38, 2007 [570]. Ángel Chamorro, Xabier Urra and Anna M. Planas, "Infection after acute ischemic stroke: A manifestation of brain-induced immunosuppression," pp. 1097-1103.

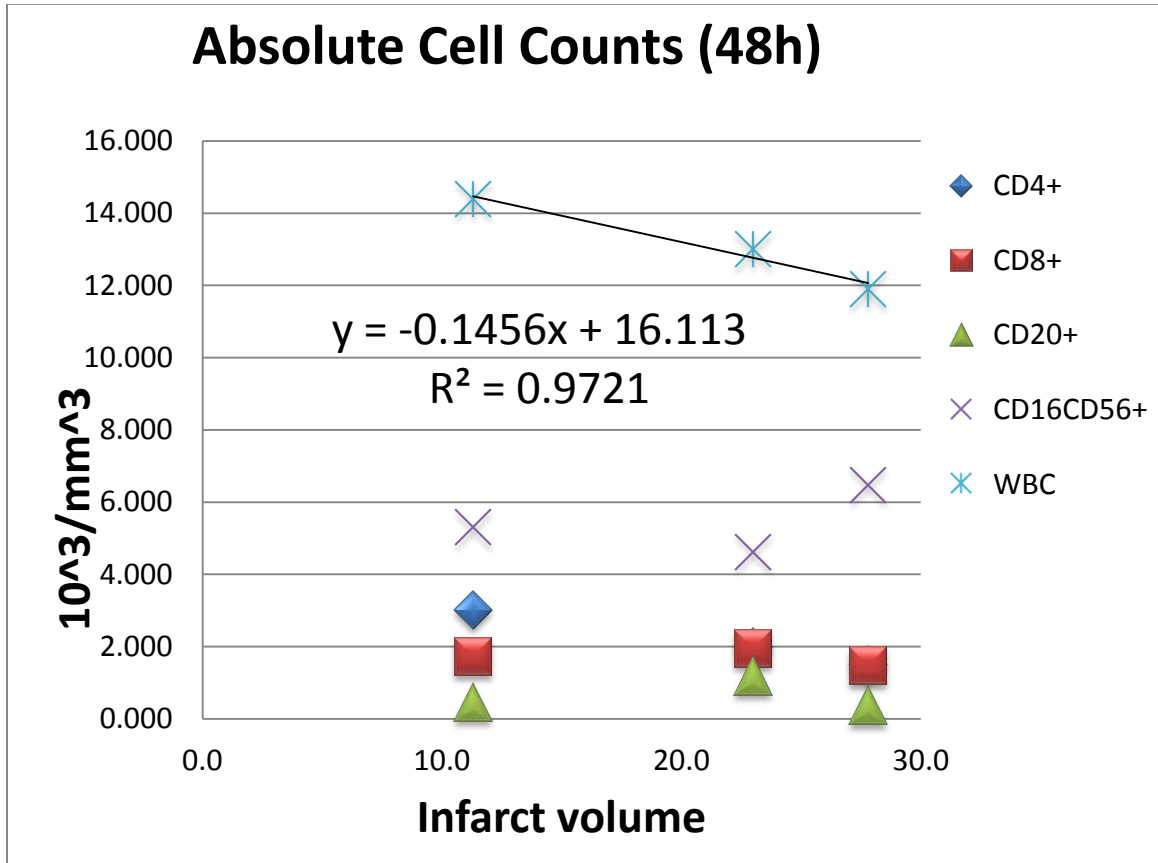


Figure 83. Day 2 white blood cell count decreases as infarct volume increases

Absolute count of WBCs (light blue x), CD4+ (Blue diamond), CD8+ (red square), CD20+ (green triangle) and CD56+CD16+ (purple x) cells at 2 days post injury as a function of T2 infarct volume. Equation of fit for WBC versus infarct volume is shown on graph. $R^2=0.9721$.

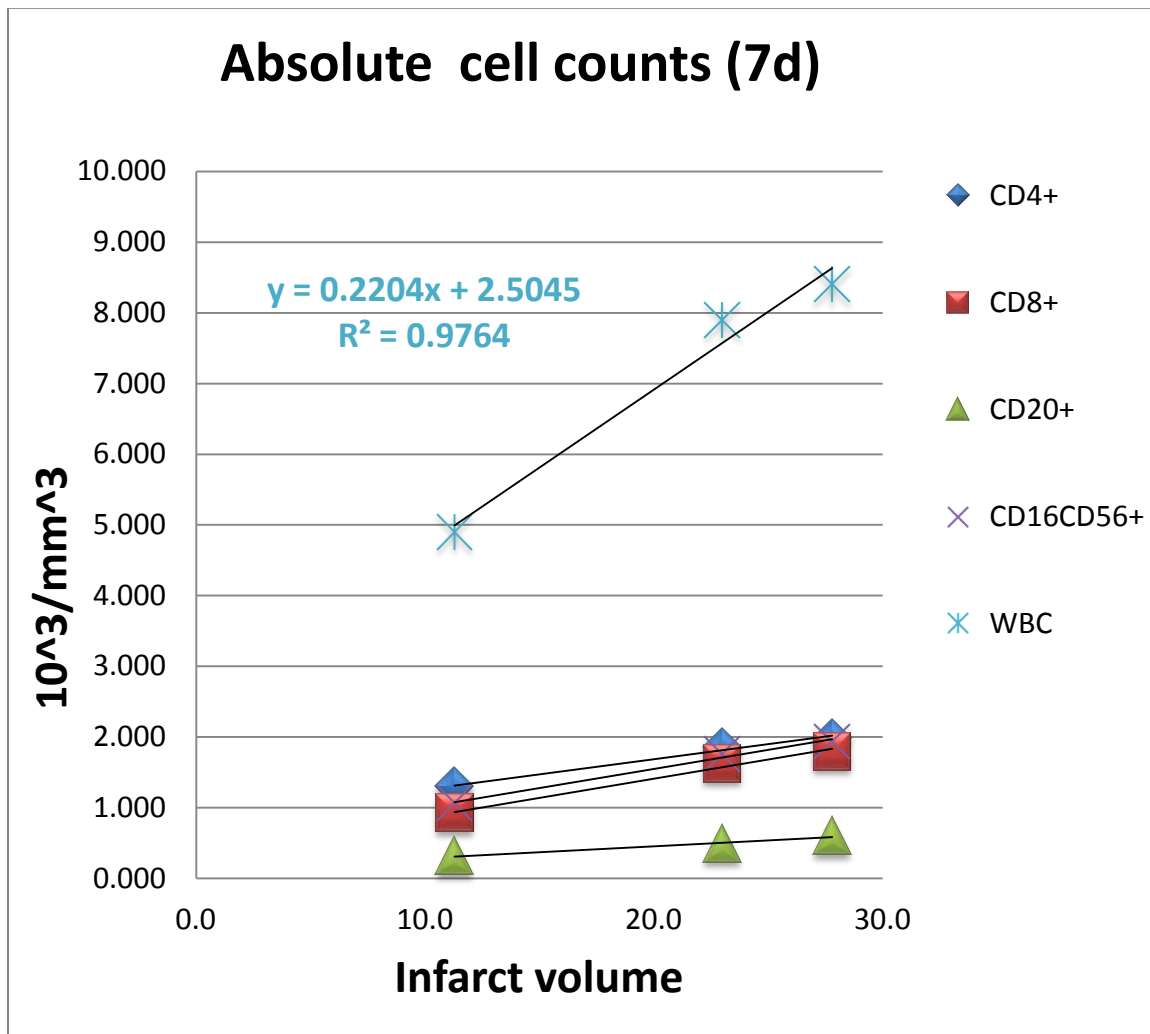


Figure 84. Day 7 white blood cell count increases with increasing infarct volume

Absolute count of WBCs (light blue x), CD4+ (Blue diamond), CD8+ (red square), CD20+ (green triangle) and CD56+CD16+ (purple x) cells at 7 days post injury as a function of T2 infarct volume. Equation of fit for WBC versus infarct volume is shown on graph. $R^2=0.9764$.

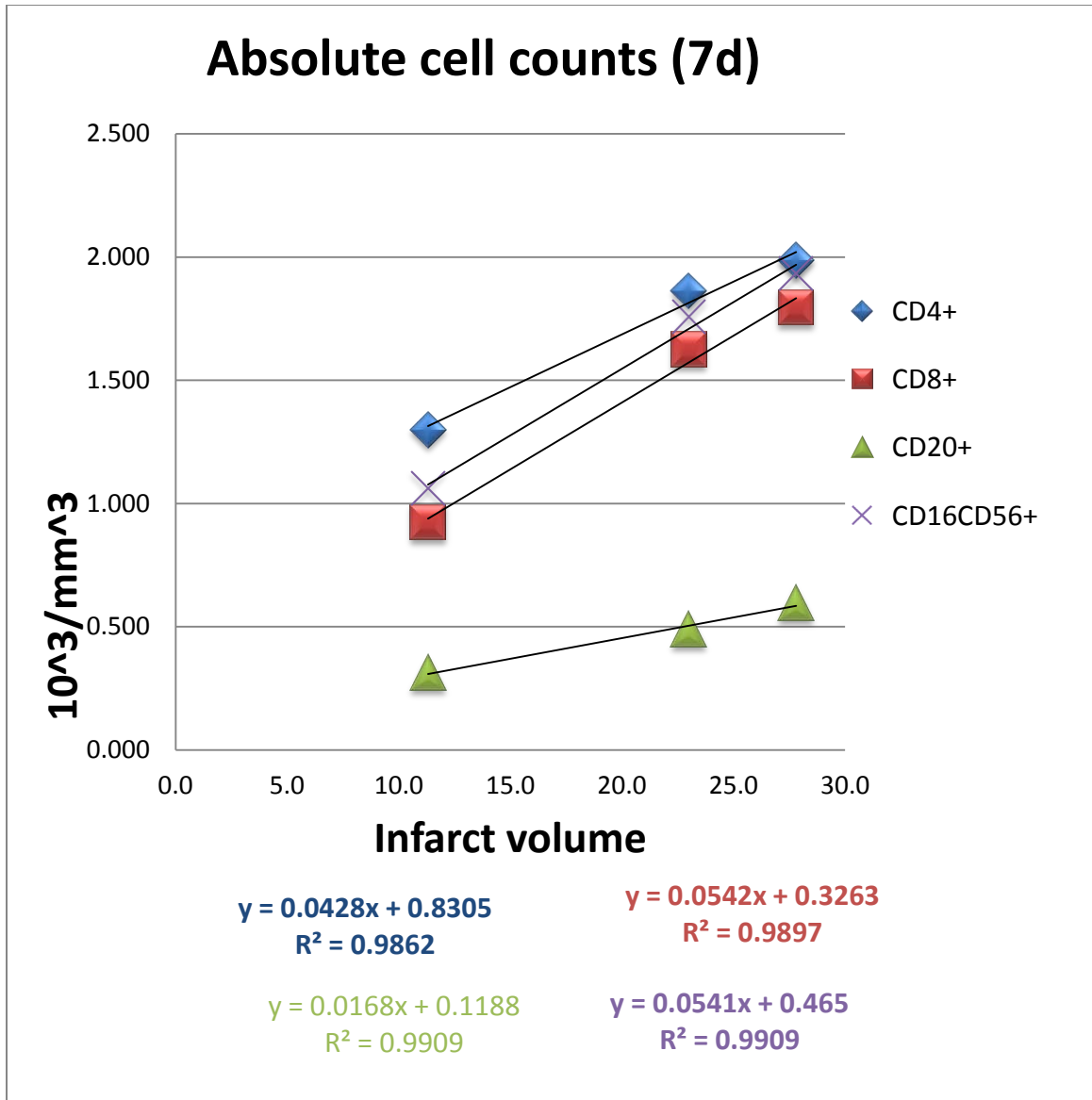


Figure 85. *CD4+ and CD8+ T cell, B cell, and NK cell counts increase with increasing with infarct volume*

Absolute count of CD4+ (Blue diamond), CD8+ (red square), CD20+ (green triangle) and CD56+CD16+ (purple x) cells at 7 days post injury as a function of T2 infarct volume. Equations of fit for individual cell populations and R² values are displayed on graph in corresponding colors.

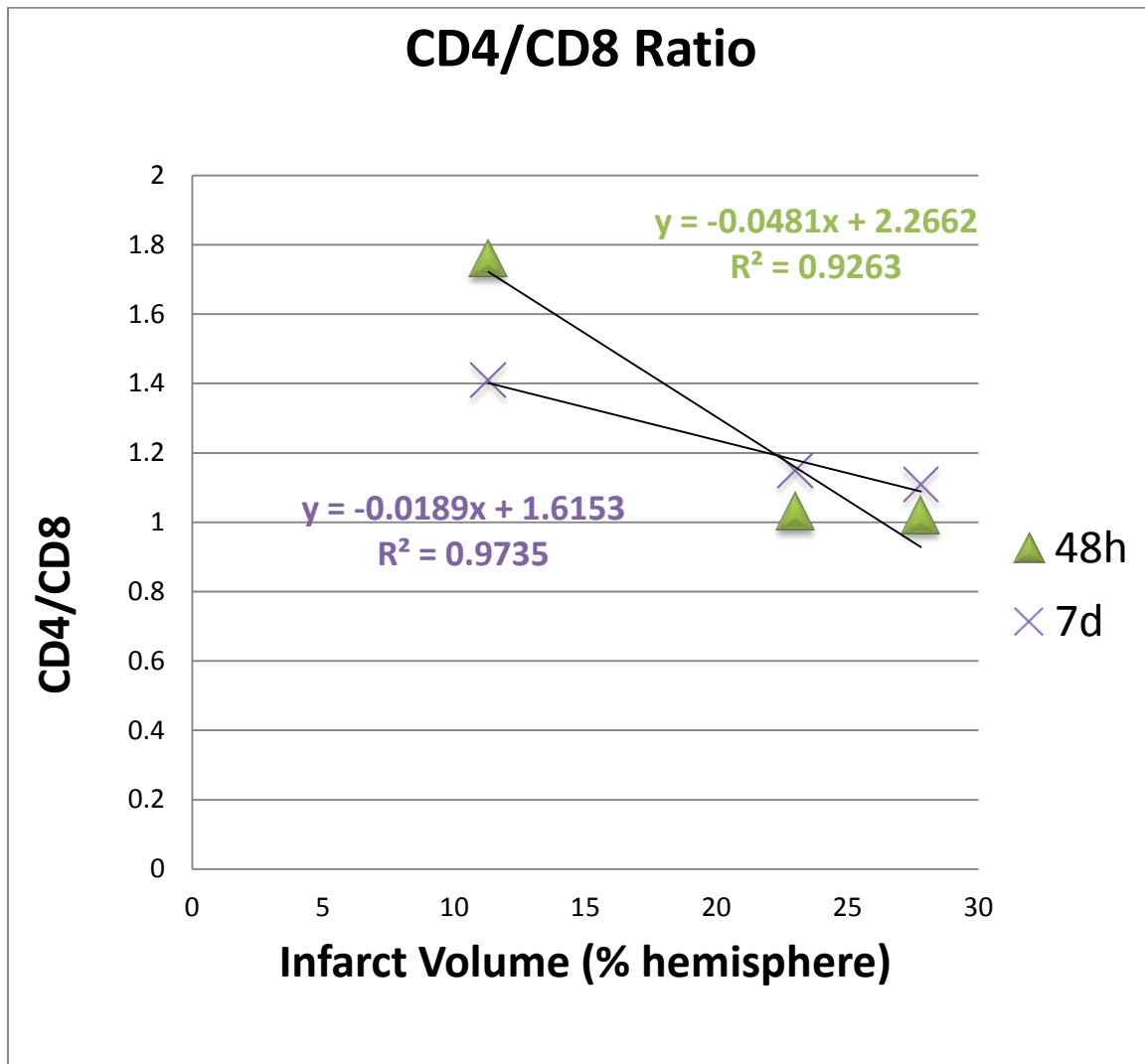


Figure 86. Ratio of CD4+ to CD8+ cells decreases with increasing infarct volume.

Ratio of CD4+ to CD8+ cells at days 2 (green triangle) and 7 (purple x) post stroke as a function of T2 infarct volume. Equations of fit for individual cell populations and R^2 values are displayed on graph in corresponding colors.

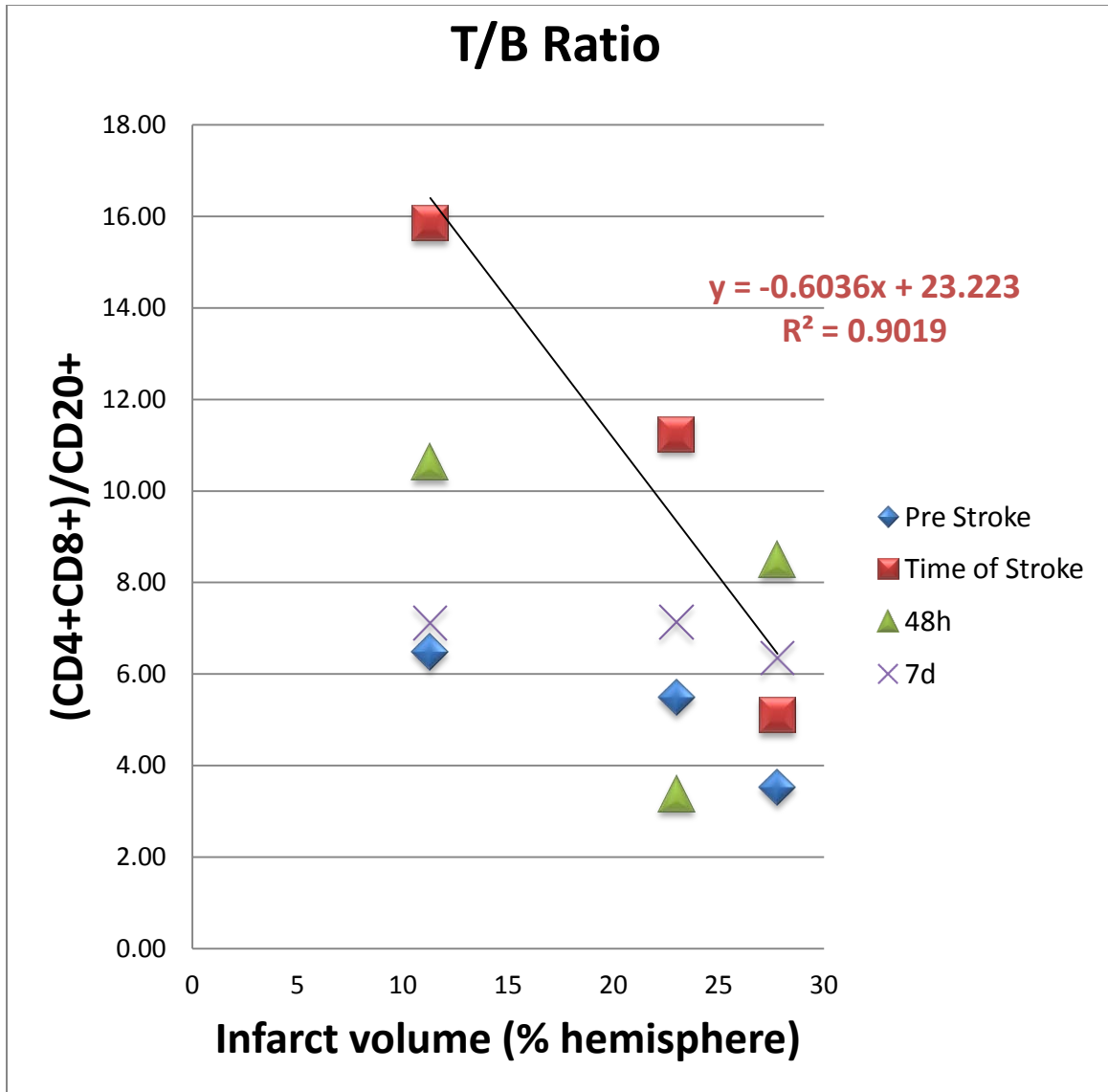


Figure 87. High T to B cell ratio at time of stroke, but not after stroke, correlates with increased infarct volume

Ratio of CD4+CD8+ T cells to CD20+ B cells 4 weeks prior to stroke (blue diamond), at the time of stroke (red square), 2 days after stroke (green triangle) and 7 days after stroke (purple x) as a function of T2 infarct volume. Equation of fit for time of stroke is displayed on graph. $R^2=0.9019$.

APPENDIX J

Characterization of the response to the two vessel occlusion model of cerebral ischemia in Chinese origin rhesus macaques

Background

Previous studies using Indian origin rhesus macaques showed highly consistent infarct volumes [324]. Extent of infarct also correlated well with duration of ischemia (**Figure 87**). Importation of Indian macaques to the United States was banned in the 1970's. Though the Oregon National Primate Research Center (ONPRC) has a large colony of Indian Rhesus macaques and an extensive breeding program, a limited number of mature (8-10 year old) male primates are available. Due to the limited availability of Indian origin macaques at the ONPRC, and the high demand of future neuroprotective studies using the two vessel occlusion model, an alternative source of NHPs was needed. Importation of Chinese origin rhesus macaques proved a viable solution. However, prior to use in drug studies, validation of the two vessel ACA/MCAO model in these primates was performed.

Material and Methods

Animals

Eight male rhesus macaques (*Macaca mulatta*) of Indian origin, one animals of Chinese origin and three animals of hybrid Chinese-Indian origin with an average age of ~9 years and an average body weight of ~8 kg were used. Animals were single-housed indoors in double cages on a 12h:12h light/dark cycle, with lights-on from 0700 to 1900h, and at a constant temperature of $24 \pm 2^{\circ}\text{C}$. Laboratory diet was provided bi-daily (Lab Diet 5047, PMI Nutrition International, Richmond, IN) supplemented with fresh fruits and vegetables, and drinking water was provided *ad libitum*. The animal care program is compliant with federal and local regulations regarding the care and use of research animals and is Association for Assessment and Accreditation of Laboratory Animal Care (AAALAC)-accredited. All animal experiments were subject to approval by the Institutional Animal Care and Use Committee (IACUC) at the Oregon National Primate Research Center.

Two-vessel Occlusion Protocol in NHP

Four weeks before surgery, animals were screened for general health, endemic disease, and neurological disorders. The right middle cerebral artery (distal to the orbitofrontal branch) and both anterior cerebral arteries were exposed and occluded with vascular clips (**Figure 88**), as previously described [324]. Surgical procedures were

conducted by a single surgeon. Briefly, anesthesia was induced with ketamine (~10 mg/kg, intramuscular injection) and animals were then intubated and maintained under general anesthesia using 0.8% to 1.3% isoflurane vaporized in 100% oxygen. A blood sample was taken and a venous line was placed for fluid replacement. An arterial line was established for blood pressure monitoring throughout surgery to maintain a mean arterial blood pressure of 60 to 80mmHg. End-tidal CO₂ and arterial blood gases were continuously monitored to titrate ventilation to achieve a goal PaCO₂ of 35 to 40 mm Hg. The surgery was performed as described previously [324]. Post-operative analgesia consisted of intramuscular hydromorphone HCl and buprenorphine.

Infarct measurement

Measurement of infarct volume was performed using T₂-weighted magnetic resonance images taken after 48 hours of reperfusion [324]. All scans were performed on a Siemen's 3T Trio system, housed near the surgical suite at ONPRC. Because of the small filling capacity of the rhesus macaque head, an extremity coil was used to achieve better image quality of the brain. Anesthesia was induced initially with ketamine (10mg/kg intramuscular injection) and a blood sample was obtained. The animals were then intubated and administered 1% isoflurane vaporized in 100% oxygen for anesthesia maintenance. Animals were scanned in the supine position 2 days after surgery, and most animals also received baseline scans before surgery. Animals were monitored for physiologic signs, including pulse-oximetry, end-tidal CO₂, and respiration rate. All animals received anatomical MRI scans, which included T₁- and T₂-weighted, high-

resolution time of flight scans, and a diffusion-weighted scan. The T₁ scan was an MPRAGE protocol, with TR=2500ms, TE=4.38ms, number of averages=1 and the flip angle=12°. Full brain coverage was attained at a resolution of 0.5mm isovoxel. The T₂ scan was a turbo spin-echo experiment, with TR=5280ms, TE=57ms, number of averages=4, an echo train length of 5, and a refocusing pulse flip angle of 120°. The entire brain was imaged with a 0.5x0.5 mm in-plane resolution and a slice thickness of 1mm. Measurements of infarct volume as a percentage of the ipsilateral hemisphere or cortex were made using the following formula: (area damaged/total area)x100%.

Results

Initial two vessel occlusion procedures with Chinese or hybrid origin rhesus macaques showed highly variable levels of cerebral infarct volume (**Figure 89**). Generally, infarct volume was larger than previously seen in Indian origin animals at the same occlusion duration, and resulted in increase morbidity. Many of these animals were found to have a visible midline shift on their MRIs (**Figure 89**), indicative of cerebral edema. Careful mapping of the cerebral vasculature documented increased anatomical variability in animals of Chinese or hybrid origin (**Figure 90**). Specifically, alteration in the number of anterior cerebral arteries complicated clip placement and may have led to variances in extent of ischemia.

Subsequent studies over the following two months tested the variability of infarct volume in an additional 8 macaques of Indian origin (**Figure 91**). Surprisingly, these animals also showed increased variability in infarct volume as compared to previous cohorts [324]. Additionally, a prominent midline shift (**Figure 91**), indicative of cerebral edema, was seen in MRIs from two animals. Possible variables that changed since previous experimental cohorts

included: personnel changes in the surgical team, post-operative care personnel changes due to inclement weather, post-operative administration of intravenous (i.v.) fluids for some but not all animals, and variable use of ventilation during MRI scans. Additionally, during these studies it was noted that intensity of T2 MRIs was highly variable, even between animals with similar infarct volumes (**Figure 92**).

Conclusions

Implementation of more standardized post-operative procedures were implemented subsequent to the studies presented here. All animals received acute post-operative i.v. fluids during recovery. Further, all animals were ventilated during MRI procedures to ensure consistent oxygen saturation. Follow up studies with additional Chinese origin macaques continued to show increased in variability in infarct volume as compared to Indian origin animals. However, the range of infarct was slightly reduced, potentially due to the implementation of standardized procedures and consistency in surgical and post-operative care personnel. Future drug studies also implemented higher N numbers for Chinese origin macaque, following a power analysis with the newly established baseline infarct range.

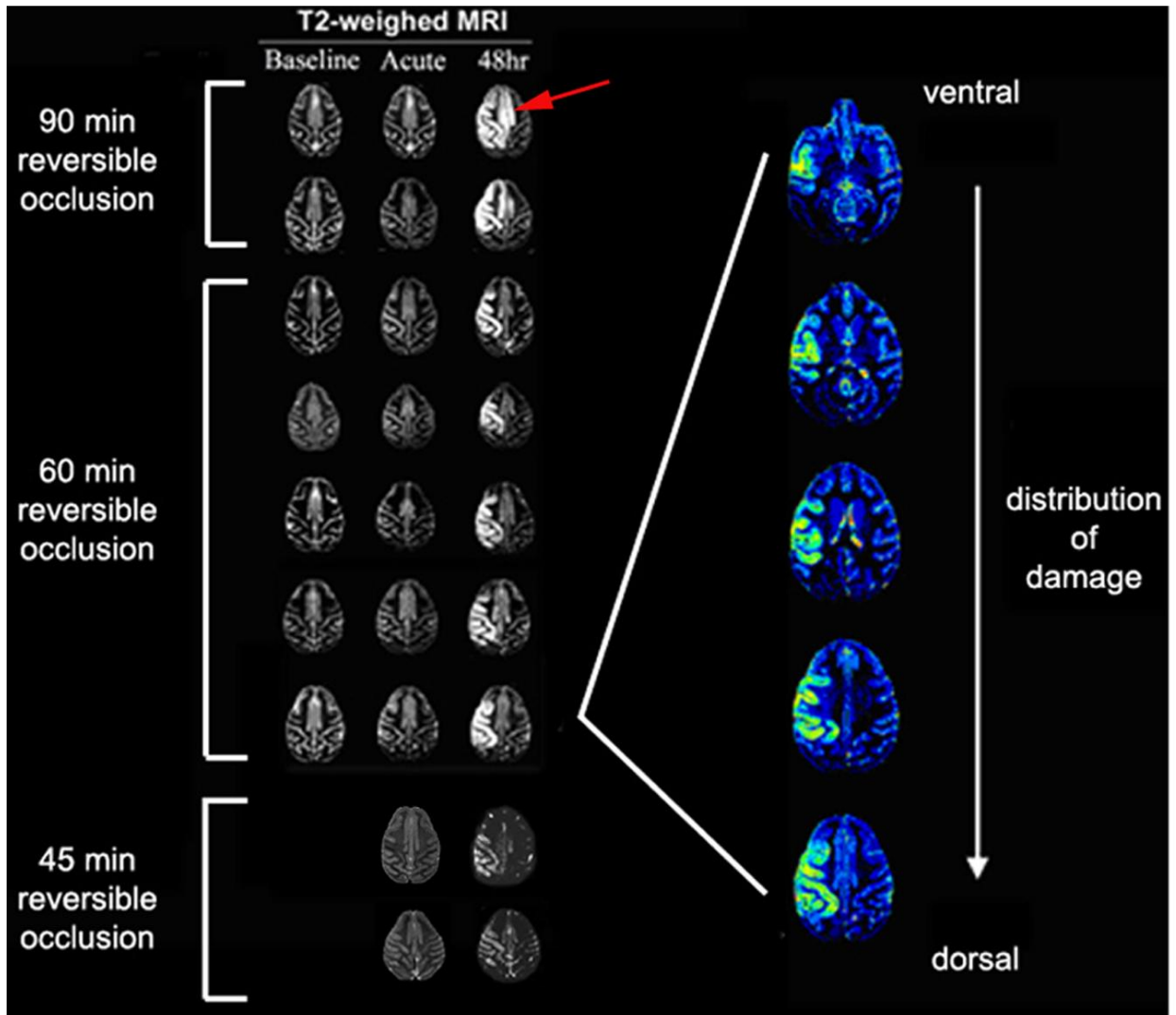


Figure 88. Comparison of stroke volume with T2-weighted MRI across various durations of reversible, two-vessel occlusion in Indian origin animals

A single transverse T2 MRI slice per animal is shown at 2 days post-occlusion, in animals that underwent 45, 60 or 90 min of ischemia. Similar cortical regions were involved at all timepoints, but ninety minutes of ischemia resulted in increased intensity and distribution of cortical involvement, which included the bilateral cingulate (red arrow) as well as rostral caudate (not shown). A pseudo-colored distribution of damage is shown for a 60 min stroke.

Table 12. Summary of infarct volumes following 2 vessel occlusion in Indian origin animals

Study	#	Ischemia (min)	Survival (days)	% ipsilateral hemisphere infarcted	
				T2 MRI	Cresyl violet
	1	45	7	18.3	21.53
	2	45	7	19.7	28.84
Ischemia	3	60	7	18.9	25.25
Duration	4	60	7	25.4	26.88
	5	90	2	47.3	39.9
	6	90	2	41.6	28.9
	7	60	2	23.3	21.1
	8	60	2	24.2	26.9
Infarct	9	60	2	27.0	25.0
Reproducibility	10	60	2	25.7	24.3
	11	60	2	26.6	23.3

Adapted from *Journal of Cerebral Blood Flow and Metabolism* 29(6) 2009 [324]. G Alexander West, Kiarash J Golshani, Kristian P Doyle, Nikola S Lessov, Theodore R Hobbs, Steven G Kohama, Martin M Pike, Christopher D Kroenke, Marjorie R Graf, Maxwell D Spector, Eric T Tobar, Roger P Simon and Mary P Stenzel-Poore “A New model of cortical stroke I the rhesus macaque” pp. 1175-86.

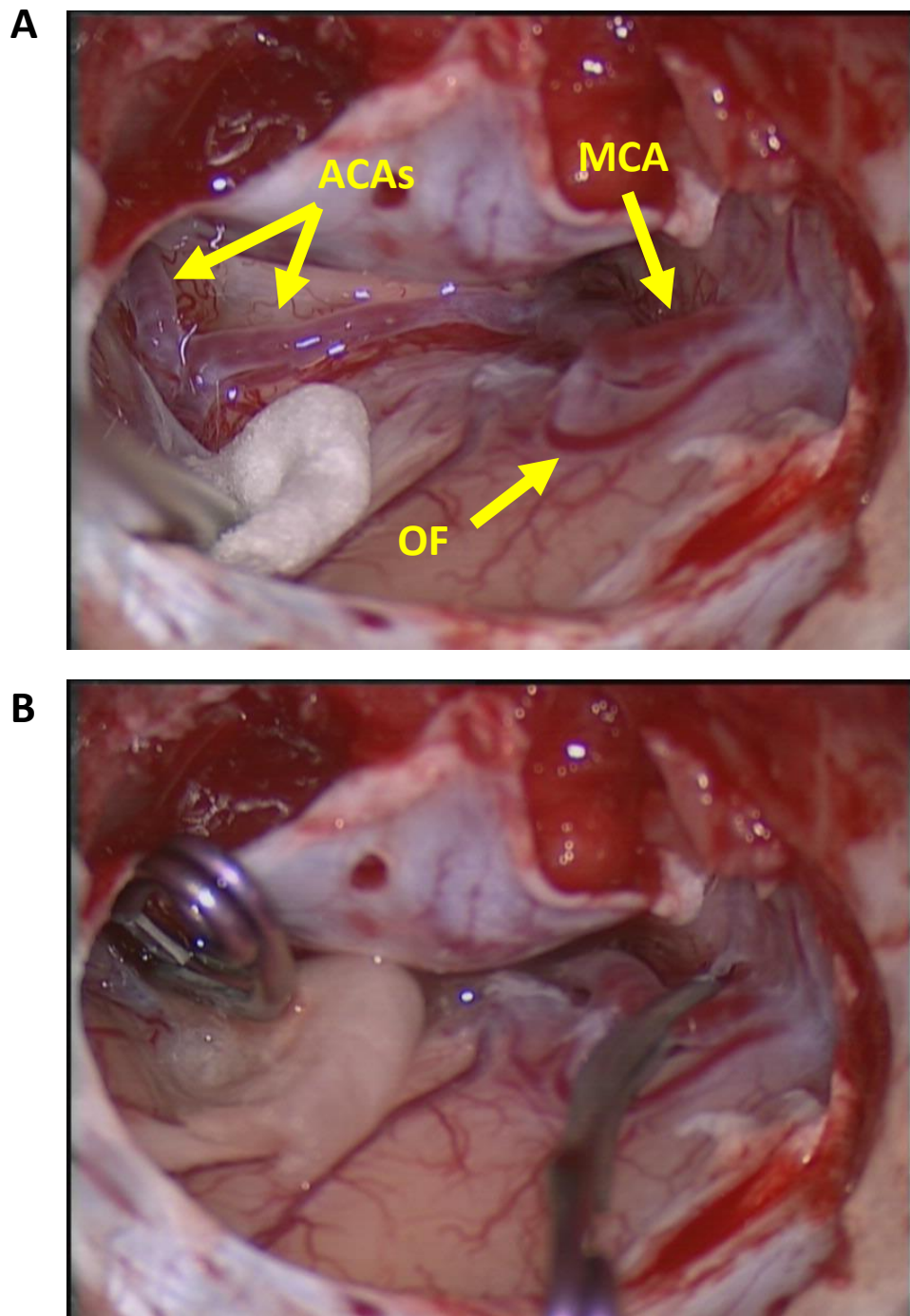


Figure 89. *View of middle cerebral and anterior cerebral arteries from cranial window*

View of cerebral vasculature from cranial window created via enucleation of eye. **(A)** Vessels prior to aneurysm clip placement **(B)** Vessels with clips in place. MCA, middle cerebral artery; ACA, anterior cerebral artery; OF, orbital frontal branch.

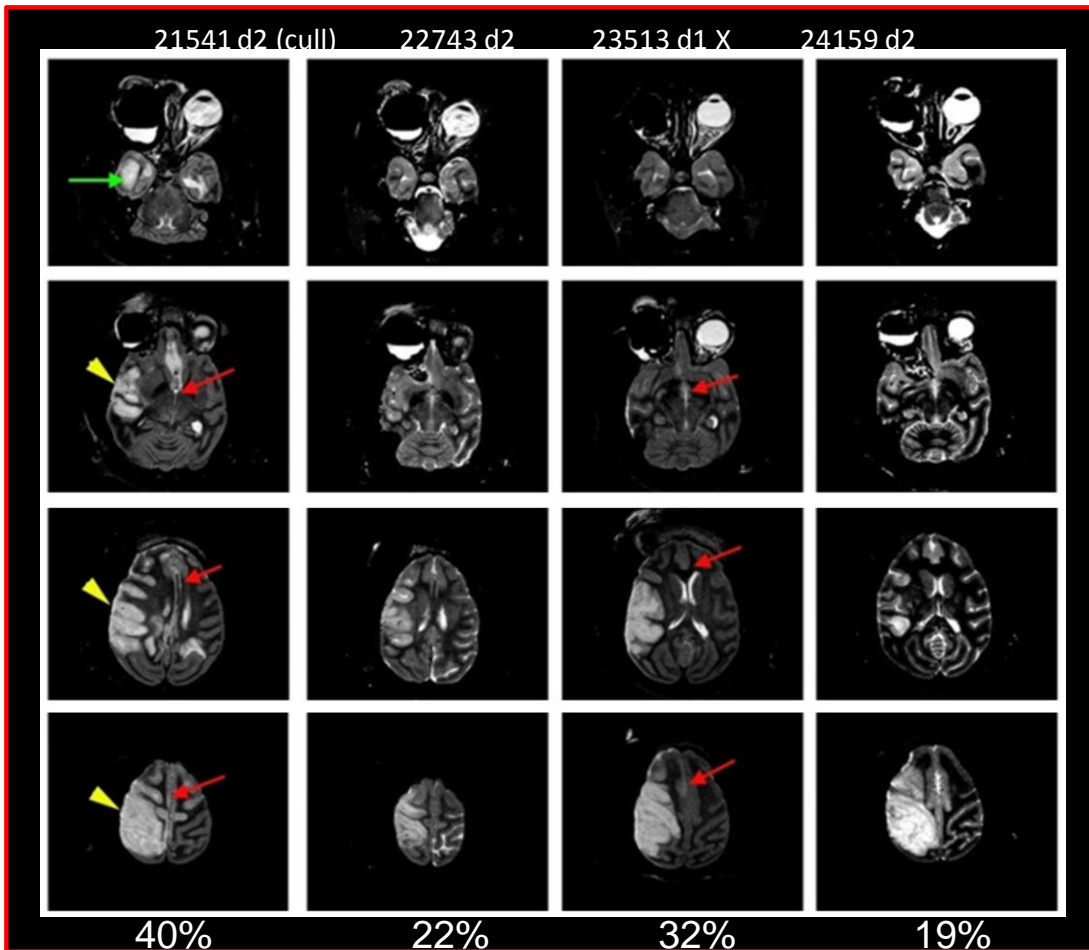


Figure 90. Serial MRI section from Chinese or hybrid origin animals 2 days post occlusion

Four serial MRI slices per animal following 60 minutes of two vessel occlusion. Red arrows indicate midline shift caused by cerebral edema. Green arrow indicates atypical involvement of caudate in ischemia damage. Yellow arrow highlights extensive infarct involving motor cortex.

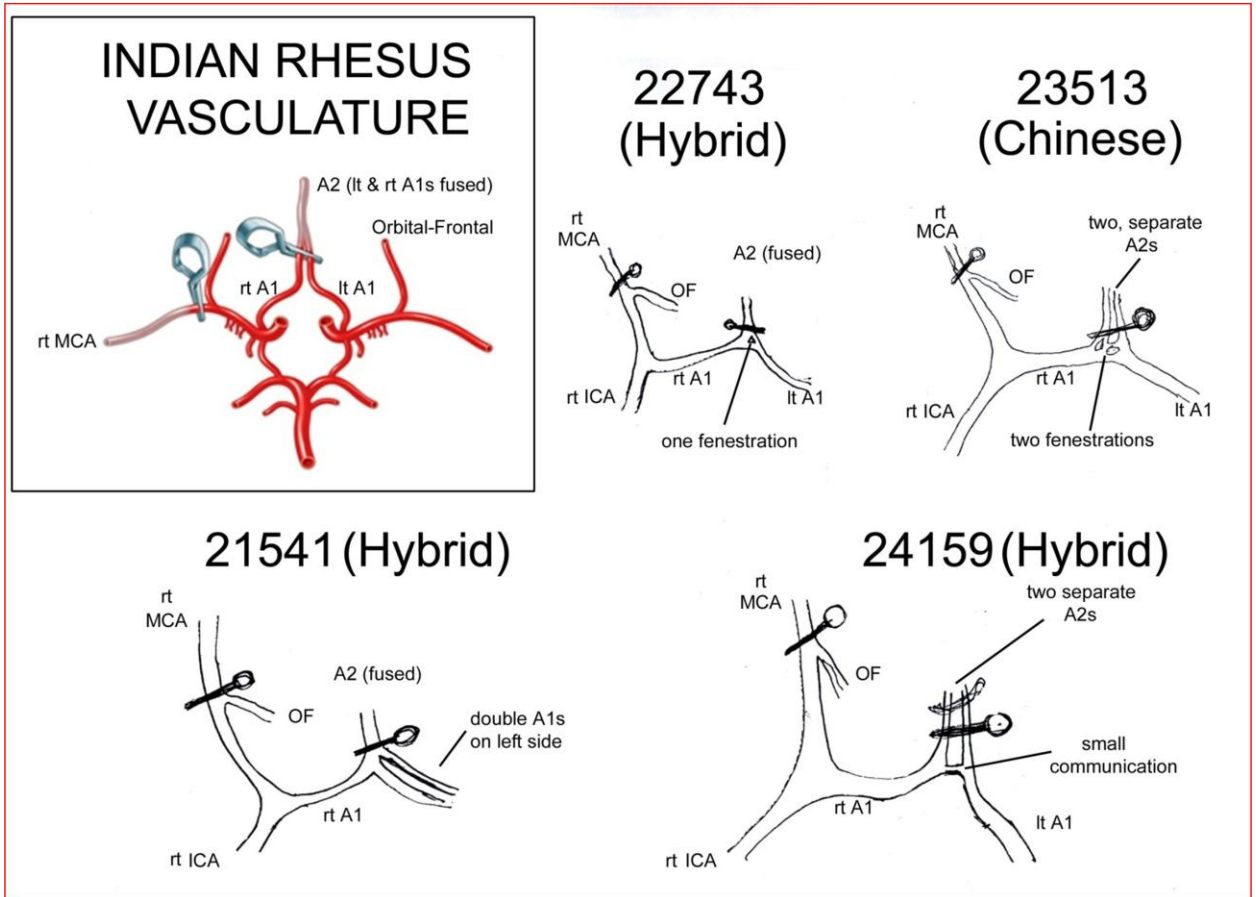


Figure 91. Vascular architecture of Indian origin rhesus compared to Chinese or hybrid origin

Increase variability seen in cerebral vascular of Chinese and Chinese-Indian hybrid origin macaques. Top left (insert) shows typical vascular pattern seen in Indian origin macaques, which was highly consistent. Drawings depict variable vasculature in Chinese or hybrid animals, and bars with circles represent placement of aneurysm clips during occlusion.

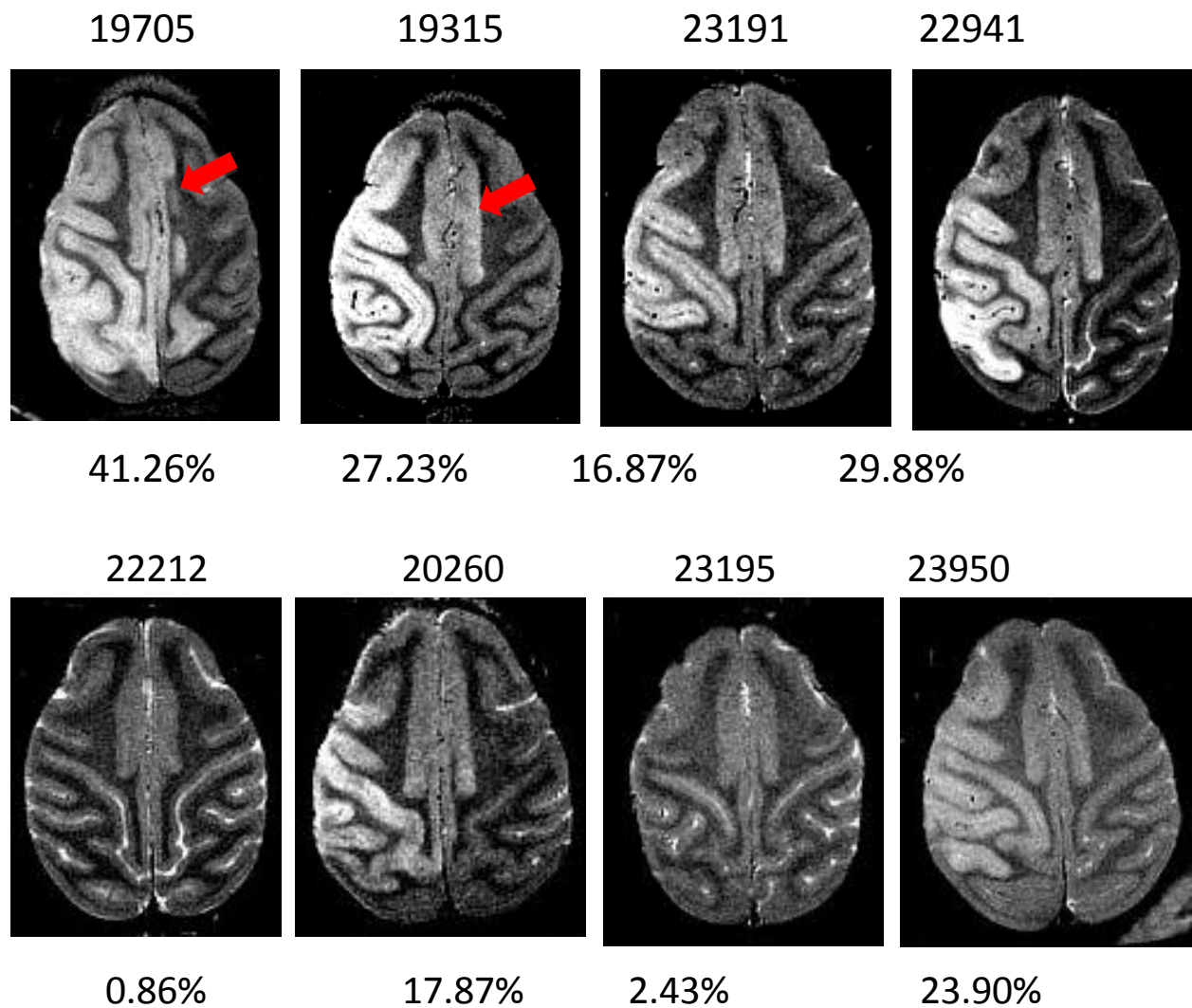
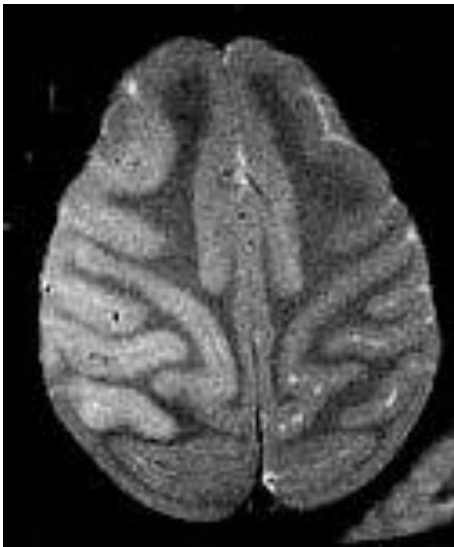


Figure 92. Representative MRIs from 8 Indian origin rhesus macaques 2 days post occlusion

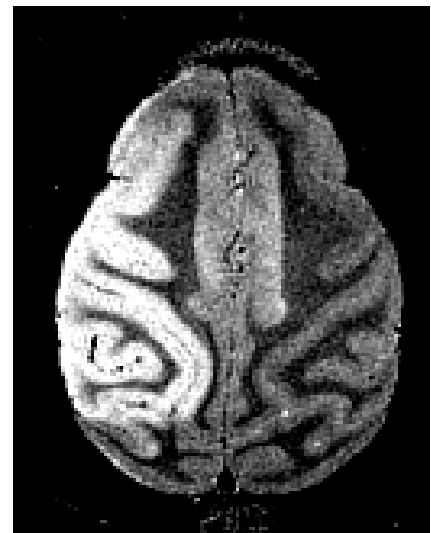
Subsequent studies with Indian origin macaques showed increased variability in infarct volume as compared to what was seen in previous studies. Red arrows mark midline shift, indicative of cerebral edema.

23950 – 45 min



23.9%

19315 – 60 min



27.2%

Figure 93. *Variable intensity but similar infarct volume in two separate T2 MRIs*

Intensity of T2 MRI scan varied considerably between animals. Though infarct volume is identical between the two animals pictured above, it is unclear if increased signal correlated to increased neurological deficit.

APPENDIX K

Supplemental figures referred to in main text

Figure 94 *Reduction of MCAO-associated neurological deficit in mice
Following preconditioning with CpG ODNs*

Figure 95 *Boison Lab*

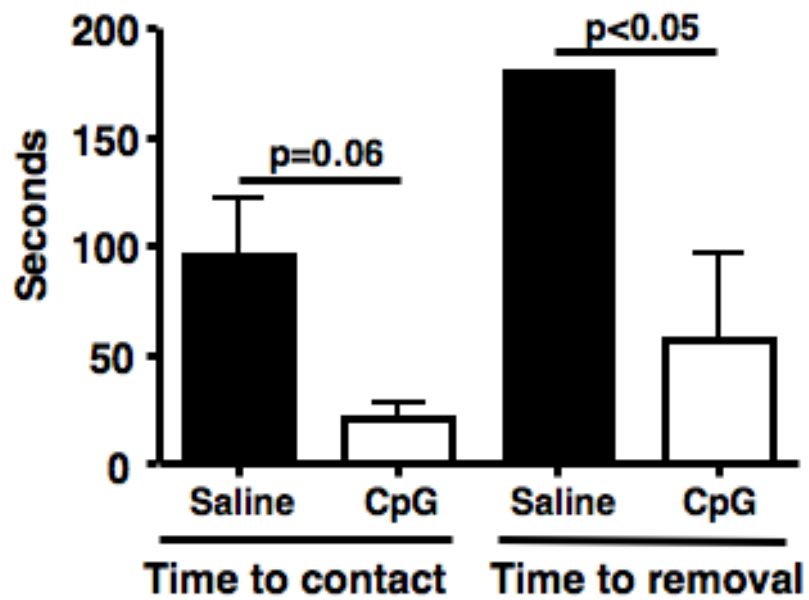


Figure 94. Reduction of MCAO-associated neurological deficit in mice following preconditioning with CpG ODNs

Seventy-two hours after MCAO, forepaw sensitivity, somatosensory neglect, and motor impairments were assessed. Adhesive tapes of equal size were applied to each paw and the duration to contact and to removal were measured. Values are group means \pm SEM; n=3.



Figure 95. *Boison Lab*

Front row (left to right): Panos Theofilas, Tien Coffman, Chaitra Sriram, Marissa Hanthorn, Jessica Yahm, Rebecca Williams-Karnesky, Ursula Sandau, Michael Williams, Tianfu Li

Back Row (left to right): Krishnaveni Subbiah, Haiying Shen, Nikki Lytle, Wes Plinke, Teresa Lusardi, Khon Truong, Detlev Boison, Kiran Akula

Not pictured: Sue Crawford

Fin